University of Southampton

Faculty of Environmental and Life Sciences

School of Ocean and Earth Science

Investigating Zooplankton Ecology and Biogeochemistry in the Twilight Zone, One of the Least Studied Ecosystems on Earth

by

Eloïse Linda-Roselyne Savineau

BSc, MSc

ORCID ID 0000-0003-2038-2010

Thesis for the degree of Doctor of Philosophy

February 2026

University of Southampton

Abstract

Faculty of Environmental and Life Sciences

School of Ocean and Earth Science

Investigating Zooplankton Ecology and Biogeochemistry in the Twilight Zone, One of the Least Studied Ecosystems on Earth

by

Eloïse Linda-Roselyne Savineau

The biological carbon pump (BCP) is crucial to the regulation of Earth's climate. Through a suite of processes that convert inorganic carbon dioxide (CO_2) into particulate organic carbon (POC) and subsequent transfer to depth, the BCP is estimated to reduce atmospheric CO_2 concentrations by 50 % of what they would otherwise be. Zooplankton are a key component of the BCP by grazing on phytoplankton, fragmenting and repackaging POC, and actively transporting carbon to depth through diel- and ontogenetic vertical migration. However, the role of zooplankton in POC transformation and vertical flux attenuation in the mesopelagic zone (100 – 1000m), where most POC attenuation occurs, remains poorly understood. This thesis investigates how vertical changes in zooplankton ecology and physiology shape carbon cycling within the mesopelagic. In the Scotia Sea, lipid-storing copepods were found to be emerging from overwintering, metabolically inactive, and not feeding on the spring diatom bloom. This highlights how the physiology of lipid-storing copepods causes a decoupling between primary production and when this organic matter is remineralised by these animals. In the northern Benguela Upwelling System (nBUS), zooplankton biomass peaked within the oxygen minimum zone (OMZ), whereas the larger animals were distributed above and below this region. These results suggest that the OMZ provides zooplankton with a refuge from predation. The main contribution of zooplankton to carbon sequestration was via their respiration at depth during diel vertical migration. This highlights the role of these animals in the spatial decoupling between carbon fixation in surface waters and remineralisation at depth. Lastly, analysis of zooplankton community size spectra in the Scotia Sea revealed that large, lipid-storing copepods, which integrate energy over an entire season, skew the shape of the size spectra, favouring larger size classes. This can mislead interpretations of energy flow unless taxonomy and physiology are integrated into size-based approaches. Collectively, results from this thesis highlight the role of zooplankton ecology and physiology in decoupling carbon cycling in both time and space in the mesopelagic.

Table of Contents

Table of Tables

Table of Tables

Table of Figures

Table of Figures

Table of Figures

List of Accompanying Materials

The data used in this thesis is available from the University of Southampton's Pure repository via the DOI https://doi.org/10.5258/SOTON/D3847

Research Thesis: Declaration of Authorship

Print name: Eloïse Linda-Roselyne Savineau

Title of thesis: Investigating Zooplankton Ecology and Biogeochemistry in the Twilight Zone, One of the Least Studied Ecosystems on Earth

I declare that this thesis and the work presented in it are my own and has been generated by me as the result of my own original research.

I confirm that:

1. This work was done wholly or mainly while in candidature for a research degree at this University;
2. Where any part of this thesis has previously been submitted for a degree or any other qualification at this University or any other institution, this has been clearly stated;
3. Where I have consulted the published work of others, this is always clearly attributed;
4. Where I have quoted from the work of others, the source is always given. With the exception of such quotations, this thesis is entirely my own work;
5. I have acknowledged all main sources of help;
6. Where the thesis is based on work done by myself jointly with others, I have made clear exactly what was done by others and what I have contributed myself;
7. Parts of this work have been published as:

Savineau, E.L-R., Cook, K.B., Blackbird, S.J., Stowasser, G., Kiriakoulakis, K., Preece, C., Fielding, S., Belcher, A.C., Wolff, G.A., Tarling, G.A. and Mayor, D.J., 2024. Investigating the physiological ecology of mesopelagic zooplankton in the Scotia sea (Southern ocean) using lipid and stable isotope signatures. *Deep Sea Research Part I: Oceanographic Research Papers*, *208*, p.104317. https://doi.org/10.1016/j.dsr.2024.104317

Signature: ..... Date:.....

Acknowledgements

I would like to express my sincere gratitude to my supervisory team: Dan Mayor, Kathryn Cook, Ben Ward, Kostas Kiriakoulakis and B.B. Cael. Thank you for all your support during my PhD. To Dan Mayor and Kathryn Cook, thank you for your constant encouragement, advice, generous time, support, and wisdom. Thank you for all the invaluable opportunities you have given me to gain experience in open-ocean expeditions and allowing me to develop into a well-rounded researcher. I will cherish all our fun times at sea and hundreds of crosswords completed!

This thesis could not have been completed without support from: Gabi Stowasser and Geraint Tarling at the British Antarctic Survey, who kindly shared all their COMICS stable isotope data and their wisdom when it comes to Scotia Sea ecosystems; George Wolff and Sabena Blackbird from the University of Liverpool for teaching me the intricacies, both theoretical and in the laboratory, of lipid biomarker analyses; all the researchers involved in the COMICS programme who have made the foundation of my thesis possible; and the financial support provided by the INSPIRE doctoral training partnership.

To the Ocean Plankton team – it's been amazing getting to work with such a passionate team of like-minded plankton enthusiasts. Special thanks to my Oithona University partner in crime, Josephine "Eloïse" Tod, for providing me with a second home whenever I visited the team in Exeter and for always feeding me delicious (and sometimes spicy) meals!

I would like to thank everyone involved in the JC231, DY157/AMT30, DY180 and JC269 research expeditions for making my time at sea so enjoyable and teaching me so much about oceanographic fieldwork. Thank you to the captains and crews of RRS James Cook and RRS Discovery, without whom our research would not be possible.

Thank you to the Pelagic Ecosystems Lab at the University of British Columbia for welcoming me during my research placement and making my time in in Vancouver so special.

Thank you too all my fellow PhD students at NOC and beyond for making my PhD experience so amazing, whether it be silly 12:30 lunch-time chats, sunset drinks at Dancing Man, hanging off the climbing wall at Parthian, chilling at the beach, or in the middle of the Atlantic Ocean. To Farin, my OG flatmate, thank you for baking the most delicious cakes and always being down for a Supernatural binge watch. To Rowan, thank you for being an amazing friend, flatmate, tarot card reader, sailing partner and fellow salty soul with whom I could always escape to Swanage. To Beth, thank you for being the bestest friend, flatmate and all-round legend to have gone through this whole experience with. From coffee breaks in the green kitchen, ditching work at 11 am to go surfing or snorkelling, peaceful sunrise swims at Lepe, jump-starting the Corsa battery

more times than we can count, finding moss and bluebells in the forest, Avon sauna sessions, cycling the Isle of Wight, and hiking in Snowdonia – you've made my time in Southampton unforgettable! To Seb, thank you for accepting to run an ultra-marathon with me "no questions asked" and becoming such a great running partner and friend. I'm going to sorely miss Biscoff Bun Long Runs with you and Beth every Sunday!

Ma maman, you will forever be credited as the one who fuelled my desire to be a marine biologist and oceanographer. Who knew that showing me how to build a homemade plankton net made from tights for a high school project would lead to this thesis 12 years later! Dad, thank you for always making me question the natural world around me and for nurturing and encouraging my passion for STEM. The student has surpassed the master! To my brother Tanguy, thank you for being my #1 jester and always finding ways to make me smile and laugh no matter my mood or stress level. Merci à toute ma famille - les Français, les Belges et les Américains - de m'avoir soutenue à travers les années, votre sirène des eaux froides vous promet de sauver notre océan tant aimé.

Pour mon pépé,

“On aime ce qui nous émerveille, et on protège ce que l'on aime."

(Jacques Yves Cousteau)

Merci de m’avoir fait aimer l’océan.

Definitions and Abbreviations

ABF.....Angola-Benguela front

ACC.....Antarctic circumpolar current

ALAGEL .....Alanine-gelatine

ALC .....Fatty alcohol

ANOVA .....Analysis of variance

APF.....Atlantic polar front

AVISO .....Altimetry-derived geostrophic velocities

BAS .....British Antarctic Survey

BATS.....Bermuda Atlantic Time-series Study

BCD.....Bacterial carbon demand

BCP .....Biological carbon pump

BN .....Benguela North station

BSTFA.....N,O-bis-(trimethylsilyl)trifluoroacetamide

BUS .....Benguela Upwelling System

C .....Carbon

COMICS .....Controls over Ocean Mesopelagic Interior Carbon Storage

CPR .....Continuous plankton recorder

CTD .....Conductivity, temperature, depth

DCM .....Deep chlorophyll maxima

DHA.....Docosahexaenoic acid

DIC.....Dissolved inorganic carbon

DO.....Dissolved oxygen

DOC .....Dissolved organic carbon

DVM .....Diel vertical migration

DW .....Dry weight

EBUEs .....Eastern boundary upwelling ecosystems

EPA.....Eicosapentaenoic acid

ESD .....Equivalent spherical diameter

ETS .....Electron transport system

FA.....Fatty acid

GC.....Gas chromatography

GEL .....Gelatine

GF/F .....Glass fibre filter

GLYGEL.....Glycine-gelatine

GS-MS .....Gas chromatography-mass spectrometry

HCl.....Hydrochloric

HNLC .....High nutrient, low chlorophyll

HOT.....Hawaii Ocean Time-Series

ID .....Identification

INT.....2-p-iodophenyl-3-p-nitrophenyl monotetrazolium chloride

IPCC.....Intergovernmental Panel on Climate Change

IUPAC.....International Union of Pure and Applied Chemistry

Mammoth.....Mammoth multi-net (Hydrobios)

MEDUSA.....Model of Ecosystem Dynamics, nutrient Utilisation, Sequestration and Acidification

MLD.....Mixed layer depth

MOCNESS .....Multiple Opening and Closing Net and Environmental Sampling System

MUFA .....Monounsaturated fatty acid

MZ .....Mesopelagic zone

N .....Nitrogen

NADH .....Nicotinamide adenine dinucleotide

NADPH.....Nicotinamide adenine dinucleotide phosphate

NBSS .....Normalised biovolume size spectra

nBUS .....Northern Benguela Upwelling System

NERC.....Natural Environmental Research Council

NMDS.....Non-metric multidimensional scaling

NMFRI .....National Marine Facilities Research Institute

OBIS .....Ocean Biogeographic Information System

OMZ .....Oxygen minimum zone

OVM .....Ontogenetic vertical migration

PAC .....Particle associated copepods

PERMANOVA.....Permutational multivariate analysis of variance

PF.....Polar front

POC.....Particulate organic carbon

POETS-WCB.....Polar Ocean Ecosystem Time Series - Western Core Box

POM .....Particulate organic matter

PUFA .....Polyunsaturated fatty acid

RDA .....Redundancy analysis

RMT25 .....Rectangular Midwater Trawl, 25 m^2

RQ .....Respiration quotient

SACCF.....Southern Antarctic circumpolar current front

SACW .....South Atlantic Central Water

SAPs.....Standalone pumps

SB-ACC .....Southern boundary of the Antarctic circumpolar current

sBUS .....Southern Benguela Upwelling System

SCOOBIES.....Scotia Sea Open-Ocean Observatory

sd .....Standard deviation

SFA.....Saturated fatty acid

SIMPER.....similarity percentage

SUERC.....Scottish Universities Research Centre

TAG .....Triacylglycerol

TIC.....Total ion current

TL .....Trophic level

TTE .....Trophic transfer efficiency

UK .....United Kingdom

WE.....Wax esters

WMD .....Weighted mean depth

WoRMS .....World Register of Marine Species

WW .....Wet weight

ZCD .....Zooplankton carbon demand

Chapter 1 Introduction

1.1 The biological carbon pump and global climate regulation

The ocean has a major role in regulating Earth's climate, influencing the rate of climate change by storing excess heat and carbon and slowly redistributing these over time. Ocean biogeochemical cycling of carbon is influenced by physical, chemical (solubility pump) and biological processes, with the later, being the focus herein. The biological carbon pump (BCP) describes a myriad of processes that cycle and export carbon from the euphotic, epipelagic zone to the mesopelagic zone and the deep ocean (Boyd *et al.*, 2019). The BCP is crucial to the Earth's climate and is estimated to lower atmospheric carbon dioxide (CO_2) concentrations by up to 50 % of what it would otherwise be relative to pre-industrial climate (Parekh *et al.*, 2006; Tjiputra *et al.*, 2025). Inorganic CO_2 from the atmosphere is drawn into the ocean where it dissolves into seawater, is fixed by phytoplankton during photosynthesis and converted into particulate organic carbon (POC) (Turner, 2015). This carbon forms the base of heterotrophic marine ecosystems and is subsequently grazed by zooplankton and cycled through the rest of the food web through predation. Because the BCP plays such an important role in carbon cycling, it is fundamental to understand what governs the fate of sinking carbon. The strength of the BCP is described as the magnitude of POC flux out of the euphotic zone and the efficiency of the BCP as the fraction of that POC that is transported to depth (Buesseler *et al.*, 2020) – with the latter influencing the length of time this exported carbon is sequestered in the ocean before being released back into the atmosphere (Kwon *et al.*, 2009). It is estimated that 10 – 25 % of the 45 – 50 Gt of carbon produced by phytoplankton in the euphotic zone sinks down into the mesopelagic (Falkowski *et al.*, 1998; Henson *et al.*, 2011; Henson *et al.*, 2012). However, ~90 % of POC is remineralised within the mesopelagic (100 – 1000 m), with this flux attenuation of POC with depth most widely quantified via a power-law relationship known as the "Martin curve" (Martin *et al.* (1987); Figure 1.1):

$$F_z = F_{100} \times \left({}^{z}/_{100}\right)^{-b} \qquad (eq\ 1.1)$$

Where F_z is the sinking flux of POC at depth z, F_{100} is the flux of POC at a fixed 100 m reference depth and exponent b is the flux attenuation coefficient calculated from the slope of the log-log transformation of POC flux and depth.

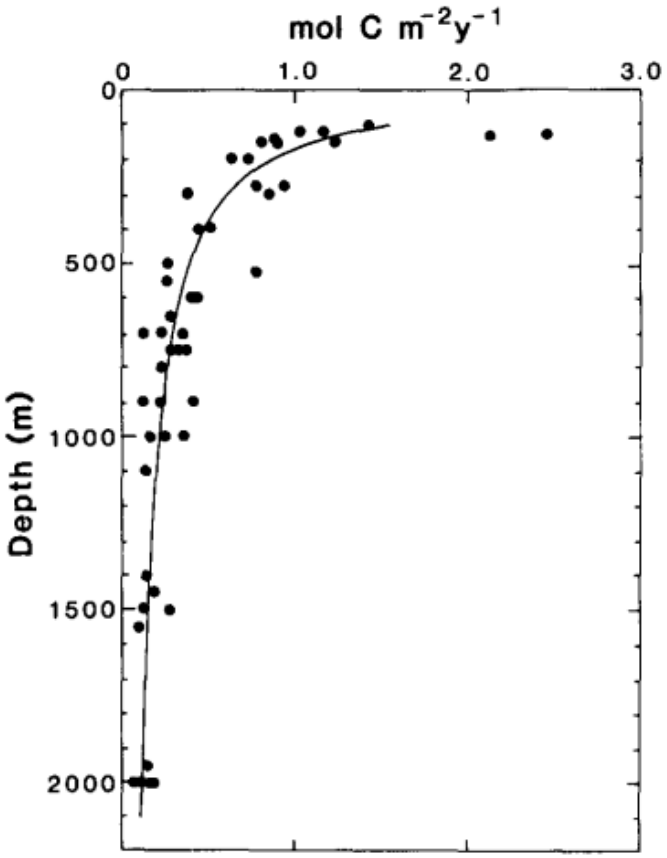

Figure 1.1 The "Martin curve" from Martin *et al.* (1987) showing POC flux (mol C m^{-2} y^{-1}) attenuation with depth in the North Pacific. Data (circles) were obtained from sediment traps and fitted with the power law function from equation 1.1 and a b-value of 0.86.

Within the BCP, carbon export is influenced by the reworking of POC by heterotrophic bacteria and zooplankton (Giering *et al.*, 2014; McDonnell *et al.*, 2015; Turner, 2015; Doherty *et al.*, 2021; Nguyen *et al.*, 2022), particle fragmentation by zooplankton (Mayor *et al.*, 2014) and vertical migration of animals (Steinberg *et al.*, 2000; Archibald *et al.*, 2019) (Figure 1.2). It is well documented that animal breakdown, ingestion and repacking of organic material influences the rate of export of organic matter to the deep ocean (Turner, 2015). Due to the inefficiency of marine food webs, a majority of this carbon is released back into the water as dissolved organic matter (DOC), faecal pellets, or respired by animals into dissolved inorganic carbon (DIC). The mesopelagic or "twilight" zone (100 – 1000 m) describes the region of the ocean just below the base of the euphotic zone, where light is insufficient for photosynthesis to occur, but downwelling irradiance (less than 1 % surface light levels) still enables visual predation and diurnal/nocturnal cycles to occur (Robinson *et al.*, 2010; Sutton, 2013). Due to the 'transitional' nature of the mesopelagic, communities display a multitude of trophic behaviours and strategies, including organisms feeding on microbes/bacteria (Pond and Ward, 2011), detritus (Steinberg *et al.*, 1998; Yamaguchi *et al.*, 2002), phytoplankton (Yang *et al.*, 2016), zooplankton

(Lourenço *et al.*, 2017), and nekton (Potier *et al.*, 2007). Some organisms moreover undergo daily vertical migrations to feed in surface epipelagic waters at night before returning to deeper mesopelagic waters during the day (Klevjer *et al.*, 2016). Ocean ecology therefore has a crucial role in the vertical coupling between the surface and deep ocean (Sutton, 2013).

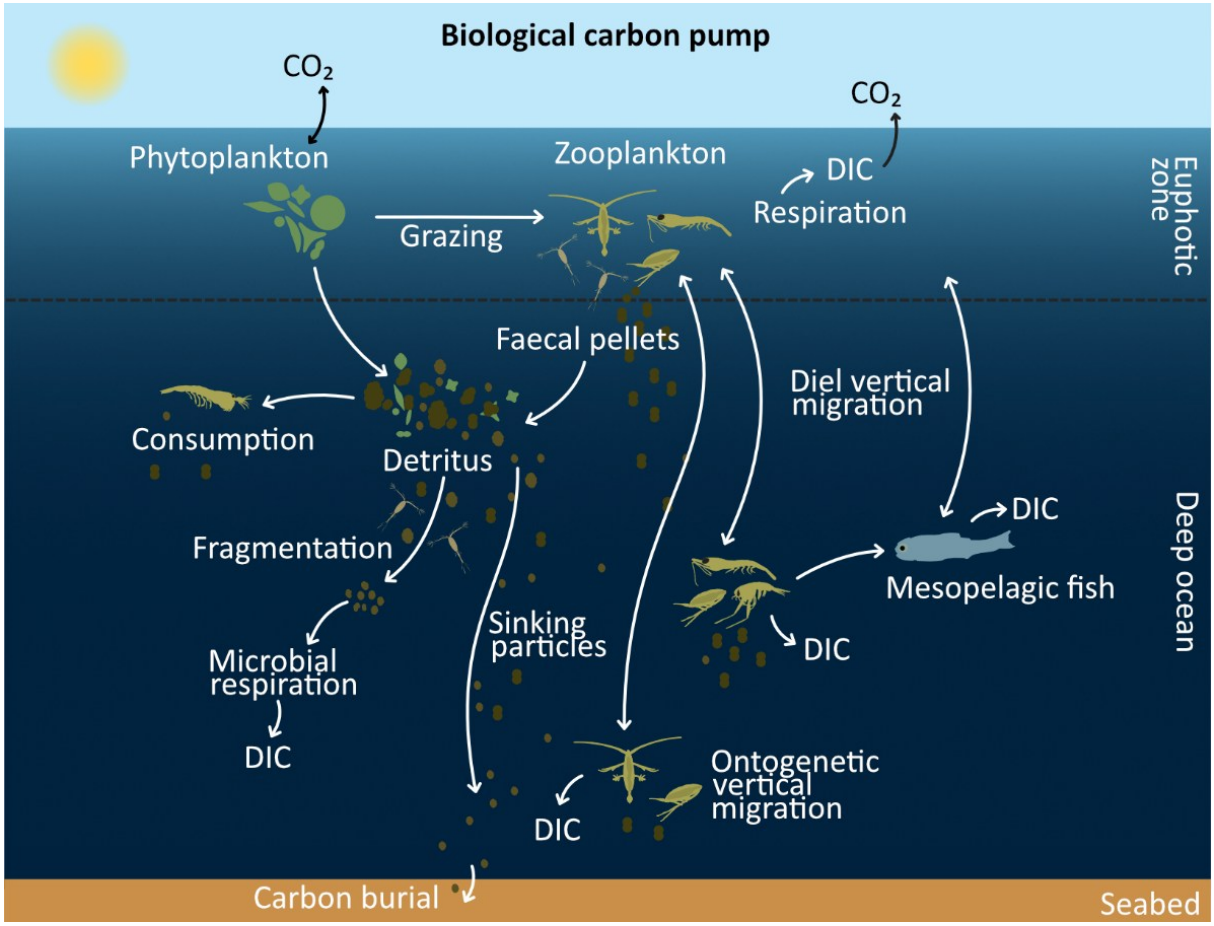

Figure 1.2 Schematic illustrating some of the processes involved in the biological carbon pump. Organic carbon is formed by phytoplankton in the epipelagic zone and is grazed by heterotrophs. Phytoplankton are repackaged into detritus and faecal pellets, passively sink and are further recycled by heterotrophs and microbes. Animals perform diel and ontogenetic vertical migration, actively transporting carbon to depth. As organisms respire, they convert organic carbon into dissolved inorganic carbon (DIC, carbon dioxide - CO_2).

1.2 Role of zooplankton in the biological carbon pump

1.2.1 Zooplankton passive transport of POC

Mortality of zooplankton in the epipelagic has been proposed as a contributor to the passive export of POC, however, quantifying this process remains difficult due to the challenge of distinguishing between carcasses that passively sink into sediment traps and live zooplankton

that swim into the trap and subsequently die due to formaldehyde preservatives (Buesseler *et al.*, 2007a; Steinberg and Landry, 2017). Zooplankton passively export POC through grazing on phytoplankton and repacking this organic matter into faecal pellets, which may act as fast-sinking agents of the downward flux of POC in the ocean (Turner, 2002). The contribution of faecal pellets to the total sinking POC flux is highly variable. The composition and size structure of zooplankton communities influence the rate of passive export, with larger zooplankton which produce large, dense faecal pellets, suggested to contribute more to passive flux of POC (Poulsen and Kiørboe, 2006). The robustness of faecal pellets mean they do not disaggregate as easily as other phytodetrital aggregates and have high volume-specific sinking velocities (Ploug *et al.*, 2008). Gelatinous zooplankton such as Salpa and Appendicularia, which have high filtration rates and produce dense faecal pellets, are moreover observed to play a major role in the passive flux of POC during phytoplankton bloom events (Bruland and Silver, 1981; Lalande *et al.*, 2011). While most estimates suggest faecal pellets contribute on average 40 % to total sinking POC flux (Turner, 2015), this can be as much as 94 % during spring bloom events and as little as 1.9 % in autumn (Stukel *et al.*, 2013). Zooplankton also influence the passive export of POC by fragmenting larger particles into smaller ones. Small mesozooplankton (< 1 mm), such as *Oithona* spp. and Oncaeidae, are hypothesised to be the primary drivers of the attenuation of sinking particles in the upper ocean (Mayor *et al.*, 2014). These animals are considered to be the most abundant and ubiquitous multicellular zooplankton in the global ocean (Gallienne and Robins, 2001) and the 'gate-keepers' of POC flux at the base of the euphotic zone (González and Smetacek, 1994; Jackson and Checkley, 2011; Koski *et al.*, 2020). These small, particle-associated copepods (PAC) are hypothesised to have a "search and destroy" mode of feeding as they scavenge for interstitial particle-attached microbes, and as a result inadvertently break down large, fast-sinking particles into smaller, suspended ones (Mayor *et al.*, 2020). In turn, this makes small, suspended particles hotspots for microbial colonisation - a process called microbial gardening (Mayor *et al.*, 2014). In experimental studies, fragmentation of aquaria-reared Antarctic krill faecal pellets was observed to increase microbial POC turnover by 1.9 times (Cavan *et al.*, 2021). The breakdown of particles and colonisation by microbes results in an estimated 70 – 91 % of remineralisation being carried out by prokaryotes in the twilight zone (Giering *et al.*, 2014). Zooplankton-mediated fragmentation contributed to a reduction in particle size with increasing depth at the Porcupine Abyssal Plain (PAP) site in the North Atlantic, an observation that contrasted with model predictions anticipating a decline in small particles with depth due to attenuation processes (Cavan *et al.*, 2017). The discrepancy was suggested to partly arise from the models' failure to account for biological fragmentation by zooplankton (Cavan *et al.*, 2017). The explicit inclusion of particle-associated copepods (PAC) and their effects on sinking POC into a biogeochemical model, such as MEDUSA (Model of Ecosystem Dynamics, nutrient Utilisation, Sequestration and Acidification), provided the first

mechanistic way of explaining particle flux attenuation and demonstrated that these zooplankton may be the main drivers for particle flux attenuation in the mesopelagic (Mayor *et al.*, 2020).

1.2.2 Zooplankton active transport of POC

Zooplankton active transport describes the component of the BCP whereby POC is directly transported from surface waters to the mesopelagic by the vertical movement of zooplankton. This includes diel vertical migration (DVM), ontogenetic vertical migration, and mortality of migrating species at depth.

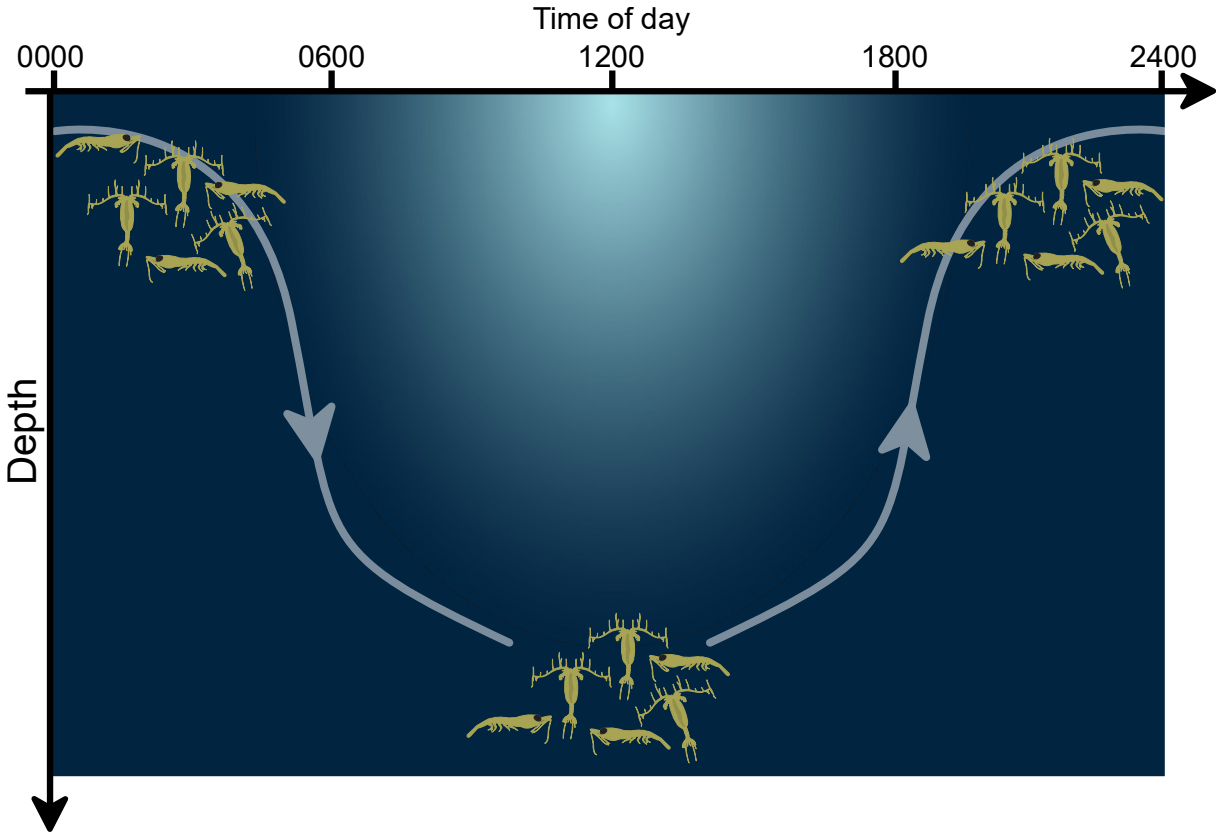

Figure 1.3 Schematic of classic (nocturnal) diel vertical migration, whereby zooplankton migrate to food rich epipelagic waters at night and migrate to deeper waters during the day to reduce risks of visual predation.

DVM is the daily synchronised movement of zooplankton and micronekton from their daytime residence in the mesopelagic zone to the euphotic zone (Figure 1.3), where they feed on phytoplankton at night (Steinberg and Landry, 2017). DVM is generally described as a trade-off between the need to feed in surface waters where food availability is high and the risks of being eaten due to visual predation (Zaret and Suffern, 1976; Hays *et al.*, 1994; Hays, 2003). DVM is costly, as migration and residence at depth during the day means zooplankton cannot feed on high quality algal cells at this time, therefore counterbalancing this cost is the reduced risk of

predation in the mesopelagic from visually orienting animals compared with staying in surface waters during the day (Hays, 2003). However, DVM is complex, and is observed to be highly variable and dependent on environmental conditions, species composition and developmental stage. For example, in periods of extreme bloom events where high food concentrations penetrate deeper into the mesopelagic, DVM may be reduced, as deeper residing zooplankton do not have to risk going to surface waters to feed, and high food concentrations may offset the risk of visual predation for surface-dwelling species. The depth of the mixed layer or deep chlorophyll maxima (DCM) has been reported to influence the vertical distribution of zooplankton (Harris, 1988). Cook *et al.* (2023) found limited evidence of synchronised DVM in the upper 500 m in the Scotia Sea, with only *Metridia* spp. and *Salpa thompsoni* showing consistent DVM, and proposed this was due to abundant phytoplankton and excellent feeding conditions throughout the water column negating the need to DVM, as has previously been observed in the Southern Ocean (Cisewski *et al.*, 2010; Cisewski and Strass, 2016). Smaller mesozooplankton may offset the risk of visual predation in surface waters with the advantage of increased growth rates due to continuous food availability in surface waters. Indeed, larger copepods have been observed to have larger DVM signals than smaller ones, with the former being more conspicuous and therefore spending less time in surface waters compared to smaller copepods (Barth *et al.*, 2023). DVM by *Metridia okhotensis* has been observed to change with growth and developmental stage, with adult females staying below the permanent pycnocline in waters deeper than 300 m except for in April when DVM was relatively active, whilst copepodite stages C4 and C5 showed pronounced DVM throughout the year (Takahashi *et al.*, 2009). Through DVM, zooplankton may enhance POC flux to the mesopelagic by consuming POC at the surface and releasing it at depth as faecal pellets, excreted DOC, and DIC, e.g. carbon dioxide, from respiration (Steinberg *et al.*, 2000; Buesseler and Boyd, 2009). Respiration by vertically migrating species may be a good means to quantify carbon export by DVM, as DIC released at depth from respiration is likely centred around the maximum depth of residence, where zooplankton spend the most time during the day (Archibald *et al.*, 2019). Unlike POC released as faecal pellets, respiration releases DIC, meaning this carbon is no longer bioavailable to use by other heterotrophs. Respiratory carbon flux from migrating zooplankton has been observed to range from 2.8 % to 88.3 % of passive POC flux (Longhurst *et al.*, 1990; Dam *et al.*, 1995; Zhang and Dam, 1997; Hernández-León *et al.*, 2019b). Such large range in DVM respiratory carbon fluxes underscores the varying impact of DVM on carbon flux.

Some species of zooplankton are also observed to undergo seasonal migration, known as ontogenetic vertical migration (OVM). During OVM, zooplankton migrate to deep waters of the mesopelagic (500 – 2500 m) at the end of summer and enter a state of diapause – a period of dormancy that allows them to conserve energy during food-scarce winter months (Hirche, 1996;

Baumgartner and Tarrant, 2017). OVM is most common in herbivorous calanoid copepods of mid and high latitudes (temperate/polar regions), such as *Calanus finmarchicus* (Hirche, 1996), *C. hyperboreus* (Hirche, 1997), *C. glacialis* (Freese et al., 2016) in the North Atlantic, and *Calanoides acutus* and *Rhincalanus gigas* in the South Atlantic sector of the Southern Ocean (Atkinson, 1991). It is also observed under certain oceanographic conditions such as upwelling areas (Arashkevich *et al.*, 1996). The descent of lipid-rich calanoid copepods and metabolism of these lipids at depth, termed the 'lipid pump', represents an efficient route of active carbon transport and sequestration from epi- to mesopelagic waters (Jónasdóttir *et al.*, 2015; Visser *et al.*, 2017). Unlike the typical Redfield ratio of organic matter, which has elemental ratios of Carbon:Nitrogen:Phosphorus (C:N:P = 1.00:0.15:0.01), lipids have ratios of nutrients to carbon which are extremely low (C:N:P = 1:<0.0001:<0.0001) (Jónasdóttir *et al.*, 2015). Because lipids are rich in carbon but contain low nutrients, and lipids are actively transported to the mesopelagic zone by OVM, the lipid pump results in a decoupling between surface nutrient and deep ocean carbon cycling – a process termed the lipid shunt (Jónasdóttir *et al.*, 2015). The lipid shunt allows for enhanced carbon sequestration without depleting surface nutrients and therefore allows for continued surface productivity that is not dependent on nutrient availability for carbon export. In the Southern Ocean, seasonal migration is estimated to annually transport 65 Mt of carbon to depths beyond 500 m, 80 % of which is transported by mesozooplankton (Yang *et al.*, 2025). This equated to 38 – 56 % and 78 – 103 % of POC flux at 500 m and 1000 m respectively (Yang *et al.*, 2025).

Several studies have highlighted discrepancies between the change in sinking POC flux and metabolic requirements of resident bacteria and zooplankton in the mesopelagic zone. In the subarctic Pacific, bacterial carbon demand (BCD) and zooplankton carbon demand (ZCD) were measured to be 10-fold and 3- to 9-fold greater than the POC flux, respectively, while in the subtropical Pacific, BCD and ZCD were 3- to 4-fold and 1- to 2-fold greater than the sinking POC flux, respectively (Steinberg *et al.*, 2008). These findings suggest alternative sources of POC, such as zooplankton vertical migration and carnivory, must be important means by which resident biota meet metabolic demands (Steinberg *et al.*, 2008). Maynard (1975) estimated that around 57 % of micronekton in Hawaiian mesopelagic waters do not undergo DVM, implying reliance on local food sources, such as predation. In the North Pacific, distinct mesopelagic layers show peaks in carnivorous zooplankton, with these peaks linked to the presence of large populations of ontogenetic vertical migrators which carnivorous zooplankton may feed on (Steinberg *et al.*, 2008). Indeed, Mackas and Tsuda (1999) estimated that 33 % of *Neocalanus plumchrus* mortality in the subarctic Pacific occurs between 400 m to 1000 m due to predation by small micronekton and chaetognaths. Around 50 % of predation on migrating zooplankton occurs in the mesopelagic, suggesting mortality of migrating zooplankton plays a substantial

role in the vertical transport of carbon to the mesopelagic. The extent and occurrence of both DVM and OVM therefore have important implications for the strength and efficiency of the biological carbon pump. Altogether, the mesopelagic migrant pump is estimated to lead to an exported carbon sequestration timescale of approximately 250 years (Boyd *et al.*, 2019).

1.3 Role of mesopelagic fish in the biological carbon pump

Mesopelagic fish are considered one of the most abundant groups of marine vertebrates in the ocean. Although biomass estimates are complicated due to fish net avoidance (Kaartvedt *et al.*, 2012), estimates using acoustic backscatter and ecosystem-based modelling place estimates between 1.8 and 16 gigatons (Irigoien *et al.*, 2014; Anderson *et al.*, 2019; Proud *et al.*, 2019). Mesopelagic fish hold an important trophic position in the food web, acting as the link between lower (zooplankton) and higher trophic levels (Cherel *et al.*, 2010; Iglesias *et al.*, 2023). Many mesopelagic fish have been observed to migrate vertically and perform DVM, residing in deeper mesopelagic waters during the day and travelling to shallower epipelagic waters during the night to forage (Klevjer *et al.*, 2016; Olivar *et al.*, 2017; Eduardo *et al.*, 2020b). The representation of mesopelagic fish as carbon exporters is often over-looked, however studies suggest these animals may account for 10 % of primary production via respiration in deep waters (Irigoien *et al.*, 2014). Localised studies found mesopelagic fish to contribute 15 – 17 % of carbon flux in the top 400m in the northeast Pacific (Davison *et al.*, 2013) and myctophid fish to contribute ~8 % of gravitational carbon flux at the mid-Atlantic ridge (Hudson *et al.*, 2014). Recent studies suggest mesopelagic fish may be equally as important in active carbon flux as migrating zooplankton (Pinti *et al.*, 2023; Getzlaff and Kriest, 2024).

1.4 Knowledge gaps in resolving zooplankton-mediated carbon cycling

Despite the current understanding that zooplankton are fundamental contributors to the biological carbon pump and drivers of particle flux attenuation, they remain one the largest uncertainties in marine biogeochemical models used to describe how marine ecosystems will respond to climate change, and how this feeds back into the global climate context (Henson *et al.*, 2022; Ratnarajah *et al.*, 2023; Rohr *et al.*, 2023; Henson *et al.*, 2024). Uncertainties in zooplankton contribution to biogeochemical cycling result from lack of knowledge and quantitative data on mesopelagic zooplankton biomass and metabolic rates (Ratnarajah *et al.*, 2023; Rohr *et al.*, 2023). Until recently, research activity on the mesopelagic zone has been comparatively sparse compared to the epipelagic, with studies mainly focussed on microbial processes and carbon flux (Hidalgo and Browman, 2019). For example, of the 31.3 million

records within Ocean Biogeographic Information System (OBIS), >50 % of marine species recorded came from the epipelagic zone, but <20 % from the mesopelagic (Egorova *et al.*, 2025). A tenfold decrease in OBIS records has moreover been observed below 200 m (Webb *et al.*, 2010). These discrepancies are related to difficulties in quantifying zooplankton rate-based metabolic processes *in-situ* in the mesopelagic (Yebra *et al.*, 2017; Menden-Deuer *et al.*, 2021) as well as patchiness of biomass measurements (Buitenhuis *et al.*, 2013; Moriarty and O'Brien, 2013) and inconsistencies due to disparate sampling methodologies (Lombard *et al.*, 2019).

To resolve uncertainties regarding the role of zooplankton in carbon cycling, we need increased knowledge of how zooplankton community composition and trophic ecology changes throughout the mesopelagic - that is of who eats what and where – to map out the cycling of energy and carbon in the mesopelagic. Quantifying vertically resolved changes in zooplankton biomass, magnitude of DVM and metabolic rates (e.g., respiration and ingestion rates) throughout the mesopelagic can also help us gain a better understanding of the metabolic carbon budgets of these animals, how this change with depth and hence how these relate to observed changes in the flux attenuation of POC. Altogether, resolving the above knowledge gaps should increase our understanding of the spatial controls of zooplankton-mediated carbon cycling. Improved knowledge of zooplankton physiology, for example copepod diapausing behaviour, and the extent that these animals do or do not interact with primary production depending on the time of year and developmental stage is important to understand the temporal controls of zooplankton-mediated carbon cycling. The mesopelagic is not a homogenous layer and can therefore experience strong gradients in environmental conditions such as temperature and oxygen (e.g., oxygen minimum zone). These gradients are moreover likely to influence the distribution of zooplankton and elicit strong physiological responses and behavioural adaptations (Robinson *et al.*, 2010). For, example oxygen minimum zones (OMZ) may act as a barrier preventing extensive DVM or lead to variability of vertical distributions depending on species-specific behaviours and tolerances to hypoxic waters (Wishner *et al.*, 2013; Tutasi and Escribano, 2020; Wishner *et al.*, 2020; Färber Lorda and Färber Data, 2023).

1.5 COMICS programme

This thesis has analysed data collected as part of the Natural Environmental Research Council (NERC) COMICS programme (Controls over Ocean Mesopelagic Interior Carbon Storage). The programme aimed to gain a mechanistic understanding of the key processes controlling carbon remineralisation in the mesopelagic, to balance and close the budget of supply and consumption of organic matter at discrete layers within the mesopelagic and build new parameterisation for mesopelagic remineralisation within IPCC (Intergovernmental Panel on

Climate Change) class global biogeochemical models (Sanders *et al.*, 2016). From a zooplankton perspective, quantifying the vertical distribution and movement, trophic ecologies, and physiological properties such as metabolic requirements and ontogenetic behaviours, is key to understanding how these animals influence carbon remineralisation in the mesopelagic. COMICS focused on investigating three potential controls over remineralisation depth: temperature, oxygen concentration and ecosystem structure. This was done through two cruises in contrasting oceanic regions, with the first cruise, DY086, sampling the high productivity region downstream of South Georgia in the Scotia Sea (Southern Ocean), and the second cruise, DY090, sampling in the northern Benguela Upwelling System, an area with strong vertical gradients in dissolved oxygen concentration.

1.5.1 Scotia Sea

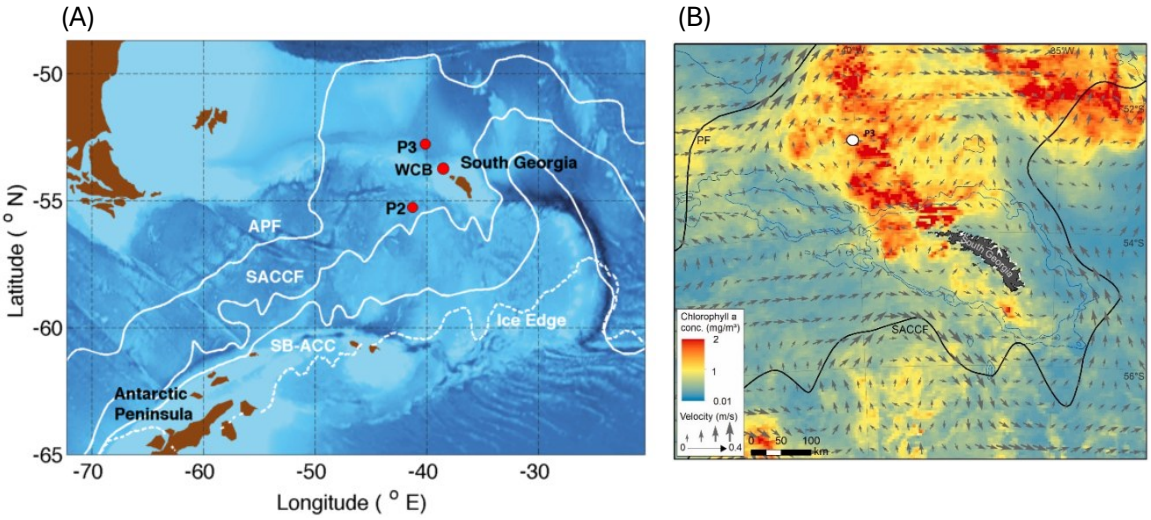

Figure 1.4 (A) Location of South Georgia in the Scotia Sea and the P3 sampling site explored during the COMICS DY086 expedition. White lines represent the different water fronts in the Scotia Sea, including the Atlantic Polar Front (APF), the Southern Antarctic Circumpolar Current Front (SACCF) and the southern boundary of the Antarctic Circumpolar Current (SB-ACC). Figure obtained from BAS (2025) (B) Map showing the chlorophyll a concentrations (MODIS Aqua) averaged for the study period of the COMICS DY086 expedition. Grey arrows indicate altimetry-derived geostrophic velocities (AVISO), also averaged for the study period, and the thick black lines show the location of the Polar Front (PF) and Southern Antarctic Circumpolar Current Front (SACCF). Blue isobaths are the 1000 m and 2000 m isobaths (GEBCO). The map was created by L. Gerrish, Mapping and Geographic Information Centre, British Antarctic Survey (BAS). Figure obtained from Manno *et al.* (2022).

The Scotia Sea, in the south Atlantic sector of the Southern Ocean (Figure 1.4A), is bounded by the Drake Passage to the west, the South Atlantic Ocean to the north and east, and the Weddell Sea to the South. Topographically, it is bounded by the Scotia Arc, a system of island chains and submarine ridges including South Georgia and the South Sandwich Islands to the north and east, and the South Orkney Islands to the south. Oceanographically, it is dominated by the eastward flow of the Antarctic Circumpolar Current (ACC), especially the Southern Antarctic Circumpolar Current Front (SACCF) and the Polar Front (PF). The Scotia Sea lies between the PF and the SACCF, with the interactions of the currents with the Scotia Sea shelf creating regions with high mixing and nutrient upwelling/availability (Kahru *et al.*, 2007). Together with iron input from the island shelf (Nielsdóttir *et al.*, 2012), this results in an area of high productivity downstream from the northwestern end of the island (Figure 1.4B), supporting large and intense phytoplankton blooms and high zooplankton biomass (Korb *et al.*, 2004; Ward *et al.*, 2012b; Cook *et al.*, 2023). This contrasts with other areas south of South Georgia and much of the Southern Ocean, which are characterised as HNLC zones (High Nutrient, Low Chlorophyll) (Korb and Whitehouse, 2004; Korb *et al.*, 2010; Park *et al.*, 2010). The productive area downstream of South Georgia has been extensively studied, with time series, such as the British Antarctic Survey's (BAS) Polar Ocean Ecosystem Time Series - Western Core Box (POETS-WCB) running since 1996. Although epipelagic and to some extent mesopelagic zooplankton have been extensively studied in this area (Ward *et al.*, 2004; Ward *et al.*, 2006; Stowasser *et al.*, 2012; Tarling *et al.*, 2012; Ward *et al.*, 2012b; Saunders *et al.*, 2018; Ward *et al.*, 2018), limited studies have done this from a vertically-resolved perspective from epi- to mesopelagic waters down to 500 m.

1.5.2 Northern Benguela Upwelling System

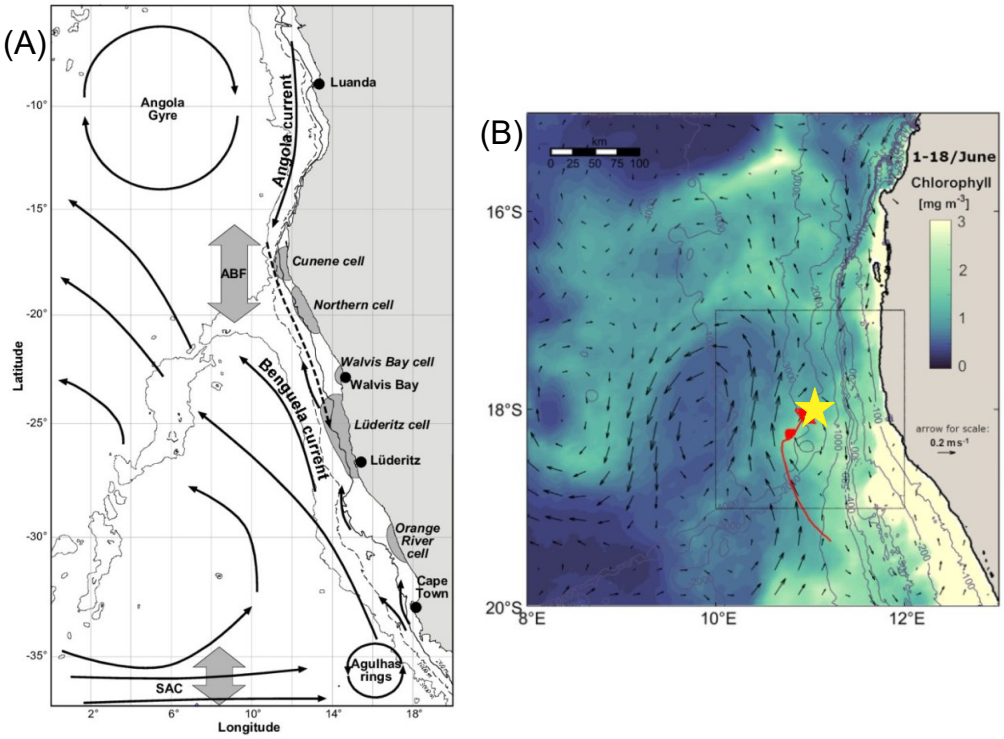

Figure 1.5 (A) Map the Benguela Upwelling System (BUS) off the eastern coast of Africa and location of the Angola-Benguela front (ABF). Figure obtained from (Ekau *et al.*, 2010) (B) Satellite chlorophyll-a concentration (CMEMS GlobColour) as colour shading and regional pattern of surface circulation (CMEMS DUACS), both averaged across the duration of COMICS DY090 expedition in the northern BUS (nBUS) in June 2018. Depth isolines are overlaid in grey and the ship sampling location is marked by the yellow star. The red line represents the pathway of a glider deployed over the duration of the expedition. Figure obtained from (Lovecchio *et al.*, 2025).

The Benguela Upwelling System (BUS), located off the southwest coast of Africa (Figure 1.5), is among the most productive marine ecosystems globally, with an estimated annual primary production of 331 – 441 g C m^2 y^{-1} (O'Reilly and Sherman, 2016). The BUS is one of the four major eastern boundary upwelling ecosystems (EBUEs) – alongside the California, Humbolt, and Canary systems – which play a disproportionately large role in global ocean productivity. Despite covering less than 1% of the ocean's surface, EBUEs contribute around 20 % of the world's marine fish catch (Chavez and Messié, 2009). The BUS spans approximately 17 °S to 34 °S and is bounded by the Benguela Current to the west, the Angola Current to the north, and the Agulhas Current to the south (Rae, 2005; Hutchings *et al.*, 2009). It is subdivided into northern (nBUS) and southern (sBUS) sectors, separated by the Luderitz upwelling cell at 26 °S (Hutchings *et al.*, 2009). The nBUS is furthermore bounded by the Angola-Benguela Front to the

north (Figure 1.5). The system is driven by the southeasterly trade wind, inducing Ekman transport and resulting in upwelling of cold, nutrient rich waters off the coast of Namibia. The nBUS is typified by coastal upwelling with cold waters, high plankton productivity, and moderate to high fish biomass (Hutchings *et al.*, 2009). The nBUS is also characterized by periodic southward advection of hypoxic, nutrient rich South Atlantic Central Water (SACW) from the Angola Gyre, with local oxygen consumption during remineralisation further exacerbating these conditions and leading to the formation of a pronounced (semi-permanent) low oxygen zone in the mesopelagic zone between 100 – 500 m (Monteiro *et al.*, 2006). The tightly coupled physical-biogeochemical interactions make the nBUS an interesting site for understanding the effects of low oxygen zones on zooplankton vertical distribution, trophic ecology and physiology, and their influence on carbon export efficiency.

1.6 Methods to investigate zooplankton ecology and their role in carbon cycling

A variety of techniques have been used to investigate the trophic ecology and physiology of marine ecosystems (Nielsen *et al.*, 2018). In the following section, I introduce the suite of complementary techniques used to investigate the knowledge gaps and research themes introduced in section 1.4. To understand what contributes to the attenuation of POC flux and how carbon is cycled through the mesopelagic, we must determine the trophic interactions between zooplankton and POC and among different zooplankton, and how physiology may influence the trophic ecology of zooplankton (section 1.6.1). A key factor in understanding the impact of zooplankton on the turnover and remineralisation of organic matter in the upper ocean is the quantification of their metabolic rates and biomass (section 1.6.2), which enables the estimation of metabolic carbon budgets. Lastly, I discuss how zooplankton size structure can be used to understand ecosystem functioning and the transfer of energy in an ecosystem (section 1.6.3).

1.6.1 Exploring the trophic ecology and physiology of zooplankton

A trophic marker is described as a compound which is transferred "metabolically untouched" to higher trophic levels and whose origin can be easily traced back to its source. Such markers provide vital information on the pathway of energy flow in an ecosystem and help qualitatively and quantitively characterise food-web structure.

1.6.1.1 Stable isotope analyses

Trophic levels (TLs) refer to the position of individuals, species or groups of organisms in a food web. Bulk nitrogen stable isotope analysis is a widely used technique to describe the trophic structure of marine ecosystems (Hobson *et al.*, 1994; Koppelmann *et al.*, 2009; Kürten *et al.*, 2013; Kim *et al.*, 2023). This technique employs bulk stable isotope ratios of nitrogen, expressed as $\delta^{15}N$ due to the heavier isotope, ^{15}N, being preferentially retained and accumulated in the tissues of organisms compared to the lighter isotope ^{14}N (Miyake and Wada, 1967). This occurs during kinetic isotope fractionation whereby the lighter ^{14}N isotope is preferentially used by enzymes during amino acid deamination and transamination, resulting in the remaining nitrogen pool being enriched in ^{15}N relative to the source (dietary) nitrogen (Macko *et al.*, 1986; Gannes *et al.*, 1998). Greater $\delta^{15}N$ ratios are therefore expected in consumers higher up the food web. Nitrogen is moreover described as having higher accuracy then methods such gut content analysis, due to tissue composition reflecting longer-term feeding habits, rather than short-term presence of prey in stomach. In marine organisms, the $\delta^{15}N$ signatures in tissues of organisms is observed to increase in a predictable way at each successive trophic level (Fry, 2006), with mean fractionation values of 3-4 ‰ per trophic level (Minagawa and Wada, 1984; Post, 2002), although 2.5 ‰ is suggested as the mean fractionation value for herbivores (Zanden and Rasmussen, 2001). Fractionation is moreover influenced by diet, with lower trophic fractionation observed when consumers eat high-protein diets similar to their own (Mill *et al.*, 2007; McMahon *et al.*, 2015). Temperature can also affect trophic fractionation, with higher temperatures resulting in lower trophic fractionations (Power *et al.*, 2003; Barnes *et al.*, 2007).

Nitrogen stable isotopes can be used to estimate trophic levels of consumers:

$$TL = \frac{\left(\delta^{15}N_{consumer} - \delta^{15}N_{primary\ producer}\right)}{\Delta_n} + 1.0 \qquad (eq\ 1.2)$$

where $\delta^{15}N_{consumer}$ is the $\delta^{15}N$ signature of the consumer of interest, $\delta^{15}N_{primary\ producer}$ is the $\delta^{15}N$ of the baseline primary producer of the system, 1.0 is the trophic level of the primary producer (Post, 2002), Δ_n is the $\delta^{15}N$ enrichment factor per trophic level. However, assumptions around what isotopic baseline to use when calculating trophic levels introduces uncertainties into calculating trophic levels based on nitrogen stable isotope analysis. In open ocean ecosystems, this relates to issues with temporal and spatial variations in the isotopic baseline signature of primary producers compared to isotopic signatures of consumers which integrate $\delta^{15}N$ over a longer time (Post, 2002). Using $\delta^{15}N$ of a baseline consumer reduces the influence of short-term seasonal changes on baseline isotopic signatures as they have lower isotopic turnover rates compared to phytoplankton (Cabana and Rasmussen, 1996). In Southern Ocean studies, *S. thompsoni* is often used as the baseline consumer (Stowasser *et al.*, 2012;

Pakhomov *et al.*, 2019). If using a primary consumer as the baseline isotopic value in the above trophic level equation (eq 1.2), then the baseline trophic level is changed to 2 instead of 1.

Bulk carbon stable isotope signatures, expressed as $\delta^{13}C$, are often used to evaluate the sources of primary production to the system, with different sources of carbon having different $\delta^{13}C$ signatures (Hobson *et al.*, 1994; Hobson, 1995). $\delta^{13}C$ signatures vary a lot less than $\delta^{15}N$ across trophic levels (0.5 – 1 ‰) (DeNiro and Epstein, 1978; Fry and Sherr, 1984) and are therefore more often used to describe different functional groups based on the source of the carbon (Rounick and Winterbourn, 1986). For example, inshore or bottom feeders have enriched $\delta^{13}C$ signatures compared to offshore/planktonic/pelagic feeders (DeNiro and Epstein, 1978; Hobson *et al.*, 1994; Quillfeldt *et al.*, 2015).

1.6.1.2 Lipid biomarker analyses

Lipid biomarkers are commonly employed to investigate the feeding ecology and physiology of zooplankton (Dalsgaard *et al.*, 2003; Wilson *et al.*, 2010; Pond *et al.*, 2012; Stevens *et al.*, 2022). Lipids are vital to organisms and are some of the most important molecules transferred from plants to animals in marine food webs (Arts *et al.*, 2001; Parrish, 2013). They play a fundamental role in the physiology of animals, notably in the structure and function of cell membranes, as precursors of hormones (eicosanoids) and in the storage of energy (Dalsgaard *et al.*, 2003). The majority of lipids are composed of fatty acids esterified to another molecule such as a fatty alcohol, glycerol, or sphingosine, with this link determining the type of lipid class the fatty acid is a part of.

1.6.1.2.1 Lipid classes

Fatty acids consist of hydrocarbon chains of various lengths, with one end finishing in a methyl group ($-CH_3$) and the opposite end finishing in a carboxyl group (-COOH) (Figure 1.6). Fatty acids can be saturated (carbon atoms linked by single covalent bonds) or unsaturated (carbon atoms linked by double bonds). Fatty acids with only one double bond are referred to as monounsaturated fatty acids (MUFAs) and those with multiple double bonds as polyunsaturated fatty acids (PUFAs). Fatty acid nomenclature is based on the number of carbon atoms and number of double bonds. The position of the first double bond is denotated by (n-x), counting from the methyl end. For example, the fatty acid eicosapentaenoic acid (EPA) is identified as 20:5(n-3), meaning it has 20 carbon atoms and 5 double bonds, with the first double bond located after the third carbon atom from the methyl end (Figure 1.6).

Wax esters consist of a fatty acid esterified to a fatty alcohol (ALC). Fatty alcohols follow the same chemical structure as fatty acids but end with a hydroxyl group (-OH) instead of a carboxyl group. Wax esters are a major lipid class in high latitude copepods (Lee *et al.*, 2006).

Triacylglycerols (TAG) are composed of three fatty acids esterified to a glycerol backbone and are the most common form of lipid storage in animals (Lee *et al.*, 2006).

Phospholipids consist of two fatty acids attached to a glycerol containing a phosphate group. This group of lipids is a vital component of biological membranes.

Sterols do not contain fatty acids, instead they consist of a fused four-ring hydrocarbon core structure, with a hydroxyl group at the 3-position of the A-ring and a branched hydrocarbon side chain attached at the 17-position on the D ring. The carbon skeleton of a sterols in known as a cyclopentanoperhydrophenanthrene skeleton.

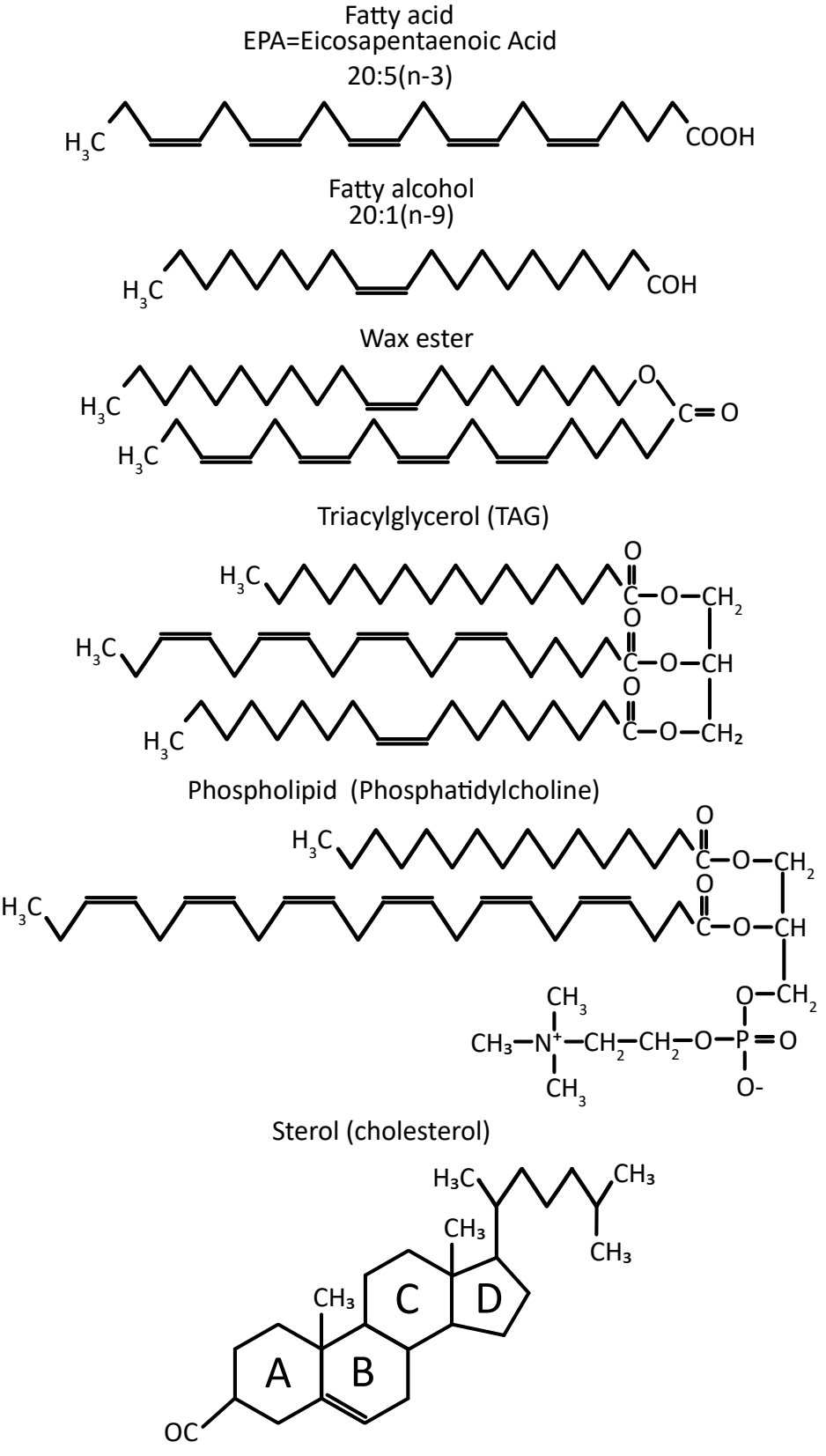

Figure 1.6 Chemical structure of key lipid groups.

1.6.1.2.2 Fatty acids and alcohol biomarkers

Fatty acids can either be acquired from the consumer's diet or internally through *de novo* biosynthesis. Certain fatty acids are biosynthesized by specific bacteria, algae and some zooplankton and, when accumulated without modification by consumers, can be useful trophic biomarkers (

Table 1.1).

Two fatty acids, EPA and docosahexaenoic acid (DHA, 22:6(n-3)), known to be a product of photosynthetic processes (although a few benthic deep-sea invertebrates may also biosynthesize them (Pond *et al.*, 2002)), are predominantly biosynthesised *de novo* by diatoms and dinoflagellates, respectively, and are considered good biomarkers for sources of herbivory (Dalsgaard *et al.*, 2003). The fatty acid 18:1(n-9) is often described as a biomarker of carnivorous zooplankton and is commonly used as a putative marker of carnivory due to it being a major fatty acid in marine organisms (Dalsgaard *et al.*, 2003). I use the term 'putative' here, because this fatty acid can be biosynthesized *de novo* in animals (Dalsgaard *et al.*, 2003), making it difficult to tell whether it derives from biosynthesis, is acquired through diet, or both (Mayor *et al.*, 2013). Many species of herbivorous calanoid copepods (e.g. *Calanoides acutus, Calanus hyperboreus, C. glacialis, C. propinquus*) biosynthesize the fatty acids 20:1(n-9) and 22:1(n-11), which are referred to as herbivorous calanoid biomarkers (Hagen *et al.*, 1993; Kattner and Hagen, 1995; Albers *et al.*, 1996; Graeve *et al.*, 2005). These long-chained MUFAs are thought to play an important role in the storage of lipids, i.e. energy, of diapausing species (Albers *et al.*, 1996). Similarly to the herbivorous calanoid fatty acid biomarkers, ALC-20:1(n-9) and ALC-22:1(n-11) are herbivorous calanoid fatty alcohol biomarkers and together with their fatty acid counterparts, form wax ester lipids (Lee *et al.*, 2006). When these fatty acids and alcohols are found in other mesozooplankton, it can be deduced that these animals have preyed upon these herbivorous calanoid copepods.

Table 1.1 Common fatty acids found in pelagic zooplankton and micronekton lipids.

Lipid class	**Biomarker**	**Biomarker source**	**References**
Fatty acid	15:0, 15:1, *iso*- and *anteiso* C15	Bacteria	(Perry *et al.*, 1979; Volkman *et al.*, 1980)
Fatty acid	16:1(n-7)	Diatoms	(Mayzaud *et al.*, 1990; Viso and Marty, 1993)
Fatty acid	17:0, 17:1, *iso*- and *anteiso* C17	Bacteria	(Perry *et al.*, 1979; Volkman *et al.*, 1980)
Fatty acid	18:1(n-9)	Zooplankton	(Sargent and Falk-Petersen, 1988; Falk-Petersen *et al.*, 1990)
Fatty acid	18:4(n-3)	Dinoflagellates	(Mayzaud *et al.*, 1990)
Fatty acid	20:1(n-9)	Herbivorous calanoid copepods	(Falk-Petersen *et al.*, 1987; Kattner and Hagen, 1995; Albers *et al.*, 1996; Scott *et al.*, 2002)
Fatty acid	20:5(n-3), EPA	Diatoms	(Mayzaud *et al.*, 1990; Viso and Marty, 1993)
Fatty acid	22:1(n-11)	Herbivorous calanoid copepods	(Falk-Petersen *et al.*, 1987; Kattner and Hagen, 1995; Albers *et al.*, 1996; Scott *et al.*, 2002)
Fatty acid	22:6(n-3), DHA	Dinoflagellates	(Mayzaud *et al.*, 1990)
Fatty alcohol	ALC-20:1(n-9), ALC-22:1(n-11)	Herbivorous calanoid copepods	(Falk-Petersen *et al.*, 1987; Kattner and Hagen, 1995; Albers *et al.*, 1996; Scott *et al.*, 2002)

1.6.1.2.3 Lipids and physiology

Although lipid biomarkers can aid in mapping out trophic interactions, mesozooplankton lipid signatures are not simply a reflection of what they eat. Instead, lipid signatures can be viewed as summation of metabolic processes that store, synthesize or catabolise various lipids to meet physiological requirements. Such a mindset of moving away from 'you are what you eat' towards 'you are what you don't respire, excrete or egest' has been discussed in the context of stable isotopes (Mayor *et al.*, 2011). Lipids can give valuable insight into key physiological

processes of zooplankton, such as energetic and physiological adaptation of diapausing species (Pond, 2012). DHA is essential for the functioning of biological cell membranes, helping to maintain membranes in a liquid-crystalline state, allowing transmembrane proteins to move and function correctly (Hulbert, 2003; Valentine and Valentine, 2004). In cold and high-pressure environments like those in the deep sea, lipids may undergo liquid to solid phase transitions, therefore DHA is especially important for migrating mesozooplankton to maintain membrane fluidity at depth (Pond *et al.*, 2012). Pond *et al.* (2014) has indeed reported that the proportion of DHA in membrane phospholipids of *Calanoides acutus* increased with depth, particularly in colder waters. Polyunsaturated fatty acids (PUFAs) are also important in buoyancy control, with the liquid-solid phase transition of PUFAs at depths greater than 500 m helping buoyant, lipid-rich copepods achieve neutral buoyancy at depth during diapause (Pond and Tarling, 2011). Due to thermal expansion and compressibility, and hence liquid-solid phase transition, solid lipids have a greater density than in a liquid state, reducing hydrostatic lift and countering the positive buoyancy of large lipid stores (Visser and Jónasdóttir, 1999; Pond, 2012). The Antarctic copepod, *C. acutus,* only initiates descent to depth when lipids have reached 50 % unsaturation (Pond and Tarling, 2011), mainly through the acquisition of EPA and long-chained moieties 20:1 and 22:1. Because EPA and DHA are essential to zooplankton physiology, but cannot be biosynthesized at biologically significant rates (Bell *et al.*, 2007), once obtained from dietary sources these fatty acids accumulate in the tissues and are conserved between trophic levels (Lee *et al.*, 1971). Therefore, although these fatty acids are originally derived from dinoflagellates and diatoms, they do not necessarily indicate herbivorous feeding as carnivorous zooplankton, which also require fatty acids such as DHA, obtain them from feeding on herbivorous species. This highlights how fatty acids are not simply trophic biomarkers but may also reflect the life-history and physiological requirements of mesozooplankton.

1.6.2 Quantifying zooplankton community carbon budgets

1.6.2.1 Electron Transport System (ETS) activity

Respiration is an important index of physiological activity and is an essential parameter in quantifying carbon fluxes in marine ecosystems. This is because respiratory rates (e.g., oxygen consumption) can be converted into carbon dioxide production via the respiratory quotient (RQ), which quantifies the volume of carbon dioxide that is released over the volume of oxygen taken up during respiration. In marine mesozooplankton, an RQ of 0.9 is often used (Ariza *et al.*, 2015), that is 0.9 mol of carbon dioxide is produced for every 1 mol of oxygen consumed. Respiration rates of mesozooplankton can therefore be used to quantify the respiratory carbon flux produced by zooplankton undertaking DVM during daytime residence at depth (Ariza *et al.*, 2015; Hernández-León *et al.*, 2019a; Hernández-León *et al.*, 2019b). Several methods have been

employed to determine respiration rates (oxygen consumption), including live incubation experiments measuring time-dependent changes in oxygen concentration (Mayzaud *et al.*, 2005; Lilley and Lombard, 2015). Although this can give us an understanding of species-specific respiration rates, these experiments are time consuming and cannot realistically cover the diversity of the ocean. Moreover, direct determination of oxygen consumption through live incubation is difficult for deeper-dwelling (e.g. mesopelagic) zooplankton due to damage and stress these animals sustain during capture and retrieval, as well as environmental conditions (e.g. pressure) in experimental setups not being representative of their natural habitat. All of this can therefore result in changes to the physiological state of the studied organisms.

An alternate approach is to measure the activity of the enzyme system involved in oxygen utilisation within an animal. This indirect method of quantifying respiration measures maximal potential oxygen consumption by looking at the rate at which the mitochondrial and microsomal respiratory electron transport system (ETS) transfers electrons from physiological substrates (NADP, NADPH and succinate) to the terminal electron acceptor (Owens and King, 1975; Gómez *et al.*, 1996). In a natural system, the terminal electron acceptor is oxygen (O_2), however in the laboratory, an artificial electron acceptor, tetrazolium salt 2-(4-iodophenyl)-3-(4-nitrophenyl)-5-phenyltetrazolium chloride (INT), is used to register the electron transmission rate, where 1 mole of oxygen consumption is equal to 2 moles of INT reduction (Gómez *et al.*, 1996). Oxygen consumption can then be converted into carbon production through simple stoichiometry, where 22.4L O_2 = 12.0 g C and the RQ=0.9. ETS measurements can be taken on samples that are immediately frozen upon collection, maintaining the integrity of *in situ* enzymatic activity and thus potential respiration rates of organisms in their natural habitat. ETS moreover has the advantage that it can be done for specific species of interests (Bode *et al.*, 2013; Hernández-León *et al.*, 2019a; Herrera *et al.*, 2019), at a community level, that is for an entire sample of zooplankton obtained from nets (Minutoli *et al.*, 2017; Protopapa *et al.*, 2019b), size-fractionated zooplankton samples (Ariza *et al.*, 2015; Herrera *et al.*, 2017; Cook *et al.*, 2023), and at depth discrete intervals (Yebra *et al.*, 2018; Hernández-León *et al.*, 2019a; Hernández-León *et al.*, 2024).

1.6.2.2 Grazing experiments

Another important factor in understanding zooplankton mediated effects on carbon export, is zooplankton grazing rate. The rate at which zooplankton consume phytoplankton mediates the transfer of organic carbon to higher trophic levels as well as organic carbon export to deeper waters (Steinberg *et al.*, 2008; Boyd *et al.*, 2019). Because zooplankton exhibit considerable functional diversity and variable spatial distributions, parameterising grazing rates is incredibly difficult and remains the largest source of uncertainty in carbon cycling in marine

biogeochemical models (Rohr *et al.*, 2023). Laboratory and field-based incubation experiments can help provide estimates of species-specific grazing rates of mesozooplankton, although these can be highly localised in space and time. Mesozooplankton grazing rates can be measured using particle-removal experiments (Båmstedt *et al.*, 2000). These experiments involve incubating a pre-determined number of mesozooplankton (e.g. 3 *Calanus*) in 1 L bottles with seawater alongside control bottles with no zooplankton. Bottles are incubated for 24 hours on a plankton wheel at the *in-situ* temperature. After this, the microplanktonic community before incubation (initial community) is compared to the final community composition and abundance at the end of the incubation in both the animal and control bottles (details in Chapter 3.3.8.1). Clearance and ingestion rates can then be calculated using the equations of Frost (1972), using the initial and final microplankton counts, phytoplankton growth constants, and filtration rates of the grazer.

1.6.2.3 Body size and biomass estimates from imaging technologies

Quantifying the biomass of zooplankton in the ocean is integral to understanding the cycling of carbon as zooplankton biomass is a product of primary production. Moreover, understanding where this biomass is located throughout the mesopelagic can help better our understanding of where zooplankton are and are not interacting with POC and thus help elucidate the processes responsible for carbon cycling.

The FlowCam Macro (Figure 1.7), manufactured by Yokogawa Fluid Imaging Technologies, is an automated bench-top particle size and shape analyser for particles/zooplankton between 150 µm and 5 mm. It uses flow imaging microscopy to digitally image, count and produce morphological data outputs (e.g. length, area-based diameter, area area-based diameter, etc.) from the imaged particles. Preserved zooplankton samples, transferred into seawater (rinsed of formaldehyde), are pumped through the FlowCam Macro via a high-capacity industrial peristaltic pump and pass through a 2 mm or 5 mm flow cell placed in front a microscope lens coupled with a high resolution (1920 x 1200 pixel) monochrome digital camera.

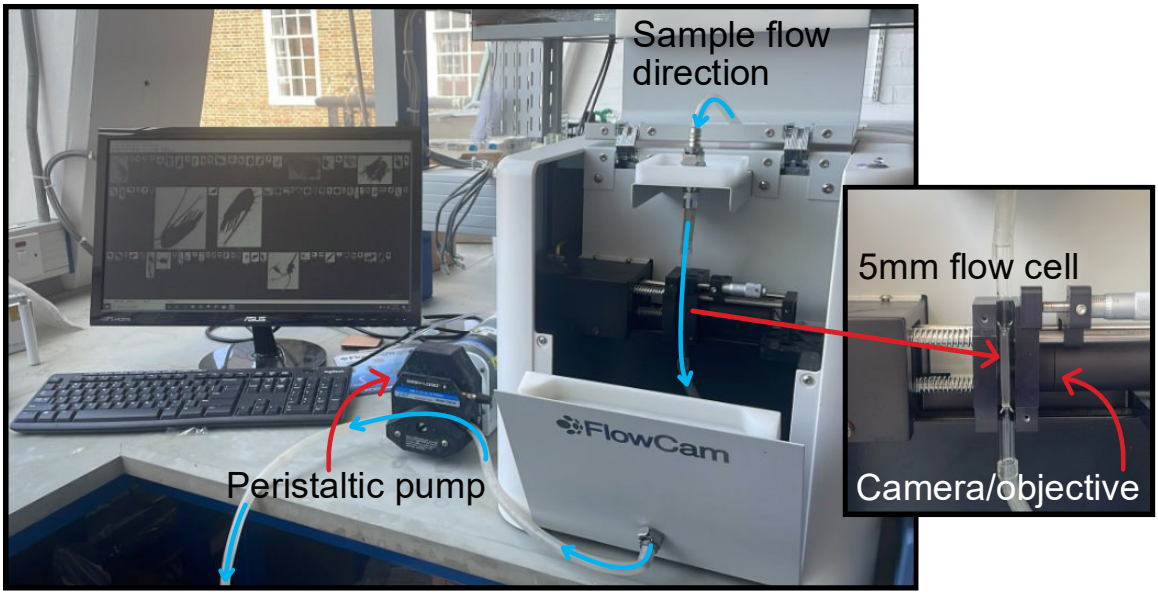

Figure 1.7. FlowCam Macro set-up.

The FlowCam VisualSpreadsheet software allows for semi-autonomous sorting and classification of collected images using image libraries built by the user and statistical pattern-recognition algorithms, however, it still relies heavily on manual validation and classification by the user. The FlowCam Macro has the advantage over traditional microscopy of rapidly providing a digital record of physical samples and collecting a myriad of associated morphological data alongside the images used for taxonomical classification (Figure 1.8). Image data can then be used alongside count and size data to describe the zooplankton size structure of the community. The FlowCam Macro can also be used to calculate zooplankton biomass via conversion of image-based area data of zooplankton into dry weight (DW) using published regressions (Lehette and Hernández-León (2009); specific details of procedure in Chapter 4.3.5).

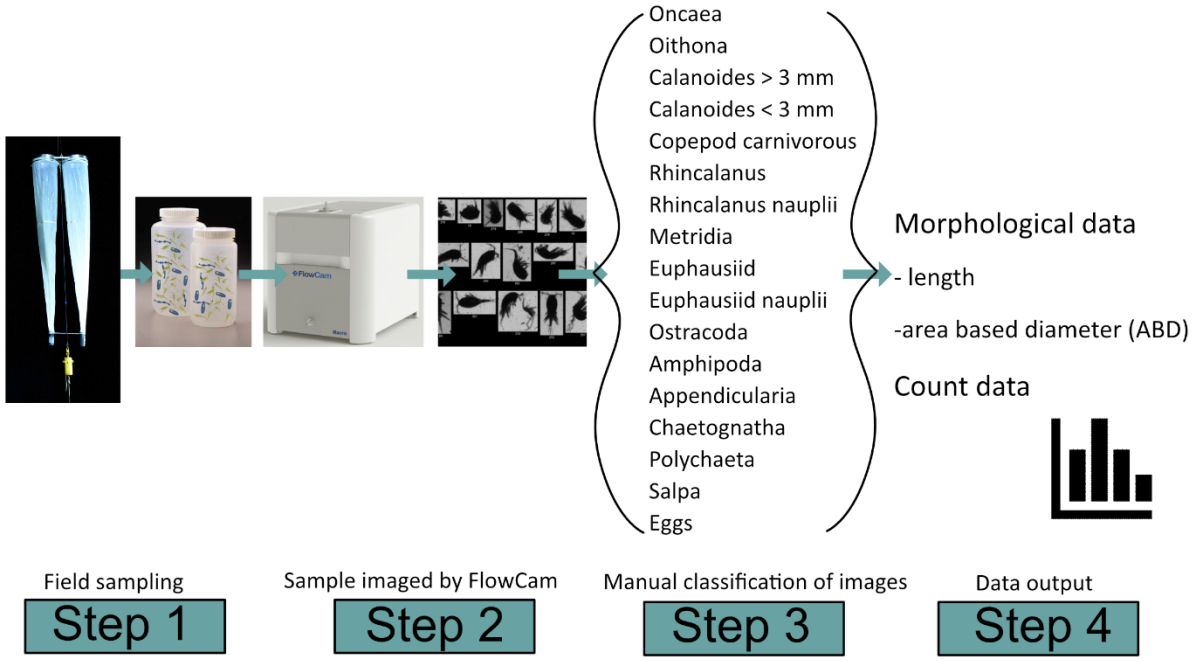

Figure 1.8 Workflow summary for processing zooplankton sample through the FlowCam Macro.

1.6.3 Understanding ecosystem functioning using zooplankton community size structure

In marine ecosystems, body size is considered a "master" trait influencing an organism's physiology (Kleiber, 1932), for instance, small organisms have a larger respiratory contribution per unit body mass compared to large organisms (Ikeda, 1966; Herrera *et al.*, 2014). Size also influences community structure and predator-prey trophic interactions, as most zooplankton are constrained by gape-size, meaning bigger animals will eat smaller ones (Cohen *et al.*, 1993; Hansen *et al.*, 1994; Barnes *et al.*, 2010; Andersen *et al.*, 2016). There are some exceptions to this rule, with some gelatinous zooplankton such as jellyfish able to feed upon both small and large prey. Despite this caveat, size may be a better determinant of understanding trophic interactions than species identity, as food preference is observed to change with parameters such as life-stage of zooplankton or resource availability (Jonsson and Tiselius, 1990; Vega, 1999; Holm *et al.*, 2019). Organisms at specific developmental stages may have more in common with other species of the same size compared to conspecifics at a different developmental stage (Andersen *et al.*, 2016). Size can moreover reflect key functional groups e.g., small particle feeders/detritovores (Turner, 2004; Svensen *et al.*, 2011), medium sized herbivores (Ariffian *et al.*, 2025), large carnivores (Pakhomov and Perissinotto, 1996; Froneman *et al.*, 1998; Olsen *et al.*, 2000). The one measure of size may therefore provide a comprehensive representation of ecosystem functioning, something potentially very useful to modelers when it comes to parameterising zooplankton in biogeochemical models in a 'simplistic' way. Indeed,

Andersen *et al.* (2016) suggest size to be one of the most important traits characterising pelagic organisms, and one by which many ecological/physiological traits (e.g. trophic interactions, metabolic rates) are controlled.

1.6.3.1 Normalised biovolume size spectra

Size spectra describe the size distribution of organisms in ecosystems. The theory predicts an inverse relationship between the size and total abundance of organisms on a log-log scale (Sheldon *et al.*, 1972; Platt and Denman, 1977; Sprules and Barth, 2016). High abundances of small organisms are observed at the bottom of the food web with a progressively decreasing abundance of larger organisms up the food web (Figure 1.9A), equating to an equal biomass of organisms in each size bin scale (Sheldon *et al.*, 1972; Platt and Denman, 1977). In marine ecosystems, this remarkable trend is observed from microscopic/planktonic organisms, all the way up to whales (Sheldon *et al.*, 1972; Hatton *et al.*, 2021).

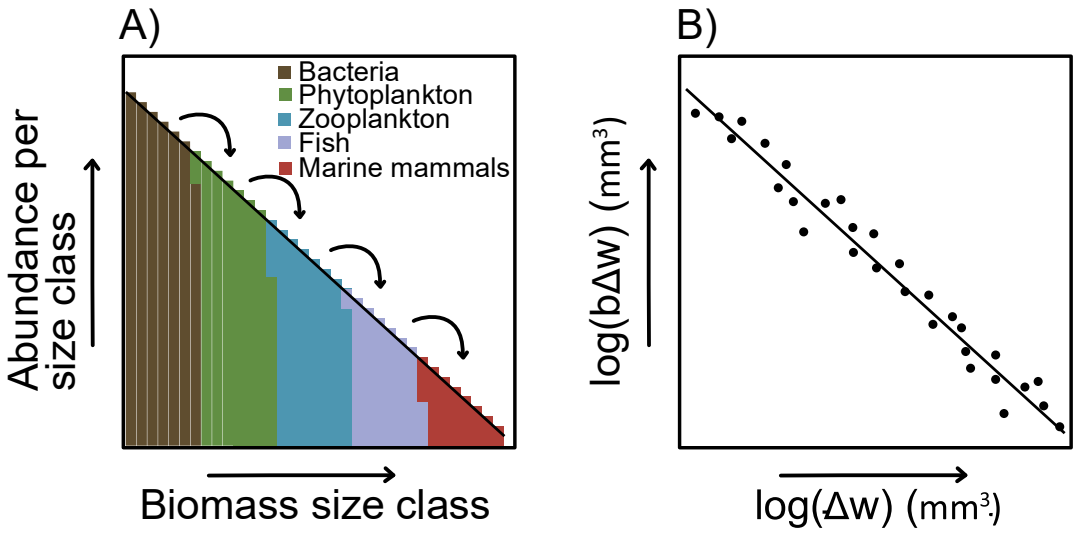

Figure 1.9 (A) Global ocean size spectrum "From bacteria to whales" (Heneghan *et al.*, 2019) on a log-log scale. The spectrum is based on Sheldon's theoretical -1 slope illustrating the inverse relationship between abundance and biomass. Each bin shows the total abundance of individuals per body mass size class. (B) Normalised biovolume size spectrum plot, where ($b\Delta w$ in mm^3) is the normalised biovolume in each size bin (Δw in mm^3)

Normalised biovolume size spectrum (NBSS; Figure 1.9B), using abundance and biovolume (as the unit of size), is commonly used to represent the size structure of zooplankton communities (Dai *et al.*, 2016; Dai *et al.*, 2017; De Figueiredo *et al.*, 2025). Parameters of the NBSS, such as the elevation of the intercept and the slope, can provide powerful means by which to explore the productivity and efficiency of an ecosystem or community. The gradient of the slope and the elevation of the intercept on the y-axis represent the overall productivity of the system, with a

higher intercept indicative of high system productivity, whereas a low intercept suggests less overall productivity of a system. The slope of the NBSS can be used as an index of trophic transfer efficiency (TTE) of a community, with a steeper slope indicative of low TTE, i.e. energy is lost to the system so supports fewer organisms higher up the food web. By contrast, a shallower slope is indicative of a high TTE, i.e. biomass stays high throughout the food web, often representing more internal recycling of energy and matter (Zhou, 2006). Size-spectrum theory furthermore predicts a slope of -1 in a stable planktonic marine environment, due to only 10% of energy/biomass being transferred between trophic levels, from small to large organism (Sheldon *et al.*, 1972; Brown *et al.*, 2004). However, empirical data suggest that the shape and slope may vary with environmental conditions or community structure (Heneghan *et al.*, 2019; Atkinson *et al.*, 2021; Atkinson *et al.*, 2024).

1.6.3.2 What drives changes in size spectrum shape?

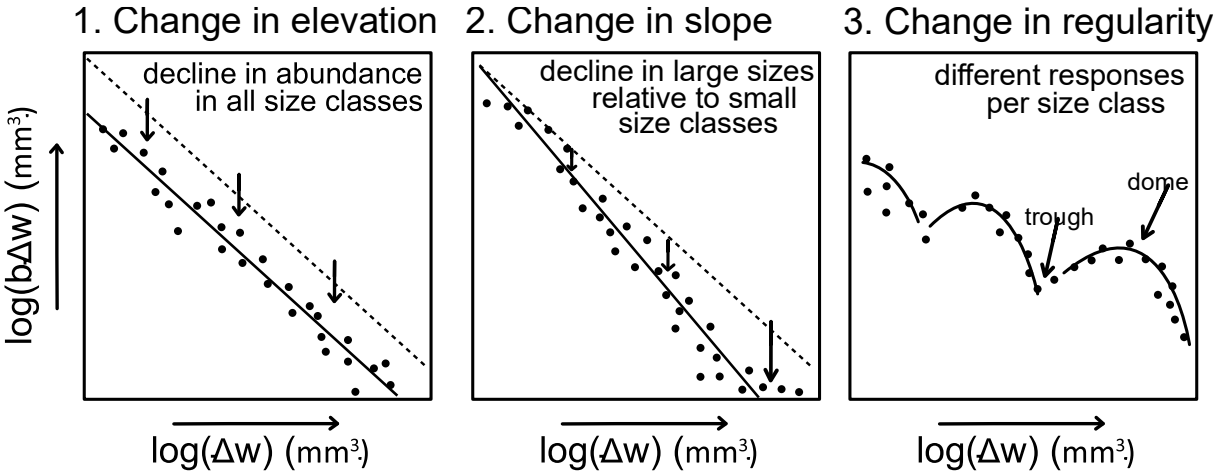

Figure 1.10 Different responses of a normalised biovolume size spectrum to perturbations. The dashed line represents the hypothetical NBSS under stable conditions, where the slope is approximately -1 on a log-log scale. (1) Changes in the elevation of the slope affecting all size classes equally (2) Changes in the slope due to changes in the trophic transfer efficiency between size classes (3) Changes in the regularity of the slope due to differences in responses to change between size classes.

Changes to the overall productivity of a marine ecosystem, such as increases or decreases in net primary production are likely to result in proportional changes in elevation throughout the NBSS (Figure 1.10) as this would influence the baseline energy available to support the overall biomass in a community/ecosystem. Similarly, if the system shows universal temperature-dependent responses of metabolism, then this would also be reflected in proportional changes to the elevation of the NBSS (warmer temperature = faster metabolism and energy consumption = overall decrease in the amount of biomass that can be supported) (Brown *et al.*, 2004; Yvon-Durocher and Allen, 2012; Yvon-Durocher *et al.*, 2012; Schramski *et al.*, 2015). In contrast,

changes to the slope of the NBSS are expected from factors that affect the interactions across size classes. For example, a decrease in the trophic transfer efficiency would result in less biomass in the larger size classes compared to the smaller ones. This effect, termed trophic amplification has been observed in response to warmer sea temperatures (Chust *et al.*, 2014; Ullah *et al.*, 2018; Kwiatkowski *et al.*, 2019). At an ecosystem level, e.g., entire pelagic community, changes in the regularity of the slope, often termed as domes and troughs in the slope, can be representative of top-down control, with a trough being positioned to the left of a dome, i.e. a peak in biomass of the larger size class (Rossberg *et al.*, 2019). On a smaller, scale, such as within zooplankton communities, domes are expected to result from factors that affect specific size classes or taxonomic or functional groups. For example, in zooplankton NBSS of high-latitude environments, high abundances of lipid-storing copepods result in accumulation of biomass in larger size classes compared to smaller size classes and hence a dome to form (Tarling *et al.*, 2012). Understanding the causes of domes and troughs, their links to community function (such as feeding strategies or physiological life-history traits), and how the size structure of zooplankton communities change with depth can provide key insights into how carbon is acquired and transferred within these communities, and thus how zooplankton-mediated carbon cycling varies with depth.

1.7 Objectives of the thesis

This thesis aims to better understand vertically resolved changes in zooplankton ecology and physiology, and how this influences the fate of carbon in the upper ocean using a combination of approaches, including lipid biomarkers, stable isotopes, grazing experiments, respiration measurements, and size-spectrum analysis.

This thesis addresses the following key research questions:

- How the physiological ecology of lipid storing copepods could influence carbon budgets at different stages of their ontogeny (Chapter 2).

- How diel vertical migration (DVM), ontogenetic vertical migration (OVM) and oxygen minimum zones (OMZs) are thought to influence the distribution of animals throughout the mesopelagic, and the associated consequences for carbon budgets (Chapter 3).

- How the relationships between zooplankton size and their trophic/functional ecology, and the necessary changes in trophic strategy with increasing depth, causes changes to the size structure of mesopelagic zooplankton and associated consequences on carbon cycling (Chapter 4).

Chapter 2 uses lipid biomarker and nitrogen stable isotope data to resolve the food web dynamics and physiological ecology of mesozooplankton in epi- and mesopelagic waters in the Scotia Sea (Southern Ocean) during an intense spring diatom bloom. This work specifically explored how the lipid-storing copepods interact with ambient particulate organic carbon (POC) during the diapausing stage of their ontogeny. This chapter found a decoupling between zooplankton feeding dynamics and ambient POC in the upper 500 m and highlights the need to account for ontogenetic changes in lipid-storing copepod physiology when quantifying zooplankton-mediated biogeochemical cycling. This chapter has been published in Deep Sea Research Part I (Savineau *et al.*, 2024). Outputs from this chapter have also been used in a companion paper, focussing on POC (Preece et al., in prep), to which I contributed as a co-author.

Chapter 3 examines the trophic ecology, physiology, metabolic carbon budget and respiratory active carbon flux of mesopelagic zooplankton and micronekton in the northern Benguela Upwelling System using lipid biomarkers, stable isotopes, biomass data, grazing experiments and respiration measurements via ETS activity. Notably, our study found high biomass of mesozooplankton within the lower boundary of the OMZ, highlighting the importance of the OMZ as an ecological refuge for many temporary and permanent mesozooplankton residents. In contrast, micronekton showed extensive DVM throughout the water column, irrespective of the OMZ, but peak biomass distributions either above or below the OMZ. This chapter highlights how hypoxia tolerance, DVM behaviour and residence (or not) of animals in the OMZ is likely to have a significant influence on the flux of carbon throughout the mesopelagic in marine ecosystems with OMZs.

Chapter 4 examines vertically resolved mesozooplankton size spectra throughout the upper 500 m of the water column in the Scotia Sea (Southern Ocean) using flow imaging microscopic analysis (FlowCam Macro) of zooplankton net samples. This study highlights the influence of physiology, particularly copepod OVM and diapause, on the size structure and inferred energy flow in high latitude mesozooplankton communities. This chapter provides a new perspective on how size and taxonomy can be used to infer depth associated changes in zooplankton trophic ecology and demonstrates that high-throughput and semi-autonomous techniques can provide a cost-effective alternative to time- and labour-intensive microscopy.

Chapter 5 discusses the findings of chapters 2 – 4 in the context of how they increase our understanding of zooplankton ecology in the mesopelagic and the implications with regards to zooplankton-mediated carbon cycling. I moreover identify further knowledge gaps and discuss future research priorities.

Chapter 2 Investigating the physiological ecology of mesopelagic zooplankton in the Scotia Sea (Southern Ocean) using lipid and stable isotope signatures

Eloïse L-R. Savineau[1,2], Kathryn B. Cook[2,3], Sabena J. Blackbird[4], Gabriele Stowasser[5], Konstadinos Kiriakoulakis[6], Calum Preece[4], Sophie Fielding[5], Anna C. Belcher[5], George A. Wolff[4], Geraint A. Tarling[5], Daniel J. Mayor[2,3]

[1] School of Ocean and Earth Science, University of Southampton, Southampton, SO14 3ZH, UK

[2] National Oceanography Centre, Southampton, SO14 3ZH, UK

[3] Present address: Biosciences, Hatherly Building, University of Exeter, Exeter, EX4 4PS, UK

[4] School of Environmental Sciences, University of Liverpool, Liverpool, L69 3GP, UK

[5] British Antarctic Survey, Cambridge, CB3 0ET, UK

[6] School of Biological and Environmental Sciences, Liverpool John Moores University, Liverpool, L3 3AF, UK

Savineau, E.L.R., Cook, K.B., Blackbird, S.J., Stowasser, G., Kiriakoulakis, K., Preece, C., Fielding, S., Belcher, A.C., Wolff, G.A., Tarling, G.A. and Mayor, D.J., 2024. Investigating the physiological ecology of mesopelagic zooplankton in the Scotia sea (Southern ocean) using lipid and stable isotope signatures. *Deep Sea Research Part I: Oceanographic Research Papers*, *208*, p.104317. doi: https://doi.org/10.1016/j.dsr.2024.104317

ES analysed the data and wrote the manuscript with support from KC and DM. KC, GS, KK, GT, SF, AB and DM conducted on board sample collection and processing. CP and SB conducted laboratory lipid analyses of POM and zooplankton, respectively. GW helped with the lipid data. GS conducted laboratory analyses and provided the stable isotope data. All authors contributed feedback on the manuscript.

Keywords: Copepods; Amphipods; Euphausiids; Salps; Chaetognatha; Trophic Interactions; Fatty Acids; South Georgia; Twilight Zone

2.1 Abstract

The mesopelagic zooplankton community plays an important role in the cycling and sequestration of carbon via the biological pump. However, little is known about the physiology and ecology of key taxa found within this region, hindering our understanding of their influence on the pathways of energy and organic matter cycling. We sampled the eight most abundant zooplankton (*Calanoides acutus, Rhincalanus gigas, Paraeuchaeta* spp.*,* Chaetognatha*, Euphausia triacantha, Thysanoessa* spp.*, Themisto gaudichaudii* and *Salpa thompsoni*) from within the mesopelagic zone in the Scotia Sea during a sinking diatom bloom and investigated their physiological ecology using lipid biomarkers and stable isotopic signatures of nitrogen. Data suggest that the large calanoid copepods, *C. acutus* and *R. gigas*, were in, or emerging from, a period of metabolic inactivity during the study period (November 15th – December 15th 2017). Abundant, but decreasing lipid reserves in the predominantly herbivorous calanoid copepods, suggest these animals may have been metabolising previously stored lipids at the time of sampling, rather than deriving energy solely from the diatom bloom. This highlights the importance of understanding the timing of diapause of overwintering species as their feeding is likely to have an impact on the turnover of particulate organic matter (POM) in the upper mesopelagic. The $\delta^{15}N$ signatures of POM became enriched with increasing depth, whereas all species of zooplankton except *T. gaudichaudii* did not. This suggests that animals were feeding on fresher, surface-derived POM, rather than reworked particles at depth, likely influencing the quantity and quality of organic matter leaving the upper mesopelagic. Our study highlights the complexity of mesopelagic food webs and suggests that the application of broad trophic functional types may lead to an incorrect understanding of ecosystem dynamics.

2.2 Introduction

The biological carbon pump (BCP) refers to the myriad processes that export photosynthetically-fixed particulate organic matter (POM) from the ocean's surface into deeper waters (Boyd *et al.*, 2019) where it may subsequently be stored for tens or hundreds of years, depending on the depth of remineralisation (Kwon *et al.*, 2009). Zooplankton are known to influence the strength of the BCP through numerous processes, including grazing on phytoplankton, repackaging POM into faecal pellets, active transport of carbon by diel and ontogenetic vertical migration, and fragmentation of sinking particles (Turner, 2015; Steinberg and Landry, 2017; Mayor *et al.*, 2020; Anderson *et al.*, 2022).

Zooplankton in the mesopelagic zone, between ~100 – 1000 m, act as a trophic filter between surface productivity and the deep ocean (Giering *et al.*, 2014; Mayor *et al.*, 2014; Mayor *et al.*, 2020). However, relatively little is known about the physiology and trophic interactions of these

animals, hindering our understanding of the pathways of energy and organic matter processing in this environment. Zooplankton obtain their food in several ways, including feeding on phytoplankton, consuming detritus/sinking particles, or carnivory. Moreover, trophic interactions are rarely "black and white", with zooplankton showing feeding plasticity due to both spatial and temporal variability in food availability (Søreide *et al.*, 2008; Moura *et al.*, 2016).

Stable isotope ratios of nitrogen ($\delta^{15}N$) are commonly used to estimate trophic position as the heavier isotope, ^{15}N, is retained and accumulated in the tissues of organisms preferentially over the lighter isotope, ^{14}N, with increasing trophic level (Miyake and Wada, 1967). Stable isotope analysis allows for the calculation of trophic levels within a food web but does not provide information on the specificity of a consumer's diet and is therefore often conducted in parallel with other complementary techniques, such as lipid biomarkers (Protopapa *et al.*, 2019a). Lipid biomarkers have widely been used as a tool to investigate the feeding ecology and physiology of zooplankton (Dalsgaard *et al.*, 2003; Wilson *et al.*, 2010; Pond *et al.*, 2012; Stevens *et al.*, 2022). Fatty acids can be obtained either through the consumer's diet or *de novo* biosynthesis. Bacteria, algae and some zooplankton biosynthesize specific fatty acids, which can then be transferred through the food web and accumulated in lipids of consumers, sometimes without modification, making them useful trophic biomarkers. Many species of calanoid copepods biosynthesize the fatty acids 20:1(n-9) and 22:1(n-11), which are referred to as calanoid biomarkers (Hagen *et al.*, 1993; Kattner and Hagen, 1995). These fatty acids, and their fatty alcohol counterparts, are prominent moieties in the wax esters that many calanoid copepods use to store energy (Hagen *et al.*, 1993; Lee *et al.*, 2006). Two polyunsaturated fatty acids (PUFAs), 20:5(n-3) and 22:6(n-3) (commonly known as EPA and DHA, respectively), are predominantly biosynthesised *de novo* by diatoms and dinoflagellates, respectively, and are considered valuable biomarkers for sources of herbivory as they cannot be biosynthesized by zooplankton at biologically significant rates (Dalsgaard *et al.*, 2003). Lipids can give insight into key physiological processes of zooplankton, such as energetic and physiological adaptation of diapausing species (Visser and Jónasdóttir, 1999; Pond, 2012). Vertically migrating zooplankton increase the proportion of 22:6(n-3) in their phospholipids in response to increasing pressure and decreasing temperature throughout the epi- to mesopelagic (Pond *et al.*, 2014). Fatty acid signatures are therefore not simply biomarkers of diet, but rather a reflection of metabolic processes that store, synthesize, and catabolise lipids to meet physiological requirements (Mayor *et al.*, 2011; Mayor *et al.*, 2013).

The Scotia Sea is considered to be one of the most productive areas of the Southwest Atlantic/Southern Ocean, with large phytoplankton blooms dominated by diatoms (Korb *et al.*, 2012) and high zooplankton biomass (Atkinson *et al.*, 2004; Ward *et al.*, 2012b). Here, we explore the trophic- and physiological ecology of zooplankton from within the mesopelagic

region of the Scotia Sea using $\delta^{15}N$ and lipid signatures in the eight most abundant and biomass-dominant taxa. We integrate these data and use them to examine how different diet- and life-history-related physiologies influence the observed patterns in biomarkers in the different animals sampled. We moreover compare zooplankton lipid and stable isotope signatures to those of POM (see also Preece *et al.* (in prep)), to determine the fate of POM within the food web during a spring bloom and hence how zooplankton influence the cycling of POM within the epi- and upper mesopelagic.

2.3 Methods

2.3.1 Sample collection

This study is part of the COMICS (Controls over Ocean Mesopelagic Interior Carbon Storage) programme, which aims to shed light on the processes controlling carbon remineralisation in the mesopelagic (Sanders *et al.*, 2016). Samples were collected aboard the *RRS Discovery* during the research cruise DY086 to the Scotia Sea in the Southern Ocean (12 November – 19 December 2017) in the vicinity of the British Antarctic Survey Scotia Sea open-ocean observatory site P3 (SCOOBIES, 52.40 S, 40.06 W)(Giering *et al.*, 2019a). The same station was visited 3 times, defined as P3A (15 – 22nd November), P3B (29th November – 5th December) and P3C (9 – 15th December).

Samples for stable isotope analyses of POM were collected in Niskin bottles via a CTD rosette deployed at depths approximately corresponding to the sampled net horizon depths (5, 25, 50, 75, 125, 200, 450 m). Samples were filtered onto pre-combusted (450 °C; 12 hours) 47 mm GF/F filters (Whatman glass fibre filter, nominal pore size 0.7 µm) and stored frozen at -80 °C prior to analysis. Samples for lipid analyses of POM were obtained using standalone pumps (SAPs) deployed within the mixed layer (ML; 0 – 90 m), the upper mesopelagic, 150-170 m (i.e. ca. ML + 100 m), 250-260 m (ca. ML + 200 m), and 440-460 m. Two size fractions were sampled. Large particles (>53 µm) were collected on nylon mesh screens (Nitex; pore size 53 µm; 10 % HCl acid cleaned). Small particles (0.7 – 53 µm, <53 µm hereafter) were collected on pre-combusted (400 °C; 4 hours) 293 mm GF/F filters (nominal pore size 0.7 µm) located under the nylon mesh (Full SAPs filtration protocol can be found in Preece *et al.* (in prep)). All visible zooplankton/organisms were removed from the filters.

A range of nets were used to capture the vertical distribution of the epipelagic and upper mesopelagic (0 – 500 m) mesozooplankton, macrozooplankton and micronekton > 0.3 mm. Animals were collected with a combination of RMT 25 (Rectangular Midwater Trawl, 25 m^2 net mouth, 4 mm cod-end mesh), MOCNESS (Multiple Opening and Closing Net and Environmental

Sampling System, 1 m^2 rectangular opening, 330 µm (0.33 mm) mesh nets) and Mammoth Net (300 µm mesh, 1 m^2 opening) (see Appendix A Table A 1 and Table A 2). The nets were deployed over a range of discrete depth intervals from 500 m to the surface, deployed either obliquely (RMT25 and MOCNESS), or vertically (MAMMOTH). Full net deployment protocols can be found in Cook *et al.* (2023). Once onboard, the net cod ends were immediately transferred into a temperature-controlled laboratory (2 ˚C) and specimens of the eight most abundant zooplankton taxa were subsequently picked: *Calanoides acutus*, *Rhincalanus gigas* and *Paraeuchaeta* spp. (Calanoida); Chaetognatha; *Euphausia triacantha* and *Thysanoessa* spp. (Euphausiacea); *Themisto gaudichaudii* (Amphipoda); and *Salpa thompsoni* (Salpida). Chaetognaths were not identified to species level. Insufficient *T. gaudichaudii* were collected at depths beyond 250 m for analysis. Samples for stable isotope and lipid analyses were stored in petri dishes and glass vials, respectively and frozen at -80°C.

2.3.2 Stable isotope analysis

Invertebrate specimens were weighed (wet weight), freeze-dried whole and then re-weighed (dry weight). Samples were homogenised using an oscillating mill (MM200, Retsch). Isotopic analyses were carried out at the Scottish Universities Research Centre (SUERC), East Kilbride, Glasgow, UK. Aliquots for nitrogen isotopes were weighed into tin capsules (0.6 – 1mg) and measured on a Thermo-Fisher-Scientific (Bremen, Germany) Delta XP Plus Isotope-Ratio Mass Spectrometer linked to an Elementar (Hanau, Germany) Pyrocube Elemental Analyser. The internal reference materials were GEL (gelatin solution, $\delta^{15}N$= 5.71 ± 0.15‰), ALAGEL (alanine-gelatine solution, $\delta^{15}N$ = 2.52 ± 0.08‰), and GLYGEL (glycine-gelatine solution spiked with ^{15}N-alanine, $\delta^{15}N$ = 23.60 ± 0.12‰), each dried for two hours at 70 °C. The glutamic acid standard USGS40 was run four times as independent checks of precision and accuracy. Delta values were corrected for instrument drift and linearity. Delta (δ) values are used to express the relative difference between the ratios of two stable isotopes, ^{15}N and ^{14}N in organisms, expressed as $\delta^{15}N$, compared to the international reference standard for nitrogen isotopes ($\delta^{15}N$ of atmospheric nitrogen gas).

Trophic level (TL) was calculated from $\delta^{15}N$ following equation 2.1:

$$TL = \frac{\left(\delta^{15}N_{consumer} - \delta^{15}N_{primary\ consumer}\right)}{\Delta_n} + 2.0 \qquad (eq\ 2.1)$$

where $\delta^{15}N_{consumer}$ is the $\delta^{15}N$ signature of the consumer of interest, $\delta^{15}N_{primary\ consumer}$ is the $\delta^{15}N$ of a primary consumer, here assumed to be the herbivorous copepod *C. acutus,* 2.0 is the trophic level of the primary consumer (Post, 2002), Δ_n is the $\delta^{15}N$ enrichment factor per trophic level (2.5 ‰ for herbivores; Zanden and Rasmussen (2001)). Using $\delta^{15}N$ of a primary

consumer allows for reduced susceptibility of short-term phytoplankton seasonal changes influencing baseline isotopic signatures (Cabana and Rasmussen, 1996). The use of a herbivorous calanoid copepod as the baseline consumer has been suggested as a more appropriate method in high-chlorophyll α conditions dominated by diatoms, which often pass through other primary consumers, such as salps, undigested (von Harbou *et al.*, 2011; Metfies *et al.*, 2014; Pakhomov *et al.*, 2019).

2.3.3 Lipid analysis

Zooplankton lipid extractions were carried out on each homogenised freeze-dried (-60°C; 10^{-2} mBar) sample (1 – 60mg dry weight) (Cook *et al.*, 2023). A known quantity of an internal standard (3 - 10 µgL of 5α(H)-cholestane) was added to each sample, followed by a mixture of dichloromethane (DCM) and methanol (9:1; 15 mL). The samples were then sonicated (15 min, x2) and the resulting extract was decanted into round bottom flasks. The solvent obtained was evaporated to dryness under vacuum using a rotary evaporator at ~30°C. Each sample was then passed through a Pasteur pipette filled with anhydrous sodium sulphate using DCM (3 mL). The solvent was blown down with nitrogen gas and the samples were stored (-20°C) before transmethylation and derivatisation with N,O-bis-(trimethylsilyl)trifluoroacetamide (BSTFA). Lipids from the POM samples were extracted in a similar way (see also Kiriakoulakis *et al.* (2004)).

Gas chromatography-mass spectrometry (GC-MS) analyses of the total lipid extracts were conducted using a GC Trace 1300 fitted with a split-splitless injector and column DB-5MS (60m x 0.25mm (i.d.), with film thickness 0.1 µm, non-polar stationary phase of 5 % phenyl and 95 % methyl silicone), using helium as a carrier gas (2 mL min^{-1}). The GC oven was programmed after 1 minute from 60°C to 170°C at 6°C min^{-1}, then from 170°C to 315°C at 2.5 °C min^{-1} and held at 315 °C for 15 min. The eluent from the GC was transferred directly via a transfer line (320°C) to the electron impact source of a Thermoquest ISQMS single quadrupole mass spectrometer. Typical operating conditions were: ionisation potential 70 eV; source temperature 215°C; trap current 300 µA. Mass data were collected at a resolution of 600, cycling every second from 50–600 Daltons and were processed using Xcalibur software.

Compounds were identified either by comparison of their mass spectra and relative retention indices with those available in the literature, and/or by comparison with authentic standards. Shorthand notations of fatty acids and alcohols follows the IUPAC (International Union of Pure and Applied Chemistry, hhtp://www.iupac.org) systematic nomenclature ‘n-x’ notation. Quantitative data were calculated by comparison of peak areas of the internal standard with those of the compounds of interest, using the total ion current (TIC) chromatogram. The relative

response factors of the analytes were determined individually for 36 representative fatty acids and sterols using authentic standards. Response factors for analytes where standards were unavailable were assumed to be identical to those of available compounds of the same class.

Total lipid concentrations were expressed relative to zooplankton dry weight and nitrogen biomass (mg g N^{-1}). Nitrogen biomass was chosen over carbon biomass as amino acids/proteins are more representative of metabolically-active tissues than carbon, particularly in lipid-rich species (Ikeda, 1988; Ventura, 2006).

2.3.4 Data analysis

The relationships between $\delta^{15}N$ and depth, $\delta^{15}N$ of zooplankton and $\delta^{15}N$ of POM and fatty acid/alcohol compositions with depth were investigated using linear regression. To deal with differences in individual compound concentrations between zooplankton taxa/POM samples, quantitative data (individual fatty acids/alcohols) were converted to relative abundances (mol%) of total identified lipid. Relative abundances for each lipid class were also calculated by summing the concentrations (nmol) of individual moieties into their respective classes and dividing each lipid class by the total lipid concentration of the individual zooplankton. The relationship between 18:1(n-9) and depth was investigated using linear regression. This fatty acid was of particular interest, as it is biosynthesized by animals (Dalsgaard *et al.*, 2003), but not phytoplankton, and is therefore representative of zooplankton-sourced materials to the particle pool. The influence of POM size fraction (<53 µm vs. >53 µm), time of collection (P3A/P3B/P3C) and sampling depth on the composition (mol%) of the 13 most abundant fatty acids, which made up >80 % of total fatty acid composition, were examined using redundancy analysis (RDA). The influence of zooplankton taxa and time of collection (P3B and P3C; no P3A zooplankton lipid data available) on the composition (mol%) of fatty acids were also examined using RDA analysis. The significance of individual model terms were determined using a permuted (n=9999) forward selection procedure (Mayor *et al.*, 2013). Fatty acids that accounted for <3 % of total fatty acids and missing values for individual taxa were excluded from the RDA analysis as RDA sees zero values as similar (Zuur *et al.*, 2007). Fatty acids with single missing values were imputed by taking a mean of all other values for the individual taxon and fatty acid. Additional RDA analyses were conducted to investigate whether the compositions of lipid classes were influenced by the different taxa. All statistical analyses were conducted in the R v4.1.3 programming environment (R Core Team, 2022) using the 'Vegan' package (Oksanen *et al.*, 2020a). Data obtained at the P3 station during each visit is summarised in Table 2.1.

Table 2.1. Summary of particulate organic matter (POM) and zooplankton data available at each visit of the P3 station in the Scotia Sea, South Georgia.

	P3A	**P3B**	**P3C**
POM lipid data	✓	✓	✓
POM stable isotope data	✓	✓	✓
Zooplankton lipid data	X	✓	✓
Zooplankton stable isotope data	X	✓	✓

2.4 Results

2.4.1 Stable isotope compositions

The $\delta^{15}N$ signatures of POM at P3 ranged between 1.24 ‰ and 8.22 ‰ and became progressively ^{15}N-enriched with depth (ANOVA, $F=25.1_{(1,18)}$, $p<0.001$; Figure 2.1). POM $\delta^{15}N$ values did not change significantly between the three visits to P3 (ANOVA, $F=0.130_{(2,17)}$, $p=0.879$).

The mean $\delta^{15}N$ signatures of the zooplankton varied between 3.50 ‰ and 8.97 ‰, with the lowest being in the salp *S. thompsoni* and the copepod *R. gigas*, followed by the amphipod *T. gaudichaudii* and copepod *C. acutus*, increasing to euphausiids and chaetognaths and the copepod *Paraeuchaeta* spp. which was most enriched in ^{15}N (Table 2.2; Appendix A Figure A 1). The $\delta^{15}N$ values of *T. gaudichaudii* and *R. gigas* were both correlated with POM $\delta^{15}N$ values ($F \geq 12.76_{(1,\geq 11)}$, $p<0.001$ in both cases), and depth ($F=14.26_{(1,11)}$, $p=0.003$ and $F=11.76_{(1,17)}$, $p=0.003$ respectively) whereas all other species were not ($p>0.05$ in all cases). *T. gaudichaudii* $\delta^{15}N$ values increased with depth ($y = 45.7x - 199.5$; $R^2 = 0.56$) whereas those for *R. gigas* decreased ($y = -106.5x + 734.6$; $R^2 = 0.41$) (Figure 2.2). Estimated trophic levels ranged from 3.61 to 5.46 (Figure 2.3). The lowest trophic levels were found in *S. thompsoni* and *R. gigas,* followed by *T. gaudichaudii*, *Thysanoessa* spp., Chaetognatha, *E. triacantha* and lastly *Paraeuchaeta* spp..

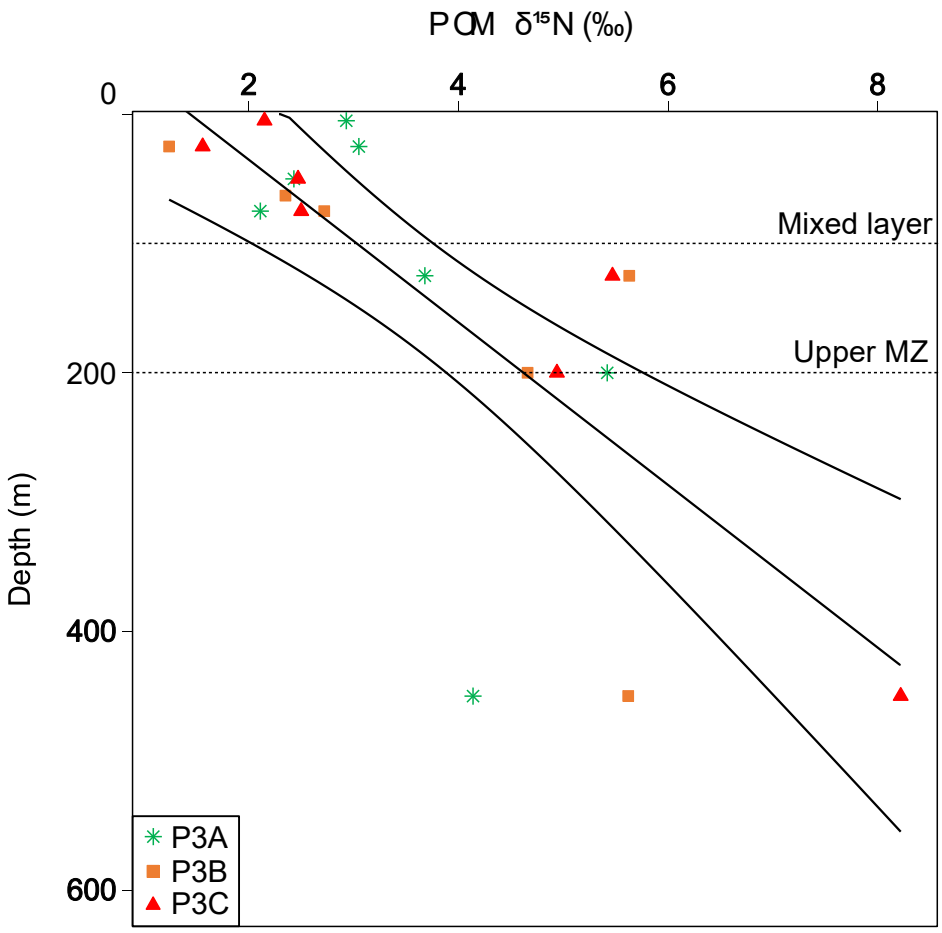

Figure 2.1. $\delta^{15}N$ signatures of particulate organic matter (POM) in relation to sampling depth at station P3 (P3A + P3B + P3C) in the Scotia Sea. The regression line indicates a statistically significant ($p<0.05$) relationship between $\delta^{15}N$ of POM and depth. $y = -90.55x (\pm 50.91) + 62.88 (\pm 12.55)$. $R^2 = 0.58$. Standard errors are illustrated either side of the regression line and given in brackets next to the equation coefficients. Horizontal dotted lines indicate the boundaries of the mixed layer depth (0 – 95 m) and the upper mesopelagic zone (MZ) (96 – 200 m) (Giering *et al.*, 2023).

Table 2.2. Dry weight (DW, mg), organic nitrogen content per DW (mg N), organic carbon content per DW (mg C), mg of lipid to DW content (mg lipid g DW-1), lipid to organic nitrogen content (mg g N-1) and lipid to organic carbon content (mg g C-1) and $\delta^{15}N$ signatures of zooplankton (mean ± standard deviation) sampled at the P3 (P3B + P3C) station in the Scotia Sea. One outlier value in the lipids data was removed when calculating the means for *T. gaudichaudii* due to the value being an order of magnitude larger than the rest of the data. The number of replicates (n) for lipid analyses are indicated for each taxa in the top row of each station visit. Replicate sizes for the stable isotope data are indicated within the $\delta^{15}N$ row for each station visit.

		Calanoides acutus	**Chaetognatha**	***Euphausia triacantha***	***Paraeuchaeta* spp.**	***Rhincalanus gigas***	***Salpa thompsoni***	***Themisto gaudichaudii***	***Thysanoessa* spp.**
	n	3	3	3	0	4	1	0	2
P3B	mg DW	1.9 ± 1.1	7.4 ± 5.0	76.6 ± 43.7	-	3.1 ± 1.2	4.4	-	23.4 ± 6.2
	mg N	0.1 ± 0.06	0.4 ± 0.1	5.1 ± 3.2	-	0.2 ± 0.09	0.2	-	2.2 ± 0.4
	mg C	1.1 ± 0.7	1.6 ± 0.4	40.8 ± 23.6	-	1.7 ± 0.7	0.8	-	9.1 ± 2.9
	mg lipids g DW^{-1}	516.9 ± 117.5	118.8 ± 52.3	100.0 ± 38.5	-	427.3 ± 28.6	43.2	-	154.0 ± 145.0
	mg lipids g N^{-1}	30.6 ± 6.5	8.9 ± 5.8	6.4 ± 1.5	-	25.8 ± 4.7	1.70	-	14.1 ± 12.5
	mg lipids g C^{-1}	289.8 ± 61.1	37.1 ± 25.9	54.9 ± 31.5	-	231.6 ± 25.0	8.0	-	60.9 ± 59.3
	δ15N (‰)	5.4 ± 1.4 (n=3)	6.2 ± 0.6 (n=9)	6.3 ± 0.9 (n=12)	7.3 (n=1)	4.9 ± 0.3 (n=3)	5.0 ± 1.1 (n=10)	5.4 ± 0.1 (n=4)	6.3 ± 0.7 (n=16)
	n	3	4	2	1	3	1	2	3
P3C	mg DW	3.0 ± 0.4	6.5 ± 9.6	45.6 ± 8.1	1.7	4.8 ± 1.4	12.8	6.4 ± 4.1	43.5 ± 52.5
	mg N	0.2 ± 0.02	0.6 ± 0.9	4.8 ± 0.1	0.2	0.3 ± 0.08	0.1	0.5 ± 0.3	4.8 ± 6.3

		Calanoides acutus	Chaetognatha	*Euphausia triacantha*	*Paraeuchaeta* spp.	*Rhincalanus gigas*	*Salpa thompsoni*	*Themisto gaudichaudii*	*Thysanoessa* spp.
	mg C	1.7 ± 0.1	2.4 ± 3.5	19.6 ± 3.2	0.8	2.6 ± 0.9	0.7	2.5 ± 1.7	17.5 ± 21.9
	mg lipids g DW^{-1}	438.7 ± 106.4	61.9 ± 15.3	155.5 ± 16.6	194.1	276.0 ± 42.8	28.3	122.4 ± 36.1	107.8 ± 66.5
	mg lipids g N^{-1}	31.5 ± 5.9	5.8 ± 1.5	16.9 ± 4.4	18.4	18.5 ± 1.0	0.3	9.2 ± 2.4	11.1 ± 7.9
	mg lipids g C^{-1}	245.8 ± 48.4	23.7 ± 7.1	67.2 ± 8.3	93.4	152.7 ± 31.4	1.5	46.4 ± 10.7	42.6 ± 29.1
	$\delta^{15}N$ (‰)	7.0 ± 1.7 (n=5)	7.1 ± 0.4 (n=6)	7.2 ± 0.8 (n=10)	7.7 ± 1.5 (n=2)	5.1 ± 0.8 (n=16)	5.0 ± 0.8 (n=9)	6.2 ± 0.8 (n=9)	6.2 ± 0.7 (n=14)

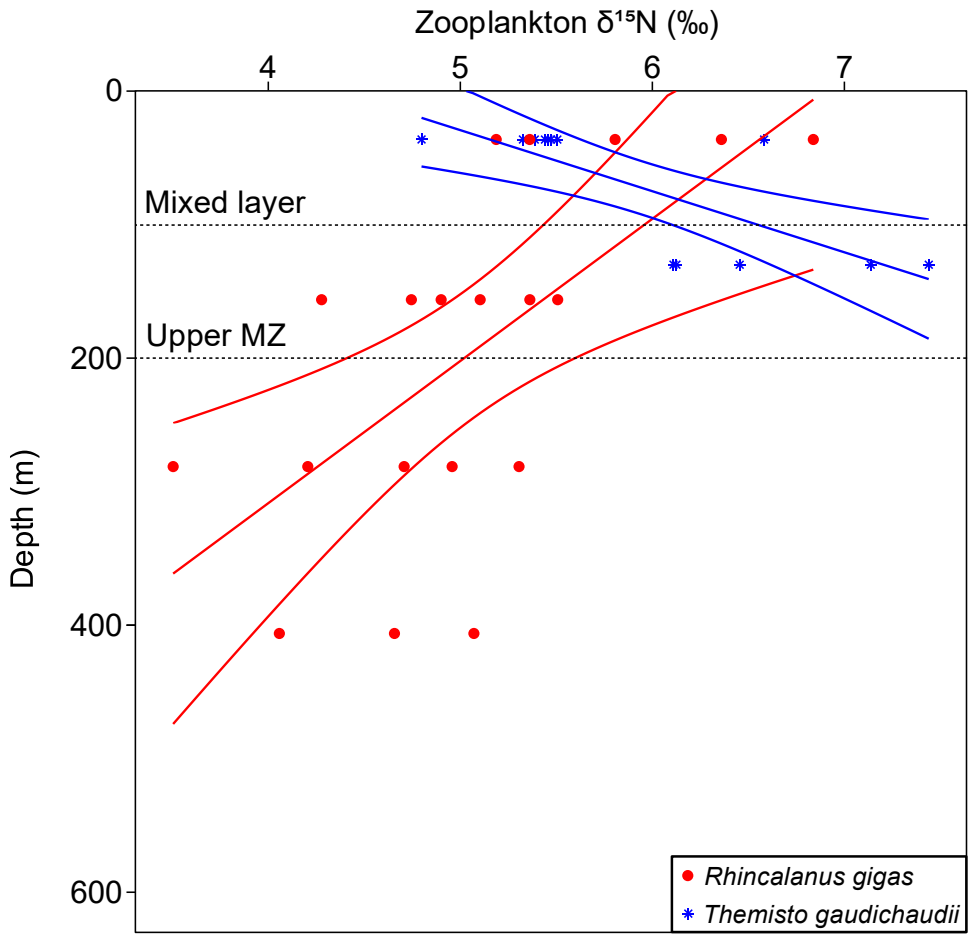

Figure 2.2. $\delta^{15}N$ signatures of *Rhincalanus gigas* and *Themisto gaudichaudii* in relation to depth at station P3 (P3B + P3C) in the Scotia Sea. Depth values represent mean depth of the net from which specimens were collected from. *T. gaudichaudii* were collected in the upper 250 m, using either a RMT 25 net sampling between 10 – 250 m or a MOCNESS net sampling 10 – 62 m (see supplementary figure S2 for details). Insufficient *T. gaudichaudii* were collected at depths beyond 250 m for analysis. The regression lines indicate a statistically significant ($p<0.05$) relationship between the $\delta^{15}N$ values of the zooplankton and depth (*T. gaudichaudii* = blue: $y = 0.779x$ (± 0.218) + 4.106 (± 0.536) ($R^2 = 0.54$); *R. gigas* = red: $y = -0.238x$ (± 0.066) + 6.268 (± 0.364) ($R^2 = 0.44$). Standard error values for the equation coefficients are given in brackets. Only taxa with significant linear relationships are plotted. Horizontal dotted lines indicate the boundaries of the mixed layer depth (0 – 95 m) and the upper mesopelagic zone (MZ) (96 – 200 m) (Giering *et al.*, 2023).

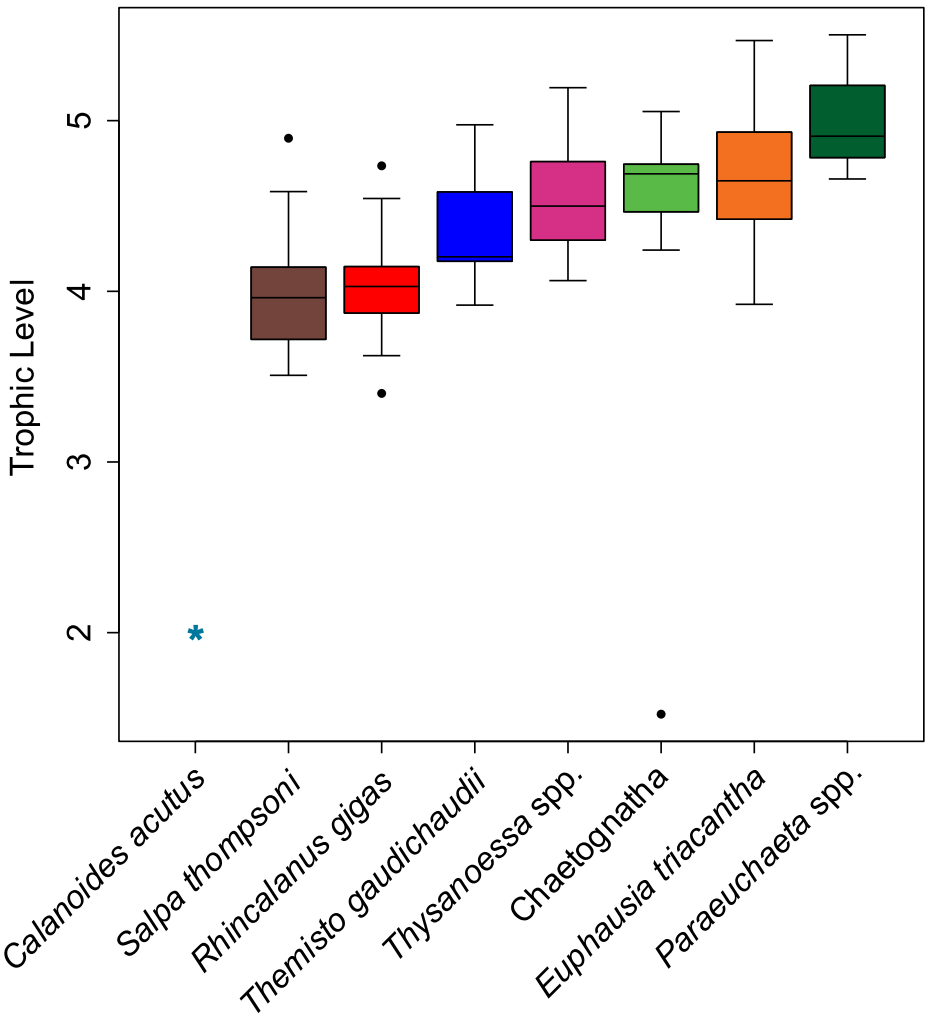

Figure 2.3. Estimated trophic level for the 8 zooplankton taxa at station P3 (P3B + P3C) in the Scotia Sea. The boxplot represents the minimum, maximum, median, first quartile and third quartile values. Circles represent outliers. Trophic level was calculated from $\delta^{15}N$, assuming a trophic enrichment factor of 2.5 ‰ per trophic level. The baseline consumer $\delta^{15}N$ signature used to calculate trophic levels was based on the mean $\delta^{15}N$ of *Calanoides acutus* ($\delta^{15}N$ = 6.38 ± 1.73; asterisk) and a baseline consumer trophic level = 2.0 (asterisk). *C. acutus* $\delta^{15}N$ signatures were not affected by sampling depth ($F=0.002_{(1,6)}$, p=0.963).

2.4.2 Fatty acid signatures of particulate organic matter

The lipid composition of POM is described in Preece et al. (submitted). Briefly, the fatty acid composition (mol%) of the <53 µm POM was dominated by 20:5(n-3), followed by 16:1(n-7) and 22:6(n-3) (40.7 ± 6.4, 14.5 ± 5.1 and 11.6 ± 5.8 mol% respectively; Table 2.3). The fatty acid composition of the >53 µm POM was dominated by 16:1(n-7), 18:1(n-9) and 20:5(n-3) (26.8 ± 9.3, 15.8 ± 10.7 and 11.2 ± 11.4 mol% respectively; Table 2.3). The percentage of the 18:1(n-9) fatty acid in POM increased with depth (Figure 2.4) in both <53 µm and >53 µm size fractions ($F=8.20_{(1,20)}$, p=0.009; $F=23.6_{(1,20)}$, p<0.001, respectively). Other fatty acids with percentage compositions that increased with depth included 18:2(tr-9) for both size fractions (<53 µm: $F=7.77_{(1,20)}$, p=0.011, R^2=0.28; >53 µm: $F=6.16_{(1,20)}$, p=0.022, R^2=0.24) and 18:0 for the <53 size fraction ($F=42.6_{(1,20)}$, p<0.001, R^2=0.68; Figure A 2; Table A 3). The percentage composition of 14:0 decreased with increasing depth in the >53 µm size fraction ($F=7.54_{(1,20)}$, p=0.012, R^2=0.27; Figure A 3; Table A 3). No other POM fatty acid changed with depth (Table A 3).

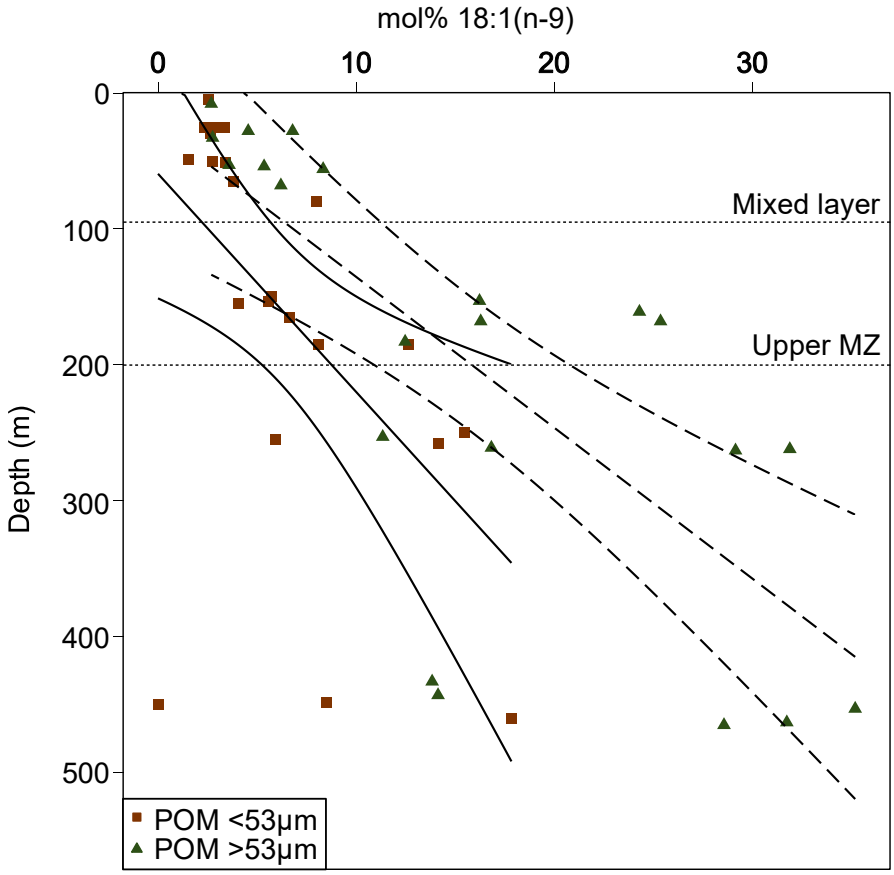

Figure 2.4. Relationships between depth and the relative abundance of the biomarker 18:1(n-9) (mol%) fatty acid in the <53 µm (filled squares) and >53 µm (filled triangles) size-fractions of particulate organic matter (POM) sampled at station P3 (P3A + P3B + P3C) in the Scotia Sea. This fatty acid is biosynthesized by animals (Dalsgaard, 2003), but not phytoplankton, and is therefore representative of zooplankton-sourced materials to the particle pool and more reworked POM. The regression lines indicate statistically significant ($p<0.05$) linear relationships. POM <53 µm (solid line): $y = 16.06x (\pm 5.61) + 59.44 (\pm 43.92)$ ($R^2 = 0.29$); POM >53 µm (dashed line): $y = 11.08x (\pm 2.28) + 24.41 (\pm 43.19)$ ($R^2 = 0.54$). Standard errors are illustrated either side of the regression line and given in brackets next to the equation coefficients. Horizontal dotted lines indicate the boundaries of the mixed layer depth (0 – 95 m) and the upper mesopelagic zone (MZ) (96 – 200 m) (Giering *et al.*, 2023).

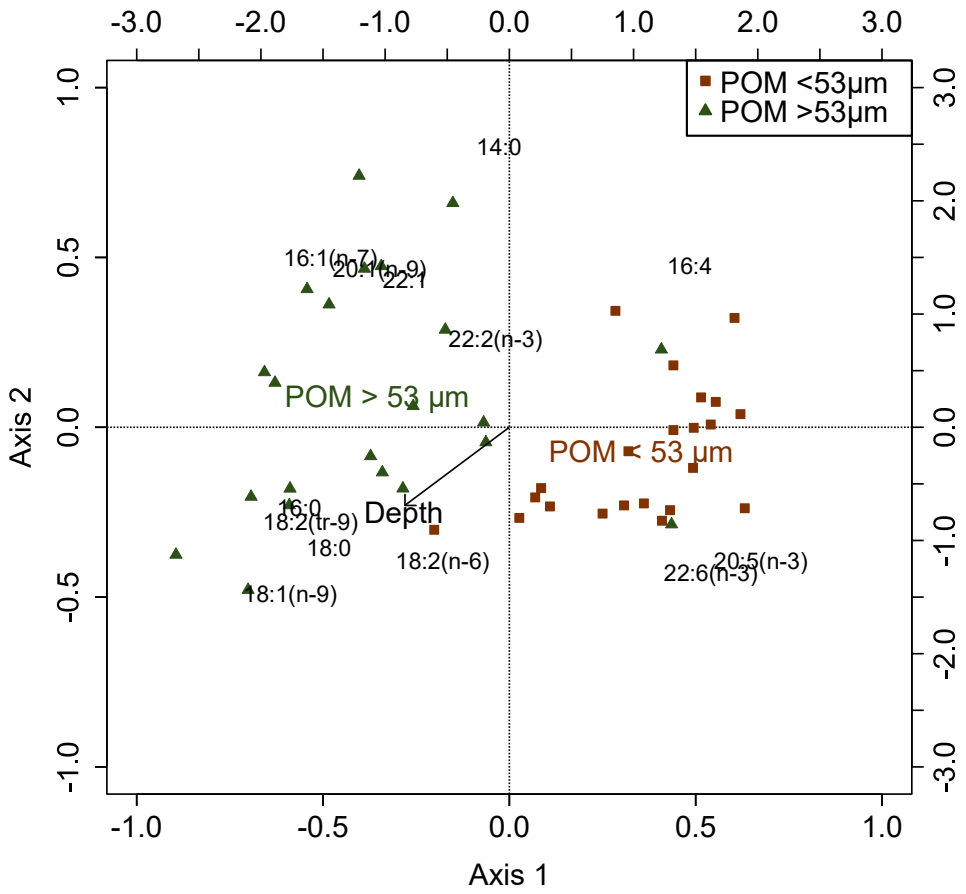

Figure 2.5. Fatty acid composition (mol%) of size-fractionated particulate organic matter (POM) from station P3 (P3A + P3B + P3C) in the Scotia Sea. Redundancy analysis distance triplot of the proportional abundance of each fatty acid for the two particle sizes and the continuous variable depth. Each single point refers to a single sample of POM. The effect of depth is plotted as a vector (solid black line). The primary and secondary sets of axes relate to the individual samples and fatty acid loadings, respectively.

The fatty acid composition of the POM varied as a function of particle size (<53 µm or >53 µm) and sampling depth (RDA, $F=13.67_{(1,42)}$, $p<0.001$ and $F=6.34_{(1,42)}$, $p<0.001$ respectively; Figure 2.5; see also Preece *et al.* (in prep)). Including time of collection (P3A/P3B/P3C) had no effect on the model fit ($F=1.73_{(2,42)}$, $p=0.073$) and was therefore excluded from the model. The final RDA model explained 35.4 % of the total variance in the data, with the first and second axes accounting for 28.1 % and 7.32 % of the overall variability, respectively. Particle size was ordinated across the first axis, with <53 µm and >53 µm POM generally having positive and negative values on this axis, respectively. The PUFAs 20:5(n-3), 22:6(n-3) and 16:4, were more closely associated with the <53 µm fraction. All other fatty acids were more closely associated to the >53 µm POM.

Table 2.3. Fatty acid composition (mol%, mean ± standard deviation) of <53 µm and >53 µm POM throughout epi- and mesopelagic waters at station P3 (P3A + P3B + P3C) in the Scotia Sea, focusing on the 13 most abundant fatty acids (making up > 80% of fatty acid composition). Fatty acid values were averaged across 5 depth bins. The number of replicates (n) is indicated for each depth bin. Data reproduced from Preece *et al.* (in prep).

	POM <53 µm						**POM >53 µm**					
Depth bin (m)	5 – 30 n=5	49 – 80 n=5	150 – 185 n=6	250 – 258 n=3	448 – 460 n=3	Mean n=22	5 – 30 n=4	45 – 65 n=4	150 – 180 n=5	250 – 260 n=4	430 – 462 n=5	Mean n=22
14:0	2.9 ± 1.6	3.1 ± 0.3	1.8 ± 0.5	1.3 ± 0.6	2.1 ± 0.7	2.2 ± 1.0	4.4 ± 3.3	6.3 ± 3.4	2.2 ± 2.1	2.3 ± 0.7	1.5 ± 1.2	3.2 ± 2.8
16:0	2.6 ± 0.9	6.4 ± 8.2	3.9 ± 1.4	3.7 ± 0.8	8.4 ± 1.2	4.8 ± 4.2	7.8 ± 6.5	9.4 ± 4.7	4.9 ± 3.2	8.7 ± 3.0	8.7 ± 3.7	7.8 ± 4.2
18:0	0.2 ± 0.0	0.3 ± 0.1	0.5 ± 0.3	0.8 ± 0.4	3.7 ± 1.9	0.9 ± 1.3	3.1 ± 4.2	1.4 ± 0.5	1.4 ± 0.6	3.1 ± 1.1	3.9 ± 2.1	2.6 ± 2.2
16:1(n-7)	17.1 ± 3.6	13.1 ± 7.1	11.4 ± 6.5	15.1 ± 1.9	17.5 ± 2.6	14.5 ± 5.1	26.1 ± 11.8	36.7 ± 7.0	21.5 ± 10.4	22.8 ± 6.2	28.0 ± 4.2	26.8 ± 9.3
18:2(n-6)	1.9 ± 1.4	3.0 ± 0.3	2.8 ± 1.2	3.4 ± 1.3	3.5 ± 0.9	2.9 ± 1.1	2.4 ± 1.1	2.3 ± 1.4	2.6 ± 0.4	4.9 ± 5.0	4.1 ± 1.2	3.3 ± 2.3
18:1(n-9)	2.8 ± 0.4	2.4 ± 0.9	6.0 ± 1.4	11.2 ± 4.1	8.8 ± 8.9	6.3 ± 4.8	4.2 ± 1.9	5.9 ± 2.0	18.9 ± 5.6	22.3 ± 9.9	24.7 ± 10.1	15.8 ± 10.7
18:2(tr-9)	1.9 ± 0.8	2.7 ± 0.8	3.2 ± 0.4	4.8 ± 1.5	4.1 ± 1.1	3.3 ± 1.4	4.2 ± 3.7	5.5 ± 2.4	4.6 ± 2.1	6.8 ± 1.4	8.0 ± 3.2	5.9 ± 2.9
20:5(n-3)	41.0 ± 5.2	40.4 ± 3.1	47.7 ± 4.6	37.3 ± 5.7	34.5 ± 7.0	40.7 ± 6.4	11.7 ± 12.6	5.3 ± 6.2	19.1 ± 16.0	13.9 ± 9.6	5.6 ± 6.9	11.2 ± 11.4
20:1(n-9)	2.4 ± 2.8	0.2 ± 0.1	0.3 ± 0.2	2.2 ± 3.2	0.7 ± 0.3	1.2 ± 2.0	0.2 ± 0.4	5.5 ± 6.5	6.9 ± 3.9	5.8 ± 2.5	3.1 ± 1.7	4.4 ± 4.0
22:6(n-3)	9.1 ± 6.4	11.7 ± 6.6	13.3 ± 7.9	13.9 ± 3.8	10.3 ± 3.1	11.9 ± 5.8	2.5 ± 4.1	0.6 ± 0.6	5.2 ± 7.5	2.2 ± 4.40	1.1 ± 1.7	2.4 ± 4.4
22:1	2.8 ± 3.4	0.6 ± 0.2	0.9 ± 0.9	0.6 ± 0.6	3.6 ± 3.1	1.6 ± 2.2	6.5 ± 9.9	5.1 ± 5.5	8.1 ± 6.8	3.7 ± 2.5	3.3 ± 2.6	5.4 ± 5.7

Table 2.4. Fatty alcohol composition (mol%, mean ± standard deviation) of <53 µm and >53 µm POM throughout epi- and mesopelagic waters at station P3 (P3A + P3B +P3C) in the Scotia Sea, focusing on the 4 most abundant fatty alcohols. Fatty alcohol values were averaged across 5 depth bins. The number of replicates (n) is indicated for each depth bin. Data reproduced from (Preece *et al.*, in prep).

	POM <53 µm						**POM >53 µm**					
Depth bin (m)	5 – 30 n=5	49 – 80 n=5	150 – 185 n=6	250 – 258 n=3	448 – 460 n=3	Mean =22	5 – 30 n=4	45 – 65 n=4	150 – 180 n=5	250 – 260 n=4	430 – 462 n=5	Mean =22
ALC-14:0	1.1 ± 0.9	2.6 ± 3.0	1.5 ± 1.1	2.5 ± 3.0	1.0 ± 0.9	1.7 ± 1.9	1.3 ± 1.8	1.1 ± 0.8	6.9 ± 5.4	4.1 ± 2.7	4.2 ± 3.6	3.7 ± 3.8
ALC-16:0	1.1 ± 1.1	2.8 ± 3.4	2.8 ± 3.2	4.5 ± 4.1	2.1 ± 1.2	2.5 ± 2.8	1.3 ± 2.1	1.1 ± 1.2	10.4 ± 4.9	7.0 ± 4.3	10.3 ± 8.7	6.4 ± 6.3
ALC-20:1	3.7 ± 4.8	0.6 ± 0.7	1.6 ± 2.7	0.9 ± 1.2	0.3 ± 0.5	1.6 ± 2.8	-	1.1 ± 0.8	9.9 ± 7.4	7.6 ± 5.0	4.2 ± 1.7	4.8 ± 5.4
ALC-22:1	1.7 ± 2.4	0.3 ± 0.3	0.1 ± 0.1	0.1 ± 0.2	-	0.5 ± 1.3	2.1 ± 4.1	0.1 ± 0.2	3.9 ± 2.8	1.6 ± 1.9	0.1 ± 0.2	1.6 ± 2.6

2.4.3 Fatty acid and alcohol signatures of zooplankton

Fatty acids made up >60 mol% of the total lipids within each taxa sampled (Table 2.5). The relative abundances of monosaturated fatty acids (MUFAs) and PUFAs were similar across taxa, with higher amounts of PUFAs compared to MUFAs, apart from *Paraeuchaeta* spp., which contained a greater amount of MUFAs (49.4 mol%) and less PUFAs (9.2 mol%; note only one *Paraeuchaeta* specimen was sampled; Table 2.5). The dominant MUFAs in all taxa were 16:1(n-7) and 18:1(n-9) (as well as 20:1(n-9) in *C. acutus*). 20:5(n-3) and/or 22:6(n-3) were the most abundant PUFA(s) in all taxa (Table 2.6). Other PUFAs included 16:4, 18:2(n-6) and 18:3(n-5). Saturated fatty acids (SFAs), mainly 14:0 and 16:0, made up between 15 - 27 mol% of total lipids for all except the three copepod species (*C. acutus, R. gigas* and *Paraeucheta* spp.), where total SFAs accounted for <8 mol% (Table 2.5). All non-copepod zooplankton taxa had low or moderate contributions of fatty alcohols (<12 %; Table 2.5). By contrast, fatty alcohols in the three copepod species represented >25 % of the total lipid pool. *C. acutus* alcohols were dominated by unsaturated compounds, specifically ALC-20:1 and ALC-22:1, whereas *R. gigas* alcohols were dominated by saturated alcohols, predominately ALC-14:0 and ALC-16:0 (Table 2.7). *Paraeuchaeta* spp. had a more equal distribution of saturated and unsaturated alcohols.

Table 2.5. Lipid class composition (mol%, mean ± standard deviation) of each zooplankton taxa sampled at station P3 (P3B + P3C) in the Scotia Sea. Saturated-, monounsaturated- and polyunsaturated-fatty acids are abbreviated as SFA, MUFA and PUFA respectively. The number of replicate samples (n) is indicated for each taxon. Replicate samples of *C. acutus* each contained 5 individuals. Replicate samples of *R. gigas* each contained 2 individuals. All other taxa replicates contained 1 individual per replicate.

	Calanoides acutus	**Chaetognatha**	***Euphausia triacantha***	***Paraeuchaeta* spp.**	***Rhincalanus* gigas**	***Salpa thompsoni***	***Themisto gaudichaudii***	***Thysanoessa* spp.**
	n=6	**n=7**	**n=5**	**n=1**	**n=7**	**n=2**	**n=3**	**n=5**
SFA	7.4 ± 0.5	15.5 ± 4.3	20.5 ± 3.5	2.2	2.5 ± 0.7	21.0 ± 4.1	20.1 ± 3.4	26.9 ± 5.5
Branched Acids	0.2 ± 0.2	0.5 ± 0.2	1.9 ± 0.7	0.6	0.0 ± 0.0	1.4 ± 0.4	0.9 ± 0.5	0.6 ± 0.4
MUFA	23.7 ± 2.6	26.4 ± 2.9	22.5 ± 4.8	49.4	21.9 ± 1.8	13.6 ± 5.3	25.6 ± 2.7	17.1 ± 2.6
PUFA	32.4 ± 6.6	45.4 ± 7.4	43.0 ± 10.9	9.2	49.9 ± 3.8	46.7 ± 11.8	42.1 ± 3.5	40.2 ± 11.1
Saturated Alcohols	8.4 ± 0.7	1.5 ± 1.7	5.1 ± 1.4	21.6	20.7 ± 1.8	2.3 ± 3.0	2.0 ± 1.3	0.4 ± 0.3
Unsaturated Alcohols	27.5 ± 3.3	3.2 ± 6.2	4.4 ± 1.2	16.5	4.6 ± 0.7	9.5 ± 8.7	7.0 ± 3.6	11.6 ± 6.4
Sterols	0.3 ± 0.2	7.4 ± 3.4	2.3 ± 0.3	0.5	0.6 ± 0.2	5.5 ± 0.7	2.4 ± 1.2	3.2 ± 2.5
Phytadienes	0.00	0.00	0.4 ± 0.8	0.00	0.00	0.00	0.00	0.00
Total fatty acids	63.6 ± 7.1	87.3 ± 90.4	86.0 ± 12.4	60.7	74.2 ± 4.2	81.4 ± 13.5	87.8 ± 5.6	84.2 ± 12.7
Total alcohols	36.0 ± 3.3	4.8 ± 6.5	9.5 ± 1.8	38.1	25.2 ± 1.8	11.8 ± 9.2	8.9 ± 3.8	12.0 ± 6.5

Table 2.6. Fatty acid composition (mol% mean ± standard deviation) of the 8 studied zooplankton taxa sampled at station P3 (P3B + P3C) in the Scotia Sea, focusing on the 15 most abundant fatty acids included in the RDA model. *The fatty acid 22:1 was tentatively assigned hereafter as 22:1(n-11) based on the knowledge of 22:1(n-11) being a fatty acid only biosynthesised by herbivorous calanoid copepods such as *C. acutus* (Hagen *et al.*, 1993; Dalsgaard *et al.*, 2003). The number of replicate samples (n) is indicated for each taxon. Replicate samples of *C. acutus* each contained 5 individuals. Replicate samples of *R. gigas* each contained 2 individuals. All other taxa replicates contained 1 individual per replicate.

	Calanoides acutus	**Chaetognatha**	***Euphausia triacantha***	***Paraeuchaeta* spp.**	***Rhincalanus gigas***	***Salpa thompsoni***	***Themisto gaudichaudii***	***Thysanoessa* spp.**
	n=6	n=7	n=5	n=1	n=7	n=2	n=3	n=5
14:0	7.8 ± 1.3	5.2 ± 4.1	12.7 ± 2.6	1.1	0.9 ± 0.5	12.3 ± 0.4	10.0 ± 2.5	17.9 ± 8.4
16:0	3.6 ± 0.6	10.7 ± 1.8	9.1 ± 1.7	2.3	2.2 ± 0.5	11.2 ± 0.9	10.8 ± 1.6	12.1 ± 0.5
16:4	4.5 ± 3.5	1.0 ± 1.2	0.8 ± 1.3	0.2	9.8 ± 0.9	2.0 ± 1.5	1.5 ± 1.0	0.3 ± 0.1
16:1(n-7)	10.6 ± 0.7	8.9 ± 1.8	6.9 ± 3.8	40.0	14.4 ± 1.7	7.7 ± 0.7	10.4 ± 1.4	4.4 ± 1.0
18:3(n-6)	2.8 ± 0.6	0.3 ± 0.2	0.8 ± 0.5	0.3	1.7 ± 0.4	1.2 ± 0.5	1.9 ± 0.6	1.4 ± 0.6
18:4	4.2 ± 2.7	0.6 ± 0.6	0.9 ± 0.4	0.0	4.9 ± 0.5	2.8 ± 0.5	3.4 ± 1.3	0.7 ± 0.3
18:2(n-6)	2.3 ± 0.4	5.2 ± 4.4	6.5 ± 1.1	3.2	5.6 ± 4.3	2.6 ± 0.3	3.1 ± 0.5	3.3 ± 0.4
18:1(n-9)	3.3 ± 0.8	8.0 ± 3.4	8.4 ± 3.0	34.1	12.9 ± 1.2	2.2 ± 0.8	6.6 ± 2.8	7.0 ± 0.3
18:1(tr-9)	0.8 ± 0.3	2.9 ± 1.6	3.8 ± 2.0	1.3	2.1 ± 1.0	2.9 ± 0.8	2.5 ± 0.9	4.5 ± 0.4
20:5(n-3)	17.9 ± 14.0	16.9 ± 2.1	12.8 ± 1.7	4.2	25.3 ± 3.0	22.1 ± 1.4	18.4 ± 2.2	16.8 ± 3.6
20:1(n-9)	12.5 ± 2.3	3.1 ± 1.9	2.6 ± 0.6	2.0	0.3 ± 0.1	3.3 ± 3.8	5.4 ± 0.9	2.5 ± 0.6
22:6(n-3)	8.9 ± 1.6	21.8 ± 5.8	11.5 ± 1.7	4.5	5.2 ± 0.6	18.4 ± 5.9	9.2 ± 6.5	14.2 ± 7.0
22:1(n-9)	1.9 ± 0.5	2.0 ± 2.3	0.8 ± 0.4	0.1	0.0 ± 0.0	0.9 ± 0.5	0.9 ± 0.1	0.7 ± 0.2
20:4	2.3 ± 1.2	1.0 ± 1.0	1.0 ± 0.2	0.1	1.0 ± 0.2	0.8 ± 0.4	3.3 ± 3.0	1.2 ± 0.4
22:1(n-11)*	6.4 ± 1.5	2.7 ± 3.9	1.1 ± 0.6	0.8	0.1 ± 0.1	1.5 ± 2.1	2.0 ± 0.7	1.2 ± 0.3

Table 2.7. Fatty alcohol composition (mol% mean ± standard deviation) of the 8 studied zooplankton taxa sampled at station P3 (P3B + P3C) in the Scotia Sea, focusing on the 8 most abundant fatty alcohols included in the RDA model. The number of replicate samples (n) is indicated for each taxon. Replicate samples of *C. acutus* each contained 5 individuals. Replicate samples of *R. gigas* each contained 2 individuals. All other taxa replicates contained 1 individual per replicate.

	Calanoides acutus	**Chaetognatha**	***Euphausia triacantha***	***Paraeuchaeta* spp.**	***Rhincalanus* gigas**	***Salpa thompsoni***	***Themisto gaudichaudii***	***Thysanoessa* spp.**
	n=6	n=7	n=5	n=1	n=7	n=2	n=3	n=5
ALC-14:0	11.3 ± 1.0	24.3 ± 16.3	23.0 ± 0.9	30.0	35.2 ± 1.0	5.3 ± 6.2	8.8 ± 3.3	1.3 ± 1.3
ALC-16:0	11.1 ± 0.6	23.7 ± 16.7	25.1 ± 0.7	23.5	37.4 ± 1.9	6.6 ± 6.1	9.6 ± 2.3	1.7 ± 1.5
ALC-18:0	0.5 ± 0.3	5.1 ± 6.2	3.8 ± 0.3	0.8	8.0 ± 1.3	1.3 ± 0.6	0.7 ± 0.0	0.6 ± 0.4
ALC-16:1	6.5 ± 0.8	2.1 ± 2.1	3.9 ± 0.3	8.4	8.5 ± 2.6	2.2 ± 3.0	4.5 ± 2.3	0.9 ± 0.4
ALC-18:1	2.8 ± 0.9	7.7 ± 10.8	8.0 ± 1.7	13.3	7.3 ± 0.6	3.3 ± 1.2	2.2 ± 0.8	36.7 ± 8.9
ALC-20:1	41.6 ± 2.4	24.2 ± 19.8	21.4 ± 0.9	6.1	0.7 ± 0.2	58.1 ± 12.9	39.5 ± 2.6	39.9 ± 7.3
ALC-22:1	24.9 ± 2.2	11.4 ± 9.0	11.5 ± 3.5	6.3	0.5 ± 0.1	12.1 ± 13.6	32.7 ± 4.6	17.8 ± 6.6
ALC-24:1	0.6 ± 0.3	0.3 ± 0.2	1.4 ± 0.8	6.8	0.8 ± 0.3	10.8 ± 14.4	1.1 ± 0.7	0.2 ± 0.2

2.4.4 RDA analysis of zooplankton lipid data

Taxon identity explained 77.2 % of the total variance in the zooplankton lipid class composition data (RDA, $F = 13.55_{(7,28)}$, $p<0.001$; Figure 2.6), with the first and second axes accounting for 36.0 % and 18.1 % of the variability, respectively. Including time of collection (P3B/P3C) did not improve the model fit ($F = 0.599_{(1,34)}$, $p=0.670$) and was therefore omitted. There was a distinct separation of the three copepods from the rest of the zooplankton. Copepods had strong negative loadings on the first axis and associations with alcohols, unsaturated alcohols and MUFAs, while all other species had positive loadings on the first axis and associations with sterols and SFAs. *R. gigas* was strongly associated with saturated alcohols, whereas *C. acutus* and *Paraeuchaeta* spp. were associated with unsaturated alcohols and MUFAs.

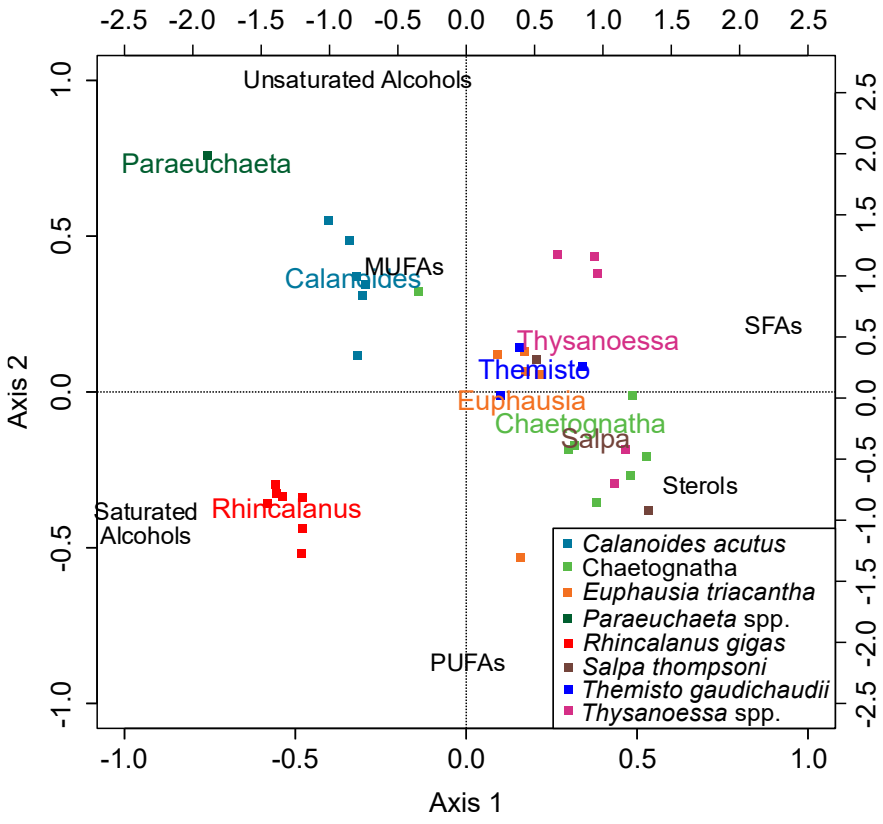

Figure 2.6. Lipid class composition (mol%) of the zooplankton taxa from station P3 (P3B + P3C) in the Scotia Sea. Redundancy analysis distance triplot of the proportional abundance of each lipid class in each sampled zooplankton taxa and 6 different lipid classes. The primary and secondary sets of axes relate to the individual zooplankton samples and lipid class loadings, respectively. Each single point refers to an individual taxon replicate.

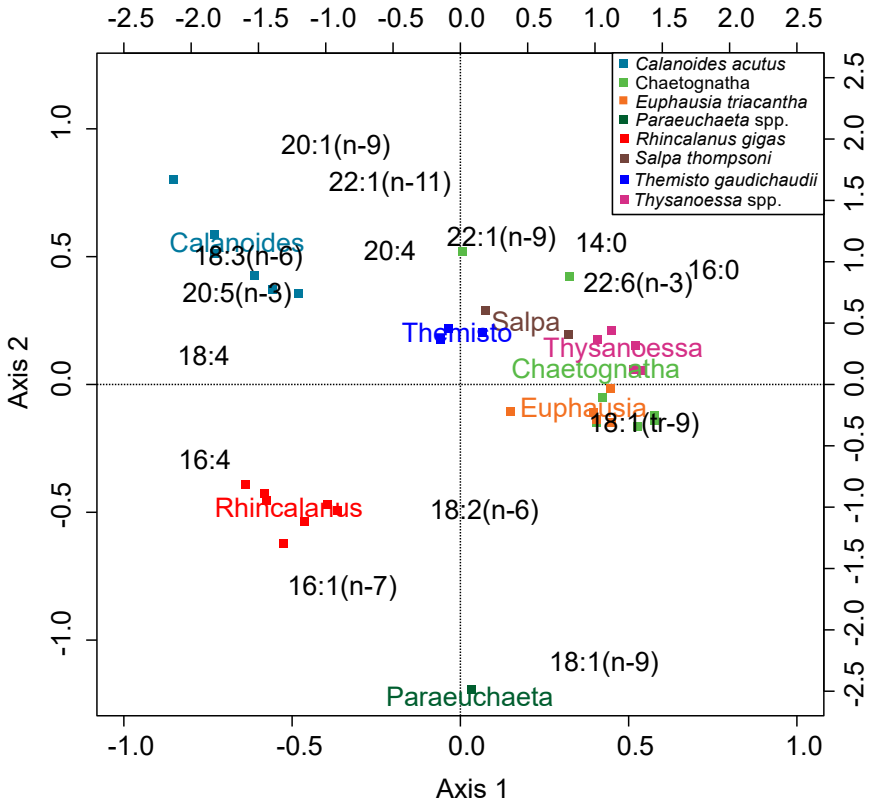

Figure 2.7 Fatty acid composition (mol%) of the zooplankton taxa from station P3 (P3B + P3C) in the Scotia Sea. Redundancy analysis distance triplot of the proportional abundance of fatty acids in each sampled zooplankton taxa and 16 fatty acids. The primary and secondary sets of axes relate to the individual zooplankton samples and fatty acid loadings, respectively. Each single point refers to an individual taxon replicate.

Taxon identity explained 73.0 % of the total variance in the zooplankton fatty acid compositional data (RDA, $F = 10.8_{(7,28)}$, $p<0.001$), with the first and second axes accounting for 32.7 % and 21.9 % of the variability, respectively (Figure 2.7). Including time of collection (P3B and P3C) did not improve the model fit ($F = 0.467_{(1,34)}$, $p=0.856$) and was therefore omitted. *E. triacantha*, Chaetognatha, *Thysanoessa* spp., *S. thompsoni* and *T. gaudichaudii* grouped together and were positively associated with the fatty acids 14:0, 18:1(tr-9), 16:0 and 22:6(n-3), 14:0 and 22:1(n-9). Chaetognatha demonstrated a range of both strong positive and negative loadings on the second axis, with some individuals being closely associated to 22:1(n-9) and others to 18:1(tr-9).

The three copepod species were ordinated away from the other taxa and each other, with *C. acutus* having strong negative loadings on the first axis and positive loadings on the second axis. *R. gigas* had strong negative loadings on both the first and second axes. *Paraeuchaeta* spp. had a strong negative loading on the second axis. *C. acutus* was particularly associated with 20:1(n-9), with the composition of this MUFA being higher in *C. acutus* (12.5 mol%) compared to all

other species (<6 mol%; Table 2.6). *C. acutus* was also closely associated with the PUFAs 20:5(n-3) and 18:3(n-6), and to a lesser extent 22:1(n-11) and 20:4. *R. gigas* was particularly associated with the short-chained fatty acids 16:4 and 16:1(n-7). *Paraeuchaeta* spp. was strongly associated with 18:1(n-9) and 16:1(n-7).

2.5 Discussion

2.5.1 Lipid content of particulate organic matter

The occupation of station P3 was characterised by a phytoplankton bloom dominated by large diatoms, with live, intact cells at depths within and below the epipelagic zone (Manno *et al.*, 2022; Ainsworth *et al.*, 2023). Lipid composition data of POM are originally presented and discussed in detail in Preece *et al.* (in prep) and reiterated here to facilitate the interpretation of the zooplankton data. The dominance of diatom markers 20:5(n-3) and 16:1(n-7) in both POM size fractions throughout the water column down to 500 m (Table 2.3) is entirely consistent with the occurrence of diatoms at depth. The differences in the fatty acid compositions of the two particles size classes (Figure 2.5) were driven by the increased relative abundances of the PUFAs, 20:5(n-3) and 22:6(n-3), in the <53 µm samples, and increased relative abundances of 18:1(n-9), 18:2(tr-9), and 20:1(n-9) in the >53 µm samples. The MUFA 18:1(n-9), which is biosynthesized by zooplankton (Dalsgaard *et al.*, 2003), contributed on average 15.8 mol% to the >53 µm POM fatty acids, compared to 6.3 % in the <53 µm size fraction (Table 2.3) and increased in relative concentration with increasing depth (Figure 2.4). Similar contributions of 18:1(n-9) in POM have previously been observed (Richoux, 2010), and its increased relative abundance with depth suggests that zooplankton-sourced materials become increasingly more important in midwater particle pools (Sheridan *et al.*, 2002). The presence of 18:1(n-9) within the large POM fraction may moreover be attributed to live particle associated copepods (PAC) too small to be removed from the SAPs filters, such as Oithonidae and Oncaeidae (<1 mm). These copepods produce large lipid stores that are dominated by 18:1(n-9) as well as the fatty alcohols ALC-14:0 and ALC-16:0 and to a lesser extent ALC-20:1(n-9) and ALC-22:1(n-11) (Kattner *et al.*, 2003). Indeed, there was an increased contribution of copepod lipids, largely unsaturated alcohols, to the >53 µm POM size fraction in the upper mesopelagic possibly derived from *Oithona* (Figure A 3; up to 35 %, Preece *et al.* (in prep)). This is consistent with the idea that small PACs are important in reworking and attenuating sinking POM in the upper mesopelagic (Mayor *et al.*, 2014; Koski *et al.*, 2020; Mayor *et al.*, 2020).

2.5.2 Trophic ecology of the zooplankton

The calculated zooplankton trophic levels ranged between 3.6 and 5.5 (Figure 2.3), suggesting a degree of trophic overlap within the zooplankton food web. We observed a subtle continuous, rather than stepwise, increase in trophic level, with *S. thompsoni* being at the lowest- and the carnivorous copepod *Paraeuchaeta* spp. at the highest trophic level, respectively. The isotopic signatures of copepods were broadly aligned with their trophic ecology inferred from the fatty acid analysis. Indeed, the high contributions of 16:1(n-7) and 20:5(n-3) in *C. acutus* and *R. gigas* suggest diatoms to be a dominant source of food and supports the idea that these species are broadly herbivorous (Kates and Volcani, 1966; Kattner *et al.*, 1994; Ward *et al.*, 1996; Falk-Petersen *et al.*, 1999). The top trophic position of *Paraeuchaeta* spp. aligns with previous studies describing this species as predatory (Øresland, 1991; Øresland and Ward, 1993). Isotopic and fatty acid data for the euphausiids were broadly consistent with these species being omnivores (Falk-Petersen *et al.*, 1999; Richoux, 2010), as suggested by the presence of both phytoplankton and calanoid biomarkers. The high percent contributions of ALC-20:1 and ALC-22:1 in both species moreover suggests their feeding on *C. acutus* (Table 2.7), the most abundant copepod. Other Southern Ocean calanoid species such as *Calanus propinquus* and *Calanus simillimus* also biosynthesize the calanoid biomarkers 20:1(n-9) and 22:1(n-11) (Hagen *et al.*, 1993; Ward *et al.*, 1996), however, these species were present in negligible amounts in nets during the study period (Cook *et al.*, 2023).

The $\delta^{15}N$ and trophic position of Chaetognatha were similar to those of the omnivorous euphausiids, despite them being considered active predators (Pakhomov *et al.*, 1999). Chaetognatha fatty acid composition was consistent with other studies; 22:6(n-3) and 20:5(n-3), and to a lesser extent 16:0, 16:1(n-7) and 18:1(n-9), dominate the composition of Antarctic chaetognaths (Kruse *et al.*, 2010). The calanoid biomarker 20:1(n-9) was observed in high proportions in one of the seven individuals sampled and was also abundant in alcohol form (Table 2.7), suggesting feeding on *C. acutus*. The wide array of fatty acids present in Chaetognatha may reflect their known behaviour as opportunistic feeders (Froneman and Pakhomov, 1998; Froneman *et al.*, 1998).

The fatty acids of *T. gaudichaudii* were dominated by 20:5(n-3), 16:0, 16:1(n-7), 14:0 and 22:6(n-3), in agreement with other studies (Fricke and Oehlenschläger, 1988; Nelson *et al.*, 2001; Mayzaud and Boutoute, 2015). The presence of the calanoid biomarker 20:1(n-9), both in fatty acid and alcohol forms, indicates feeding on *C. acutus* or other calanoid copepods. The $\delta^{15}N$ and estimated trophic level of the amphipod *T. gaudichaudii* was much lower than expected given the species' known behaviour as a raptorial predator (Pakhomov and Perissinotto, 1996; Froneman *et al.*, 2000; Watts and Tarling, 2012). However, other studies have also reported

relatively low $\delta^{15}N$ signatures in *T. gaudichaudii*, and together with herbivorous fatty acid biomarkers, suggests that this species is likely more omnivorous than previously thought, especially in juvenile stages (Stowasser *et al.*, 2012). Interestingly, the $\delta^{15}N$ values of *T. gaudichaudii* increased with corresponding increases in $\delta^{15}N$ of POM with depth (Figure 2.1, Figure 2.2), suggesting that this species may be tightly linked to the ambient food supply at the depth of its capture. The increased $\delta^{15}N$ signatures with depth may reflect differences in the developmental-stage due to vertical ontogenetic partitioning, with younger stages in surface waters and older stages (with heavier $\delta^{15}N$) at depth, which is commonly observed in pelagic amphipods (Bowman *et al.*, 1982).

The $\delta^{15}N$ signatures of *R. gigas* decreased relative to increasing $\delta^{15}N$ of POM with depth (Figure 2.1, Figure 2.2), suggesting that this species may not have been feeding directly on ambient POM at the depth at which they were captured, but in surface waters. *R. gigas* has been observed to undergo shallow diel vertical migration (DVM) (Atkinson *et al.*, 1992a;b; Conroy *et al.*, 2020). However, no pronounced synchronised DVM of zooplankton was observed at the time of the study (Cook *et al.*, 2023), suggesting that *R. gigas* in deep waters may not be feeding in surface waters at night. The negative relationship between $\delta^{15}N$ signatures of *R. gigas* and POM may be due to the deeper-dwelling individuals being metabolically inactive and therefore not feeding on ambient POM. Deeper-dwelling *R. gigas* collected concurrently with the present study had lower specific respiration rates than animals from shallower depths (Cook *et al.*, 2023), supporting this suggestion. This interpretation is further supported by high, but decreasing, lipid levels from visit P3B to P3C (Table 2.2), suggesting the use of internal energy reserves (see section 2.5.3).

2.5.3 Physiological ecology of copepod species

Differences in lipid and $\delta^{15}N$ signatures may reflect important, species-specific aspects of zooplankton life cycles and physiological requirements. The lipid class and fatty acid RDA analyses revealed a separation between *C. acutus, R. gigas* and *Paraeuchaeta* spp. and the rest of the zooplankton, with each copepod species forming a distinct cluster (Figure 2.6; Figure 2.7). The lipid class RDA (Figure 2.6) and compositional data (Table 2.5) demonstrate that fatty alcohols were important for discriminating these copepods from the rest of the species. Fatty alcohols are essential in the production of wax esters (WE), which are a major lipid class in these animals (Hagen *et al.*, 1993; Graeve *et al.*, 1994; Hagen *et al.*, 1995; Kattner and Hagen, 1995; Falk-Petersen *et al.*, 1999; Lee *et al.*, 2006; Ward *et al.*, 2012b). The copepods *C. acutus* and *R. gigas* had higher body lipid content (Table 2.2) compared to the other species, consistent with the seasonal production of large lipid reserves in polar non-carnivorous calanoid copepods (Hagen *et al.*, 1993; Graeve *et al.*, 1994; Kattner *et al.*, 1994; Falk-Petersen *et al.*, 1999). Large

lipid reserves are important in the ontogenetic behaviour of diapausing copepods, which migrate to deeper waters to overwinter and use stored lipids to fuel reproductive processes (sexual maturation, gonad development, and egg production/spawning) (Hagen and Schnack-Schiel, 1996) and regulate buoyancy (Pond and Tarling, 2011). *C. acutus* has a 1-year life cycle with intense grazing in spring/summer followed by a descent into deep waters where they undergo diapause and become inactive (Marin, 1988; Marin and Schnack-Schiel, 1993). *C. acutus* fatty acids were dominated by the PUFA 20:5(n-3) and the MUFAs 20:1(n-9), 16:1(n-7) and 22:1(n-11), in agreement with our understanding of the importance of long-chained moieties for diapausing species (Hagen *et al.*, 1993; Kattner and Hagen, 1995; Falk-Petersen *et al.*, 1999; Dalsgaard *et al.*, 2003).

R. gigas did not contain the calanoid copepod markers, 20:1(n-9) and 22:1(n-11), but instead was dominated by 20:5(n-3) and short-chained fatty acid and alcohol moieties, in agreement with the understanding that fatty acid biosynthesis in *R. gigas* likely ends with the elongation to 18:0 and conversion to 18:1 (Kattner *et al.*, 1994; Ward *et al.*, 1996). This contrasts with the wax ester composition of *C. acutus*, which is dominated by esters of 20:1(n-9) or 20:5(n-3) acids paired to ALC-20:1(n-9) (Pond and Tarling, 2011; Pond, 2012). *R. gigas* has been observed to have both 1- and 2- year life cycles, and various levels of diapause, with trophic inactivity, semi-activity and active feeding in winter (Marin, 1988; Hopkins *et al.*, 1993; Marin and Schnack-Schiel, 1993; Ward *et al.*, 1997; Pasternak and Schnack-Schiel, 2001; Tarling *et al.*, 2007). Intraspecific differences in life-strategies are likely related to environmental conditions, with *R. gigas* populations at the southern end of their geographical extent having 2-year life cycles due to slow growth rates and harsher environmental conditions (Ward *et al.*, 1997). Given its large, but decreasing lipid reserves and low $\delta^{15}N$ values, we suggest *R. gigas,* particularly deeper-dwelling individuals, at the P3 site in the Scotia Sea were metabolically inactive and using internal energy stores – indicative of some form of diapause. This highlights the need to understand how animal physiologies influence lipid and $\delta^{15}N$ signatures, rather than signatures being a reflection of just ecological and feeding dynamics. If overwinter behaviour was not considered, the low $\delta^{15}N$ signatures and dominance of diatom fatty acid biomarkers in *R. gigas* could be interpreted as their feeding on fresh diatoms from the surface.

The fate of primary production within the food webs of the epipelagic and upper mesopelagic is a major determinant of subsequent carbon sequestration in deeper waters. The different physiological ecologies elucidated from the lipid and stable isotope data highlight the importance of considering physiology when tracing carbon cycling. Determining the extent to which large herbivorous copepod species such as *R. gigas* and *C. acutus* undergo overwintering and hence do or do not always interact with the spring phytoplankton bloom will influence how we represent their role in attenuating the flux of sinking POM in the epi- and upper mesopelagic.

Similarly, determining where and on what zooplankton are feeding will increase our understanding of how these animals interact with and cycle organic matter. For instance, the preferential feeding on fresh, surface-derived POM rather than re-worked particles may modify the quality and quantity of organic matter leaving the upper mesopelagic.

2.6 Conclusion

The $\delta^{15}N$ signatures of particulate organic matter (POM) sampled at the P3 site in the Scotia Sea increased with depth, whereas the $\delta^{15}N$ signatures of zooplankton species generally did not. This suggests a decoupling between the feeding dynamics of zooplankton and ambient POM throughout the upper mesopelagic (>500m) at this location. We propose that non-carnivorous zooplankton in this region typically prefer to feed on surface-derived POM and not reworked particles found in deeper waters. The diatom fatty acid biomarkers, 16:1(n-7) and 20:5(n-3), were abundant in POM sampled at all depths, supporting the idea that fresh, surface-derived sinking POM was available throughout the epi- and upper mesopelagic, negating the need for migration to surface waters to access this material. *R. gigas* was the only non-carnivorous species not to conform to the consumption of diatom-based material throughout the water column; its $\delta^{15}N$ signature decreased with depth, suggesting that it was not feeding on ambient POM at their depth of capture. We suggest that the deeper-dwelling *R. gigas* and *C. acutus* were likely in the process of emerging from their overwintering physiology and still using stored energy reserves, as indicated by their large but decreasing lipid reserves between sampling visit P3B and P3C. Fatty acid and alcohol profiles of the non-copepod species were similar and characterised by both herbivorous and carnivorous biomarkers, suggesting generalist feeding strategies, in agreement with their life-strategies of active year-round feeding. *T. gaudichaudii* showed signs of potential vertical ontogenetic partitioning, with juvenile stages being more herbivorous than expected given the predatory nature of this species. Our study highlights the complexity of mesopelagic food webs and the importance of taking into account zooplankton physiology and suggests that the application of broad trophic functional types may lead to an incorrect understanding of ecosystem dynamics.

Chapter 3 Trophic ecology, metabolic budgets and mesozooplankton refuge in an oxygen minimum zone of the northern Benguela Upwelling System

Eloïse L-R. Savineau[1,2], Kathryn B. Cook[2,3], Sabena J. Blackbird[4], Gabriele Stowasser[5], Anna Belcher[5,6], Sophie Fielding[5], Nathan D. Hubot[2], Ryan A. Saunders[5], Daniel Bondyale Juez[7], Rona McGill[8], George A. Wolff[4], Geraint Tarling[5], Daniel J. Mayor[2,3]

[1] School of Ocean and Earth Science, University of Southampton, Southampton, SO14 3ZH, UK

[2] National Oceanography Centre, Southampton, SO14 3ZH, UK

[3] Present address: Biosciences, Hatherly Building, University of Exeter, Exeter, EX4 4PS, UK

[4] School of Environmental Sciences, University of Liverpool, Liverpool, L69 3GP, UK

[5] British Antarctic Survey, Cambridge, CB3 0ET, UK

[6] Present address: UK Centre for Ecology and Hydrology, Penicuik, EH26 0QB, UK

[7] EOMAR, Universidad de Las Palmas de Gran Canaria, Spain

[8] SUERC, East Kilbride, Glasgow, G75 0QF, UK

ES analysed the data and wrote the manuscript with support from KC and DM. KC, GS, AB, SF, NH and RS conducted sample collection and processing at-sea. KC and ES conducted the FlowCam sample processing and image classification. KC, DBJ and AB processed the ETS samples. KC calculated grazing rates. RM processed the stable isotope samples. SB processed the lipid samples. DM and KC contributed feedback on the manuscript.

Key words: fatty acids; lipids; stable isotopes; respiration; ingestion; grazing experiments; copepod; euphausiid; mesopelagic; fish; particulate organic matter; oxygen minimum zone

3.1 Abstract

The biological carbon pump (BCP) plays a critical role in sequestering atmospheric carbon dioxide (CO_2) by exporting particulate organic carbon (POC) from surface to deep ocean layers. However, the mesopelagic zone, where most POC attenuation occurs, remains poorly understood, particularly regarding the roles of mesozooplankton and micronekton in POC transformation and vertical carbon flux. This study characterized the trophic and physiological ecology, vertical distribution, diel vertical migration (DVM), and metabolic rates of mesozooplankton and micronekton from 0 – 750 m in the northern Benguela Upwelling System (nBUS), with a focus on interactions with the oxygen minimum zone (OMZ, <60 µmol/kg, ~200 – 450 m). Mesozooplankton biomass showed a bimodal distribution with peaks in biomass in the top 60 m of the water column and again within the OMZ between 250 – 500 m and showed no consistent synchronised DVM of biomass. The OMZ notably played an important role as a refuge from predation for both mesozooplankton temporary residents and permanently residing diapausing copepods. Micronekton performed extensive DVM, inhabiting surface waters at night and retreating below the OMZ during the day. While micronekton generally performed extensive DVM across the OMZ, OMZ expansion hindered DVM in Decapoda spp., highlighting the impacts of OMZs as a barrier to the vertical movement of some taxa. Our results moreover show that mesozooplankton and micronekton play a central role in the processing of carbon in the mesopelagic and within the OMZ, with elevated C:N ratios and animal-derived lipid signatures indicating significant heterotrophic reworking of POM.

3.2 Introduction

The ocean's biological carbon pump (BCP) plays a central role in regulating atmospheric carbon dioxide (CO_2) concentrations (Parekh *et al.*, 2006) by exporting organic carbon from surface to deep waters. The BCP is mainly driven by the production of particulate organic carbon (POC) in surface waters and subsequent transformation and remineralisation back into CO_2 by biological processes throughout the water column. The depth to which organic carbon reaches before being remineralised by organisms is key to determining the strength of the BCP, with deeper depths resulting in longer sequestration of carbon (Kwon *et al.*, 2009; Stukel *et al.*, 2023). However, POC flux is observed to attenuate most rapidly in the mesopelagic zone, that is, between the bottom of epipelagic productive waters and 1000 m (Buesseler *et al.*, 2007b). Mechanistically understanding the processes responsible for POC flux attenuation remains a major challenge in oceanography.

Metazoans such as zooplankton and micronekton are key contributors to the BCP. Zooplankton particle fragmentation, whereby zooplankton breakdown large particles into small suspended ones is thought to be the primary driver of POC attenuation and subsequent colonisation and remineralisation by microbes (Giering *et al.*, 2014; Mayor *et al.*, 2014; Mayor *et al.*, 2020). Zooplankton may act passively via repackaging of slow sinking POC into dense, fast sinking faecal pellets, and actively via grazing on POC and vertical migration, which transports carbon from surface waters to deeper waters (Steinberg and Landry, 2017). Diel vertical migration (DVM), whereby animals reside in deeper waters during the day and migrate to surface waters at night to feed, can enhance carbon export by transporting surface-derived carbon to depth, where a fraction of it is excreted, egested as faecal pellets or respired back into CO_2 (Jónasdóttir *et al.*, 2015; Steinberg and Landry, 2017). Carbon flux from migrating zooplankton respiration alone has been quantified to account for 2.8 % to 88.3 % of passive POC flux (Longhurst *et al.*, 1990; Dam *et al.*, 1995; Zhang and Dam, 1997; Hernández-León *et al.*, 2019b), and DVM is estimated to increase global carbon flux by 14 % (Archibald *et al.*, 2019). DVM is widely observed across trophic levels of zooplankton, micronekton and mesopelagic fish (Bandara *et al.*, 2021; Marohn *et al.*, 2021) and provides a link between epi- and mesopelagic zones and higher trophic levels (Davison *et al.*, 2013; Anderson *et al.*, 2019; Iglesias *et al.*, 2023). Understanding the vertical trophic ecology and physiology of mesozooplankton and micronekton, e.g., where they eat, what they eat, how much they eat, the depth at which they reside, how much they respire, and whether they perform DVM is therefore vital to understanding controls of carbon remineralisation in the ocean.

Despite clear consensus that mesopelagic zooplankton and micronekton are important to the BCP, the magnitude of contribution that these animals make to downward carbon flux is still uncertain. These uncertainties arise due to variability in sampling techniques for biomass estimates (Irigoien *et al.*, 2014; Underwood *et al.*, 2020), inter-taxa variability in DVM (Antezana, 2009; Barth *et al.*, 2023), intra-taxa variability in vertical distribution due to ontogeny (Hidalgo *et al.*, 2005), difficulties in measuring in-situ metabolic rates in the mesopelagic (McMonagle *et al.*, 2023), and the influence of hydrography and seasonality on their abundance, composition, physiology and DVM behaviour (Cisewski *et al.*, 2010; Bode *et al.*, 2014; Tutasi and Escribano, 2020; Cotté *et al.*, 2022; Liu *et al.*, 2022; Wiebe *et al.*, 2023; Baker *et al.*, 2025). The lack of a mechanistic understanding of these processes makes it difficult to accurately parametrise and represent POC remineralisation in biogeochemical models – which further affects our ability to reliably predict future ocean carbon storage and concomitant effects on climate.

The COMICS (Controls over Ocean Mesopelagic Interior Carbon Storage) programme aimed to shed light on the processes controlling mesopelagic zone remineralisation (Sanders *et al.*, 2016). Part of this programme focussed on exploring the role of dissolved oxygen (DO)

concentration in carbon export via the effects of low DO on metazoan physiological rates and DVM behaviour. DO concentration is thought to be an important control of interior ocean POC remineralisation, with Henson *et al.* (2012) demonstrating a reduction in mesopelagic remineralisation in low DO concentrations. Oxygen minimum zones (OMZs) have moreover been observed to experience high POC export (Van Mooy *et al.*, 2002; Roullier *et al.*, 2014; Keil *et al.*, 2016). The Benguela Upwelling System (BUS), located off the southwest coast of Africa, is among the most productive marine ecosystems globally, with an estimated annual primary production of 331 – 441 g C $m^2 y^{-1}$ (O'Reilly and Sherman, 2016). The northern BUS (nBUS) is typified by coastal upwelling with cold waters, high plankton productivity, and oxygen depleted waters (Hutchings *et al.*, 2009).

Hypoxic waters (<60 µmol O_2/kg, OMZ) constitute stressors for marine organisms, inducing physiological stress affecting metabolism, growth, and reproduction (reviewed by Roman *et al.* (2019)). Calanoid copepods have been observed to change their vertical distribution, depth of maximum occurrence, extent of DVM, and depth of diapause in response to the depth and intensity of the OMZ (Wishner *et al.*, 2020). Within the Eastern Tropical North Pacific OMZ, anoxic waters resulted in trophic partitioning of the pelagic food web, with zooplankton and fish below the anoxic core having greater $\delta^{15}N$ signatures, suggesting these animals were positioned higher up the food web (Gutiérrez-Bravo *et al.*, 2025). Tao *et al.* (2022) found the OMZ to act as a barrier to most species, preventing DVM through the entire water column, but also acting as a refuge and ecological niche for certain species adapted to low oxygen levels. In the Humboldt current, up to 60 % of krill have been observed to migrate into the OMZ during the day (Riquelme-Bugueño *et al.*, 2020). Seasonal ontogenetic vertical migrators, such as *Eucalanus inermis* have been observed to remain in constant low-oxygen habitats during diapause, likely as a predator avoidance mechanism (Wishner *et al.*, 2020). DVM behaviour is moreover suggested to exert control upon OMZs, with respiration by migrating animals intensifying oxygen-depletion in the upper layer of OMZs (Bianchi *et al.*, 2013). In the context of vertically expanding oxygen minimum zones (OMZs) (Stramma *et al.*, 2010), as observed in the nBUS over the past decades (Stramma *et al.*, 2008), quantifying the vertical distribution, DVM behaviour, trophic ecology and metabolic rates of mesozooplankton and micronekton in OMZ waters is integral to understanding how ocean biology and DO influences mesopelagic biogeochemistry.

Here, we address the effects of DO on the trophic ecology and physiology of mesozooplankton and micronekton inhabiting epi- and mesopelagic waters of the nBUS and subsequent effects on carbon cycling. Vertically stratified day and night depth profiles of mesozooplankton and micronekton biomass were collected down to 750 m to determine the extent of DVM and effects of DO on vertical biomass distributions. The trophic and physiological ecology of mesozooplankton and micronekton was investigated using stable isotope analyses of carbon

and nitrogen and lipid biomarkers to determine the movement of carbon within the ecosystems. The respiration rates of mesozooplankton and micronekton were measured using Electron Transport System (ETS) activity to determine metabolic respiratory carbon demands. Grazing experiments were conducted for the most common Copepoda species covering a range of different functional types. Biomass, grazing and respiration data were used to generate a carbon budget for mesopelagic zooplankton and micronekton communities and quantify active carbon export.

3.3 Methods

This study is part of the COMICS programme, which aims to shed light on the processes controlling carbon remineralisation in the mesopelagic (Sanders *et al.*, 2016). Samples were collected aboard the *RRS Discovery* during the DY090 research cruise, which targeted the low oxygen region offshore Namibia (23rd May – 28th June 2018) in the northern Benguela Upwelling System region in austral autumn (Henson et al., 2018). Sampling was focused at station BN (Benguela North, 18S, 11E), where three station cycles, defined as BN1 (1st – 7th June), BN2 (8 – 13th June) and BN3 (14 – 19th June) were completed.

3.3.1 Environmental data

Vertical profiles of temperature were obtained from Conductivity-Temperature-Depth (CTD) unit (SBE 9 plus) deployments. Oxygen data were collected using an SBE 43 dissolved oxygen sensor mounted on the ship's CTD frame. Oxygen sensor data were calibrated against dissolved oxygen concentration in water samples obtained from the CTD Niskin bottles and measured using the Winkler titration method (Henson *et al*, 2018). Temperature was measured using an SBE 3P temperature sensor. Fluorescence, used as a proxy for chlorophyll-a, was measured using a CTG Aquatracka MKIII fluorometer. CTD fluorescence was calibrated against Niskin bottle chlorophyll-a concentration samples collected concurrently with the CTD.

3.3.2 Particulate organic matter (POM) sample collection

Water samples for stable isotope analyses of POM were obtained via Niskin bottles attached to a CTD rosette. Samples were collected in surface waters and depths covering the net horizons (5, 25, 50, 75, 100, 200, 450, 750 m). Samples were filtered onto pre-combusted (450 °C; 12 h) 47 mm GF/F filters (Whatman glass fibre filter, nominal pore size 0.7 µm) and stored at -80 °C prior to analysis.

Samples for lipid analyses of POM were obtained using standalone pumps (SAPs) deployed within the mixed layer (ML; top 35 – 50 m), the base of the ML (35 – 50 m), 100 m, 250m, and 500 m. Two size fractions were sampled. Large particles (>53 µm) were collected on nylon mesh screens (Nitex; pore size 53 µm; 10 % HCl acid cleaned). Small particles (0.7 – 53 µm, <53 µm hereafter) were collected on pre-combusted (400 °C; 4 hours) 293 mm GF/F filters (nominal pore size 0.7 µm) located under the nylon mesh. All visible zooplankton/organisms were removed from the filters. After filtering, samples were folded, wrapped in foil and frozen at -80 °C for later analysis.

3.3.3 Mesozooplankton and micronekton

3.3.3.1 Net sampling

A range of nets were used to capture the vertical distribution of epipelagic and mesopelagic (0 – 750 m) mesozooplankton and micronekton communities. Animals were collected with a combination of RMT25 (Rectangular Midwater Trawl, 25 m^2 net mouth, 4 mm mesh), a Multiple Opening-Closing Net and Environmental Sampling System (MOCNESS) net (330 µm, 1m^2 rectangular opening), a Hydrobios Mammoth MultiNet (fitted with either nine 300 µm mesh nets (Mammoth-300 hereafter) or four 100 µm mesh nets (Mammoth-100 hereafter), and a Bongo net (100 µm, 53 cm diameter ring openings). The nets were deployed over a range of discrete depth intervals from 750 m to the surface, deployed either obliquely (RMT25 and MOCNESS), or vertically (Mammoth-300, Mammoth-100 and Bongo). The RMT25 had two nets with independent opening/closing mechanisms. Throughout the expedition, two RMT25 deployments were made per station, with the first deploying from 750 – 500 m and 500 – 250 m, sampling for 40 minutes per net. The second deployment was made from 250 – 125 m and 125 – 10 m, sampling for 20 minutes per net. The MOCNESS opening/closing mechanisms failed during DY090, therefore for all deployments only one net was towed open from 0 – 125 m and back to the surface. The Mammoth-300 was consistently deployed at preset opening/closing depths dividing the water column into the following intervals: 750 – 625, 625 – 500, 500 – 375, 375 – 250, 250 – 187, 187 – 125, 125 – 62, 62 – 31, 31 – 5 m. The Mammoth-100 was consistently deployed at preset opening/closing depths dividing the water columns in the following intervals: 750 – 500, 500 – 250, 250 – 125, 125 – 5 m. Bongo nets were deployed to 120 m. All nets were deployed during both the day and night. An infographic of how all the nets were deployed, and at which depths, is illustrated in Figure 3.1. Full net sampling protocol can be found in the DY090 cruise report (Henson *et al*, 2018). Once onboard, the net cod ends were immediately transferred into a temperature-controlled laboratory (8 °C) for sample handling. A summary of the animals caught in the different nets can be found in Appendix B Table B 1.

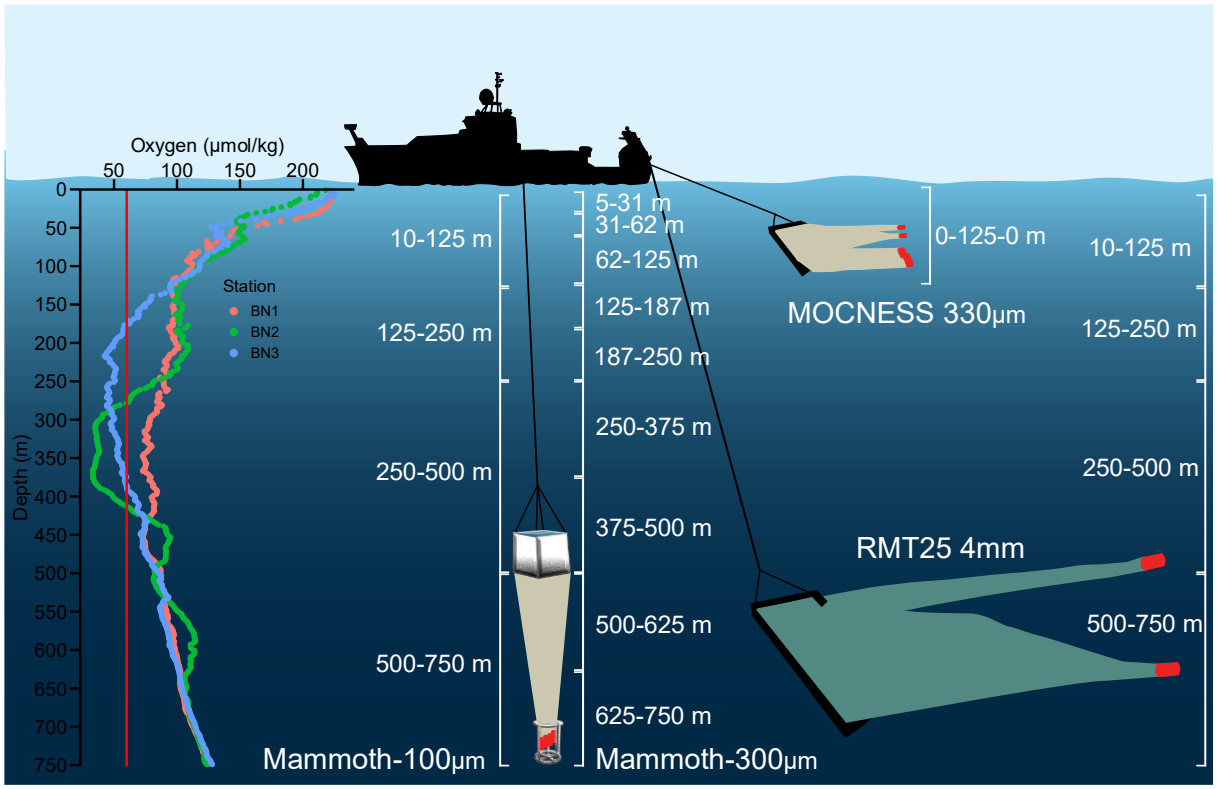

Figure 3.1 Schematic of zooplankton and micronekton nets used during this study and their respective depth profiles. Mean oxygen concentration (µmol/kg) depth profiles during each station visit (BN1-BN3) in the northern Benguela Upwelling System. Vertical red line represents the cut-off for hypoxic waters defined as oxygen concentrations < 60 µmol/kg.

3.3.3.2 Sample handling

MOCNESS catches were split into two aliquots, with one half of the catch being retained in 4 % borax buffered formaldehyde for biomass analysis and the remaining half being used to pick animals for stable isotope, lipid and ETS analyses. Mammoth-300 catches were split into two aliquots, using a Folsom plankton splitter, with one half being preserved in 4 % borax buffered formaldehyde for biomass analysis and the second aliquot being filtered onto pre-ashed 47 mm GF/F filters for Electron Transfer System (ETS) activity analysis and frozen at -80 °C. Mammoth-100 catches were split into four aliquots and preserved for ETS analysis (1/4, liquid nitrogen, -80 °C), stable isotope analysis (1/4, -80 °C), biomass (1/4, 4 % borax buffered formaldehyde). Bongo catches were divided in two, with the entire content of one of the Bongo cod-ends being preserved in 4 % borax buffered formaldehyde, and the other cod-end catch being size fractionated (100 µm, 200 µm, 500 µm, 1000 µm, 2000 µm), filtered onto a GF/F and frozen at -80 °C for subsequent ETS activity analysis. RMT25 catches were processed to record total wet weight (WW) in each net haul. The most common individual macrozooplankton, squid, and fish were identified to species level where possible, and number of animals taken for ETS and stable

isotope analysis were weighed and recorded. Specimens for stable isotope analysis and lipid analysis were frozen at -80 °C and samples for ETS were flash-frozen in liquid nitrogen and stored at -80 °C. The mean individual WW of micronekton species were calculated using the total WW and total abundance for each species. The remainder of the catches were preserved in 4 % borax buffered formaldehyde.

3.3.4 Stable isotopes analyses

Animal specimens were weighed (wet weight), freeze-dried whole and then re-weighed (dry weight). Samples were homogenised using an oscillating mill (MM200, Retsch). To prevent lipid associated bias in $\delta^{13}C$ measurements (Post *et al.*, 2007) tissue samples were split and the aliquot used for carbon isotope measurement was delipidated. Lipid was extracted using a solvent mixture of chloroform:methanol (2:1) (several washes until the solution appeared clear). Samples were then rinsed with distilled water and oven-dried for 24 hours at 50 °C prior to isotope analysis.

Filters containing particulate organic matter (POM) were freeze-dried and split into two halves. To remove inorganic carbon, the filter halves intended for carbon isotope measurements were fumed for 24 hours with 37 % HCL in a desiccator and then oven-dried at 50 °C for 24 h.

Isotopic analyses were carried out at the Scottish Universities Research Centre (SUERC), East Kilbride, Glasgow, UK. Aliquots for nitrogen isotopes were weighed into tin capsules (0.6 – 1 mg) and measured on a Thermo-Fisher-Scientific (Bremen, Germany) Delta XP Plus Isotope-Ratio Mass Spectrometer linked to an Elementar (Hanau, Germany) Pyrocube Elemental Analyser. The internal reference materials were GEL (gelatin solution, $\delta^{15}N$= 5.71 ± 0.15 ‰), ALAGEL (alanine-gelatine solution, $\delta^{15}N$ = 2.52 ± 0.08 ‰), and GLYGEL (glycine-gelatine solution spiked with 15N-alanine, $\delta^{15}N$ = 23.60 ± 0.12 ‰), each dried for two hours at 70 °C. The glutamic acid standard USGS40 was run four times as independent checks of precision and accuracy. Delta (δ) values were corrected for instrument drift and linearity. δ values are used to express the relative difference between the ratios of two stable isotopes, e.g., ^{15}N and ^{14}N in organisms, expressed as $\delta^{15}N$, compared to the international reference standard for nitrogen isotopes ($\delta^{15}N$ of atmospheric nitrogen gas).

3.3.5 Lipid analyses

Zooplankton and micronekton lipid extractions were carried out on each homogenised freeze-dried (-60 °C; 10^{-2} mBar) sample (1 – 60 mg dry weight). A known quantity of an internal standard (3 - 10 µgL of 5α(H)-cholestane) was added to each sample, followed by a mixture of dichloromethane and methanol (9:1; 15 mL). The samples were then sonicated (15 min, x2) and

the resulting extract was decanted into round bottom flasks. The solvent obtained was evaporated to dryness under vacuum using a rotary evaporator at ~30 °C. Each sample was then passed through a Pasteur pipette filled with anhydrous sodium sulphate using dichloromethane (3 mL). The solvent was blown down with nitrogen gas and the samples were stored (-20 °C) before transmethylation and derivatisation with N,O-bis-(trimethylsilyl)trifluoroacetamide (BSTFA). Lipids from the POM samples were extracted in a similar way (Kiriakoulakis *et al.*, 2004).

Gas chromatography-mass spectrometry (GC-MS) analyses of the total lipid extracts were conducted using a GC Trace 1300 fitted with a split-splitless injector and column DB-5MS (60 m x 0.25 mm (i.d.), with film thickness 0.1 µm, non-polar stationary phase of 5 % phenyl and 95 % methyl silicone), using helium as a carrier gas (2 mL min^{-1}). The GC oven was programmed after 1 minute from 60 °C to 170 °C at 6 °C min^{-1}, then from 170 °C to 315 °C at 2.5 °C min^{-1} and held at 315 °C for 15 min. The eluent from the GC was transferred directly via a transfer line (320 °C) to the electron impact source of a Thermoquest ISQMS single quadrupole mass spectrometer. Typical operating conditions were: ionisation potential 70 eV; source temperature 215 °C; trap current 300 µA. Mass data were collected at a resolution of 600, cycling every second from 50 – 600 Daltons and were processed using Xcalibur software.

Compounds were identified either by comparison of their mass spectra and relative retention indices with those available in the literature, and/or by comparison with authentic standards. Shorthand notations of fatty acids and alcohols follows the IUPAC (International Union of Pure and Applied Chemistry, hhtp://www.iupac.org) systematic nomenclature ‘n-x’ notation. Quantitative data were calculated by comparison of peak areas of the internal standard with those of the compounds of interest, using the total ion current (TIC) chromatogram. The relative response factors of the analytes were determined individually for fatty acids and sterols using authentic standards. Response factors for analytes where standards were unavailable were assumed to be identical to those of available compounds of the same class.

3.3.6 Biomass

3.3.6.1 Mesozooplankton

The preserved Bongo, Mammoth-100 and Mammoth-300 samples were sub-sampled, where necessary, using a folsom splitter, and diluted to 1L using filtered seawater. The number of splits ($Frac_{split}$, e.g., ½, ¼) for each sample was recorded. Samples were pumped through and imaged using a FlowCam Macro (Yokogawa Fluid Imaging Technologies Inc.), fitted with a 5 mm flow cell, a flow rate of 700 ml min^{-1} and an auto-image mode rate of 10 frames per second.

Images were classified into broad taxonomic groups (Table B 1) using Visual Spreadsheet (v4.19.5 and v5.6.14) to determine abundance.

Biomass was calculated using area data from the images, via the FlowCam's area area-based diameter algorithm (areaABD). Firstly, dry weight (DW, µg ind $^{-1}$) was calculated following the regression between body area of an individual taxa and its DW (Lehetter and Hernandez-Leon, 2009):

$$DW_{ind} = a \times areaABD_{ind}{}^{b} \times \frac{1}{1000} \qquad (eq\ 3.1)$$

Where a and b are coefficients. Different coefficients were used for each species/taxa where available (see Table B 2). If no species or taxa specific coefficients were found, 'general mesozooplankton' coefficients were used (Table B 2).

Integrated DW (DW_{int}, µg m^{-3}) was calculated by summing all individual DW for a taxa, dividing by the split fraction ($Frac_{split}$) and the volume of water sampled (V_{net}, m^3):

$$DW_{int} = \frac{\sum DW_{ind}}{Frac_{split} \times V_{net}} \qquad (eq\ 3.2)$$

Biomass, in molar carbon content (C, µmol m^{-3}) was calculated using C:DW ratios of individual taxa obtained from literature (Table B 2) and dividing by the molar mass of carbon (12.011).

3.3.6.2 Micronekton

Micronekton biomass was calculated based on WW, converted to DW using the regression:

$$\log(DW) = a + b \times \log(WW) \qquad (eq\ 3.3)$$

Where a and b are regression coefficients for different taxa, either from our own measurements of DW/WW or from literature (Table B 3), or using the equation:

$$DW = WW \times c \qquad (eq\ 3.4)$$

Where c is the conversion factor for specific taxa (Table B 4).

Biomass, in molar carbon content (C, µmol m^{-3}) was calculated using C:DW ratios of individual taxa obtained from literature (Table B 3 and Table B 4) and dividing by the molar mass of carbon (12.011).

3.3.6.3 Weighted Mean Depth

To analyse the vertical distribution of the total biomass and selected taxa of interest, the Weighted Mean Depth (WMD) during the day and night were calculated according to the following equation:

$$WMD\ (m) = {\Sigma(b_i \times d_i)}/{B} \qquad (eq\ 3.5)$$

Where b_i is the biomass (µmolC m^{-3}) in the net i, d_i is the mid-depth (m) of the net i, and B is the biomass in all the nets, for an event. Day WMD was subtracted from night WMD to determine the depth change due to diel vertical migration (ΔWMD).

3.3.7 Respiration

3.3.7.1 Electron transport system (ETS) activity

Mesozooplankton and micronekton respiration was estimated via ETS activity. ETS activity assays were carried out following the method of Owens and King (1975) with modifications from Gómez *et al*. (1996). Frozen specimens were reweighed in the laboratory. For mesozooplankton measurements, the whole net sub-sample (split or size fractionated) were used for the assays. For micronekton species, whole individuals were used. For fish, we used a weighed sub-sample of tissue collected from just behind the head. Each sample was homogenised in a phosphate buffer, using either an electric homogeniser or a sonicator, for 30 – 60 s, before being centrifuged at 4000 rpm for 10 min at 0 °C. 100 µL of the homogenate supernatant and 300 µL of reaction buffer (0.1 M, pH 8.5) containing substrates nicotinamide adenine dinucleotide (NADH) and nicotinamide adenine dinucleotide phosphate (NADPH) (saturating concentrations of 1.7 and 0.25 mM, respectively) were added to a semi-micro quartz cuvette. 100 µL 2-p-iodophenyl-3-p-nitrophenyl monotetrazolium chloride (INT, 4 mM) was added to each cuvette to commence the reaction. All procedures were carried out on ice. The reaction was measured continuously for 8 min at a wavelength of 490 nm in a Cary 60 UV–Vis spectrophotometer (Packard and Christensen, 2004). The temperature of the reaction was controlled at 12 °C. A blank assay was also performed without ETS substrates for each sample to account for the non-enzymatic reduction of INT (Maldonado *et al.*, 2012). Reagent blanks were taken daily.

Formazan is produced during the kinetic assay as INT is reduced. INT takes the place of oxygen as the electron acceptor in the ETS and accepts two electrons (oxygen would accept four). Therefore, the rate of formazan produced is related to oxygen consumption by a factor of two. Using the formazan production rate and our measured INT extinction coefficient (measured at 490 nm for each batch of INT; 13.3–16.4 $mM^{-1}\ cm^{-1}$) we calculated the potential respiration rate

(Φ, μmol O_2 h^{-1}) following Packard and Christensen (2004). Using a conservative respiration to ETS (R:ETS) ratio of 0.5 (Ikeda, 1985; Hernández-León and Gómez, 1996), we then estimated the respiration at the experimental temperature of 12 °C. Where a subsample was taken (i.e. for fish), the total respiration rate per individual was calculated based on the ratio between the subsample and the total weight of the fish. To estimate the respiration rate at in situ temperatures, defined as the temperature from the CTD averaged over the net depth horizon, we used the Arrhenius equation and an activation energy of 62.8 kJ mol^{-1} (15 kcal mol^{-1}) (Packard *et al.*, 1975; Ariza *et al.*, 2015; Hernández-León *et al.*, 2019a). Respiration rates per hour were multiplied by 24 to give respiration rates per day and converted from oxygen to carbon using the stoichiometric relationship between carbon and oxygen (22.4 μL O_2 = 12.01 μg C) and respiratory quotient of 0.9 (Ariza *et al.*, 2015).

3.3.7.2 Mesozooplankton respiration

Carbon specific respiration rates (μmol C μmol C^{-1} d^{-1}, expressed as d^{-1}) were calculated from ETS measurements and applied to the biomass estimates from the Mammoth-100 and Mammoth-300 samples. WW of the ETS samples were converted to DW using a conversion factor of 0.25 (Kiørboe, 2013) and then to C using a conversion factor of 0.45 (Giering *et al.*, 2019b).

3.3.7.3 Micronekton respiration

For the species where we measured ETS activity, we calculated allometric regressions relating WW (mg) to ETS-derived respiration (μL O_2 Ind^{-1} h^{-1}), with the following equation:

$$\ln(Respiration) = a_0 + a_1 \times \ln(WW) \qquad (eq\ 3.6)$$

Where a_0 and a_1 are constants for the different taxa for which ETS-assays were run (Table B 5). It was not feasible to sample and conduct ETS assays on all species, therefore we used allometric relationships from the literature to estimate respiration rates (μL O_2 Ind^{-1} h^{-1}) for species we did not measure (Belcher *et al.*, 2020). The respiration rate of taxa not sampled for ETS were calculated taking the data from, and following the form of the regressions given in, Ikeda (2014):

$$\ln(Respiration) = a_0 + a_1 \times \ln(DW) + a_2 \times 1000/T + a_3 \times \ln(z) \qquad (eq\ 3.7)$$

Where DW is dry weight (mg), T is temperature (K) and z is habitat depth (m) and a_0, a_1, a_2 and a_3 are constants for specific taxa (Table B 6). For cephalopods, we used the data from Ikeda (2016) and carried out the same procedure as above but using body mass as WW. Where allometric equations required DW, we made appropriate conversions using a combination of our own measurements and conversions from the literature (Table B 3 and Table B 4). Once individual respiration rates were calculated, these were then divided by the tow volume and

multiplied by 24 to give respiration rates in units of μL O_2 m^{-3} d^{-1}. We converted from oxygen to carbon using the stoichiometric relationship between carbon and oxygen (22.4 μL O_2 = 12.01 μg C) and respiratory quotient of 0.9 (Ariza *et al.*, 2015).

3.3.7.4 Total community respiration

Total community respiration was summed over the depth ranges that samples were taken from for each net.

3.3.8 Ingestion

3.3.8.1 Copepod grazing experiments

Experiments were conducted to quantify copepod grazing rates in surface waters. Experimental animals were collected using the Bongo net deployed in the upper 120 m and sorted using a dissection microscope. All experiments were conducted in a refrigerated container at 12 °C. Experimental water was collected via the CTD or using the Marine Snow Catcher. Grazing rates were examined using particle-removal experiments (Mayor *et al.*, 2006). In brief, glass incubation bottles were filled with un-screened seawater a little at a time to maximise homogeneity. Visibly discernible copepods were removed from the incubation bottle via a dip-tube. Experimental animals were carefully introduced into bottles and incubated in triplicate alongside triplicate control bottles in the dark on a plankton wheel rotating at 1 rpm for 24 h. Microplankton samples (200 mL) from the start of the experiment and from each of the incubated bottles were collected and preserved with acidified Lugol's iodine (1%).

Experiments were conducted for the dominant copepod species that represented different functional feeding types in the copepod community: small particle associated copepods (*Oithona* spp.), small (*Nannocalanus minor, Pleuromamma* spp., *Centropages brachiatus*), intermediate (*Calanoides natalis,* formerly identified as *Calanoides carinatus*) and large (*Eucalanus hyalinus*) filter-feeding copepods, and strongly migrating copepods (*Metridia* spp.).

The concentration of different cell types from the preserved microplankton samples were counted using a FlowCam 8400 (Yokogawa Fluid Imaging Technologies Inc.) fitted with a 10x objective and a FOV100 flow cell, at a flow rate of 0.25 ml min^{-1}. Images were collected using auto-image mode at a rate of 37 frames per second. Libraries of dominant cell types were created and used in conjunction with size filters to classify particles automatically into broad taxonomic groups (flagellates, small dinoflagellates, large athecate dinoflagellates, large thecate dinoflagellates, ciliates, pennate diatoms, centric diatoms and unidentified cells) using VisualSpreadsheet software (Version 4.3.55). Automatic classifications were checked manually

and corrected when necessary (~50 % of particles). Biomass (µg C) was calculated using particle volume (µm^3) and published carbon to volume relationships (Alldredge, 1998; Menden-Deuer and Lessard, 2000). Ingestion rates were calculated using the equations of Frost (1972) and converted to carbon specific ingestion rates using published estimates of copepod biomass (Schukat *et al.*, 2013b; Bode-Dalby *et al.*, 2022).

3.3.8.2 Total community ingestion

Carbon specific ingestion rates (amount of carbon ingested per carbon biomass of the animal per day, µg C µg C^{-1} d^{-1}) were applied to the biomass of taxa from the net samples to calculate total daily ingestion rates (µmol C m^{-3} d^{-1}). Specific ingestion rates obtained from the grazing experiments were applied to other copepod taxa sharing similar body size and feeding strategies. Where available, published values for specific ingestion rates were used for other taxa and micronekton (Table B 7). Where no published data was available, mean specific ingestion rates of the compiled data was used.

3.3.8.3 Community ingestion from respiration

Community ingestion was also estimated from community respiration using the following equation from (Ikeda and Motoda, 1978):

$$I_s = 100 \times R_s/(70 - 30) = 2.5R_s \qquad (eq\ 3.8)$$

Where I_s is ingestion for a sample, R_s is the community respiration for that sample, 70 is the value for absorption efficiency of zooplankton and 30 is the mean value for gross growth efficiency (K_1) of zooplankton (Ikeda and Motoda, 1978; Straile, 1997). For micronekton an absorption efficiency of 75 % and K_1 of 18 % was used (Ikeda, 1996).

3.3.9 Migrant biomass and active flux

Migrant biomass was obtained as the difference between the integrated values of night and day biomass in the upper 125 m of the water column. This depth was chosen to allow for consistency across all sampling gear due to coarser resolution of the Mammoth-100 and RMT25 nets, which had surface layers down to 125 m. This choice of depth is likely to result in conservative estimates of migrant biomass and active flux by zooplankton as the mixed layer depth was consistently < 50 m, therefore it can be assumed that any migration beyond 50 m would be quantified as active migration beyond the mixed layer.

For mesozooplankton, the active respiratory flux was obtained from whole community ETS assay derived average carbon specific respiration rates (d^{-1}) in the 125 – 750 m layer during the day when normal DVM was observed or during the night when reversed DVM was observed. The

average carbon specific respiration rate (d^{-1}) was divided by 24 to get the average carbon specific respiration rates (h^{-1}) and then multiplied by 11 h of zooplankton residence at depth during the day (or 13 h at night for reverse DVM). This respiration at depth was then multiplied by the migrant biomass to assess the respiratory flux of zooplankton DVM in µmol C m^{-3} 11 h^{-1} (13 h^{-1} for reverse DVM). Total active flux was estimated considering respiration, excretion and mortality at depth. Dissolved organic carbon (DOC) excretion flux by zooplankton was assumed to be equal 31 % of respiratory carbon flux (Steinberg *et al.*, 2000). Growth was assumed to be equal to mortality, therefore mortality was calculated to be equal 75 % of respiratory carbon flux (Ikeda and Motoda, 1978).

For micronekton from the RMT net, active respiratory flux for the migrating biomass (µL O_2 m^{-3} h^{-1}) was calculated based on the allometric regressions relating WW (mg) to ETS-derived respiration (section 3.3.7.3), using the mean depth of daytime residence (here described as the mean depth between 125 – 750 m) and the mean temperature at depths of 125 – 750 m. Finally, this was multiplied by 11 h (daytime length) to give respiration and converted from oxygen to carbon using the stoichiometric relationship between carbon and oxygen (22.4 µL O_2 = 12.01 µg C) and respiratory quotient of 0.9 (Ariza *et al.*, 2015). We then converted respiration rates back into µmol C m^{-3} 11 h^{-1}. DOC excretion data for micronekton and fishes are lacking, therefore the same excretory quotient as zooplankton (31 % of respiratory flux) was used for micronekton (Hudson *et al.*, 2014). Mortality was calculated to be equal to 66 % of respiratory flux (Brett and Groves, 1979; Kwong *et al.*, 2020).

3.3.10 Data analysis

Wilcoxon rank sum tests were used to test whether the biomass of zooplankton and micronekton and stable isotope signatures of POM changed between station visits. The relationships between $\delta^{15}N$, $\delta^{13}C$, depth and station visit for POM, zooplankton and micronekton were investigated using linear regressions. To deal with differences in individual compound concentrations between zooplankton/micronekton/POM samples, quantitative lipid data (individual fatty acids/alcohols) were converted to relative abundances (mol%) of total identified lipid. The relationships between individual lipids and depth were investigated using linear regression. The influence of POM size fraction (<53 µm vs. >53 µm), station visit (BN1, BN2, BN3) and environmental variables on the composition (mol%) of fatty acids were examined using redundancy analysis (RDA). The influence of animal taxa, station visit and environmental variables on the composition (mol%) of fatty acids were also examined using RDA analysis. Fatty acids that accounted for <3 % of total fatty acids and had missing values for individual taxa were excluded from the RDA analysis as RDA sees zero values as similar (Zuur *et al.*, 2007). Collinearity between variables was examined using pairwise correlation matrices with

correlations above 0.7 or below -0.7 suggesting strong collinearity. Temperature and salinity were removed due to strong collinearities with depth (see correlation matrix in Appendix B Figure B 1). The significance of individual model terms were determined using a permuted (n=9999) stepwise procedure to assess how the addition of each explanatory variable increased or decreased the adjusted R^2. Additional RDA analyses were conducted to investigate whether the compositions of lipid classes were influenced by the different taxa. All statistical analyses were conducted in the R v4.2.3 programming environment (R Core Team, 2023) using the 'Vegan' package (Oksanen *et al.*, 2020b). Data obtained at the BN station during each visit is summarised in Table 3.1.

Table 3.1 Summary of particulate organic matter (POM), zooplankton and micronekton data available at each visit of the BN station in the northern Benguela Upwelling System.

	BN1	**BN2**	**BN3**
POM stable isotopes	✓	✓	✓
Zooplankton/micronekton stable isotopes	✓	✓	✓
POM lipids	✓	✓	✓
Zooplankton/micronekton lipids	✓	✓	✓
Bongo size-fractionation	✓	✓	✓
Mammoth-100 biomass (>100 µm)	✓	✓	
Mammoth-300 biomass (>300 µm)	✓	✓	
RMT25 biomass (>4 mm)	✓	✓	✓
ETS	✓	✓	✓
Grazing experiments	✓	✓	✓

3.4 Results

3.4.1 Physical properties

Hypoxic waters at depths between ~200 and 450 m were observed during all 3 visits to the northern Benguela station (BN1 - BN3, Figure B 2). Chlorophyll-a concentrations were highest in the top 50 m of the water column (Figure B 2) and the mean mixed layer depth (MLD) rarely exceeded 50 m (Lovecchio *et al.*, 2022). Temperature ranged between 20.8 °C in surface waters

and decreased down to 4.7 °C at 750 m (Figure B 2). Detailed description of the sampling environment and water masses movements at the nBUS during this cruise can be found in (Lovecchio *et al.*, 2022; Lovecchio *et al.*, 2025).

3.4.2 Ecosystem biomarkers

3.4.2.1 Stable isotope signatures of POM

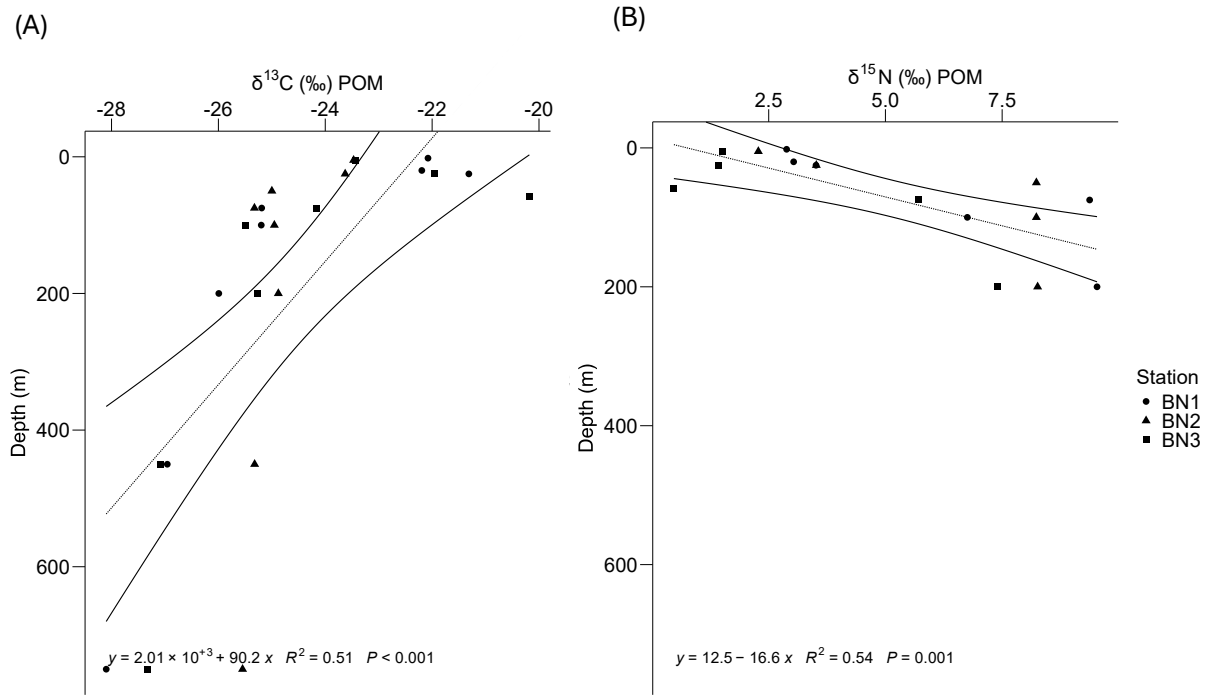

Figure 3.2 (A) $\delta^{13}C$ and (B) $\delta^{15}N$ stable isotope signatures (‰) of particulate organic matter (POM) at station BN in the northern Benguela Upwelling System. The regression lines indicate statistically significant ($p < 0.05$) relationships between $\delta^{13}C$ and depth and $\delta^{15}N$ and depth. Limited $\delta^{15}N$ measurements were available beyond 200 m due to insufficient nitrogen being present on the filters to get reliable values, with only one measurement > 200 m ($\delta^{15}N$ of 6.80 ‰ at 750 m) being recorded. This datum was omitted from the linear regression of $\delta^{15}N$. Standard errors are illustrated either side of the regression line. $\delta^{13}C$: y = 2011.6 (±465.7) – 90.2 (±18.9) x ; $\delta^{15}N$: y = 12.5 (±24.4) – 16.6 (±4.1) x

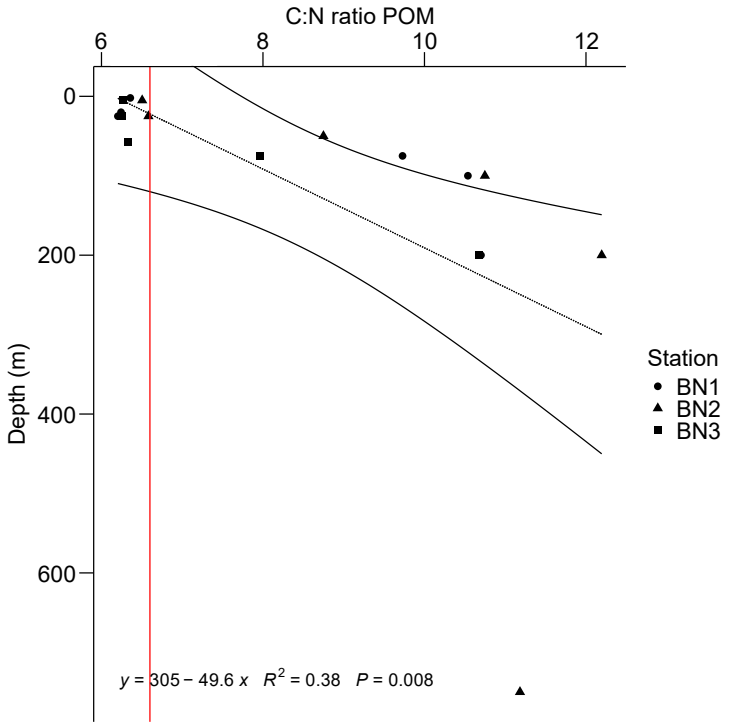

Figure 3.3 Molar POC:PN (particulate organic carbon/particulate nitrogen, C:N) for POM collected at station BN in the northern Benguela Upwelling System. The red dashed line represents a Redfield ratio of C:N = 106:16. The regression line indicates a statistically significant ($p < 0.05$) relationship between C:N ratios of POM and depth. Standard errors are illustrated either side of the regression line, y = 305 (±141) -49.6 (±16.3) x.

The $\delta^{15}N$ signatures of POM ranged between 0.47 – 9.53 ‰ and became isotopically enriched with depth down to 200 m ($F=16.43_{1,14}$, $p=0.001$, $R^2=0.54$; Figure 3.2). $\delta^{13}C$ signatures of POM ranged between -28.1 and -20.2 ‰ and became isotopically depleted with depth ($F=22.81_{1,22}$, $p<0.001$, $R^2=0.51$; Figure 3.2). No change in $\delta^{13}C$ or $\delta^{15}N$ signatures of POM with station visit (BN1-BN3) were observed ($p>0.05$). C:N ratios of POM ranged between 6.2 – 12.2 and increased with depth down to 200 m ($F=9.29_{1,15}$, $p=0.008$, $R^2=0.38$; Figure 3.3). Station visit had no effect ($F=0.41_{1,14}$, $p=0.42$, $R^2=0.12$).

3.4.2.2 Stable isotope signature of animals

The $\delta^{15}N$ signatures of the animals ranged between 4.86 ‰ and 14.70 ‰, with lowest values observed in *Rhincalanus nasutus* (Figure 3.4). All mesozooplankton species, except for Chaetognatha spp., had lower $\delta^{15}N$ values compared to the mesopelagic fish. Nemichthyidae spp. and Gymnoscopelus sp. were on average less $\delta^{15}N$ enriched compared to Chaetognatha spp.. *Cyclothone* spp. had the greatest $\delta^{15}N$ values. The $\delta^{13}C$ signatures of the animals ranged between -14.5 ‰ and -19.2 ‰ (Figure 3.4) and were more enriched than that of POM.

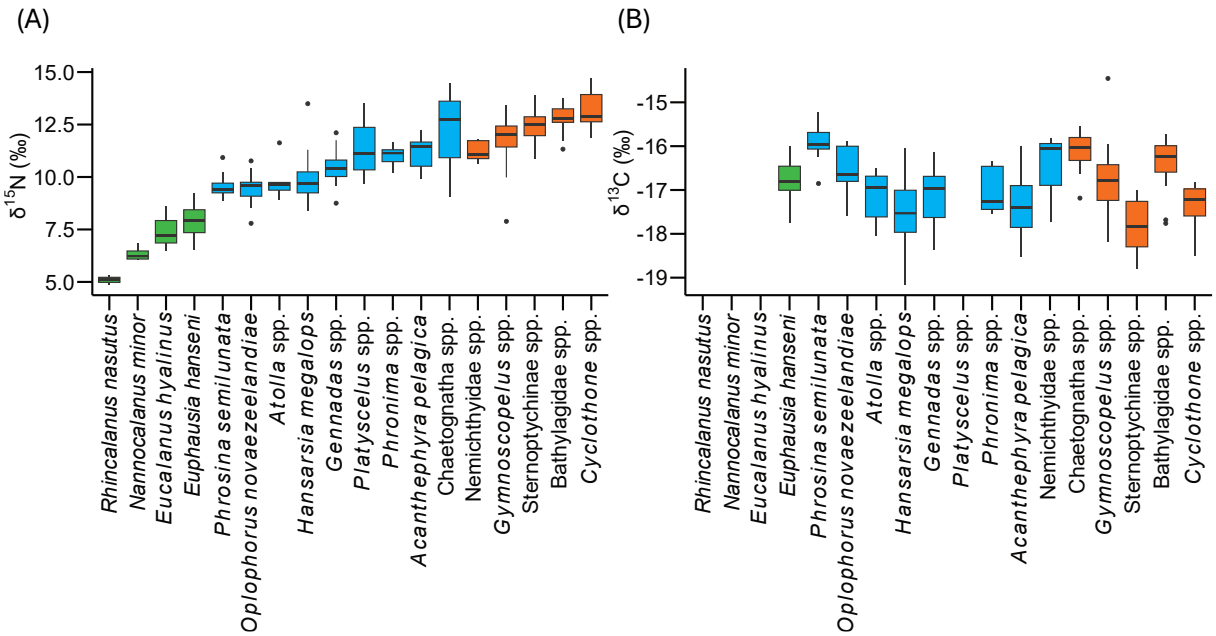

Figure 3.4 (A) $\delta^{15}N$ and (B) $\delta^{13}C$ stable isotope signatures (‰) of mesozooplankton and micronekton at station BN in the northern Benguela Upwelling System. The boxplot represents the minimum, maximum, median, first quartile and third quartile values. Circles represent outliers. Green denotes mesozooplankton taxa, blue denotes macrozooplankton and orange denotes mesopelagic fish taxa. No $\delta^{13}C$ signatures were available for *Eucalanus hyalinus*, *Nannocalanus minor, Rhincalanus nasutus* and *Platyscelus* spp. because the lipids from within these species were not successfully extracted prior to carbon isotope measurements and resulted in these samples not being reliable for $\delta^{13}C$ analyses. *Rhincalanus nasutus* analysed were all stage C6 females. *Nannocalanus* spp. were all C6 females. *Eucalanus* spp. were all C6 females.

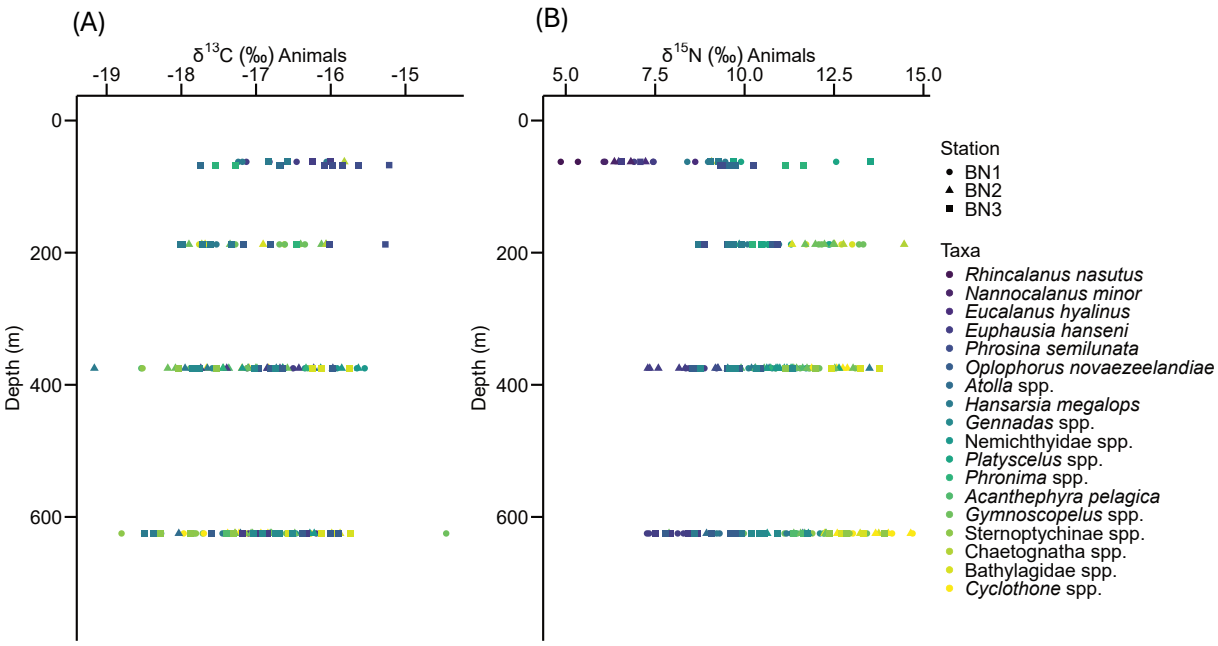

Figure 3.5 Vertically resolved (A) $\delta^{13}C$ and (B) $\delta^{15}N$ stable isotope signatures (‰) of animals at station BN in the northern Benguela Upwelling System. No $\delta^{13}C$ signatures were available for *Eucalanus hyalinus*, *Nannocalanus minor, Rhincalanus nasutus* and *Platyscelus* spp. because the lipids from within these species were not successfully extracted prior to carbon isotope measurements and resulted in these samples not being reliable for $\delta^{13}C$ analyses. *Rhincalanus nasutus* analysed were all stage C6 females. *Nannocalanus* spp. were all C6 females. *Eucalanus* spp. were all C6 females.

The $\delta^{13}C$ signatures of zooplankton and micronekton did not change with depth nor station visit ($F=2.73_{1,193}$, p=0.1, $R^2=0.01$; $F=1.24_{2,192}$, p=0.29, $R^2=0.003$ respectively; Figure 3.5). There was a weak overall trend of increasing $\delta^{15}N$ values with depth, driven by Bathylagidae spp., *Acanthephyra pelagica* and *Euphausia hanseni* ($F=5.36_{(1,13)}$, p=0.038, $R^2=0.29$; $F=6.03_{(1,9)}$, p=0.036, $R^2=0.40$; $F=5.62_{(1,23)}$, p=0.026, $R^2=0.20$ respectively; Figure B 3). Station visit had no effect (p>0.05). All other species showed no relation between $\delta^{15}N$ and depth (p>0.05). C:N ratios of zooplankton and micronekton ranged between 3.11 – 9.85 (Figure 3.6) and did not change with depth ($F=0.438_{1,217}$, p=0.51, $R^2=0.002$), nor station visit ($F=2.46_{2,216}$, p=0.09). C:N ratios were greatest in *Rhincalanus nasutus*.

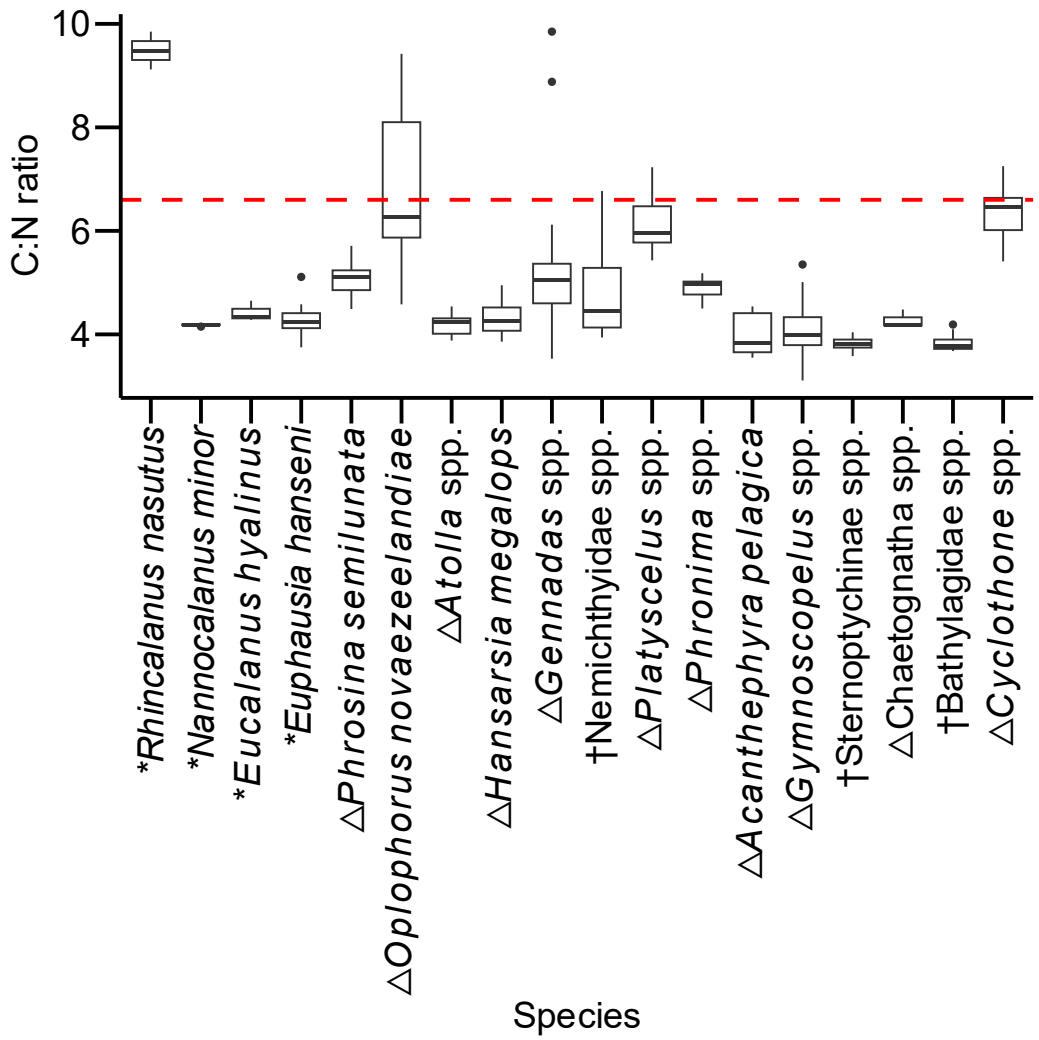

Figure 3.6 Molar carbon:nitrogen (C:N) ratio of zooplankton and micronekton collected at station BN in the northern Benguela Upwelling System. The boxplot represents the minimum, maximum, median, first quartile and third quartile values. Circles represent outliers. The red dashed line represents a Redfield ratio of C:N = 106:16. Asterisks (*) denote mesozooplankton taxa, triangles (△) macrozooplankton and obelus (†) mesopelagic fish taxa. *Rhincalanus nasutus* analysed were all stage C6 females. *Nannocalanus* spp. were all C6 females. *Eucalanus* spp. were all C6 females.

3.4.2.3 Lipid biomarker signatures of POM

The lipid class composition of POM varied as a function of particle size (<53 µm or >53 µm), station visit, water oxygen concentration and depth (RDA, $F=10.14_{1,42}$, $p<0.001$; $F=4.65_{2,42}$, $p<0.001$; $F=3.87_{1,42}$, $p=0.002$; $F=3.21_{1,42}$, $p=0.005$ respectively; Figure 3.7). The final model explained 38.7 % of the total variance in the data. The <53 µm particle pool was more closely associated with saturated fatty acids (SFAs), branched fatty acids and alcohols, whilst the >53

µm particle pool was more closely associated with monounsaturated fatty acids (MUFAs), polyunsaturated fatty acids (PUFAs) and sterols.

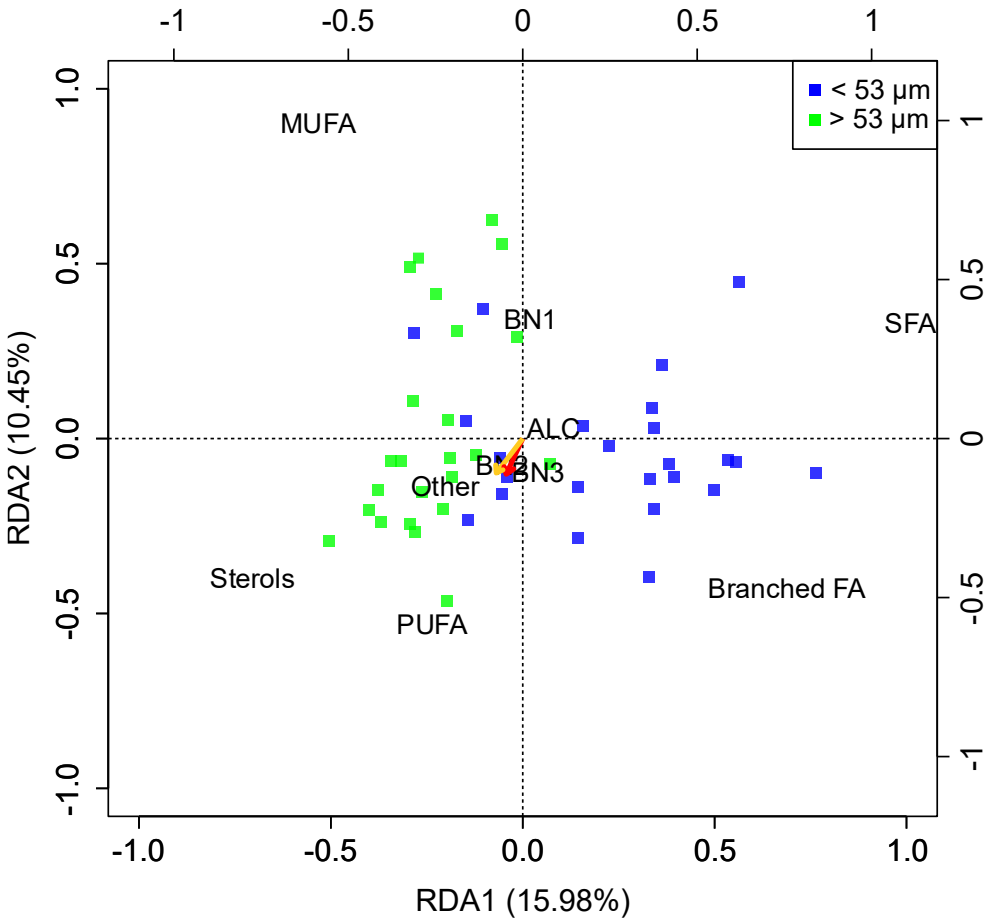

Figure 3.7 Lipid class composition (mol%) of size-fractionated particulate organic matter (POM) from station BN in the northern Benguela Upwelling System. Redundancy analysis distance triplot of the proportional abundance of each lipid class for the two particle sizes, 3 station visits, oxygen concentration and depth. Each point refers to a single sample of POM. The arrows represent the effects of water depth (yellow) and oxygen concentration (red) on the sample coordinates. The primary and secondary sets of axes relate to the individual samples and fatty acid loadings, respectively.

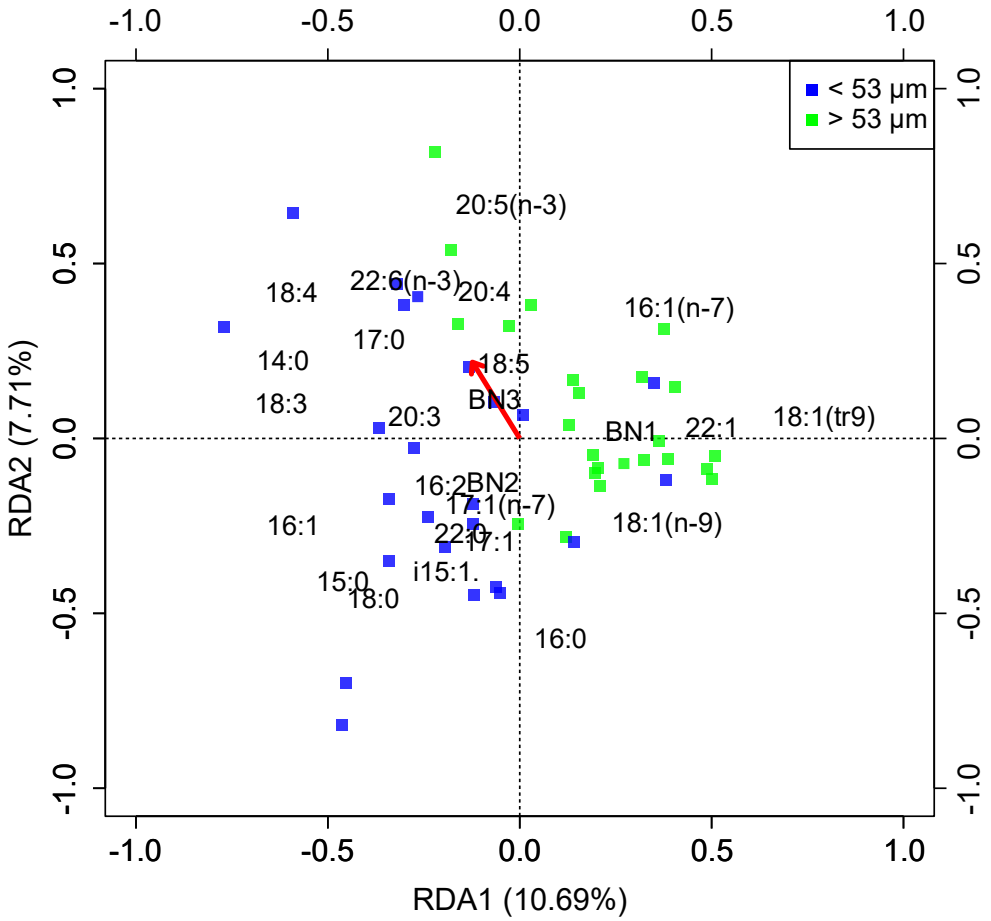

Figure 3.8 Fatty acid composition (mol%) of size-fractionated particulate organic matter (POM) from station BN in the northern Benguela Upwelling System. Redundancy analysis distance triplot of the proportional abundance of each fatty acid for the two particle sizes. Each point refers to a single sample of POM. The red arrow represents the effects of oxygen concentration on the sample coordinates. The primary and secondary sets of axes relate to the individual samples and fatty acid loadings, respectively.

The fatty acid composition of POM varied as a function of particle size (<53 µm or >53 µm), station and water oxygen concentration (RDA, $F=4.81_{1,43}$, $p<0.001$; $F=2.80_{2,43}$, $p<0.001$; $F=3.99_{1,43}$, $p<0.001$ respectively; Figure 3.8). Including depth did not increase the model fit ($F=1.12_{1,42}$, $p=0.31$). The final model explained 25.09 % of the total variance in the data. The >53 µm particle pool was closely associated with MUFAs such as 18:1(n-9), 16:1(n-7) and 22:1. Closer examination of the data revealed that diatom 20:5(n-3) and dinoflagellate 22:6(n-3) markers tended to decrease in proportional contribution to the <53 µm particle pool with depth ($F=13.04_{1,22}$, $p=0.002$, $R^2=0.37$; $F=5.18_{1,22}$, $p=0.03$, $R^2=0.19$), whereas the proportional contribution of animal biomarker 18:1(n-9) increased with depth in the > 53 µm particle pool ($F=7.75_{1,22}$, $p=0.01$, $R^2=0.26$) (Figure 3.9). No significant relationship was found between the ratio

of PUFA:MUFA with depth nor particle size fraction, however PUFA:MUFA ratios were lowest at depths 250 – 400 m (Figure 3.9).

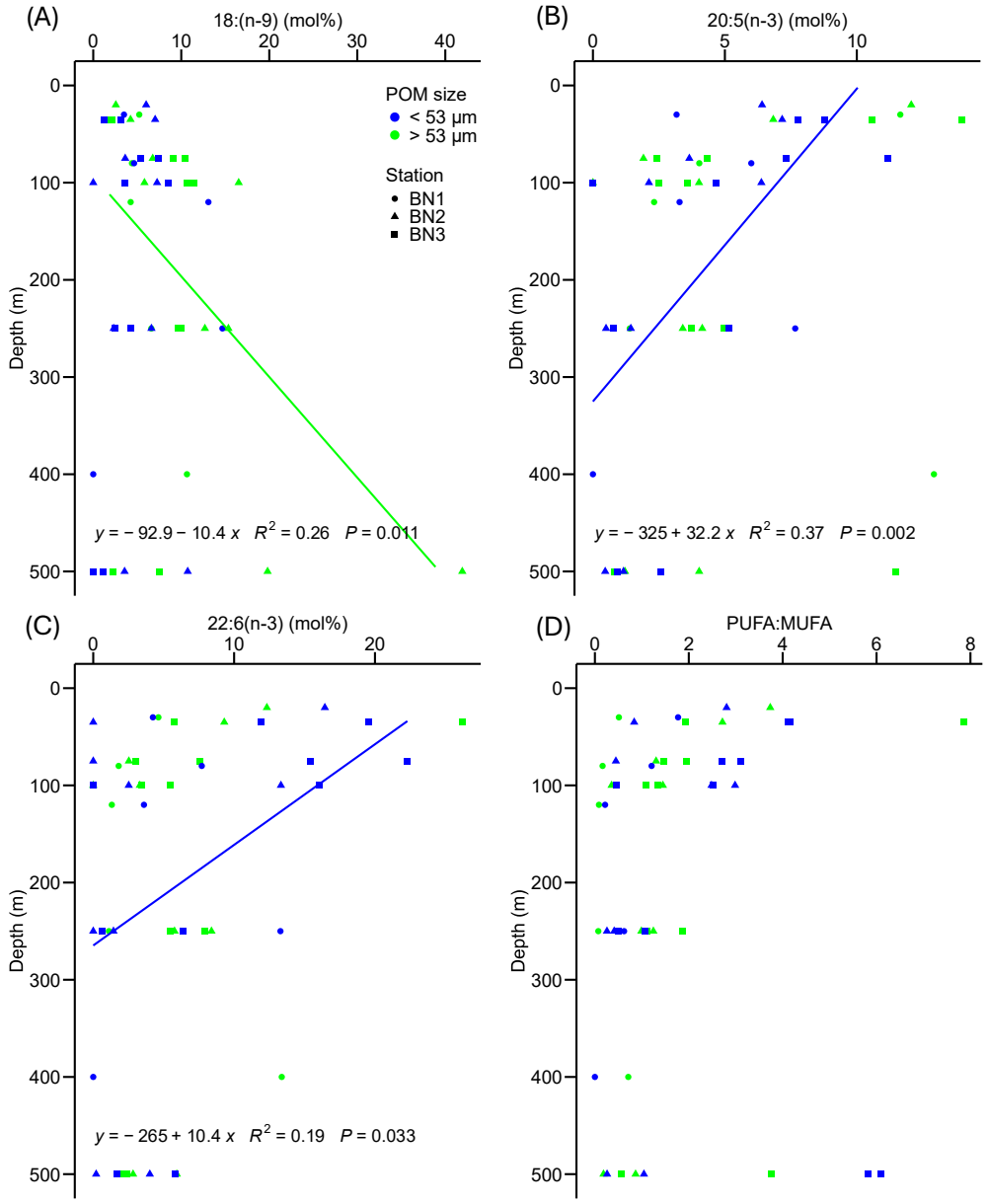

Figure 3.9 Change in the composition (%mol) of key lipid biomarkers (A) 18:1(n-9), (B) 20:5(n-3), (C) 22:6(n-3) and (D) PUFA:MUFA ratio (polyunsaturated fatty acid:monounsaturated fatty acid) in particulate organic matter (POM) in the top 500 m of the water column at the BN station in the northern Benguela Upwelling System. The regression lines indicate statistically significant ($p < 0.05$) relationships between the lipids analysed and depth, with the colour of the regression line indicating whether the regression line applies to the <53 µm (blue) or >53 µm (green) size fraction of POM.

3.4.2.4 Lipid biomarker signature of animals

Fatty acids made up > 65 mol% of the total lipids within the zooplankton taxa sampled, apart from the two herbivorous calanoid species, *C. natalis* and *R. nasutus*, where fatty acids made up less than 50 mol% of the total lipid composition (Table 3.2).These two species were characterized by a high fatty alcohol content making up more than 50 mol% of the total lipid composition. *Euchaeta* spp. and *Atolla* spp. also had contributions of fatty alcohols, making up 33 mol% and 17 mol% of the total lipid composition. The mesopelagic fish sampled all had fatty acid contents greater than 88 mol%, except for *Cyclothone* spp., for which fatty acid and fatty alcohol content made up 68 mol% and 29 mol% of the total lipid composition respectively. Sterols made up between 1.8 – 11 mol% of the total lipids for zooplankton, except for *Euchaeta* spp., *C. natalis* and *R. nasutus*, where sterols made up 0.9, 0.1 and 0.3 mol%. Mesopelagic fish sterols made between 1.8 and 7.2 mol% of the total lipid composition. Branched fatty acids made up less than 5 mol% of the total lipid composition for all taxa sampled. MUFAs were proportionally greater or equal to PUFAs for all taxa sampled except for the 3 amphipod species (*Phrosina semilunata, Platyscelus* spp. and *Phronima* spp.) and *Euphausia hanseni* where MUFAs were greater than PUFAs. Overall, the dominant SFAs were 16:0 and 18:0, MUFAs, 16:1(n-7) and 18:1(n-9) and PUFAs 20:5(n-3) and 22:6(n-3) (Table 3.3). For *C. natalis,* MUFAS were moreover dominated by 20:1(n-9) and 22:1, making up 21.6 % of total fatty acid composition. *R. nasutus* fatty acids were dominated by 16:1(n-7) and 18:1(n-9), with these making up 28 mol% and 33 mol% of total fatty acid composition respectively. All other fatty acid moieties individually had compositions of less than 8 mol%. *C. natalis* alcohols were dominated by monounsaturated compounds, especially ALC-20:1 and ALC-22:1, whereas *R. nasutus* and *Euchaeta* spp. alcohols were dominated by the saturated alcohols ALC-14:0, ALC-16:0 and ALC-18:0 (Table 3.4). *Atolla* spp. and *Cyclothone* spp. alcohols were made up of both saturated ALC-14:0 and ALC-16:0 and monounsaturated compounds ALC-20:1 and ALC-22:1 (and to a lesser extent ALC-24:1 in *Cyclothone* spp.). All taxa but Chaetognatha, Bathylagidae spp., *Gymnoscopelus* spp., *R. nasutus* and Nemichthyidae spp. contained the herbivorous calanoid biomarkers ALC-20:1 and ALC-22:1 making up >5 % of alcohol composition. The corresponding herbivorous calanoid fatty acid biomarkers 20:1(n-9) and 22:1 were also present in these species.

Table 3.2 Lipid group composition (mol% mean (x̄) and standard deviation (sd)) of the zooplankton and micronekton sampled at station BN in the northern Benguela Upwelling system. Saturated fatty acids (SFAs), branched fatty acids (Br. FAs), monounsaturated fatty acids (MUFAs), polyunsaturated fatty acids (PUFAs), saturated fatty alcohols (Sat. ALCs), unsaturated fatty alcohols (Unsat. ALCs), Sterols, total fatty acids (FAs), total fatty alcohols (ALCs). *Calanoides natalis* analysed were all copepodite stage C5. *Rhincalanus nasutus* were all stage C6 females. *Eucalanus* spp. were all C6 females. *Nannocalanus* spp. were all C6 females.

		Calanoides natalis	***Rhincalanus nasutus***	***Nannocalanus* spp.**	***Eucalanus* spp.**	***Euchaeta* spp.**	***Euphausia hanseni***	***Phrosina semilunata***	***Oplophorus novaezeelandiae***	***Atolla* spp.**	***Hansarsia megalops***	***Gennadas* spp.**	**Nemichthyidae spp.**	***Platyscelus* spp.**	***Phronima* spp.**	***Cristaspis cristata***	***Acanthephyra pelagica***	***Gymnoscopelus* spp.**	**Hatchet Fish**	**Chaetognatha spp.**	**Bathylagidae spp.**	***Cyclothone* spp.**
SFAs	x̄	15.7	3.7	40.9	53.1	9.1	37.1	33.2	27	18.7	35.6	28.6	32.3	33.9	33.9	26.7	24.8	34.5	29.9	21.5	35.5	18.4
	sd	5	1.2	4.4	20.9	6.3	6.3	2.8	1.2	18	11.2	4.9	2.3	1.1	7.7	-	4.6	3.4	6.4	-	3.9	2.9
Br. FAs	x̄	0.3	0.2	1.3	0.8	0.4	1.9	4.9	1.1	0.7	1.5	0.5	1	2.2	2.9	1.1	2.1	0.9	2.3	1.3	0.8	0.9
	sd	0.1	0.2	0.4	0.4	0.1	0.4	1.6	0.3	0.6	0.5	0.3	0.5	0.2	0.7	-	0.7	0.4	2.3	-	0.6	0.2
MUFAs	x̄	18.1	31	21.2	22.2	43.1	25.1	25.2	45.5	45	29.3	59.6	52.8	23.4	23.6	48.4	42.6	45.3	34.4	23.4	30.2	36
	sd	2.5	8	5.7	11.2	7.3	3.3	2.3	1.8	16.5	6.2	5.3	6.8	2.7	1.5	-	2.8	4.7	8.1	-	10.3	4.0
PUFAs	x̄	10.7	12.1	20.9	14.5	12.9	28	30.9	21.6	14.8	22.2	9	11.7	36.2	31.1	21.1	21	16.1	23.9	25.1	25.8	13.6
	sd	2.8	2.8	7.5	7.6	1.7	5	5	1.6	11.7	7.2	2.7	4.2	2.4	8.5	-	3.8	2.5	4.8	-	10.4	1.4
Sat. ALCs	x̄	23.5	50.8	4.6	3.4	27.1	0.2	0.1	0.9	7.6	0.9	0.1	0	0.2	0.7	0.6	2.5	0	0.8	0.1	0.2	16.7
	sd	2.7	12.3	4.9	3.3	7.2	0.1	0.1	0.7	6.9	0.8	0.1	0.1	0.1	0.6	-	3	0	1.5	-	0.2	4.4

		Calanoides natalis	*Rhincalanus nasutus*	*Nannocalanus* spp.	*Eucalanus* spp.	*Euchaeta* spp.	*Euphausia hanseni*	*Phrosina semilunata*	*Oplophorus novaezeelandiae*	*Atolla* spp.	*Hansarsia megalops*	*Gennadas* spp.	Nemichthyidae spp.	*Platyscelus* spp.	*Phronima* spp.	*Cristaspis cristata*	*Acanthephyra pelagica*	*Gymnoscopelus* spp.	Hatchet Fish	Chaetognatha spp.	Bathylagidae spp.	*Cyclothone* spp.
Unsat. ALCs	x̄	31.6	1.8	0.1	0.5	6.5	0.2	0.1	1.9	9.8	2.4	0.1	0	0.1	0.4	0.3	5	0	1.9	0	0.2	12.4
	sd	4.1	0.2	0.2	0.8	8.4	0.5	0.1	1.1	10.6	2.4	0.1	0	0.2	0.6	-	6.9	0	3.7	-	0.4	2.5
Sterols	x̄	0.1	0.3	11.1	5.4	0.9	7.5	5.6	2	3.4	8.1	2.1	2.3	3.9	7.4	1.8	1.8	3.2	6.8	28.6	7.2	1.8
	sd	0	0.2	13.2	5.8	0.4	4.4	2.3	0.5	2	3.8	1	1.3	2.4	1.2	-	2.1	3	2.5	-	4.9	0.9
Total FAs	x̄	44.5	46.8	82.9	89.8	65.1	90.2	89.3	94.1	78.5	87.1	97.2	96.7	93.6	88.6	96.2	88.5	95.9	88.2	70	91.5	68.1
	sd	4.4	11.8	17.6	6	15.3	4.7	2.5	1.4	15.8	5.7	1	1.9	2.2	2.2	-	10.1	2.8	2.6	-	4.9	7.7
Total ALCs	x̄	55.1	52.6	4.7	4	33.6	0.4	0.2	2.8	17.4	3.3	0.1	0	0.3	1.2	1	7.5	0	2.7	0.2	0.4	29
	sd	4.3	12.2	4.7	4	15.6	0.6	0.2	1.6	16.8	3.1	0.2	0.1	0.3	1.2	-	9.8	0	5.2	-	0.6	6.8

Table 3.3 Fatty acid composition (mol% mean (x̄) and standard deviation (sd)) of the zooplankton and micronekton sampled at station BN in the northern Benguela Upwelling system, focusing on the most abundant fatty acids included in the redundancy analysis model. Total Calanoid = sum of 20:1(n-9), 22:1(n-9), 20:1iso and 22:1. *Calanoides natalis* analysed were all copepodite stage C5. *Rhincalanus nasutus* were all stage C6 females. *Eucalanus* spp. were all C6 females. *Nannocalanus* spp. were all C6 females.

		Calanoides natalis	***Rhincalanus nasutus***	***Nannocalanus* spp.**	***Eucalanus* spp.**	***Euchaeta* spp.**	**Euphausia hanseni**	***Phrosina semilunata***	***Oplophorus novaezeelandiae***	***Atolla* spp.**	***Hansarsia megalops***	***Gennadas* spp.**	**Nemichthyidae spp.**	***Platyscelus* spp.**	***Phronima* spp.**	***Cristaspis cristata***	***Acanthephyra pelagica***	***Gymnoscopelus* spp.**	**Hatchet Fish**	**Chaetognatha spp.**	**Bathylagidae spp.**	***Cyclothone* spp.**
14:0	x̄	13.3	1.6	1	9	0.6	6.2	5.4	3.2	3.4	4.1	0.7	3.8	5.2	1.8	2.8	3.8	4	4	1.1	4.2	4.3
	sd	2.4	1.2	0.6	5.8	0.5	1.9	2.3	0.7	3.2	2	0.3	1.2	0.4	1.3	-	0.3	1.8	3	-	3.2	1
16:0	x̄	13.8	4.9	24.9	39.1	9	27.6	21.6	20.4	16.7	29.4	23.6	19.3	22.8	25.8	20.6	16.6	26.5	22.7	20.4	29.1	17.3
	sd	2.1	0.8	8.1	14.4	4.7	5.4	2	1	16.1	13.2	2.8	2.9	1	5.3	-	1.6	3.7	7.9	-	6.6	0.9
18:0	x̄	2.7	1.1	17.3	6.5	3.1	3.2	4.2	3.2	4	3.4	4.3	7.2	4.1	4.5	2.8	3.9	3.9	4.6	5.3	3.6	3.6
	sd	0.6	0.2	5.1	1.8	1.9	0.8	0.4	0.2	3.8	0.7	2.1	1.1	0.4	1.9	-	0.5	1.2	1.5	-	1	1.2
16:4	x̄	2.6	7.2	0.2	0.3	2.4	0.6	0	0.1	0	0.3	0	0.1	0	0	0	0.1	0.1	0.3	0	0.1	2.3
	sd	2.6	1.3	0.3	0.6	3.4	0.3	0.1	0.1	0	0.4	0	0.1	0	0	-	0.2	0.2	0.3	-	0.1	2.9
16:3	x̄	1.3	2.9	0	0.4	0.4	0.6	0.1	0.1	0.1	0.1	0	0.1	0	0	0	0	0.1	0.2	0	0.1	0.2
	sd	0.4	0.7	0	0.5	0.5	0.7	0.2	0.1	0.1	0.1	0	0.1	0.1	0	-	0	0.2	0.2	-	0.1	0.3
16:1(n-7)	x̄	8.8	28.3	2.2	9.1	8.9	5.1	5.8	5.2	6.7	4.2	1.6	5.7	2.2	1.7	2.4	7.5	4.5	4.8	9	2.9	11.1
	sd	5.7	0.9	1.1	6.1	9.8	0.8	2.2	0.6	1	1.4	0.6	1.7	0.3	0.8	-	0.7	1.6	2.7	-	2.3	1.3
18:2(n-6)	x̄	1.1	3.4	1.6	2.5	1.7	2.1	2.4	1	0.9	1.6	0.2	0.7	0.8	1.3	0.6	1.4	0.6	1.6	1.9	0.5	1.4
	sd	0.3	3	0.5	2.3	0.2	1	1	0.2	0.5	0.6	0.1	0.6	0.1	0.4	-	0.4	0.5	0.5	-	0.3	0.1
18:1(n-9)	x̄	4.3	33.1	17	8.9	44.3	13	12.3	31.1	36	18.1	51.6	39.8	10.3	14.7	39	25.4	24.6	19.6	9.8	16.8	30.8

		Calanoides natalis	*Rhincalanus nasutus*	*Nannocalanus* spp.	*Eucalanus* spp.	*Euchaeta* spp.	Euphausia hanseni	*Phrosina semilunata*	*Oplophorus novaezeelandiae*	*Atolla* spp.	*Hansarsia megalops*	*Gennadas* spp.	Nemichthyidae spp.	*Platyscelus* spp.	*Phronima* spp.	*Cristaspis cristata*	*Acanthephyra pelagica*	*Gymnoscopelus* spp.	Hatchet Fish	Chaetognatha spp.	Bathylagidae spp.	*Cyclothone* spp.
18:1(n-9)	sd	1.8	2	3	5.6	4.6	2	2.6	3.6	9.9	5.3	8.3	8.3	0.9	1.8	-	2.5	8	7.4	-	3.1	3
18:1(tr-9)	x̄	0.5	1.3	1.2	3	2.1	4.6	3.5	4	2.7	4.7	1.2	2.5	3.4	2.9	3.7	2.9	5.8	3.5	2.7	2.5	2.2
	sd	0.1	0.4	1.7	1.9	0.7	0.8	0.5	0.2	2.7	1.1	0.2	1.5	0.3	0.4	-	0.7	7.8	1.5	-	1	0.5
20:4(n-6)	x̄	1.3	1.1	1.6	0.8	0.6	2.9	3	2.2	1.2	1.8	0.6	1.6	7.1	7.3	1.3	3.1	1.1	1.5	2.8	2.2	0.8
	sd	0.6	0.4	1.7	0.7	0.1	0.6	1.4	0.4	1.2	0.8	0.3	1.2	1	1.5	-	0.6	1.4	0.9	-	1.7	0.5
20:5(n-3)	x̄	9.3	5.6	8.4	6.2	2.8	9.3	9.8	7.5	8.1	8.2	2.6	2.8	11.1	7.2	6.8	6	3.4	6.4	10.1	3.4	5.3
	sd	1.5	4.3	1.9	5.1	3.2	1.4	1.8	0.7	3	2.9	0.6	0.9	1.2	4.5	-	1	0.9	1.2	-	1.8	0.9
20:1(n-9)	x̄	6.6	0.4	1.2	0.3	0.9	0.7	0.7	1.5	1.8	1	3.7	2.2	1.2	0.5	1.1	2	1.8	2.1	1.1	1.3	1.4
	sd	0.9	0.2	0.6	0.3	0.4	0.4	0.2	0.5	2	0.3	0.8	1.4	0.6	0.2	-	1.5	1.2	1.2	-	0.9	0.1
22:6(n-3)	x̄	2.9	1.4	9.3	2.8	10.1	12	14.8	10.4	5.3	11.1	5.4	5.4	17	16.4	12.2	11.1	10.3	14.4	19.7	21.4	8.1
	sd	0.8	1.3	2.5	1.2	1.6	3.8	3.1	1.4	6.1	4	3.2	2.2	0.3	3.9	-	2.1	3.4	4.4	-	12.8	1.7
22:1(n-9)	x̄	6.8	0.5	0.7	1.7	1	0.6	0.3	0.4	0.7	0.8	0.2	0.2	0.3	1	0.3	1.1	0.7	0.8	2.3	1.4	1
	sd	7.2	0.8	0.8	1.4	1	0.3	0.1	0.2	0.4	0.8	0.1	0.3	0.2	1.1	-	0.2	0.4	0.5	-	0.8	0.3
24:1(n-9)	x̄	0.4	0.1	0.4	0.5	0.5	0.4	0.3	1	1	0.7	0.4	0.2	0.7	0.3	0.3	0.9	1.3	1.4	4.2	0.6	0.9
	sd	0.1	0	0.1	0.6	0.1	0.2	0.2	0.4	0.8	0.3	0.3	0.2	0.1	0.3	-	0.2	0.7	0.7	-	0.5	0.6
16:1	x̄	3.9	0.1	0.1	0.2	0.1	0.3	1.3	0.3	0.2	0.4	0.9	0.2	3.9	1.9	0.7	0.8	0.3	1.2	1.2	0.9	0.4
	sd	6.6	0	0.1	0.2	0.1	0.1	0.9	0.2	0.1	0.2	1.2	0.1	2.3	0.4	-	0.4	0.2	1.8	-	0.7	0.2
16:2iso	x̄	1.8	2.1	0	1.1	0.3	0.9	0.4	0.3	0.5	0.6	0	0.4	0.7	0	0	0.1	0.3	0.4	0	0	0.4
	sd	0.9	0.2	0	0.8	0.4	0.2	0.6	0.2	0.2	0.5	0	0.2	1.6	0	-	0.1	0.3	0.5	-	0	0.4
20:1iso	x̄	0.9	1.1	0.3	0.3	2.3	0.2	0.4	0.8	1.8	0.3	0.2	0.6	0.5	0.4	0.5	1.3	2.7	0.4	0.3	0.9	0.5

		Calanoides natalis	*Rhincalanus nasutus*	*Nannocalanus* spp.	*Eucalanus* spp.	*Euchaeta* spp.	Euphausia hanseni	*Phrosina semilunata*	*Oplophorus novaezeelandiae*	*Atolla* spp.	*Hansarsia megalops*	*Gennadas* spp.	Nemichthyidae spp.	*Platyscelus* spp.	*Phronima* spp.	*Cristaspis cristata*	*Acanthephyra pelagica*	*Gymnoscopelus* spp.	Hatchet Fish	Chaetognatha spp.	Bathylagidae spp.	*Cyclothone* spp.
20:1iso	sd	0.2	1.3	0.1	0.4	2.3	0.1	0.2	0.4	0.4	0.1	0.1	0.7	0.5	0.3	-	0.9	3.4	0.2	-	1.2	0.1
22:1	x̄	7.3	0.2	1.2	0.4	2.8	0.7	0.5	1.9	4.2	0.8	0.7	0.6	0.7	0.4	0.3	1.9	3.9	2.9	0.8	3.8	2.1
	sd	6	0.2	0.8	0.2	0	0.9	0.2	1.2	3.3	0.4	0.4	0.5	0.5	0.2	-	0.8	2.7	2.7	-	2.3	0.5
Sum Calanoid	x̄	21.6	2.2	3.3	2.7	7	2.2	1.9	4.6	8.6	2.9	4.8	3.5	2.7	2.3	2.2	6.3	9.2	6.2	4.4	7.5	4.9

Table 3.4 Fatty alcohol (ALC) composition (mol% mean (x̄) and standard deviation (sd)) of the zooplankton and micronekton sampled at station BN in the northern Benguela Upwelling system, focussing on the most abundant alcohols. Total Calanoid =sum of ALC-20:1 and ALC-22:1. *Calanoides natalis* analysed were all copepodite stage C5. *Rhincalanus nasutus* were all stage C6 females. *Eucalanus* spp. were all C6 females. *Nannocalanus* spp. were all C6 females.

		Calanoides natalis	***Rhincalanus nasutus***	***Nannocalanus* spp.**	***Eucalanus* spp.**	***Euchaeta* spp.**	***Euphausia hanseni***	***Phrosina semilunata***	***Oplophorus novaezeelandiae***	***Atolla* spp.**	***Hansarsia megalops***	***Gennadas* spp.**	**Nemichthyidae spp.**	***Platyscelus* spp.**	***Phronima* spp.**	***Cristaspis cristata***	***Acanthephyra pelagica***	***Gymnoscopelus* spp.**	**Hatchet Fish**	**Chaetognatha spp.**	**Bathylagidae spp.**	***Cyclothone* spp.**
ALC-12:0	x̄	0	0.1	0	0.4	0.1	2.2	2.2	0	0.1	0.2	0.1	0.2	0.2	2	0	0	0.5	0.1	3.2	1.9	0.1
	sd	0	0	0	0.7	0.1	2.3	2.7	0	0.1	0.3	0.3	0.4	0.3	2.9	-	0	1.1	0.2	-	4.1	0
ALC-14:0	x̄	17.4	42	10.1	19.4	24.8	24.6	6.8	7	10	13	14.1	0	11.5	7.7	3.6	10.6	0	6.2	16.7	7.2	12.6
	sd	3.7	1.3	14.3	14.7	2.8	18.3	5.5	2.2	7.8	14.7	6.4	0	13.2	10.1	-	1.8	0	3.5	-	10.8	2.3
ALC-15:0	x̄	0.5	0.6	0	1.4	1.6	1.5	3	0.6	0.5	0.4	1.1	0.3	0.8	2.4	1.2	1.2	0	0.8	0	0	1.4
	sd	0.1	0.1	0	1.4	1.7	1.4	6.2	0.4	0.4	0.4	1.5	0.7	1.4	3.3	-	0.6	0	1	-	0	0
ALC-16:0	x̄	22.1	47.3	24.8	39.2	54.1	19	21.9	18.1	26.8	28.6	35.6	0.4	24.1	19.6	51.6	24.7	16.7	13.2	20.2	11.1	38.8
	sd	4.4	1.7	2.7	15.8	16.1	14.2	12.6	9.9	20.5	20.7	9.7	0.7	26.6	19.3	-	7.2	40.8	11.1	-	24.5	2.5
ALC-17:0	x̄	0	0.1	0	0.2	0.3	0.1	1.8	3	0	0.2	0.4	0	0	0.6	0.2	0.7	0	0.4	0	0	0.4
	sd	0	0.1	0	0.4	0.2	0.2	4	2.3	0	0.2	0.8	0	0	1.3	-	0.7	0	0.8	-	0	0.1
ALC-18:0	x̄	1.9	5.8	48.3	27.4	3.6	36	20.7	1.6	0.9	7.4	2.6	32	21.9	26	4.3	4.7	13.6	4	36.6	32.6	2.7
	sd	0.3	1.5	25.6	19.9	1.1	36.1	14.7	0.7	0.6	8.3	2.1	45.5	19.8	23.6	-	1.9	25.7	4.2	-	31.6	2.1
ALC-20:0	x̄	0.6	0.2	2.5	1.5	0.1	2.6	17.9	1	0.5	0.5	0.3	11.4	20.3	12.3	1.3	1.1	5.5	1.3	5.4	2	0.6
	sd	0.1	0.1	1.3	1.4	0.1	2	12.5	0.4	0.3	0.4	0.7	22.8	26.9	7.5	-	0.5	13.6	1	-	2.6	0.2
ALC-22:0	x̄	0.2	0.1	5	0.7	0.3	0	0	1	0.1	0	1.1	0	0.2	1.8	1	0.3	0	0.8	1.6	0.2	0.2

		Calanoides natalis	*Rhincalanus nasutus*	*Nannocalanus* spp.	*Eucalanus* spp.	*Euchaeta* spp.	*Euphausia hanseni*	*Phrosina semilunata*	*Oplophorus novaezeelandiae*	*Atolla* spp.	*Hansarsia megalops*	*Gennadas* spp.	Nemichthyidae spp.	*Platyscelus* spp.	*Phronima* spp.	*Cristaspis cristata*	*Acanthephyra pelagica*	*Gymnoscopelus* spp.	Hatchet Fish	Chaetognatha spp.	Bathylagidae spp.	*Cyclothone* spp.
ALC-22:0	sd	0.1	0.2	3.3	1	0.4	0	0	0.9	0	0.1	2.3	0	0.5	2.7	-	0.3	0	1.2	-	0.4	0
ALC-24:0	x̄	0	0	0.9	0.6	0	0	0	0	0	0	0	0	0	0	0.2	0.1	0	0.8	0	0	0
	sd	0	0	1.3	0.6	0	0	0	0.1	0	0	0	0	0	0	-	0.1	0	1.9	-	0	0
ALC-20:1	x̄	14.4	0.6	1.8	1.8	1.4	1.9	0	11.2	6.6	17.8	6.6	0	7.2	18.7	10.6	6.6	0	2.5	0	1.7	6.4
	sd	6.5	0.4	2.5	2.6	1.9	4.8	0	1.7	5.2	15	7.8	0	11.2	22.4	-	5.9	0	3.5	-	2.3	0.5
ALC-22:1	x̄	40.3	0.2	6.7	4.1	6.1	11.4	8.1	49.4	47.8	29	37.4	0	8.4	0	12.9	28.7	0	30.2	0	0	24.3
	sd	6.2	0.1	9.4	6.3	6.4	23.1	18.1	10.1	25.4	21.6	16.5	0	17.8	0	-	4.9	0	24.4	-	0	1.2
ALC-16:1	x̄	2.1	2.2	0	0.2	2.5	0	0.7	0.5	0.8	0	0.2	0	0.8	0	0	0.7	0	1.4	5.3	0	1.9
	sd	0.4	0.7	0	0.4	3.6	0	1.5	0.7	0.3	0	0.5	0	1.1	0	-	0.8	0	1.6	-	0	0
ALC-18:1	x̄	0.3	0.5	0	0.2	2.4	0	17	1.5	0.6	0.8	0	0	4	7	0	4.7	13.7	18.3	5.9	23.3	3.3
	sd	0.1	0.5	0	0.4	3.4	0	22.5	1.3	0.1	0.8	0	0	8.9	6.3	-	5.5	33.6	21.8	-	31.9	0.4
ALC-24:1	x̄	0.2	0.1	0	3	2.4	0.6	0	5	5.1	2.2	0.3	5.8	0.7	2	10.6	15.4	0	20	0	0	6.7
	sd	0.2	0	0	2.2	2.5	1.5	0	3.6	6.9	2.2	0.7	11.6	1.1	3.3	-	6.4	0	38.4	-	0	0.5
ALC-26:1	x̄	0	0	0	0	0.2	0	0	0	0	0	0	0	0	0	2.5	0.5	0	0	0	0	0
	sd	0	0	0	0	0.3	0	0	0	0	0	0	0	0	0	-	0.6	0	0	-	0	0
Sum Calanoid	x̄	54.7	0.8	8.4	6	7.5	13.4	8.1	60.6	54.4	46.7	43.9	0	15.5	18.7	23.5	35.3	0	32.8	0	1.7	30.7
	sd	4.9	0.4	11.9	8.5	8.4	27.8	18.1	9.7	23.1	36.1	14.9	0	28.5	22.4	-	9.3	0	24.4	-	2.3	1.6

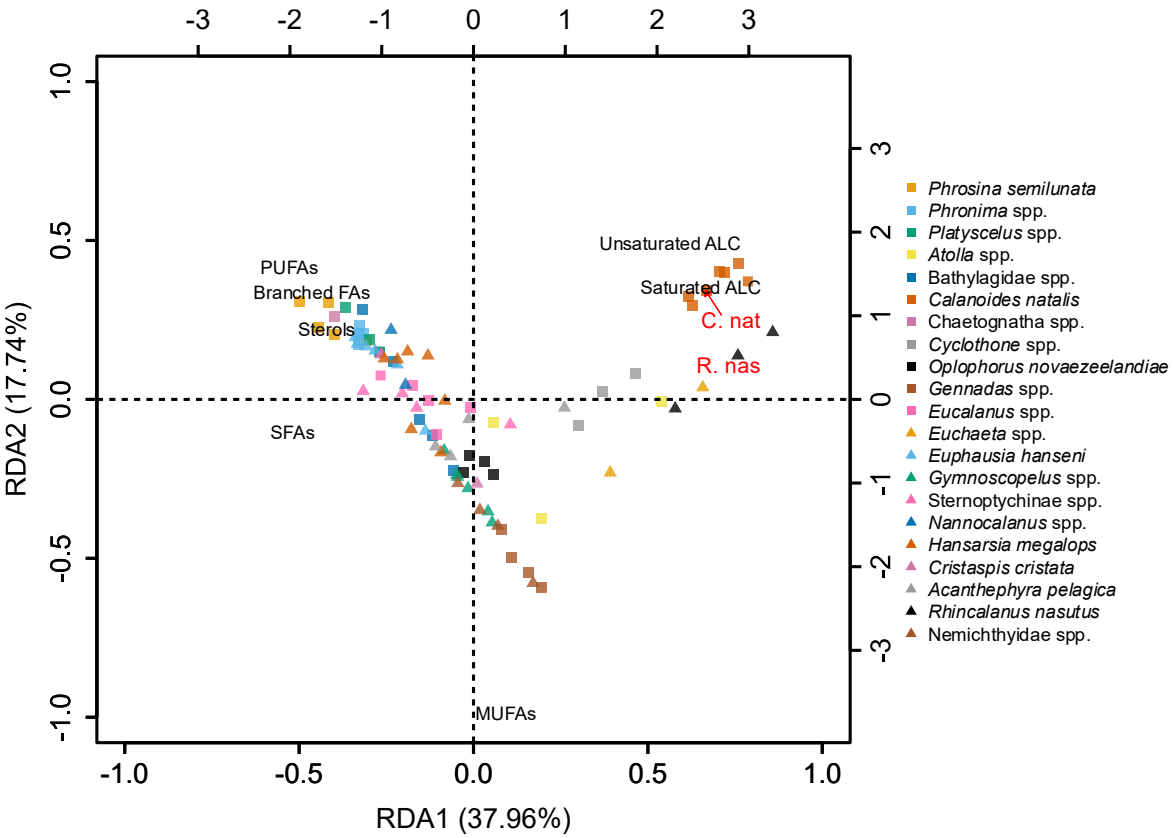

Figure 3.10 Lipid class composition (mol%) of the zooplankton and micronekton from station BN in the northern Benguela Upwelling System. Redundancy analysis distance triplot of the proportional abundance of each lipid class in each sampled zooplankton and micronekton taxa. The primary and secondary sets of axes relate to the individual zooplankton/ micronekton samples and lipid class loadings, respectively. Each shape refers to an individual taxon replicate. Centroids for *Calanoides natalis* and *Rhincalanus nasutus* are illustrated on the plot via 'C. nat' and 'R. nas' in red writing. For ease of interpretation of the plot, the *Calanoides natalis* centroid label 'C. Nat' was moved and a red arrow was added to point to the exact location of the centroid.

Taxon identity explained 77.26 % of the total variance in the zooplankton and fish lipid group composition data (RDA, $F=11.04_{20,65}$, $p<0.001$; Figure 3.10), with the first and second axes accounting for 37.96 % and 17.74 % of the variability, respectively. Including station visit (BN1/BN2/BN3), depth and chlorophyll a did not improve the model fit ($F=0.541_{2,83}$, $p=0.851$, $F=0.541_{1,63}$, $p=0.733$ and $F=2.00_{1,63}$, $p=0.085$). The herbivorous calanoid copepods *C. natalis* and *R. nasutus* were strongly associated with both saturated and unsaturated alcohols.

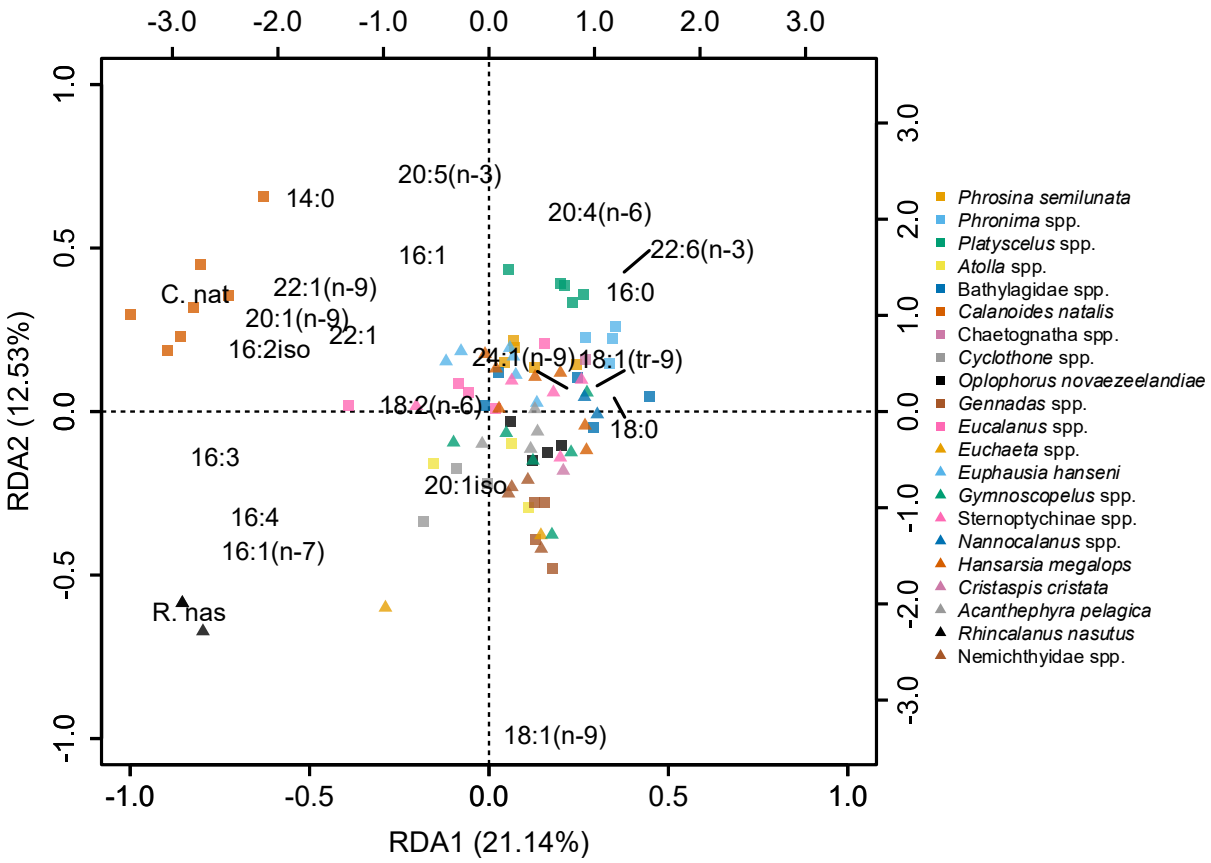

Figure 3.11 Fatty acid composition (mol%) of the zooplankton and micronekton from station BN in the northern Benguela Upwelling System. Redundancy analysis distance triplot of the proportional abundance of each lipid class in each sampled zooplankton and micronekton taxa. The primary and secondary sets of axes relate to the individual zooplankton/ micronekton samples and lipid class loadings, respectively. Each single point refers to an individual taxon replicate. Centroids for *Calanoides natalis* (C. nat) and *Rhincalanus nasutus* (R. nas) are illustrated on the plot.

Taxon identity explained 62.33 % of the total variance in the zooplankton and fish fatty acid composition data (RDA, $F=5.38_{20,65}$, $p<0.001$; Figure 3.11). Including station visit (BN1/BN2/BN3), depth and chlorophyll a or oxygen concentration did not improve the model fit ($F=0.642_{2,83}$, $p=0.903$; $F=1.25_{1,63}$, $p=0.240$; $F=1.53_{1,63}$, $p=0.131$; and $F=1.02_{1,84}$, $p=0.397$ respectively). There was a distinct separation of the two herbivorous calanoid copepod species, *C. natalis* and *R. nasutus*, from the rest of the zooplankton and fish. These species had strong negative loadings on the first axis. *C. natalis* had negative loadings on the second axis and was closely associated to the long-chained fatty acids 22:1(n-9) and 22:1, with these moieties making up 6.6 mol% and 14.1 mol% of total fatty acid composition. *R. nasutus* had strong positive loadings on the second axis and was associated with the short-chained fatty acid 16:1(n-7).

3.4.3 Biomass

The total integrated biomass of organisms in the top 750 m of the water column based on the Mammoth-100, Mammoth-300 and RMT25 net systems ranged between 158.6 – 307.5, 264.3 – 337.1 and 248.9 – 595.4 µmolC m^{-3}, respectively. In general, Mammoth-300 mesozooplankton biomass demonstrated a bimodal distribution with maximum biomass in surface waters (< 33 m) and then again around 250 – 500 m, during both the day and night (Figure 3.12). The Mammoth-100 mesozooplankton biomass also demonstrated a bimodal distribution, with peaks in biomass in the surface net (0 – 125m) and again at 250 – 500 m. CTD oxygen data indicate that the second mesozooplankton biomass peak was within the OMZ (<60 µmol O kg^{-1}) at depth between 250 – 500 m for both stations BN1 and BN2 (Figure 3.12). Mesozooplankton biomass from both the Mammoth-100 and Mammoth-300 were dominated by copepods at all depths (Figure 3.13). Calanidae were proportionally more dominant at depths beyond 375 m within the Mammoth-300 catches. RMT25 catch biomass was dominated by Cephalopoda in surface waters (10 – 125 m) at station BN1 and BN2 during the night. Amphipoda dominated the top 125 m (BN3) and 250 m (BN2) of the water column during the day RMT25 catches. Station BN1 and BN3 RMT25 catches were dominated by Gastropoda (e.g., Pteropoda) down to 250 m during the day and day/night, respectively. Mesopelagic fish dominated the biomass of the RMT25 catches between 250 – 750 m. Mesopelagic fish biomass was dominated by Myctophiformes (e.g., lantern fish), Argentiniformes (e.g., Bathylagidae spp.) and Stomiiformes (e.g., *Cyclothone* spp., Sternoptychinae spp.).

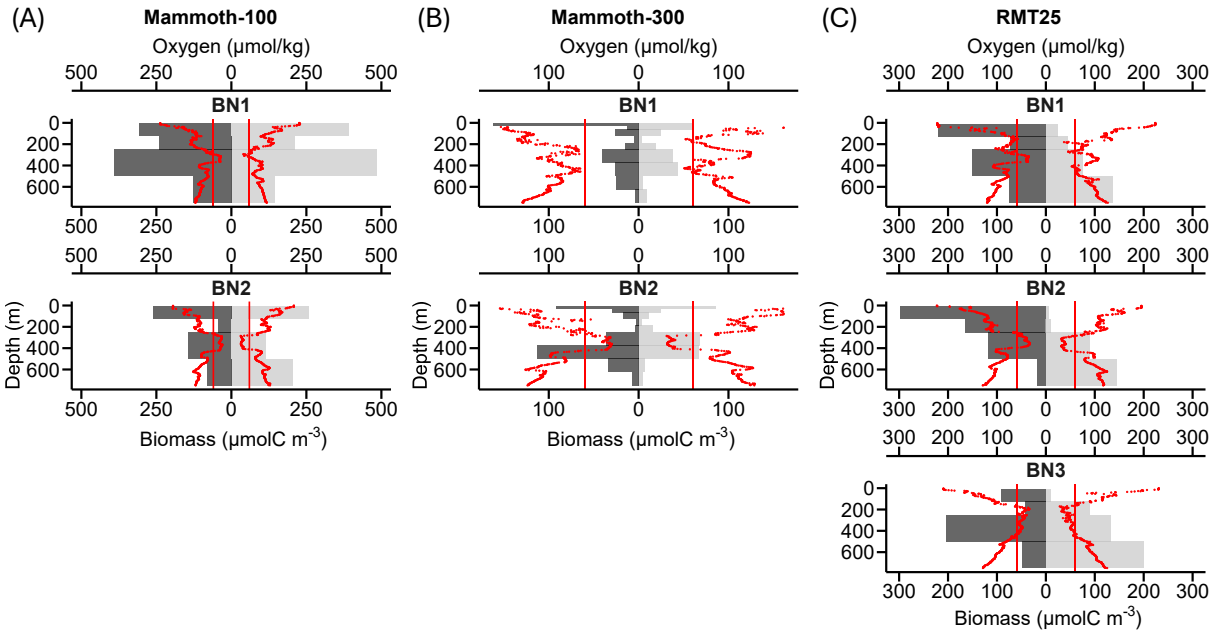

Figure 3.12 Carbon biomass (µmolC m^{-3}) of mesozooplankton sampled from (A) Mammoth-100 and (B) Mammoth-300, and (C) micronekton (RMT25 >4 mm) at station BN in the northern Benguela Upwelling System. Oxygen concentration profiles are denoted by

red points. Vertical red lines mark hypoxic waters < 60 µmol/kg Oxygen. Mammoth-100 and Mammoth-300 biomass samples were not available at BN3. Dark grey shading (left side of x-axis=0) represents nighttime observations and light grey shading (right side of x-axis=0) represents daytime observations.

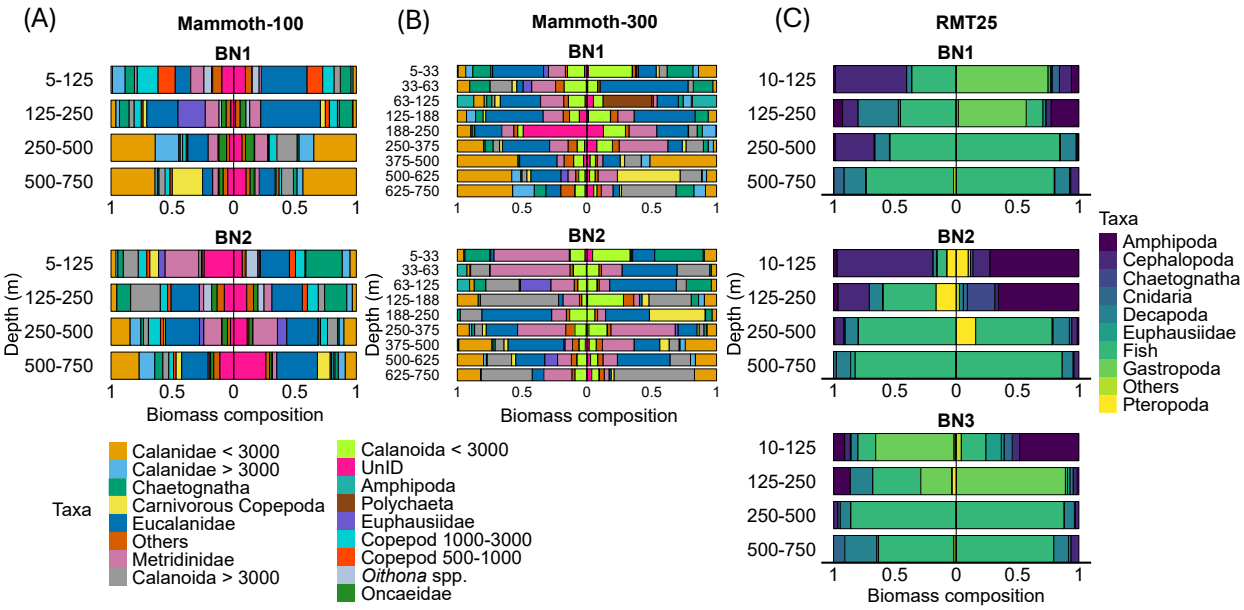

Figure 3.13 Dominant taxa (by % of total carbon biomass) of mesozooplankton sampled from (A) Mammoth-100 and (B) Mammoth-300, and (C) micronekton (RMT25 >4 mm) at station BN in the northern Benguela Upwelling System. Mammoth-100 and Mammoth-300 biomass samples not available at BN3. Taxa that individually contributed < 6 % were placed in the "Others" category. Values to the left of x-axis=0 represent nighttime observation and values to the right of x-axis=0 represent daytime observations.

The change in weighted mean depth (WMD) between day and night total biomass of mesozooplankton from the Mammoth-100 and Mammoth-300 net was < 70 m, with no consistency whether this was shallower or deeper during the day (Table 3.5). When considering specific mesozooplankton taxa, Copepoda nauplii, Copepoda < 1000 µm, *Oithona* spp., Calanidae < 3000 µm (Mammoth-300), Eucalanidae and Ostracoda were consistently distributed at shallower depths during the day than night (Figure 3.14). In contrast, Oncaeidae, Calanidae > 3000 µm (Mammoth-300) and Metridinidae spp. consistently had WMD deeper during the day than night. Total integrated micronekton (RMT25) biomass was consistently greater during than night than day at stations BN1 and BN2, with night biomass being 184 and 239 % of that during the day, respectively. Total micronekton biomass from the RMT25 was consistently deeper during the day. Fish, Cephalopoda, Gastropoda and Decapoda (apart for *Cristaspis cristata*) WMD were consistently deeper during the day (Figure 3.14). When looking at

the WMD of individual fish taxa, the majority of taxa were located above or below the OMZ during both the day and night (Figure 3.15).

Table 3.5 The change in weighted mean depth (WMD, m) between night and day (ΔWMD = Night WMD – Day WMD) of mesozooplankton and micronekton biomass at station BN in the northern Benguela Upwelling System. Mammoth-100 and Mammoth-300 samples were not available at BN3. Positive ΔWMDs indicate that biomass was distributed shallower during the day, whilst negative ΔWMDs indicate that biomass was distributed deeper during the day. A ΔWMD of 0 indicates no changes in the vertical distribution between day and night samples.

		WMD (m) Night	**WMD (m) Day**	**ΔWMD (m)**
Mammoth-100	BN1	273.4	273.4	0
	BN2	244.3	313.0	-68.7
Mammoth-300	BN1	161.9	194.1	-32.2
	BN2	271.8	228.2	43.6
RMT25	BN1	253.2	440.6	-187.6
	BN2	176.7	505.4	-328.7
	BN3	312.5	444.8	-132.3

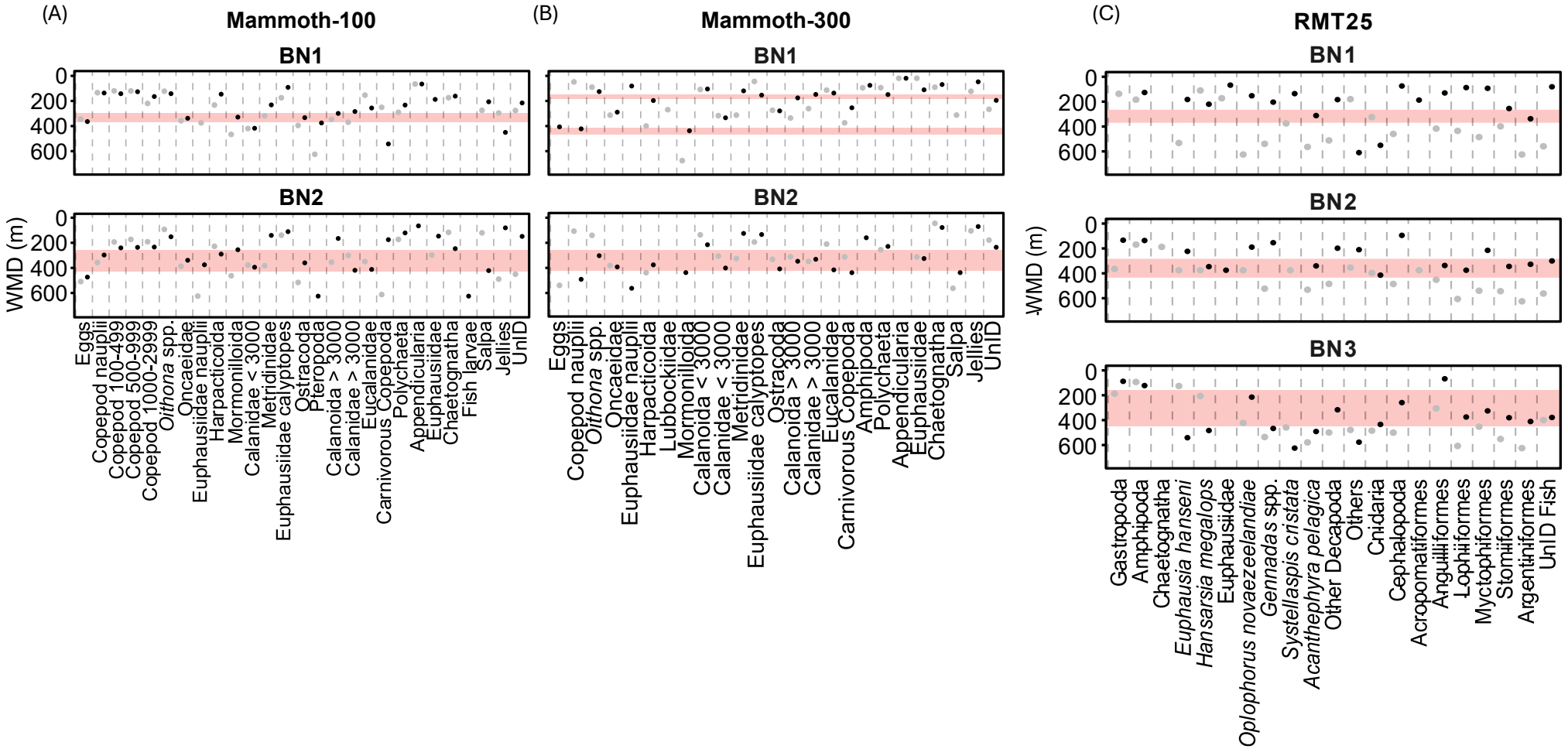

Figure 3.14 Weighted Mean Depth (WMD, m) of dominant taxa collected by the (A) Mammoth-100, (B) Mammoth-300 and (C) RMT25 nets at station BN in the northern Benguela Upwelling System. Red shading represents depths where oxygen concentrations were < 60 µmol/kg. Mammoth-100 and Mammoth-300 biomass samples not available at BN3. Black circles represent nighttime WMD and grey circles daytime WMD.

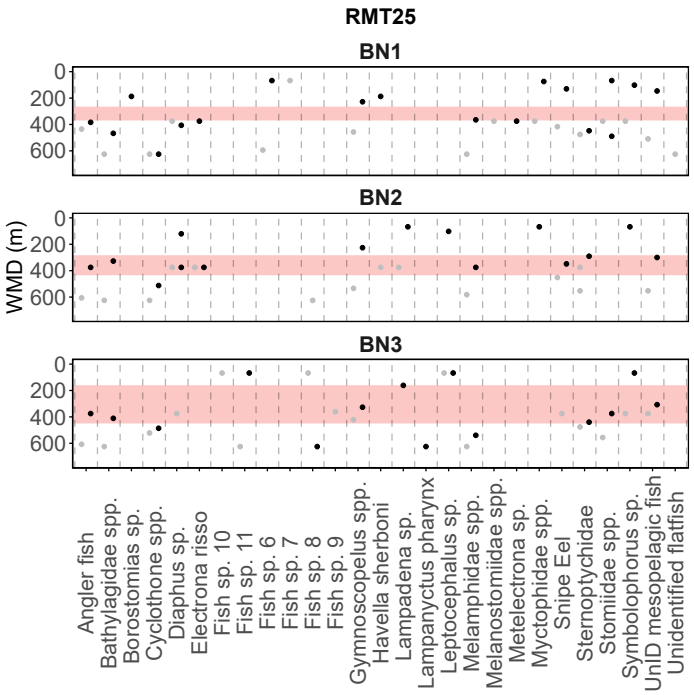

Figure 3.15 Weighted Mean Depth (WMD, m) of fish taxa collected by the RMT25 net at station BN in the northern Benguela Upwelling System. Red shading represents depths where oxygen concentrations were < 60 µmol/kg. Black circles represent nighttime WMD and grey circles daytime WMD.

3.4.4 Metabolic rates

3.4.4.1 Respiration

ETS-assay derived whole community mesozooplankton respiration rates at *in situ* temperatures (µl O^2 mg DW^{-1} d^{-1}) were highest in the top 125 m of the water column (Table 3.6). Taxa-specific ETS-assay derived respiration rates (µl O^2 mg DW^{-1} d^{-1}) for micronekton are found in Table 3.7. Total depth-integrated community respiration (CO_2 production) for the Mammoth-100, Mammoth-300 and RMT25 catches ranged between 3.40 – 24.6, 17.0 – 43.9 and 1.33 – 2.87 µmol C m^{-3} d^{-1} respectively. Pelagic respiration was dominated by mesozooplankton. Total community respiration from the Mammoth-300 catches did not show any distinct day/night trends (Figure 3.16). Total community respiration from the Mammoth-100 catches were greater at night for station BN3. ETS-assay derived taxa-specific micronekton respiration rates can be found in Table 3.7. Micronekton community respiration from the RMT25 catches was greatest at night in surface waters for all stations (Figure 3.16). Euphausiid community respiration was quantified from MOCNESS catches in the top 125 m and ranged between 10.6 – 12.3 µmol C m^{-3} d^{-1} at night and 0.0 – 0.47 µmol C m^{-3} d^{-1} during the day. Due to issues with the MOCNESS, no samples were obtained below 125 m.

Table 3.6 ETS-assay derived respiration rates (µl O^2 mg DW^{-1} d^{-1}) for whole community mesozooplankton samples from the Mammoth-300 and Mammoth-100 catches at station BN in the northern Benguela Upwelling system. Surface respiration for the Mammoth-100 sample at station BN3 was not available.

	Mammoth-300 respiration rates (µl O^2 mg DW^{-1} d^{-1})						**Mammoth-100 respiration rates (µl O^2 mg DW^{-1} d^{-1})**					
	BN1		**BN2**		**BN3**		**BN1**		**BN2**		**BN3**	
Depth (m)	Day	Night	Day	Night	Day	Night	Day	Night	Day	Night	Day	Night
5-33	23.9	11.6	14.5	15.5	11.8	21.5	39.7	55.5	11.6	17.3	-	48.5
33-63	33.8	26.9	51.9	8.9	4.6	49.4						
63-125	63.9	38.0	9.7	12.0	17.2	41.8						
125-188	9.0	14.8	3.0	7.9	5.1	23.2	5.6	8.8	9.0	4.1	9.3	43.3
188-250	7.0	8.7	2.5	2.5	4.9	11.6						
250-375	10.9	14.7	12.2	9.9	4.1	2.1	11.7	11.3	6.5	5.5	18.4	13.8
375-500	8.8	13.2	10.3	6.9	8.5	15.0						
500-625	3.1	4.9	9.4	2.4	8.0	4.8	5.5	3.3	4.5	4.0	5.9	4.1
625-750	2.9	5.1	7.3	2.7	5.3	4.1						

Table 3.7 ETS-assay derived taxa specific respiration rates (µl O^2 mg DW^{-1} d^{-1}) for micronekton catches from the RMT25 at station BN in the northern Benguela Upwelling system.

			Micronekton ETS-assay derived respiration rate (µl O^2 mg WW^{-1} d^{-1})													
Station	**Depth (m)**	**Time**	**Chaetognatha**	***Phrosina semilunata***	***Platyscelus* spp.**	***Euphausia hanseni***	***Gymnoscopelus* spp.**	***Sergestes* spp.**	**Sternoptychidae**	***Oplophorus spinosus***	***Euphausia gibboides***	**Nemichthyidae**	***Hansarsia megalops***	***Acanthephyra pelagica***	**Bathylagidae spp.**	**Melamphaidae**	***Cyclothone* spp.**
BN1	0-125	Day	0.39	6.47	4.04	-	-	-	-	-	-	-	-	-	-	-	-
	0-125	Night	-	4.10	-	6.48	9.48	6.31	12.72	-	-	-	-	-	-	-	-
	125-250	Day	-	2.97	2.83	-	-	-	-	-	5.60	0.66	-	-	-	-	-
	125-250	Night	-	3.11	2.37	5.73	-	5.22	4.42	10.88	-	8.57	7.54	-	-	-	-
	250-500	Day	-	-	3.63	6.08	2.25	2.43	3.08	-	-	3.06	-	1.02	-	-	-
	250-500	Night	-	-	-	-	-	-	2.25	-	-	-	-	-	0.53	0.46	-
	500-750	Day	-	-	-	2.86	1.47	-	3.08	2.55	-	0.37	-	0.45	0.23	1.25	0.73
	500-750	Night	-	-	-	2.35	4.91	0.63	2.70	-	-	-	4.44	1.79	0.15	-	1.53
BN2	0-125	Day	0.55	-	-	-	-	-	-	-	-	-	-	-	-	-	-
	0-125	Night	1.00	-	8.01	-	-	-	-	6.76	-	-	-	-	-	-	-
	125-250	Night	-	-	-	-	3.23	-	-	-	-	-	-	1.57	1.50	-	-
	250-500	Day	-	-	-	-	-	-	-	5.71	-	8.13	8.09	-	-	-	-

Station	Depth (m)	Time	Chaetognatha	*Phrosina semilunata*	*Platyscelus* spp.	*Euphausia hanseni*	*Gymnoscopelus* spp.	*Sergestes* spp.	Sternoptychidae	*Oplophorus spinosus*	*Euphausia gibboides*	Nemichthyidae	*Hansarsia megalops*	*Acanthephyra pelagica*	Bathylagidae spp.	Melamphaidae	*Cyclothone* spp.
BN2	250-500	Night	-	-	-	3.91	1.22	2.03	-	4.43	-	0.56	-	0.54	0.40	-	1.05
	500-750	Day	-	-	-	-	-	2.14	-	-	-	0.40	-	-	0.24	-	-
	500-750	Night	-	-	-	-	-	-	-	-	-	0.39	7.92	-	-	-	-
BN3	0-125	Day	-	-	-	6.98	-	-	-	-	-	-	-	-	-	-	-
	0-125	Night	-	6.12	-	-	-	-	-	-	-	-	-	-	-	-	-
	125-250	Day	-	-	-	-	-	-	46.06	10.11	-	-	9.47	-	-	-	-
	125-250	Night	-	-	-	5.61	-	-	-	9.66	-	-	-	-	-	-	-
	250-500	Day	-	-	-	-	7.22	3.94	-	-	-	9.26	-	-	-	-	-
	250-500	Night	-	-	-	-	-	-	-	-	-	-	-	-	-	-	1.14
	500-750	Day	-	-	-	-	-	-	-	-	-	-	-	1.59	0.20	1.44	0.62
	500-750	Night	-	-	-	3.72	-	0.33	-	3.87	-	-	4.32	-	-	-	-

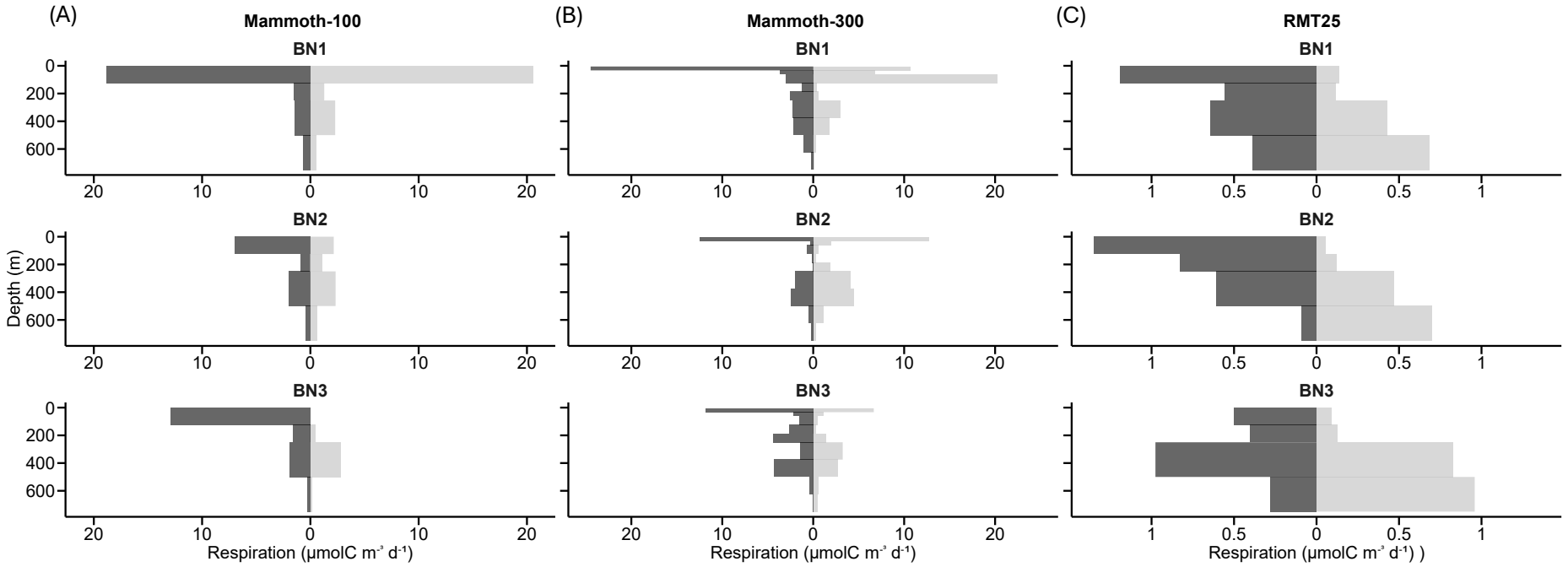

Figure 3.16 Total community respiration (µmolC m^{-3} d^{-1}) of mesozooplankton sampled from (A) Mammoth-100 and (B) Mammoth-300, and (C) micronekton (RMT25 >4 mm; MOCNESS for 0-125 Euphausiids) at station BN in the northern Benguela Upwelling System. Respiration data for the Mammoth-100 and Mammoth-300 catches were derived from ETS assays of whole community samples. Surface respiration for the Mammoth-100 sample at station BN3 was not available. Micronekton respiration data was derived based on the allometric regressions relating WW (mg) to ETS-derived respiration rates. Dark grey shading (left side of x-axis=0) represents nighttime observation and light grey shading (right side of x-axis=0) represents daytime observations.

3.4.4.2 Ingestion

Carbon specific ingestion rates ranged from 7.32 – 256.2 % µg C µg C^{-1} d^{-1} (Table 3.8). The greatest carbon specific ingestion rates were in *Centropages* spp.. Total community depth-integrated ingestion in Mammoth-100, Mammoth-300 and RMT25 catches ranged between 179.9 – 415.2, 76.1 – 106.4 and 11.5 – 31.2 µmol C m^{-3} d^{-1} (Figure 3.17). Pelagic ingestion was dominated by that of mesozooplankton. Total ingestion was greater in surface waters and 250 – 500 m. Total ingestion in Mammoth-100 surface samples at station BN1 were greater than at station BN2. RMT25 total community ingestion was more than twice greater during the night than during the day at station BN2.

Table 3.8 Summary of grazing experiments: initial carbon content of experimental bottles (µgC ml^{-1}), carbon ingested by zooplankton (µgC $ind.^{-1}$ day^{-1}), average carbon biomass of individual zooplankton (µgC $ind.^{-1}$) (Schukat *et al.*, 2013b; Bode-Dalby *et al.*, 2022) and percent carbon specific ingestion rates (% µgC µgC^{-1} d^{-1}). Initial carbon content of the bottles was calculated based on particle count and carbon biomasses of particles derived from allometric equations (Alldredge, 1998; Menden-Deuer and Lessard, 2000).

Grazing experiment ID	**Species**	**Initial carbon content (µgC ml^{-1})**	**Ingested carbon (µgC $ind.^{-1}$ day^{-1})**	**Zooplankton biomass (µgC $ind.^{-1}$)**	**Carbon specific ingestion rate (µg C µg C^{-1} d^{-1})**
6	*Oithona* spp. C4-5	0.59 ± 0.13	0.53 ± 0.33	1.17	45.40 ± 28.19
10	*Oithona* spp. C4-5	0.65 ± 0.17	1.65 ± 0.16	1.17	141.36 ± 13.93
12	*Oithona* spp. C4-5	0.60 ± 0.15	0.26 ± 0.16	1.17	22.59 ± 13.41
9	*Metridia* spp. C5-6	0.55 ± 0.06	10.1 ± 3.98	21.5	46.85 ± 18.50
5	*Nannocalanus minor C6F*	0.58 ± 0.12	19.4 ± 4.39	43	43.45 ± 10.63

Grazing experiment ID	**Species**	**Initial carbon content (µgC ml^{-1})**	**Ingested carbon (µgC ind.$^{-1}$ day^{-1})**	**Zooplankton biomass (µgC ind.$^{-1}$)**	**Carbon specific ingestion rate (µg C µg C^{-1} d^{-1})**
10	*Nannocalanus minor* C6F	0.65 ± 0.17	42.53 ± 19.30	43	98.91 ± 44.88
13	*Nannocalanus minor* C6F	0.67 ± 0.15	23.7 ± 9.0	43	55.10 ± 20.93
9	*Pleuromamma* spp. small C5/6	0.55 ± 0.06	5.67 ± 4.0	14	40.49 ± 28.61
13	*Pleuromamma* spp. large C6F	0.67 ± 0.15	30.1 ± 15.6	237	12.71 ± 6.59
8	*Calanoides natalis* C5	0.32 ± 0.04	3.81 ± 3.51	52	7.32 ± 6.75
12	*Calanoides natalis* C5-6	0.60 ± 0.15	34.5 ± 7.33	44	78.47 ± 16.66
12	*Centropages* spp. C5-6	0.60 ± 0.15	10.6 ± 3.28	4.15	256.21 ± 79.00

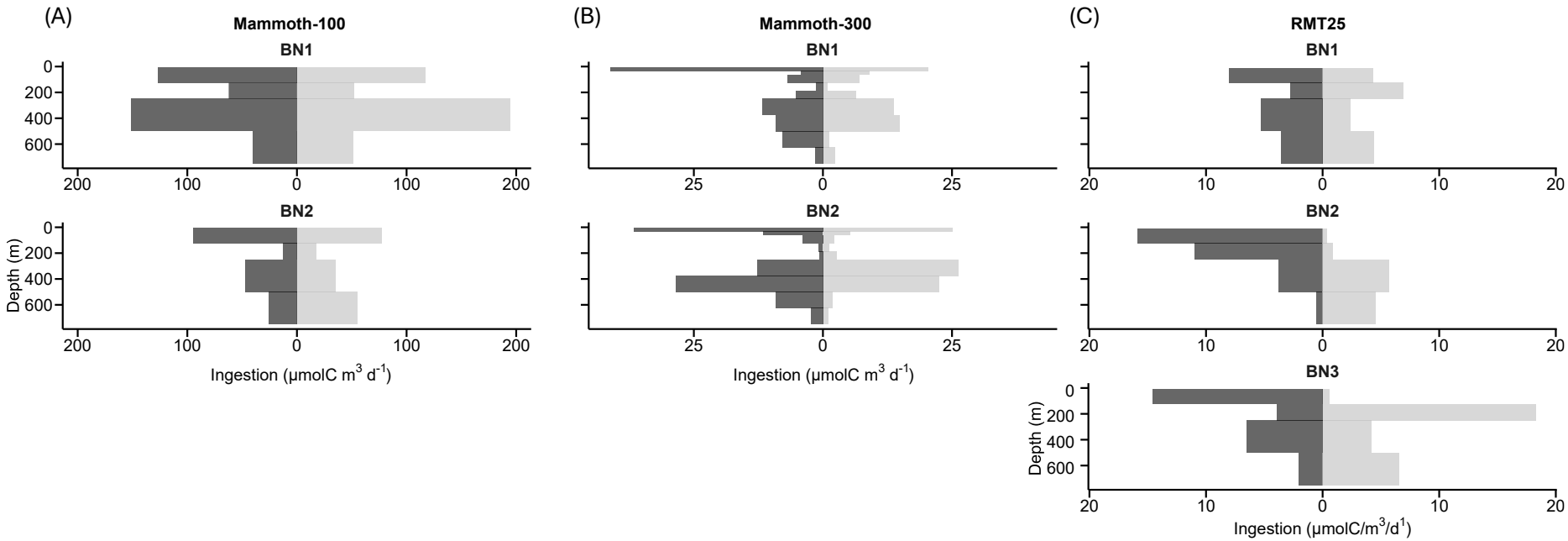

Figure 3.17 Total community ingestion (µmolC m^{-3} d^{-1}) of mesozooplankton sampled from (A) Mammoth-100 and (B) Mammoth-300, and (C) micronekton (RMT25 >4 mm) at station BN in the northern Benguela Upwelling System. Mammoth-100 and Mammoth-300 were not available for station visit BN3. Total community ingestion was calculated my multiplying catch biomass by the ingestion rates for individual taxa or functional groups and integrating them within each depth horizon sampled by the net. Dark grey shading (left side of x-axis=0) represents nighttime observations and light grey shading (right side of x-axis=0) represents daytime observations.

3.4.5 Metabolic carbon budget

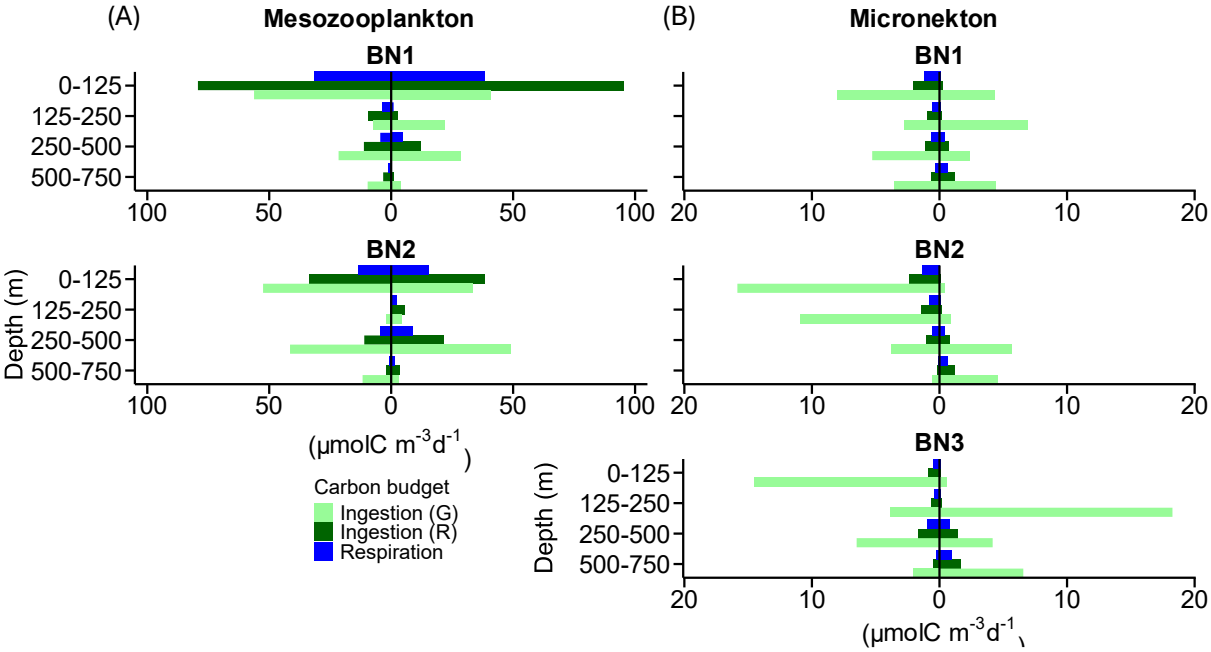

Figure 3.18 Total community carbon (µmol C m^{-3} d^{-1}) ingestion and respiration for (A) mesozooplankton and (B) micronekton at station BN in the northern Benguela Upwelling System. Ingestion is reported using two methods (1) carbon specific ingestion rates applied to biomass (Ingestion (G) = light green) and (2) ingestion calculated from respiration (Ingestion (R) = dark green; Ikeda and Motoda (1978)). Mesozooplankton ingestion was calculated from grazing experiment carbon specific ingestion rates (from this study and published literature) and applied to biomass estimates from this study. Micronekton ingestion was derived from published carbon specific ingestion rates applied to biomass estimates from this study. Values to the left side of the x-axis=0 represent nighttime observations and values to the right side of the x-axis=0 represent daytime observations. Mammoth-100 and Mammoth-300 samples not available at BN3. Mesozooplankton respiration was derived from ETS-assays on whole community samples (Mammoth-100 and Mammoth-300). Micronekton respiration was derived from allometric regressions relating WW (mg) to taxa-specific ETS-derived respiration rates (this study and published literature). When integrating the mesozooplankton data from both the Mammoth-100 and Mammoth-300, only ingestion and respiration rates of mesozooplankton <300 were included from the Mammoth-100 and added to that of the Mammoth-300, to avoid catch overlap between the two nets.

Total mesozooplankton and micronekton ingestion was greater than respiration for all station and depths using both methods (Figure 3.18). Mesozooplankton respiration accounted for 4.6 –

93.3 % of ingested carbon based on grazing experiments (i.e. Ingestion (G)). Beyond 125 m, respiration was always equivalent to < 52 % of ingestion. Micronekton respiration accounted for 0.69 – 20.0 % of Ingestion (G). When integrating throughout the entire water column, mesozooplankton respiration accounted for 38.6 ± 11.2 % and 30.5 ± 18.4 % of ingestion (G) during the day and night respectively at station BN. Depth integrated micronekton respiration accounted for 8.62 ± 2.58 % and 10.42 ± 3.25 % of Ingestion (G) during the day and night respectively at station BN.

3.4.6 Migrant biomass and active flux

Table 3.9 Total active carbon flux by mesozooplankton and micronekton diel vertical migration (DVM) at station BN in the northern Benguela Upwelling System. Migrant biomass is given as night – day biomass in the top 125 m of the water column. Negative migrant biomass indicate that biomass was greater during the day in surface waters compared to at night. All migratory fluxes are calculated for the duration spent at depth (11h for normal DVM and 13h for reverse DVM) and beyond a depth of 125 m. This depth was chosen to allow for consistency across all net sampling gear. Total active flux is the sum of respiratory, excretory and mortality fluxes, whereby excretory flux was equal to 0.31 of respiratory flux (Steinberg *et al.*, 2000) and mortality flux was equal to 0.75 and 0.66 of respiratory flux for mesozooplankton (Ikeda and Motoda, 1978) and micronekton (Brett and Groves, 1979; Kwong *et al.*, 2020) respectively.

	Mammoth-300		**Mammoth-100**		**RMT**		
	BN1	BN2	BN1	BN2	BN1	BN2	BN3
Migrant biomass µmol C m^{-3}	54.42	17.15	-84.61	3.91	195.7	291.6	81.7
Migrant respiratory flux µmol C m^{-3} d^{-1}	0.180	0.061	0.369	0.012	0.028	0.038	0.041
Migrant excretory flux µmol C m^{-3} d^{-1}	0.056	0.019	0.115	0.004	0.009	0.012	0.013
Migrant mortality flux µmol C m^{-3} d^{-1}	0.135	0.046	0.277	0.009	0.018	0.025	0.027
Total active flux µmol C m^{-3} d^{-1}	0.370	0.126	0.761	0.026	0.055	0.074	0.081

The biomass of mesozooplankton which migrated to depths > 125 m over a 24h DVM cycle was 54.4 and 17. 1 µmol C m^{-3} at stations BN1 and BN2 for the Mammoth-300 respectively, and -84.6 (more biomass in surface waters during the day) and 3.91 µmol C m^{-3} at stations BN1 and BN2 for Mammoth-100 catches respectively (Table 3.9). The total downward active carbon flux below 125 m by migrant mesozooplankton was 0.37 and 0.126 µmol C m^{-3} d^{-1} at stations BN1 and BN2 for the Mammoth-300, and 0.644 and 0.026 µmol C m^{-3} d^{-1} at stations BN1 and BN2 for Mammoth-100 (Table 3.9). The biomass of micronekton which migrated to depths > 125 m during the day was 195.7, 291.6 and 81.7 µmol C m^{-3} at stations BN1, BN2 and BN3 respectively. Micronekton active carbon flux from the RMT25 catches ranged between 0.055 – 0.081 µmol C m^{-3} DVM d^{-1} at station BN. Respiratory fluxes accounted for the highest proportion of total active flux, followed by mortality and excretory fluxes.

3.5 Discussion

This study quantified the trophic and physiological ecologies, biomass, magnitude of DVM, metabolic rates and active carbon flux of mesozooplankton and micronekton communities within the epi- and mesopelagic waters of the northern Benguela Upwelling System in the equatorial South Atlantic Ocean.

3.5.1 Zooplankton and micronekton dominate processing and fate of POM in the OMZ

The $\delta^{13}C$ signatures of POM decreased with depth (Figure 3.2), suggesting the source or composition of the organic matter changed with depth. O'Leary *et al.* (2001) found lower $\delta^{13}C$ POC values by up to 2.4 ‰ at 100 m compared to surface waters, with results pointing towards slower photosynthetic growth rates and fractionation of carbon isotopes in deeper waters. Similarly, studies have observed the $\delta^{13}C$ values of low-light phytoplankton in deeper epipelagic waters to have lower signatures by up to 6.3 ‰ compared to those in surface waters, suggesting light intensity and phytoplankton community may be important factors driving depth related changes in carbon isotope values (Henderson *et al.*, 2024).

In the present study, we observed a decrease in $\delta^{13}C$ of ~4 ‰ between the surface waters and lower epipelagic waters ~100/200 m, suggesting that differences in $\delta^{13}C$ signatures may indeed be driven by phytoplankton community photosynthetic responses to light intensity. Lower $\delta^{13}C$ values with increasing depth may also reflect the loss of labile ^{13}C-enriched components (e.g., ^{13}C-enriched carbohydrates and proteins) during heterotrophic degradation (Close *et al.*, 2014). POC:N ratios of POM were greater than the Redfield ratio of 106:16 (6.625) for station BN2 and BN3 at depths > 100 m and increased with depth (Figure 3.3), in agreement with global observations (Schneider et al., 2003). This further supports the idea of heterotrophic

degradation of POM by organisms and the preferential consumption of nitrogen rich compounds (e.g., proteins, amino acids) resulting in reworked particles having higher POC:N ratio as they sink to deeper waters (Gordon, 1971). Increased POC:N ratios with depth may also be related to increased contribution of animal faecal material to the particle pool with depth. Animals require nitrogen for growth and protein synthesis and therefore may preferentially absorb and assimilate nitrogen, resulting in faecal material and reworked particles having higher C:N ratios than fresh POM (Anderson, 1994; Steinberg and Saba, 2008; Mayor *et al.*, 2011).

The reworking of particles with depth can also be observed in the lipid data, whereby the proportional contribution of the zooplankton biomarker 18:1(n-9) increased with the depth in the > 53 µm particle pool, whereas the contribution of diatom 20:5(n-3) and dinoflagellate 22:6(n-3) biomarkers (Dalsgaard *et al.*, 2003) decreased with depth in the < 53 µm particle pool (Figure 3.9). This suggests an increased contribution of animal-sourced material (e.g., faecal material) but decreased contribution of fresh phytoplankton-derived material to POM with depth. Similar trends of increasing 18:1(n-9) contribution to POM with depth have been observed in past studies (Sheridan *et al.*, 2002; Richoux, 2010; Savineau *et al.*, 2024). The PUFA:MUFA ratios of POM were lowest within the OMZ, at depths between 250 – 400 m (Figure 3.9). Low PUFA:MUFA ratios are indicative of refractory POM, as PUFAs are more labile than MUFAs and have higher dietary absorption efficiencies in animals (Wakeham *et al.*, 1984; Hama, 1999). Harvey *et al.* (1987) found almost complete removal of PUFAs in faecal pellets of copepods compared to their diet, further providing evidence of POM from within the OMZ being enriched in faecal material compared to waters above and below. Finally, increased contribution of fatty alcohols with depths moreover suggests an increased contribution of zooplankton-derived material with depth, due to alcohols being important constituents of wax ester lipids of certain zooplankton (Table B 8; Table B 9; (Schukat *et al.*, 2014)).

The increased refractory nature of both large and small particles within the OMZ and increased contribution of 18:1(n-9) with depth to the > 53 µm particle pool suggest that particles may largely be shaped by biological processes and zooplankton/micronekton activity within the OMZ. This is further supported by glider data which observed deep particle layers between 250 – 500 m, with these “deep export” events characterized by enhanced aggregate and faecal pellet abundance (Lovecchio *et al.*, 2025). This is supported by continuous high biomass of both mesozooplankton and micronekton either permanently or partially residing within the OMZ (Figure 3.12). The mesozooplankton community within the OMZ may produce faecal pellets via egestion, hence producing large particles with the lipid, isotopic and POC:N ratio signatures observed in this study. It is furthermore possible that these particulate signatures are representative of faecal material being produced by the surface zooplankton population, with these then sinking and remaining untouched within the OMZ due to reduced biological activity

within the OMZ. Small particle-associated copepods, such as *Oithona* spp. and Oncaeidae, are hypothesized to be the main drivers of particle flux within the upper mesopelagic (Mayor *et al.*, 2020). These small particle-associated copepods are hypothesized to have a "search and destroy" mode of feeding as they scavenge for particle-attached microbes, inadvertently breaking down particles (Mayor *et al.*, 2014; Mayor *et al.*, 2020) and could therefore contribute to the reworking of and suspension of particles within this zone. Indeed particle-associated copepods such as Oncaeidae were observed to have WMDs permanently within the OMZ, with combined day/night WMDs of 344.0 ± 50.5 m and 355.4 ± 22.7 m in the Mammoth-100 and Mammoth-300 catches respectively. The high lability of a proportion of the < 53 µm particle pool at 500 m does agree with the idea that small zooplankton may break down rather than ingests large particle, thus making these smaller but with the same signatures as large "fresh" particles (this study; (Lovecchio *et al.*, 2025)). Prokaryotic count and microbial respiration was moreover reduced under low oxygen concentrations during this cruise, potentially lowering organic matter turnover by up to 7-fold in severely hypoxic waters (<20 µmol/kg) compared to oxygenated waters > 100 µmol/kg (Hemsley *et al.*, 2023; Lovecchio *et al.*, 2025), hence resulting in the sustained particle layer in the OMZ and some "fresh" material reaching depths of 500 m. This emphasizes the OMZ's role in retaining organic matter and modulating carbon cycling through reduced microbial respiration and metazoan biological activity.

3.5.2 Trophic ecology of mesozooplankton and micronekton

Overall, the $\delta^{13}C$ signatures of zooplankton and micronekton were more enriched than those of POM and ranged between -19.2 and -14.5 ‰ (Figure 3.4). This trend is observed in marine systems and is attributed to preferential consumption of labile ^{13}C enriched components of POM such as phytoplankton, especially diatoms (Fry and Wainright, 1991; De Figueiredo *et al.*, 2020). The $\delta^{13}C$ signatures of zooplankton and micronekton did not change with depth, suggesting they preferentially consumed photoautotrophic production throughout the water column (Fry and Wainright, 1991). The depleted $\delta^{13}C$ values and more refractory nature of POM with depth does indeed corroborate the idea that animals are preferentially consuming fresher material and/or migrating to surface waters where "fresher" POM was available. Mesopelagic fish signatures were in line with past studies in the nBUS (Duncan *et al.*, 2023) and micronekton showed variable signatures in line with past studies (Schukat *et al.*, 2014).

Stable isotope analysis of nitrogen revealed a $\delta^{15}N$ range of 4.86 – 14.70 ‰, with the lowest values in herbivorous calanoid copepods (Figure 3.4). A clear trophic gradient was observed, from mesozooplankton to micronekton to fish, with most zooplankton (excluding Chaetognatha) displaying lower $\delta^{15}N$ values than mesopelagic fish. This in essence suggests a positive relationship between $\delta^{15}N$ and body size and illustrates how bigger organisms are

feeding on smaller ones within the food web. This trend agrees with the idea of body size being a 'master trait' influencing trophic interactions in marine ecosystems (Andersen *et al.*, 2016) and is in agreement with past studies observing increased $\delta^{15}N$ from mesozooplankton, to macrozooplankton, micronekton and nekton (Hunt *et al.*, 2015). $\delta^{15}N$ values in mesopelagic fish matched those reported in a prior study in the nBUS (Duncan *et al.*, 2023), suggesting consistent trophic positioning of mesopelagic fish higher up the food web compared to zooplankton and micronekton. Our data showed limited evidence of vertical trophic partitioning based on $\delta^{15}N$ signatures, with a weak relationship between $\delta^{15}N$ signatures and depth (Figure 3.5), driven by subtle $\delta^{15}N$ enrichment of Bathylagidae spp., *Acanthephyra pelagica* and *Euphausia hanseni* with depth. Past studies have observed resident zooplankton and fish below the OMZ to have greater the $\delta^{15}N$ signatures than communities within or above the core of the OMZ (Gutiérrez-Bravo *et al.*, 2025). The lack of clear trophic partitioning in this study may reflect sampling limitations and biases in the present study, whereby the maximum depth sampled was 750 m, which will have excluded deep-water resident populations. Indeed, the $\delta^{15}N$ enrichment with depth in the Gutiérrez-Bravo *et al.* (2025) study was only apparent when including animals from depths > 900 m into the model. Moreover, our study did not comprehensively sample the zooplankton community when it came to stable isotope analyses but instead focussed on animals of most interest in epi- and upper mesopelagic waters and therefore may have overlooked deepwater resident taxa.

The lipid class and fatty acid profiles of mesozooplankton, micronekton and mesopelagic fish were broadly aligned with and support the trophic ecology and food web positioning inferred from the stable isotope signatures. The two herbivorous calanoid copepods *C. natalis* and *R. nasutus* ordinated away from all other species in both the lipid class and fatty acid RDAs (Figure 3.10 and Figure 3.11), highlighting the distinct herbivorous trophic ecologies of these two species compared to the more omnivorous and predatory species higher up the food web. The contribution of the 16:1(n-7) and 20:5(n-3), key diatoms biomarkers (Dalsgaard *et al.*, 2003), in *C. natalis* and *R. nasutus* suggests diatoms to be a major food source and places these species as broadly herbivorous. This is in support of past lipid biomarker studies which concluded diatoms to be an important source of food for *C. natalis* and *R. nasutus* (Verheye *et al.*, 2005; Ceballos *et al.*, 2006; Schnack-Schiel *et al.*, 2008; Daly *et al.*, 2011; Schukat *et al.*, 2014). All other species sampled overlapped significantly in their positions within the fatty acid RDA plot suggesting these species may all share more omnivorous/carnivorous diets. All taxa sampled contained 20:1(n-9) and 22:1 in their fatty acid signatures (Table 3.3). Moreover, all taxa but Chaetognatha spp., Bathylagidae spp., *Gymnoscopelus* spp., Nemichthyidae spp. and *R. nasutus* had fatty alcohols ALC-20:1 and ALC-22:1 contributions > 5 % (Table 3.4). These fatty acids and alcohols are biosynthesized *de novo* by herbivorous *Calanus* and *Calanoides* species

in polar and upwelling regions and are major constituents of their wax ester lipids (Hagen *et al.*, 1993; Kattner *et al.*, 1994; McMeans *et al.*, 2012; Schukat *et al.*, 2014). In the nBUS, these fatty acids and alcohols, hereafter referred to as calanoid biomarkers, can be attributed to the wax esters lipids of *C. natalis* (Schukat *et al.*, 2014). The presence of these long-chained fatty alcohols and acids in all taxa sampled is therefore indicative of predation on *C. natalis* or consumption of POM material reworked by *C. natalis* and underscores the importance of *C. natalis* to the food web of the nBUS.

The fatty acid signatures of *Euchaeta* spp., which contained 44.3 mol% of 18:1(n-9) is in agreement with past studies describing this species as predatory (Schukat *et al.*, 2014). 18:1(n-9) is biosynthesized de novo by zooplankton and therefore often used as a putative marker of carnivory (Dalsgaard *et al.*, 2003), although it must be noted that it is not possible to determine whether 18:1(n-9) signatures within this study originated from carnivory or de novo biosynthesis within the zooplankton. Unlike the Schukat *et al.* (2014) study for which the calanoid biomarker contributed < 2 mol% to fatty acid composition, in the present study *Euchaeta* spp. contained up to 7 mol% of these biomarkers, suggesting *C. natalis* predation to be an important contributor to *Euchaeta* diet. These fatty acid signatures align with $\delta^{15}N$ signatures of *Euchaeta* spp. being greater than the other mesozooplankton sampled, hence placing it higher up the food web (Figure 3.4).

The euphausiids *Euphausia hanseni* and *Hansarsia megalops* (previously *Nematoscelis megalops*) had mixed signatures of both phytoplankton and zooplankton-derived biomarkers, in line with their opportunistic omnivorous tendencies (Barange *et al.*, 1991; Pillar *et al.*, 1992). *H. megalops* is however suggested to be more carnivorous than *E. hanseni,* with the former species having elongated thoracic appendages thought to enhance the ability to catch prey (Berkes, 1975; Barange *et al.*, 1991). These species moreover partition their food sources based on vertical position in the water column and size, with *H. megalops* feeding on larger copepods than *E. hanseni* (Barange, 1990; Barange *et al.*, 1991). This is reflected in *H. megalops* $\delta^{15}N$ signatures being ~ 2 ‰ more enriched than those of *E. hanseni*.

The Decapoda species (*Oplophorus novaezeelandiae*, *Gennadas* spp., *Cristaspis cristata* and *Acanthephyra pelagica*) were all dominated by the zooplankton biomarker 18:1(n-9) and had fatty alcohol compositions elevated in the calanoid biomarkers ALC-20:1 and ALC-22:1, in agreement with their classification as zooplanktivorous (Schukat *et al.*, 2013a). Decapods are found to feed on various prey including copepods, euphausiids, amphipods and other decapods (Omori, 1975; Heffernan and L. Hopkins, 1981; Flock and Hopkins, 1992), aligning with $\delta^{15}N$ signatures observed in this study.

The Amphipoda taxa (*Phrosina semilunata, Platyscelus* spp. and *Phronima* spp.) in the present study were all dominated by fatty acids 16:0, 18:1(n-9), 20:5(n-8) and 22:6(n-3) and also contained calanoid biomarkers. These signatures are concurrent with the fatty acid compositions of predatory hyperiid amphipods (Gibbons *et al.*, 1992; Auel *et al.*, 2002; Savineau *et al.*, 2024) and aligns with their $\delta^{15}N$ signatures being above those of mesozooplankton which they prey upon, but below larger micronekton and mesopelagic fish (Figure 3.4).

The fatty acid composition of all mesopelagic fish were dominated by 16:0, 18:1(n-9) and 22:6(n-9) and contained signatures of the calanoid biomarkers, in agreement with wider fatty acid studies (Wang *et al.*, 2019; Voronin *et al.*, 2022; Papadimitraki *et al.*, 2023). These species are all considered carnivorous and feed on a range of prey including mesozooplankton, euphausiids, decapods, gelatinous organisms and other fish (Feagans-Bartow and Sutton, 2014; Sweetman *et al.*, 2014; Eduardo *et al.*, 2020a; Eduardo *et al.*, 2021; Bucklin *et al.*, 2024), as is observed by their top $\delta^{15}N$ trophic positioning. It is worth noting that the mesopelagic jellyfish *Atolla* spp. and the mesopelagic fish *Cyclothone* spp. had fatty alcohol contributions to total lipid content of 17.4 ± 16.8 and 29 ± 6.8 %. This is significantly higher fatty alcohol compositions than all other micronekton and fish, and together with fatty alcohol calanoid biomarker contributions > 30 % point towards consumption of *C. natalis*. Studies have indeed found *Cyclothone* spp. to have feeding strategies focused on wax-ester-rich copepods (Maar *et al.*, 2023). The elevated levels of 18:1(n-9) and calanoid biomarkers compared to phytoplankton biomarkers in *Atolla* spp. aligns with past studies (Nelson *et al.*, 2000) and is evidence of the carnivorous nature of these cnidarians.

3.5.3 Physiological ecology of mesozooplankton and micronekton

Lipid and elemental signatures may reflect species-specific physiological adaptations and requirements. The lipid class RDA revealed fatty alcohols to be important discriminants between *C. natalis* and *R. nasutus,* and the rest of the mesozooplankton and micronekton community. Fatty alcohols made up > 50 % of total lipid composition in the two aforementioned species. The prevalence of fatty alcohols suggests the storage of lipids in the form of wax esters, whereby a fatty acid is attached to a fatty alcohol. This form of storage is typically seen in copepods of seasonally or environmentally dynamic, high-latitude/upwelling systems and is thought to play an important role in fuelling reproductive processes such as gonad development and egg production following a period of metabolic inactivity (Hagen and Schnack-Schiel, 1996). Arashkevich *et al.* (1996) reported low lipid content and advanced gonad development in *C. natalis* from deep layers which, together with empty guts and low respiration rates, suggested that expended lipid reserves fuelled reproductive growth. Other studies have also reported significant decreases in the respiration rates and high lipid content in deeper waters,

underscoring the diapausing behaviour of *C. natalis* and *R. nasutus* (Timonin *et al.*, 1992; Ohman *et al.*, 1998; Auel *et al.*, 2005; Schnack-Schiel *et al.*, 2008; Schukat *et al.*, 2013b). Despite this, lipid contents of *C. natalis* (21.6 ± 5.5 % of DW) *and R. nasutus* (23.3 ± 7.7 % DW; Table B 11) in this study were lower than in previous studies. Schukat *et al.* (2014) reported values of 50.1 % and 46.2 % for *C. natalis* C5 copepodites and *R. nasutus* respectively. Similarly, Verheye *et al.* (2005) reported values of 49.5 % in *C. natalis* C5 copepodites sampled between 400 – 700 m (*C. natalis* lipids in the present study came from samples between 500 – 750 m). However, in these past studies *R. nasutus* were collected in December and *C. natalis* in March (Verheye *et al.*, 2005; Schukat *et al.*, 2014), which marks austral summer and the transition into austral autumn, whereas the present study took place in June, marking the transition into austral winter. It is possible that the lower lipid levels in this study reflect seasonal depletion of lipids later on in the season compared to a few months prior when these species would have had the highest lipids levels before entering diapause. *C. natalis* C5 copepodites did moreover have considerably lower carbon specific ingestion rates (7.32 ± 6.75 %) compared to the C5/females (78.47 ± 16.66 %), further supporting that *C. natalis* C5 copepodites were in a state of reduced metabolic activity. The lipid reserves present in *R. nasutus* can also be observed when looking at the C:N ratios of these animals, whereby *R. nasutus* had the greatest C:N ratios (Figure 3.6), indicative of preferential retainment of carbohydrates.

All fish taxa in this study, except Bathylagidae spp., had lipid compositions > 17% of DW (Table B 11). Lipids in mesopelagic fish may be an adaption to help regulate their buoyancy (Zahuranec and Pugh, 1971). Indeed, many species of *Cyclothone,* myctophiids (e.g., *Gymnoscopelus* spp.) and stomiiformes (e.g., Sternoptychinae spp.) have been observed to have fat accumulations around their swim bladders as well as extensive oil droplets within their body cavities (Capen, 1967; Zahuranec and Pugh, 1971; Kleckner and Gibbs Jr, 1972). High lipid contents are thought to be especially useful for species migrating considerable depths, as it removes the energy-consuming requirement to secrete gas (Zahuranec and Pugh, 1971). The storage of lipids, especially unsaturated fatty acids may be used as a buoyancy mechanism, as these have low phase transition temperatures, making them easily accessible to catabolise in liquid state, and influencing density and buoyancy control (Pond, 2012).

3.5.4 Micronekton vertical distribution in response to the OMZ

OMZ waters were widespread and persistent during the study period at depths between 250 – 450 m, with oxygen concentrations within the OMZ ranging from 29 – 60 µmol/kg (Figure B 2 and (Lovecchio *et al.*, 2022)). In pelagic ecosystems, oxygen concentration is an important control of the distribution of animals, with hypoxic conditions (< 60 µmol O_2/kg) influencing zooplankton,

macro-invertebrates and fish at different scales due to interspecific differences in physiologies and behaviours (Ekau *et al.*, 2010).

Micronekton demonstrated a slight bimodal trend in biomass in relation to the OMZ at night, with high biomass of animals in the surface layer <125 m and again between 250 – 500 m, although this varied a lot with station (Figure 3.12). In contrast, daytime biomass increased with depth, with the greatest biomass of micronekton found below the OMZ between 500 – 750 m. Micronekton including Decapoda, Cephalopoda and mesopelagic fish exhibited consistent DVM, with some taxa migrating completely through the OMZ (Figure 3.14). Strong DVM is a common phenomenon of mesopelagic fish, with the near surface region < 200 m becoming an important aggregation layer during the night (Sutton, 2013). Myctophids (e.g., lanternfish, *Symbolophorus* spp., Myctophidae spp., *Lampadena* spp. and *Gymnoscopelus* spp.) performed extensive DVM into surface waters at night (Figure 3.15), in agreement with past findings reporting myctophids to be strong migrators which feed in surface waters at night (Olivar *et al.*, 2012; Eduardo *et al.*, 2021). These diel vertical patterns suggest the OMZ did not act as a barrier to DVM and that these taxa are able to tolerate low oxygen levels for short amounts of time. Indeed, Olivar *et al.* (2017) found migratory mesopelagic fish able to traverse the OMZ. Some mesopelagic fish (e.g., Angler fish, Bathylagidae spp.) migrated within the lower boundary of the OMZ at night, potentially as a strategy to feed on high biomasses of mesozooplankton within this layer. Other taxa such as *Cylothone* spp. remained distributed below the OMZ and did not show strong signals of DVM, aligning with current understanding that these species are non-migratory residents of the mesopelagic (Olivar *et al.*, 2012; Maas *et al.*, 2014; Olivar *et al.*, 2017). Olivar *et al.* (2017) did find *Cyclothone* spp. inhabiting areas of low oxygen concentrations, however these concentrations were higher (60 – 80 µmol/kg) than those in our study, suggesting low concentrations between 29 – 60 µmol/kg in the present OMZ may be too low for *Cyclothone* spp. in the nBUS.

Decapoda spp. appeared to mostly avoid OMZ waters, remaining below them during the day and migrating to waters above the OMZ during the night, aligning with vertical distributions from past studies in the nBUS (Schukat *et al.*, 2013a). Studies have reported increased abundances of decapods below the OMZ in the eastern tropical North Pacific (Maas *et al.*, 2014). The vertical expansion of the OMZ during station BN3 compared to BN1 and BN2 moreover appears to have reduced the DVM behaviour of Decapoda spp., with taxa such as *Gennadas* spp. and *Acanthephyra pelagica* remaining below the OMZ at station BN3 compared to stations BN1-BN2. This suggests OMZ expansion may act as a barrier to the DVM behaviour of some micronekton taxa (Tao *et al.*, 2022).

3.5.5 Mesozooplankton vertical distribution and OMZ refuge

Mesozooplankton biomass from the Mammoth-300 catches followed a bimodal vertical distribution, with the first biomass peak concentrated in surface waters (5 – 33 m) and another peak again between 250–500 m (Figure 3.12). Field observations have reported that OMZs create metazoan habitat compression and thus high biomass in surface waters (Wishner *et al.*, 2013; Wishner *et al.*, 2020). Mesozooplankton biomass data from the Mammoth-300 catches does show biomass compression in the top 30 m of the water column, however in the present study, such compression is likely more related to the very shallow mixed layer and chlorophyll maxima being < 50 m (Lovecchio *et al.*, 2022), as the OMZ was located much deeper. In contrast, the secondary biomass peak coincided with the OMZ and was particularly evident at station visit BN2. A similar bimodal trend was observed using the Mammoth-100 net, albeit at a coarser resolution due to broader sampling depth intervals (Figure 3.12). Such bimodal distributions of mesozooplankton biomass have previously been reported in OMZ regions, with secondary peaks in mesozooplankton biomass located at the lower boundary of the OMZ (Saltzman and Wishner, 1997; Martin *et al.*, 2015). In the northern Benguela specifically, past studies have reported peaks in Copepoda abundance located in waters < 60 m and again at the lower boundary of the OMZ layer at depths > 300 m (Auel and Verheye, 2007), in agreement with our findings of peak biomasses between 250 – 500 m. It should be noted that sampling intervals within the mesopelagic zone in our study were coarse (125 m using the Mammoth-300 and 250 m using the Mammoth-100) making exact determination of mesopelagic zooplankton biomass maxima difficult in terms of whether these animals were located within the core of OMZ waters and/or at the lower boundary of the OMZ.

The mesozooplankton biomass peaks within the OMZ suggests this zone to have an important ecological role for mesozooplankton. OMZs have been suggested to provide mesozooplankton a refuge from larger predators with high oxygen requirements compared to their prey (Steinberg *et al.*, 2008; Seibel, 2011). By residing within the lower boundary of the OMZ, mesozooplankton are able to avoid the lowest oxygen concentrations but still remain within hypoxic conditions unfavourable to larger animals. Indeed, peak micronekton biomass was below the OMZ and deeper than that of mesozooplankton during the day, suggesting mesozooplankton residence within the lower OMZ may be a tactic to avoid predators. Experiments run in large indoor mesocosm systems have indeed observed the copepod *Daphnia pulicaria* to preferentially inhabit waters with oxygen concentrations of ~30µmol/kg where conditions were unfavourable for the predatory fish in the experiment, reducing *D. pulicaria* mortality rate by 1/3 compared to the oxic treatment (Larsson and Lampert, 2011). In the present study, Calanidae and Eucalanidae were proportionally important taxa to the mesozooplankton community composition beyond 250 m, suggesting these taxa have adapted to low oxygen environments.

Indeed several species of the family Eucalanidae, including *Eucalanus* spp. and *R. nasutus* are characterised by "lethargic lifestyles" whereby they substantially reduce their respiration rates or even enter a dormant state within or below the OMZ (Schukat *et al.*, 2013b; Teuber *et al.*, 2013). *C. natalis,* which dominated Calanidae composition by > 80 % at depth > 250 m (unpublished data from NMFRI Plankton Sorting and Identification Centre, Poland; Figure 3.13) and *R. nasutus* did indeed have lipid contents greater than the other mesozooplankton sampled (Table B 11). These energy reserves may allow them to reduce metabolic activity for prolonged periods and use the OMZ as a predator avoidance mechanisms during diapause (Wishner *et al.*, 2020). *C. natalis* have been associated with low-oxygen deep waters where they diapause and complete their life cycle, moulting into adults before ascending to become active adults in surface waters (Arashkevich *et al.*, 1996; Auel and Verheye, 2007).

The persistent presence of *C. natalis* and Eucalanidae, as well as daytime residence of Metridinidae within the OMZ in this study, reinforces current understanding that these taxa can survive in low oxygen environments (Saltzman and Wishner, 1997; Teuber *et al.*, 2013; Tutasi and Escribano, 2020). *C. natalis* has indeed been reported to have 100 % survival down to 46.88 µmol/kg and 80 % survival at 29.06 µmol/kg (Auel and Verheye, 2007), suggesting the OMZ oxygen concentrations of 29 – 60 µmol/kg were well within their tolerance threshold. ETS-assay derived respiration rates (µl O^2 mg DW^{-1} d^{-1}) (Table 3.6) and carbon specific respiration rates (µg C µg C % d^{-1}; Table B 12) for whole mesozooplankton community samples were indeed reduced below 125 m compared to surface waters, suggesting reduced metabolic activity. Although this could partly be attributed to low oxygen induced lower respiration rates, this trend is common in mesozooplankton irrespective of the OMZ, with other potential drivers included lower temperatures (Ikeda, 1985; Ikeda, 2014), allometric relationships between increased body size and decreased respiration (Kiørboe and Hirst, 2014), and increased proportion of metabolically inactive diapausing species.

3.5.6 Mesozooplankton DVM behaviour in an OMZ

DVM is a well-documented behavioural strategy in zooplankton and nekton, influenced by both environmental (e.g., light, temperature, oxygen, food availability) and physiological drivers (e.g., life stage), to maximise trade-offs between food availability and predator avoidance (Bandara *et al.*, 2021). While no synchronized DVM was observed across the mesozooplankton community, certain taxa, such as Metridinidae and copepod nauplii, exhibited pronounced vertical migration between epipelagic and mesopelagic waters (Figure 3.14). Metridinidae consistently migrated into the OMZ (Figure 3.14), as previously observed (Loick *et al.*, 2005) and showed normal DVM behaviour – migrating to deeper waters during the day. As with mesozooplankton taxa residing within the OMZ, Metridinidae's temporary residence in the OMZ during the day may be a strategy

to reduce predation risk during the day, whilst DVM to surface waters enables them to pay off their oxygen debt incurred during the day whilst also accessing increased food supply. Species in the genus *Pleuromamma* (Metridinidae) have indeed been observed to undergo extensive DVM into low-oxygen waters, with their nighttime ascent determined by a combination of higher oxygen levels and food supply (Teuber *et al.*, 2013; Wishner *et al.*, 2020). By contrast, copepod nauplii (Mammoth-300) showed reverse DVM, descending into the mesopelagic at night, potentially a predator-avoidance strategy. Reverse DVM has been observed in *Pseudocalanus* spp. as a strategy to reduce spatial overlap with predators (Ohman *et al.*, 1983; Ohman, 1990). *Calanus finmarchicus* in the Clyde Sea have also been observed to perform reverse DVM, sinking to depth at midnight to avoid predation by krill (Tarling *et al.*, 2002). The lack of pronounced mesozooplankton DVM, especially in the smaller size classes of mesozooplankton, may be attributed to different life-strategies promoting best survival. DVM is often attributed to larger zooplankton being more conspicuous and susceptible to visual predation (Hays *et al.*, 1994). For small zooplankton, the benefits of staying in surface waters where food concentrations are high, thus allowing consistent feeding and rapid growth, may outweigh the costs of increased risk of visual predation during the day (Irigoien *et al.*, 2004). Indeed, even those species which did show weak DVM stayed within epipelagic surface waters during the day, where food concentrations were highest.

3.5.7 Metabolic budget

As a general trend, estimated mesozooplankton ingestion using both methods was always greater than respiration (Figure 3.18), suggesting that food ingested was more than sufficient to meet metabolic requirements. Several potential drivers could explain the low respiration rates in relation to ingestion rates in both methods (up to an order of magnitude lower) in samples below 125 m. High ingestion rates of carbon relative to respiratory demand aligns with the observations of low food quality in the mesopelagic relative to the surface mixed layer. Indeed, mesopelagic POM was highly refractory and nutrient depleted compared to surface waters meaning mesozooplankton would need to consume a large quantity of POM to meet their metabolic and nutritional requirements (Mayor *et al.*, 2014).

High ingestion at depth compared to respiratory requirements may moreover be a result of overestimation of ingestion rates at depth. Mesozooplankton and micronekton ingestion rates were derived from a combination of copepod grazing experiments, which took place during this study and literature-based ingestion rates. However, limited data regarding specific ingestion rates of mesozooplankton and micronekton in the nBUS, resulted in the use of broader ingestion rates from taxa sharing similar feeding strategies or from different oceanic locations. Moreover, the same surface-derived specific ingestion rates were applied to both surface and

deep biomass measurements, which may have resulted in overestimation of ingestion at depth. To tackle the uncertainty of grazing rates, ingestion rates were recalculated based on relationship between respiration and ingestion. This suggests surface grazing rates may have indeed overestimated ingestion at depth compared to ingestion estimates using respiratory carbon demand. In environments with big variations in temperature/oxygen with depth, using respiration obtained from ETS-assays from samples at *in situ* conditions may be better suited for estimating ingestion than grazing rates obtained in surface waters – as the latter are likely to be greatly influenced by vertical changes in environmental conditions. Both these methods do still fall under the assumption that animals at depth were indeed feeding. No synchronised DVM was observed in the mesozooplankton, hence suggesting that mesozooplankton were indeed feeding where they resided. However this assumption will also itself lead to overestimations of feeding at depth given 1) Metridinidae were observed to undergo extensive DVM and it can therefore be reasoned that they were feeding in surface waters and not at depth – especially considering the idea that the reason Metridinidae (and other zooplankton) undergo DVM is to avoid predation, therefore feeding at depth would invite detection by predators 2) A proportion of the mesopelagic residents are lipid-rich diapausing species and could therefore be reliant on the consumption of internal lipid reserves rather than ambient POM 3) We don't fully understand the effects of hypoxia on mesozooplankton grazing activity, although studies suggest that filter-feeding copepods rapidly decrease their filtering rates below 3 mg O_2/L (~93.75 µmol O_2/kg) (Heisey and Porter, 1977). These uncertainties highlight the need for more experimental work to study ingestion rates of zooplankton/micronekton under hypoxia.

3.5.8 Implications of vertical distribution of mesozooplankton and micronekton for biogeochemical cycling

The occurrence and movement of mesozooplankton and micronekton in the OMZ must have consequences for the cycling of organic matter in the northern Benguela upwelling system. Zooplankton and micronekton that feed in surface waters and migrate to depth actively transport organic carbon from epi- to mesopelagic layers. These animals will then respire/excrete/produce faecal matter at depth, potentially preventing this organic matter from returning to surface waters (Steinberg *et al.*, 2008; Isla *et al.*, 2015). We found that mesozooplankton actively transported between 0.026 and 0.761 µmol C m^{-3} d^{-1} to depths below 125 m through DVM, via respiration, excretion, and mortality during their daytime (or nighttime, in the case of reverse DVM) residence at depth. Micronekton contributed a further 0.055 to 0.081 µmol C m^{-3} d^{-1}. Although most micronekton exhibited strong DVM through the OMZ to feed in surface waters during the night before retreating below the OMZ during the day, this only accounted for 21 % of total mesozooplankton and micronekton active carbon flux below 125 m.

This suggests that despite mesozooplankton not performing as extensive DVM as seen in micronekton, mesozooplankton DVM remains an important mechanism of active respiratory carbon flux within the nBUS. It should be noted that Euphausiid contribution to active flux was not quantifiable in a comparable way to that of mesozooplankton (Mammoth) and micronekton (RMT25) due to issues with the MOCNESS net that prevented sampling deeper than 125 m. However, we did observe substantial Euphausiid respiration rates of 10.6 – 12.3 µmol C m^{-3} d^{-1} at night compared to 0.0 – 0.47 µmol C m^{-3} d^{-1} during the day suggesting Euphausiids were actively migrating out of the top 125 m depth layer during the day. Although we are not able to determine where this biomass is migrating to during the daytime, the greatly reduced respiration rates suggest these animals are likely to be significant contributors to DVM active carbon flux.

3.6 Conclusion

This study provided a comprehensive characterization of the trophic and physiological ecology, vertical distribution, and role in carbon cycling of mesozooplankton and micronekton in the northern Benguela Upwelling System (nBUS), with a particular emphasis on interactions with the oxygen minimum zone (OMZ). Our findings underscore the central role of mesozooplankton and micronekton in the processing and fate of particulate organic matter (POM) across the epipelagic and mesopelagic zones. The elevated C:N ratios and refractory lipid signatures of POM within the mesopelagic collectively point to extensive heterotrophic reworking of POM, particularly within the OMZ. Stable isotope and lipid signatures revealed clear trophic structuring, with $\delta^{15}N$ values and biomarker profiles aligning with predator-prey relationships. The presence of the calanoid copepod fatty acids biomarkers throughout all species sampled suggests *Calanoides natalis* to be a foundational prey in the nBUS. Notably, our study highlights the importance of the OMZ as an ecological refuge for many temporary and permanent mesozooplankton residents. In most cases, micronekton were able to perform DVM across the OMZ, however, in a few cases, the expansion of the OMZ formed an ecological barrier to the DVM behaviour of Decapoda spp.. The lack of pronounced DVM in the majority of mesozooplankton compared to strong DVM in micronekton further highlights that body size may be an important determinant of DVM behaviour. Despite this, mesozooplankton accounted for 79 % of total meso- and micronekton active carbon flux below 125 m. Uncertainties and limitations identified in this study, regarding producing metabolic budgets for mesozooplankton and micronekton, highlight the need to better understand the physiology and metabolic rates of these animals, especially with regards to effects environmental factors of hypoxic waters, when assessing carbon budgets.

Chapter 4 Mesozooplankton size spectra reflect trophic structure and physiological ecology in the upper 500 m of the ocean in the Scotia Sea (Southern Ocean)

Eloïse L-R. Savineau[1,2], Kathryn B. Cook[2,3], Anna Belcher[4,5], Sophie Fielding[4], Gabriele Stowasser[4], Geraint A. Tarling[4], Ben Ward[1], Daniel J. Mayor[2,3]

[1] School of Ocean and Earth Science, University of Southampton, Southampton, SO14 3ZH, UK

[2] National Oceanography Centre, Southampton, SO14 3ZH, UK

[3] Present address: Biosciences, Hatherly Building, University of Exeter, Exeter, EX4 4PS, UK

[4] British Antarctic Survey, Cambridge, CB3 0ET, UK

[5] Present address: UK Centre for Ecology and Hydrology, Penicuik, EH26 0QB, UK

ES analysed the data and wrote the manuscript with support from KC and DM. KC, GS, GT, SF, AB and DM conducted sample collection and processing at-sea. KC and ES conducted the FlowCam sample processing and image classification. DM and KC contributed feedback on the manuscript.

Keywords: Zooplankton; Copepods; Mesopelagic; Epipelagic; NBSS, Normalised Biovolume; Trophic Interactions; South Georgia; Twilight Zone

4.1 Abstract

Understanding depth-related changes in zooplankton size structure and community composition is key to interpreting trophic dynamics and carbon flux in the upper ocean. This study provides the first depth-resolved analysis of mesozooplankton normalized biovolume size spectra (NBSS) from the surface to 500 m in the Scotia Sea. Mesozooplankton were collected using a 330 µm MOCNESS net and analysed via fluid imaging microscopy (FlowCam Macro). NBSS showed multi-modal distributions, reflecting both sampling biases and key functional groups dominating community composition. Surface waters (0 – 65 m) were dominated by the large, lipid-storing copepod *Calanoides acutus*, whereas the boundary of the epi- to mesopelagic (125 – 250 m) was characterised by small omnivorous and particle feeding copepods such as Metridinidae and Oncaeidae. Mesopelagic layers (250 – 500 m) contained

both small omnivorous/detritivorous taxa and large-bodied *C. acutus, Rhincalanus gigas* and carnivorous taxa. NBSS slopes were all shallower than the theoretical -1 slope, indicating high biovolume retention in larger size classes and suggesting high trophic transfer efficiency (TTE). However, much of this biomass, specifically lipid-storing copepods in diapause, may not have been actively feeding during sampling. This suggests that the observed biomass reflects energy acquired in previous weeks or months, challenging interpretations of high TTE. These findings highlight the influence of physiology, particularly copepod diapause, on the size structure and inferred energy flow in zooplankton communities. The study moreover emphasizes that size spectra alone can misrepresent ecosystem dynamics if taxonomic composition is ignored and underscores the importance of integrating functional ecology into size-based approaches when assessing zooplankton-mediated carbon cycling.

4.2 Introduction

Zooplankton play a central role in the flow of energy in pelagic ecosystems, acting as a trophic link between phytoplankton and higher trophic levels such as fish, birds and marine mammals. From a biogeochemical perspective, zooplankton are a key component of the biological carbon pump (BCP), interacting with, transforming, and transporting organic carbon from surface to deep layers of the ocean (Steinberg and Landry, 2017). Particulate organic matter (POM) sinking into the mesopelagic attenuates with depth, with zooplankton-mediated processes, e.g. grazing, faecal pellet production, particle fragmentation, and active transport, influencing carbon flux attenuation (Steinberg and Landry, 2017). In particular, particle fragmentation – whereby small, particle-associated zooplankton intercept and break down large, fast-sinking particles into small, suspended ones – is thought to be the primary driver of particle attenuation and remineralisation (Giering *et al.*, 2014; Mayor *et al.*, 2020). This process, known as microbial gardening, makes small, suspended particles available to bacteria for colonisation and microbial respiration (Mayor *et al.*, 2014). The depth at which these zooplankton-mediated processes occur, will influence the length-scale of carbon sequestration in the ocean, with deeper carbon remineralisation depths resulting in longer sequestration (Stukel *et al.*, 2023) and greater carbon dioxide removal from the atmosphere (Kwon *et al.*, 2009). Exploring how zooplankton communities and their trophic ecology change with depth through the mesopelagic is therefore key to understanding how animals at different depths are influencing the BCP and hence carbon cycling and storage in the ocean.

In marine ecosystems, body size is considered a master trait influencing an organism's physiology, community structure and trophic interactions (Kleiber, 1932; Barnes *et al.*, 2010; Andersen *et al.*, 2016). In trophic ecology, size dictates predator-prey interactions as

zooplankton are typically constrained by gape-size and feeding apparatuses, resulting in energy in a food web flowing from small to large organisms (Cohen *et al.*, 1993; Hansen *et al.*, 1994). Changes in size can be representative of the different trophic functions in zooplankton communities. Small zooplankton tend to be detritivores/particle feeders/omnivores (Turner, 2004; Svensen *et al.*, 2011), whereas primarily herbivorous species tend to be larger to feed on phytoplankton such as diatoms (Ariffian *et al.*, 2025), and predatory zooplankton larger still to feed on other zooplankton (Pakhomov and Perissinotto, 1996; Froneman *et al.*, 1998; Olsen *et al.*, 2000). The relationship between zooplankton size and trophic position is moreover illustrated by an increase in $\delta^{15}N$ and trophic level with body size (Romero-Romero *et al.*, 2016; De Figueiredo *et al.*, 2020). Quantifying how size changes with depth can therefore help elucidate how trophic ecology and functional dynamics change down through the mesopelagic.

A multitude of factors may drive changes in community structure and size, however, in the present study, we hypothesize functional traits (feeding strategies), food availability and physiology to be the main drivers in the observed changes in body size with depth. If zooplankton are to position themselves in the water column according to feeding strategies, then we would expect to see herbivores in surface waters where phytoplankton are most abundant, detritovores/particle feeders at the boundary of the epi- to mesopelagic, where the contribution of reworked particles and detritus increases compared to fresh material (Lampitt *et al.*, 1990; Jackson, 1993; González and Smetacek, 1994; Kiørboe, 2000; Koski *et al.*, 2005; Jackson and Checkley, 2011; Koski *et al.*, 2020), and carnivores throughout the water column where prey are available but also in deeper waters where POM becomes less readily available and a carnivorous lifestyle therefore becomes more advantageous (Ozaki and Ikeda, 1999; Vestheim *et al.*, 2005; Laakmann *et al.*, 2009). Based on these different 'eco-depths', we may expect to see zooplankton communities dominated by different sizes at different depths, with large herbivorous zooplankton in surface waters, small particle-associated zooplankton at the base of the euphotic, and a mix of small detritovores and larger predatory zooplankton in the mesopelagic. Changes in community composition with depth may moreover have concomitant effects on biogeochemical functioning, with depths dominated by herbivorous zooplankton interacting with the phytoplankton bloom or small particle associated copepods potentially associated with increased particle fragmentation and a slowing down of carbon flux (Koski *et al.*, 2020).

Normalised biovolume size spectra (NBSS), which describe how the biovolume of organisms within a size range shifts between size classes, can effectively summarise the size structure of zooplankton communities and how energy is transferred up the food web (Platt and Denman, 1977; Sprules and Barth, 2016). Changes in the intercept of the NBSS can be used as a proxy for the amount of energy at the base of the food web, whilst the slope is an index of how this energy

is transferred across the food web to larger organisms (Sprules and Barth, 2016). Size-spectra theory predicts a slope close to -1 in stable planktonic marine environments, due to around 10 % of biomass being transferred between trophic levels, from small to large organism (Sheldon *et al.*, 1972; Brown *et al.*, 2004). A steeper slope is indicative of low trophic transfer efficiencies (TTE), whereby a majority of energy (carbon) is lost in the system and therefore cannot support a high biomass of larger animals. Size spectral slopes steeper than -1 have been observed during summertime oligotrophic (i.e. low nutrient) conditions in planktonic communities (Atkinson *et al.*, 2021). Oligotrophic waters promote smaller sized plankton and long inefficient food chains, resulting in strong trophic amplification and decreased biomass of larger sized animals such as fish (Atkinson *et al.*, 2024). However, steep slopes can also be caused by extreme storm events resulting in high metazoan mortality compared to smaller size classes (Atkinson *et al.*, 2021). In contrast, shallower slopes are indicative of a high TTE and thus more biomass in larger size classes, as is suggested in more eutrophic systems (Atkinson *et al.*, 2024). Eutrophic systems, promoting larger size classes, are also observed to experience top-down trophic cascades, seen as domes and troughs in size spectra, whereby the increase in biomass in a larger size class results in a decrease in the biomass of the smaller size class preceding it due to predator-prey interactions (Rossberg *et al.*, 2019).

Changes in the NBSS slope can moreover be attributed to changes in community structure. Preceding studies examining size spectral changes with depth observed a shallowing of the NBSS slope from surface waters down to 3000 m in the western tropical North Pacific (Dai *et al.*, 2017; Kim *et al.*, 2025). In the subarctic this was attributed the presence of large-sized diapausing calanoids in deeper water layers (Kim *et al.*, 2025), whereas in the subtropical region this was likely a result of changes in the taxonomic composition linked to zooplankton feeding modes, with an increase in large carnivorous zooplankton at depth (Dai *et al.*, 2017).

Because a simple measure of size can provide a myriad of information regarding ecological and biogeochemical dynamics of an ecosystem, size-based ecosystem or biogeochemical models are increasingly being use (Ward *et al.*, 2012a; Blanchard *et al.*, 2017; Heneghan *et al.*, 2020; Negrete-García *et al.*, 2022). Size-based models have the advantage of being able to substantially reduce the number of free parameters in a model by using the allometric relationships between size and physiological traits to describe variables such as nutrient uptake, growth, mortality, grazing rates and predator-prey interactions (Ward *et al.*, 2012a), significantly reducing computational costs (Guiet *et al.*, 2016). However, if we are to use size-based modelling effectively, we need a fundamental and empirically derived understanding not only of how size changes with depth, but how these changes are related to shifts in the ecological and biogeochemical functioning of zooplankton in the mesopelagic. Indeed, Flynn *et*

al. (2025) highlight the present day widening gap between empirical plankton research and modelling, and the urgent need to integrate modelling with empirical science.

The increased move towards size-based approaches to ecological and biogeochemical observations and modelling may be linked to the 'digitalisation' of the ocean, whereby quantitative imaging devices are generating a mass of size-based data (Lombard *et al.*, 2019). Optical bench-top instruments, such as the FlowCam Macro (Yokogawa Fluid Imaging Technology) and ZooScan (Hydroptic), are now widely used to process and image zooplankton net samples, allowing for faster processing compared to microscopy analysis (Detmer *et al.*, 2019; Cornils *et al.*, 2022). Moreover, the development of in-situ plankton imaging systems such as Underwater Vision Profilers (Hydroptic) attached to gliders, BCG-Argo floats and moorings are allowing researchers to explore spatial and temporal plankton dynamics at high resolutions (Picheral *et al.*, 2022). From all these images we can extract a breadth of data including morphological size data, taxonomic classification, and abundance data. It is therefore important to develop a good understanding of how size relates to community structure and ecosystem functioning if we are to make good use of this emerging data. It is moreover vital to understand how imaging data compares to traditional net and microscopic taxonomy analyses if we are to move towards imaging plankton.

The Scotia Sea is considered to be one of the most productive areas in the Southwest Atlantic sector of the Southern Ocean, supporting large and intense diatom blooms (Korb *et al.*, 2012), high particulate organic carbon (POC) concentrations in the upper mesopelagic (Giering *et al.*, 2023) and high zooplankton biomass (Ward *et al.*, 2012b; Cook *et al.*, 2023). Many studies have explored mesozooplankton in the Scotia Sea around South Georgia, although these have mainly been depth-integrated (e.g., 0 – 200 m, 0 – 400 m) (Ward *et al.*, 2004; Ward *et al.*, 2006; Tarling *et al.*, 2012; Ward *et al.*, 2012b), with few studies investigating depth-stratified mesopelagic communities (Hopkins *et al.*, 1993; Atkinson and Sinclair, 2000; Cook *et al.*, 2023; Savineau *et al.*, 2024). However, no study has yet explored depth-stratified changes in mesozooplankton size structure in the upper 500 m of the Scotia Sea. Given the importance of zooplankton in the cycling of carbon in the mesopelagic, it is important to examine how community size structure and trophic ecology varies vertically from the epipelagic to the mesopelagic zone. The present study used FlowCam Macro analysis of vertically resolved zooplankton net samples to investigate changes in epi- to upper mesopelagic zooplankton community structure and body size in the Scotia Sea, with the aim of understanding if and how changes in size spectra correspond to changes in trophic strategies and the associated changes in the ecological and biogeochemical functioning of the system.

4.3 Method

4.3.1 Sample collection

Samples for this study are part of the COMICS (Controls over Ocean Mesopelagic Interior Carbon Storage) programme, which aimed to shed light on the processes controlling carbon remineralisation in the twilight zone (Sanders *et al.*, 2016). Samples were collected aboard the *RRS Discovery* during the research cruise DY086 to the Scotia Sea in the Southern Ocean (12 November – 19 December 2017) in the vicinity of the British Antarctic Survey Scotia Sea open-ocean observatory site P3 (SCOOBIES, 52.40 S, 40.06 W) (Sanders et al., 2016). The same station was visited 3 times, defined as P3A (15 – 22nd November), P3B (29th November – 5th December) and P3C (9 – 15th December).

A MOCNESS (Multiple Opening and Closing Net and Environmental Sampling System, 1 m^2 rectangular opening, 330 µm mesh nets) was used to sample the zooplankton community at 8-depth-discrete intervals of 62.5 m, starting at 500 m and going up to the surface. Both day and night samples were collected. Zooplankton samples were preserved in 4 % borax buffered formaldehyde. Full net deployment protocols can be found in Cook et al., 2023. Due to mechanical issues with the MOCNESS net during station visit P3A, samples were only obtained during visits P3B and P3C, therefore this study focusses on the latter 2 station visits.

4.3.2 Sample FlowCam Macro processing

The taxonomic characterization of abundance and size distributions of the zooplankton community were investigated using a FlowCam Macro (Yokogawa Fluid Imaging Technology). The FlowCam Macro is a flow imaging microscopy instrument which takes monochrome photographs of zooplankton and large particles between 150 µm and 5 mm, to obtain morphological data along with accurate counting and sizing measurements e.g. length, area using the FlowCam's area-based diameter algorithm (areaABD), equivalent spherical diameter (ESD). The formaldehyde-fixed samples were subsampled, where necessary, using a Folsom plankton splitter, and diluted to 1 L using filtered seawater. The fraction of sample analysed ($Frac_{split}$, e.g. ½, ¼) for each sample was recorded. Samples were pumped through the FlowCam Macro (Figure 4.1), fitted with a 5 mm flow cell, at a flow rate of 700 mL min^{-1}. Images were collected using auto-image mode at a rate of 10 frames per second.

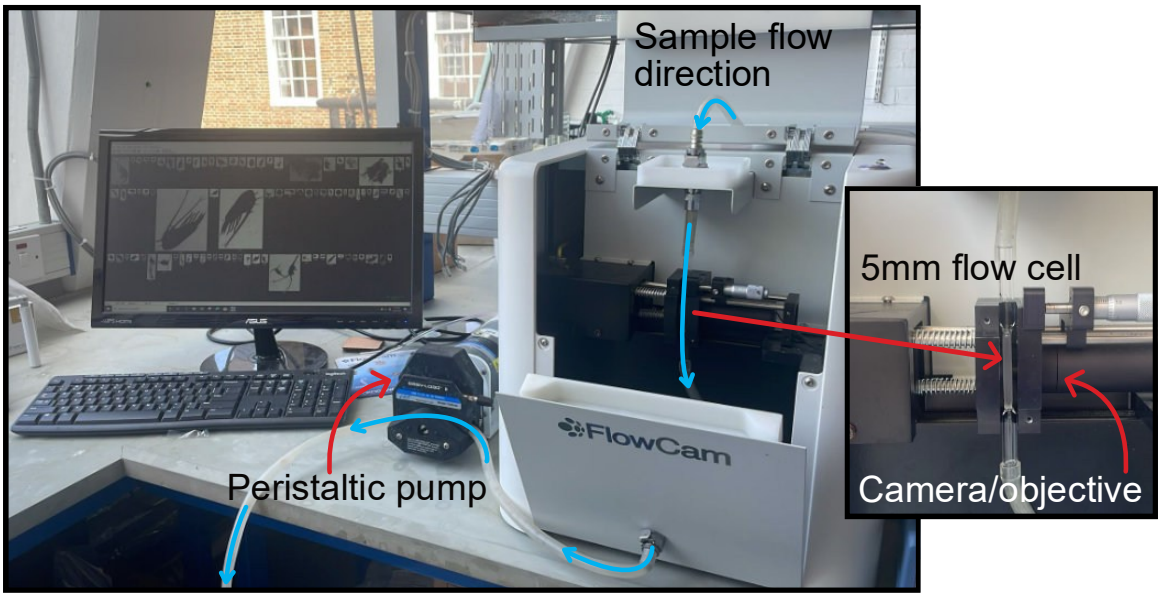

Figure 4.1. Zooplankton samples are pumped through the FlowCam Macro via a high-capacity industrial peristaltic pump and pass through a 5 mm flow cell placed in front of a microscope objective coupled with a high resolution (1920 x 1200 pixel) monochrome digital camera.

4.3.3 Image analysis

Image outputs from the FlowCam Macro were processed using Visual Spreadsheet software (Version 4.3.55). Images for each sampling event and net were manually classified into 21 broad taxonomic groups (Oncaeidae, *Oithona* spp., small Calanoida, large Calanoida, *Calanoides acutus* > 3 mm, *C. acutus* < 3 mm, carnivorous Copepoda, *Rhincalanus gigas, R. gigas* nauplii, Metridinidae, Euphausiidae, Euphausiidae calyptopes, Euphausiidae nauplii, Ostracoda, Amphipoda, Appendicularia, Chaetognatha, Polychaeta, Thaliacea, Eggs, Unidentifiable zooplankton). Image datasets were cleaned to remove unwanted images of particles, detritus and air bubbles.

4.3.4 FlowCam Macro vs. microscopy comparison

Zooplankton sample compositions obtained from the FlowCam were compared to compositions obtained from the same samples analysed by microscopic identification and enumeration at the NMFRI Plankton Sorting and Identification Centre, Poland. Detailed information of the taxa and species found in each classification, size ranges, and example images can be found in Table 4.1.

Table 4.1. Description of each FlowCam Macro classification group and the taxa and species expected to be representative of these groups based on the FlowCam Macro images and microscopy analysis. All FlowCam Macro images were obtained from samples from this study. Images are not to scale. Microscopy images were obtained from:
[1] https://inaturalist-open-data.s3.amazonaws.com/photos/67733907/medium.png,
[2] @OceanPlankton
[3] https://v3.boldsystems.org/index.php/Taxbrowser_Taxonpage?taxid=5780,
[4] Jaspers et al. (2023),
[5] https://upload.wikimedia.org/wikipedia/commons/5/58/Doliolum_sp.png

Name of taxonomic group	**Typical taxa in the category based on microscopy work**	**Average total length (based on literature)**	**Example of images**	
			FlowCam Macro	Microscopy
Oncaeidae	Oncaeidae spp. *Triconia* spp. *Oncaea* spp.	0.5 – 2 mm		 1
***Oithona* spp.**	*Oithona atlantica* *Oithona similis* *Oithona frigida* *Oithona* spp.	0.68 – 1.4 mm	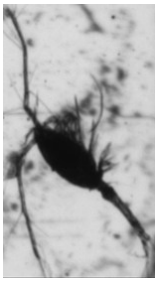	 2
Small Calanoida	Aetideidae (copepodites) *Aetideus armatus* *Aetideus australis* Calanoida spp. *Calocalanus* spp. *Clausocalanus* laticeps *Ctenocalanus* spp. *Racovitzanus antarcticus*	< 3 mm		 3

	Scaphocalanus brevicornis *Scaphocalanus farrani* *Scaphocalanus* spp. *Scolecithrichidae* spp. *Scolecithricella* spp. *Spinocalanus abyssalis* *Spinocalanus* spp.			
Large Calanoida	*Amallothrix* spp. *Amallothrix valida* *Calanus propinquus* *Calanus simillimus* *Euchirella* spp. *Euaugaptilus* spp. *Gaetanus* spp. *Haloptilus* spp. *Lophothrix* spp. *Lucicutia* spp. *Neocalanus tonsus* Phaennidae	> 3 mm		 2
***Calanoides acutus* < 3000**	*Calanoides acutus*	< 3 mm		 2
***Calanoides acutus* > 3000**	*Calanoides acutus*	> 3 mm	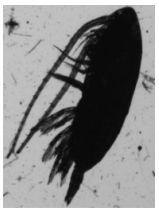	 2
Carnivorous Copepoda	*Augaptilidae* spp. *Candacia* spp. *Candacia maxima* Euchaetidae spp. *Heterorhabdus* spp.	1.4 – 10 mm		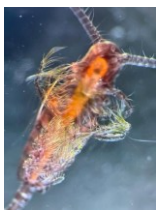 2

	Heterorhabdus norvegicus *Heterorhabdus spinifrons* *Paraeuchaeta* spp. *Paraeuchaeta antarctica* *Paraeuchaeta biloba* *Paraeuchaeta kurilensis*			
Rhincalanus gigas	*Rhincalanus gigas*	6 – 10 mm		 2
***Rhincalanus gigas* nauplii**	*Rhincalanus gigas* nauplii	0.86 – 1.8 mm	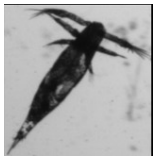	Not pictured
Metridinidae	Metridinidae spp. *Metridia gerlachei* *Metridia lucens* *Metridia curticauda* *Metridia* spp. *Pleuromamma antarctica*	1.5 – 4 mm	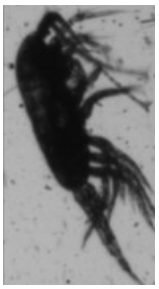	 2
Euphausiidae	Euphausiidae spp. *Euphausia triacantha* *Thysanoessa macrura* Thysanoessa spp.	12 – 28 mm 42 mm	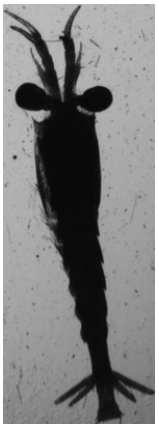	 2
Euphausiidae calyptopes	Euphausiidae spp. calyptopes	1 – 2 mm	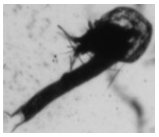	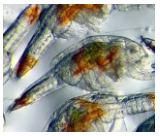

				2
Euphausiidae nauplii	Euphausiidae spp. nauplii	0.45 – 0.55 mm	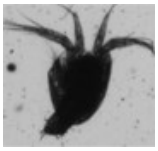	 2
Ostracoda	Ostracoda spp.	1 – 3 mm		 2
Amphipoda	Amphipoda spp. Gammaridea spp. Hyperiidae spp. *Primno macropa* *Themisto* spp. *Vibilia* spp.	4 – 28 mm	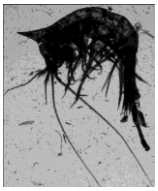	 2
Chaetognatha	Chaetognatha spp. Sagittidae spp. *Eukrohnia* spp.	9 – 105 mm	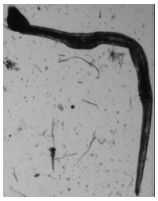	
Polychaeta	*Pelagobia* spp. Polychaeta spp. *Tomopteris* spp.	2 – 12 mm		 2
Thaliacea	Doliolidae spp. Salpidae spp.	~140 mm	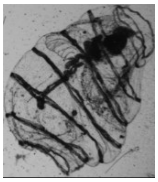	

				5
Eggs		<0.5 mm	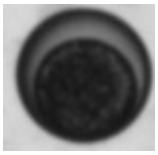	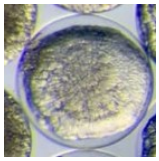 2

To assess differences in the community composition between the two methods (FlowCam vs Microscopy), permutational multivariate analysis of variance (PERMANOVA) and similarity percentage (SIMPER) analyses, both based on Bray-Curtis dissimilarities were conducted using the vegan package version 2.6.4 (Oksanen *et al.*, 2022) in R version 4.2.3 (R Core Team, 2023). PERMANOVA tested the null hypothesis that the community composition between the two methods do not differ, with a p value < 0.05 rejecting the null hypothesis. Community composition data were expressed as a proportion of total abundance and differences in community structure were investigated through PERMANOVA using the adonis2() function in R. To account for the fact that each sample was analysed using both methods, permutations were stratified (constrained) by sample ID using the strata argument. The significance of the test was evaluated using 999 permutations. SIMPER analysis with Bray-Curtis dissimilarities was used to determine which taxa contributed most to the observed compositional differences between the two methods (FlowCam vs Microscopy). Cumulative contributions were used to highlight the dominant taxa driving compositional differences. 2-dimensional non-metric multidimensional scaling (NMDS) ordination plots were generated to visualise the differences in community composition between the two methods (FlowCam vs Microscopy). NMDS using the metaMDS() function was conduction using Bray-Curtis dissimilarities The NMDS solution was evaluated based on stress values, with values below 0.2 considered as good fit and representative of community dissimilarities.

4.3.5 Zooplankton abundance and biovolume calculations

The total number of each individual taxon within a sample (N_{sample}) was obtained by dividing the count within the subsample (N_{sub}) by the split fraction ($Frac_{split}$).

$$N_{sample} = \frac{N_{sub}}{Frac_{split}} \qquad (eq\ 4.1)$$

This was then divided by the volume of water sampled by the net (V_{net}, m^3, obtained from the net flow meter) to derive the abundance of individuals (ind m^{-3}) in each taxon.

The volume of each zooplankton individual (V_{ind}, mm^3) was estimated using the area calculated using area-based diameter ($areaABD_{ind}$) as:

$$V_{ind} = \frac{4}{3}\pi\left(\frac{areaABD_{ind}}{\pi}\right)^{\frac{3}{2}} \quad (eq\ 4.2)$$

Biovolume (BV_{taxa}, mm^3) for each individual taxon in the sample was calculated by summing individual volumes for a taxon and dividing by the fraction of the subsample that was analysed:

$$BV_{taxa} = \frac{\sum V_{ind}}{Frac_{split}} \quad (eq\ 4.3)$$

This was then divided by the volume of water sampled at each depth to obtain BV_{taxa}, $mm^3\ m^{-3}$. All taxa BV were summed to obtain the biovolume of the entire zooplankton community sampled (BV_{comm}, mm^3).

4.3.6 Normalised biovolume size spectra

Normalised biovolume size-spectra (NBSS) were computed for each MOCNESS depth sampled. We created 20 size intervals (Δw in mm^3) logarithmically spaced between w_{min} and w_{max}. All individual zooplankton (V_{ind} in mm^3) were sorted into these size bins according to their respective log10(V_{ind}). The normalised biovolume in each size bin ($b_{\Delta wx}$ in mm^{-3}) was calculated as:

$$b_{\Delta w_x} = \frac{\sum(V_{ind} in \Delta w_x)}{\Delta w_x} \times \frac{1}{Frac_{split}} \times \frac{1}{V_{net}} \quad (eq\ 4.4)$$

where Δw_x is the width of a size bin in mm^3 (i.e. antilog of upper boundary minus antilog of lower boundary), $Frac_{split}$ is the split fraction (to obtain the $b_{\Delta w_x}$ of the entire sample), and V_{net} is the volume sampled by the net measured with a flow meter (m^3). NBSS were created by plotting all log10 transformed $b_{\Delta w_x}$ against the midpoint of their respective log10(Δw_x). Linear regressions were fitted to derive NBSS slopes.

4.4 Results

4.4.1 FlowCam zooplankton community composition

Throughout the upper 500 m, composition was dominated by Copepoda, making up 78 – 97% and 73 – 98 % of total numerical and biovolume composition respectively (Figure 4.2). Non-copepod biovolume was dominated by gelatinous zooplankton including Chaetognatha, Polychaeta and Thaliacea (Figure 4.3). Within Copepoda, numerical composition varied with depth, with *Calanoides acutus* dominating in the top surface layer and Metridinidae becoming more prominent in layers below (Figure 4.4). Copepoda biovolume was dominated by *C. acutus*

and *Rhincalanus gigas* (Figure 4.4). The percent composition contribution of the different taxa to each depth strata are summarised in Figure 4.2 - Figure 4.4 and Table 4.2.

Community composition was observed to vary vertically with depth (Table 4.2). Surface waters (0 – 62 m) were dominated, both numerically and in biovolume composition, by *C. acutus* (68.3 and 78.0 % respectively). Metridinidae were numerically dominant across all depth strata from 62 m downwards, alongside unidentified small Calanoida (18.5 – 28.8 %). Based on the microscopy work, small Calanoida were dominated by Scolecitrichidae and *Ctenocalanus* spp.. *C. acutus* and *R. gigas* made up the greatest proportion of biovolume composition at all depths beyond 62 m (44.0 – 89.2 %), but only 11.9 – 33.6 % of numerical composition. The numerical contribution of Oncaeidae increased with depth throughout the water column, from 0.1 % in surface waters, to 11.3 % in the deepest strata of 437 – 500 m. Carnivorous zooplankton (Amphipoda, Chaetognatha, carnivorous Copepoda, and Polychaeta) contributed more to numerical and biovolume compositions beyond 62 m compared to surface waters, and contributed more in terms of biovolume (9.1 – 18.0 %) compared to abundance (2.7 – 7.5 %). Thaliacea were only observed at depths beyond 125 m. The numerical contribution of Ostracoda to community composition increased with depth and was most notable at depths beyond 312 m. Amphipoda were most prominent in the 375 – 437 m depth strata.

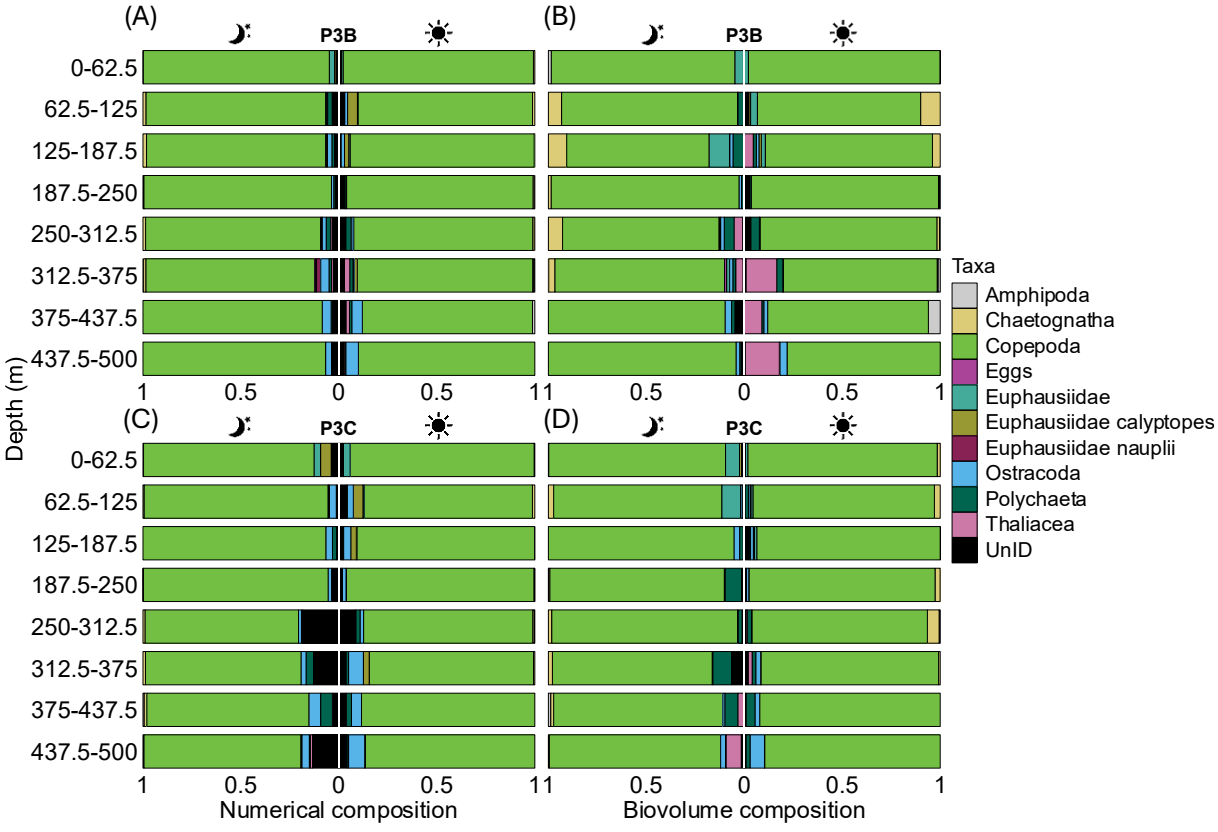

Figure 4.2. Vertical distribution of all zooplankton numerical (A, C) and biovolume (B,D) proportional composition during night and day visits of station P3 (top P3B and bottom P3C)

northwest of South Georgia in the Scotia Sea. Moon/Sun = Night/Day samples. Unidentified category represents zooplankton too small to confidently identify into specific taxa. Taxonomic classification obtained from the FlowCam Macro. Copepoda classification contains Oncaeidae, *Oithona* spp., small Calanoida, large Calanoida, *Calanoides acutus* > 3 mm, *C. acutus* < 3 mm, carnivorous Copepoda, *R. gigas*, *R. gigas* nauplii, and Metridinidae.

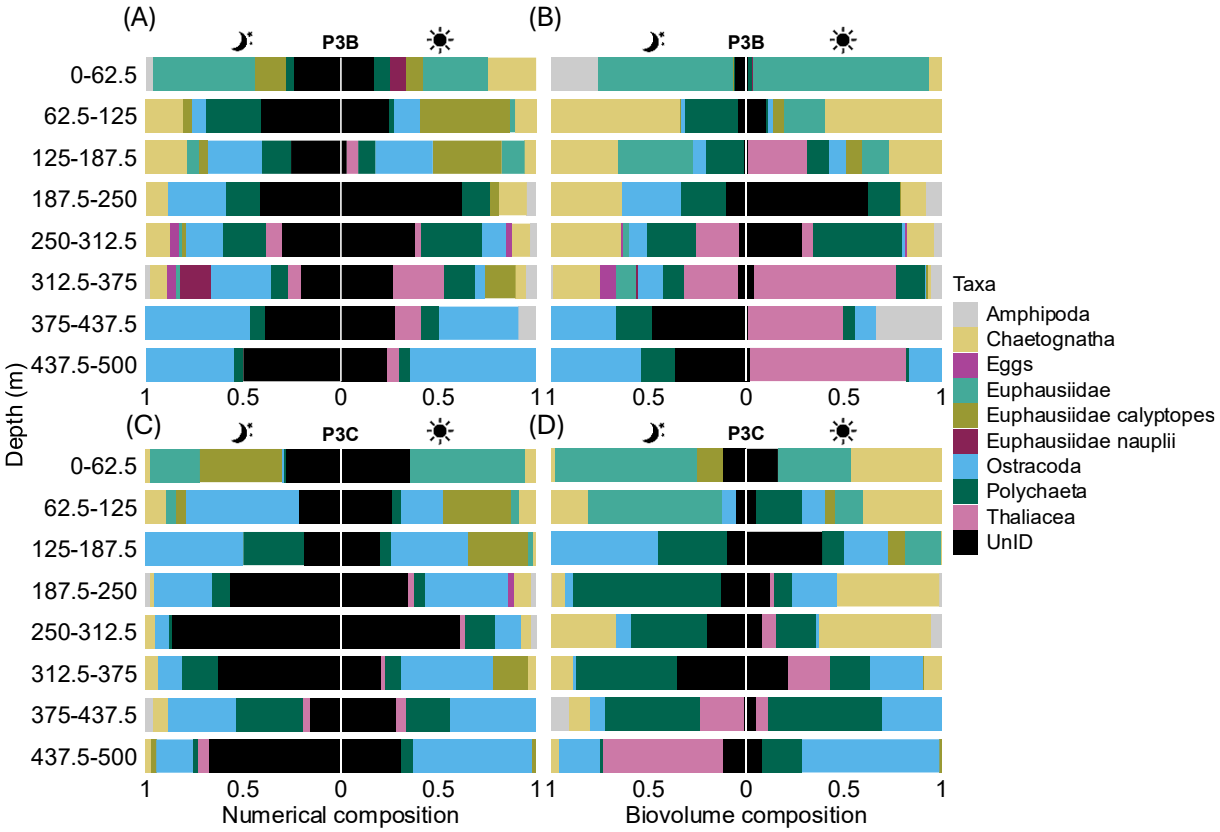

Figure 4.3. Vertical distribution of non-copepod zooplankton numerical (A, C) and biovolume (B, D) proportional composition during night and day visits of station P3 (top P3B and bottom P3C) northwest of South Georgia in the Scotia Sea. Moon/Sun = Night/Day samples. Unidentified category represents zooplankton too small to confidently identify into specific taxa. Taxonomic classification obtained from the FlowCam Macro.

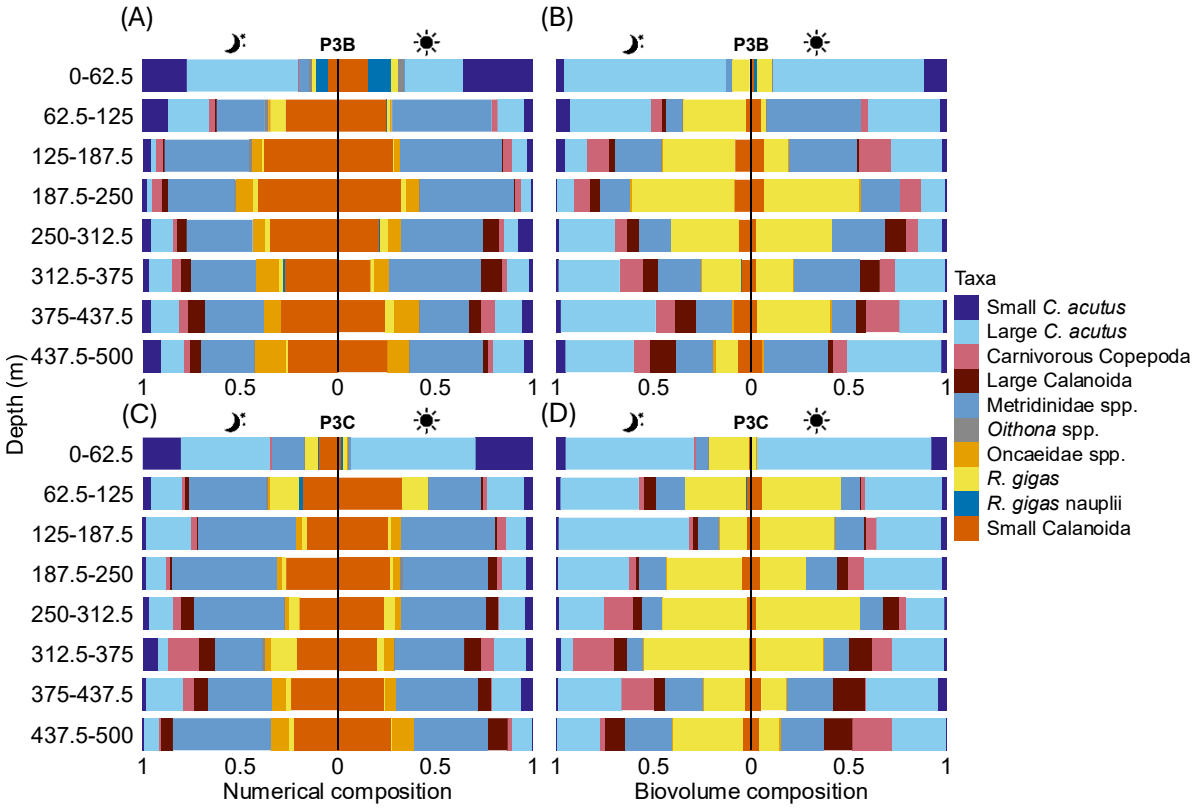

Figure 4.4. Vertical distribution of copepod numerical (A, C) and biovolume (B, C) proportional composition during night and day visits of station P3 (top P3B and bottom P3C) northwest of South Georgia in the Scotia Sea. Moon/Sun = Night/Day samples. Small *C. acutus* (*Calanoides acutus* length < 3000 µm). Large *C. acutus* (length > 3000 µm). *R. gigas* = *Rhincalanus gigas*. Small Calanoida < 3000 µm. Large Calanoida > 3000 µm.

Table 4.2. Mean (± standard deviation) percent numerical and biovolume proportional contribution of the different taxa to total community composition at the P3 station northwest of South Georgia in the Scotia Sea. Composition was summarised across station visits and day/night samples. Taxonomic classification obtained from the FlowCam Macro.

		Numerical (N) and biovolume (BV) composition (%) in each depth (m) strata															
		0 – 62		62 – 125		125 – 187		187 – 250		250 – 312		312 – 375		375 – 437		437 – 500	
Taxa		**N**	**BV**	**N**	**BV**	**N**	**BV**	**N**	**BV**	**N**	**BV**	**N**	**BV**	**N**	**BV**	**N**	**BV**
Amphipoda	mean	0.2	1.5	-	-	-	-	0.2	0.2	0.3	0.5	0.4	0.7	0.9	3.6	-	-
	sd	-	-	-	-	-	-	0.1	0.2	0.1	0.1	0.2	0.7	0.4	3.4	-	-
***Calanoides acutus* < 3000**	mean	25.3	6.7	6.2	3.3	3.1	2.2	2.1	1.1	4.3	1.3	3.6	1.2	3.9	2.1	3.5	1.8
	sd	7.8	3.4	4.0	2.0	1.1	0.9	1.2	0.7	2.0	0.4	2.0	0.7	1.9	1.3	3.9	2.0
***Calanoides acutus* > 3000**	mean	45.8	74.9	15.5	34.8	10.1	31.4	7.2	22.7	9.4	18.6	9.5	19.3	13.4	31.2	10.2	29.0
	sd	14.3	11.3	3.0	3.2	8.2	23.4	4.2	14.8	2.3	5.3	4.2	9.7	1.7	10.8	3.5	8.4
Total *Calanoides acutus*	mean	71.0	81.6	21.7	38.1	13.2	33.7	9.4	23.8	13.7	19.9	13.1	20.5	17.4	33.3	13.7	30.8
Carnivorous Copepoda	mean	0.6	0.8	2.1	3.2	3.5	7.1	3.0	7.2	2.0	7.0	6.2	10.6	4.1	9.6	1.9	8.4
	sd	0.6	0.6	0.5	1.3	1.0	5.0	1.3	3.0	1.0	4.8	4.6	4.5	2.5	6.6	1.0	6.9
Chaetognatha	mean	0.4	0.6	1.2	5.6	0.8	4.5	0.4	1.3	1.0	4.1	0.9	1.6	1.3	1.5	0.5	0.5
	sd	0.2	0.8	0.4	3.5	0.9	4.7	0.2	0.9	0.3	3.0	0.4	1.3	-	-	-	-
Eggs	mean	-	-	-	-	-	-	0.1	0.0	0.4	0.1	0.6	1.1	-	-	-	-

		0 - 62		62 - 125		125 - 187		187 - 250		250 - 312		312 - 375		375 - 437		437 - 500	
		N	**BV**	**N**	**BV**	**N**	**BV**	**N**	**BV**	**N**	**BV**	**N**	**BV**	**N**	**BV**	**N**	**BV**
Eggs	sd	-	-	-	-	-	-	-	-	0.2	0.1	-	-	-	-	-	-
Euphausiidae	mean	2.6	3.7	0.4	4.7	0.5	4.5	-	-	0.2	0.6	0.3	1.4	-	-	-	-
	sd	1.2	2.6	0.2	4.4	0.2	5.1	-	-	-	-	-	-	-	-	-	-
Euphausiidae calyptopes	mean	2.2	0.4	2.7	0.3	1.8	0.6	0.2	0.0	0.2	0.0	2.3	0.1	-	-	0.4	0.1
	sd	2.9	0.7	2.7	0.4	1.3	0.5	-	-	-	-	0.9	0.1	-	-	0.2	0.1
Euphausiidae nauplii	mean	0.2	0.0	-	-	-	-	-	-	-	-	2.2	0.1	-	-	-	-
	sd	-	-	-	-	-	-	-	-	-	-	-	-	-	-	-	-
Large Calanoida	mean	-	-	1.1	2.5	0.7	1.7	2.1	3.0	5.5	6.7	6.8	7.8	6.2	8.4	5.4	9.4
	sd	-	-	0.7	2.3	0.3	0.7	1.8	2.5	1.2	2.3	2.2	2.5	1.1	5.2	2.8	5.1
Metridinidae	mean	5.2	2.1	32.1	17.4	44.7	17.8	42.8	15.3	35.6	14.3	30.2	16.1	28.5	16.4	32.8	21.1
	sd	6.2	2.6	11.1	15.4	4.1	8.7	7.7	2.9	3.8	7.0	9.6	8.6	6.5	4.5	6.2	3.4
Oithona spp.	mean	1.3	0.0	0.9	0.0	0.9	0.1	0.8	0.0	0.4	0.0	0.8	0.0	0.6	0.0	0.6	0.0
	sd	1.0	0.0	0.5	0.0	0.8	0.1	0.3	0.0	0.0	0.0	0.7	0.0	-	-	0.0	0.0
Oncaeidae	mean	0.4	0.0	1.0	0.1	3.8	0.4	5.2	0.4	4.0	0.2	5.8	0.3	7.6	0.5	10.5	1.0
	sd	-	-	0.2	0.0	0.9	0.2	2.6	0.3	2.1	0.1	3.2	0.3	2.8	0.2	3.0	0.6
Ostracoda	mean	0.1	0.0	2.2	0.6	2.8	1.8	1.6	0.9	1.6	0.6	3.8	1.2	5.3	2.2	5.4	3.9

		0 - 62		62 - 125		125 - 187		187 - 250		250 - 312		312 - 375		375 - 437		437 - 500	
		N	**BV**	**N**	**BV**	**N**	**BV**	**N**	**BV**	**N**	**BV**	**N**	**BV**	**N**	**BV**	**N**	**BV**
Ostracoda	sd	-	-	1.4	0.3	0.9	0.7	0.3	0.4	0.4	0.8	3.0	1.1	0.6	0.9	2.4	2.4
Polychaeta	mean	0.2	0.0	1.1	1.6	1.1	2.4	0.6	2.6	1.9	3.4	2.0	4.0	2.6	3.5	0.6	0.8
Polychaeta	sd	0.0	0.0	1.1	1.3	0.7	2.1	0.2	3.8	1.0	1.6	1.2	3.7	2.4	2.6	0.2	0.9
Rhincalanus gigas	mean	3.3	9.4	8.4	23.9	1.4	21.5	2.1	38.4	3.8	37.9	4.3	26.8	2.1	20.3	1.3	17.1
	sd	1.8	6.9	5.6	15.2	0.6	11.7	0.5	12.9	1.2	8.6	4.1	13.6	1.5	9.8	0.8	12.4
Rhincalanus gigas **nauplii**	mean	4.8	0.5	1.1	0.2	-	-	-	-	0.5	0.0	0.9	0.1	-	-	-	-
	sd	5.1	0.7	1.2	0.2	-	-	-	-	-	-	-	-	-	-	-	-
Small Calanoida	mean	7.2	0.6	22.8	3.2	24.6	4.4	30.0	5.7	21.4	2.8	17.8	2.3	22.0	4.4	21.8	4.4
	sd	5.8	0.5	5.0	1.5	8.1	1.7	6.6	1.9	6.7	1.5	3.7	1.4	3.1	2.6	2.8	1.5
Thaliacea	mean	-	-	-	-	0.4	4.5	0.1	0.1	0.5	1.9	1.3	7.1	1.0	4.1	0.8	12.6
	sd	-	-	-	-	-	-	-	-	0.3	2.2	1.3	7.5	0.7	4.3	0.3	6.9
Unidentified zooplankton	mean	1.9	0.5	2.7	0.8	1.4	0.8	2.4	1.3	8.4	1.4	5.4	2.5	3.2	1.3	5.8	1.1
	sd	1.3	0.5	1.1	0.6	0.9	1.1	0.9	1.0	7.3	1.0	4.9	2.8	0.4	2.2	5.1	0.5
Total carnivorous zooplankton	mean	1.4	2.9	4.4	10.3	5.4	14.0	4.2	11.3	5.2	14.9	9.5	16.9	8.9	18.2	3.0	9.8

4.4.2 Microscopy vs FlowCam numerical composition comparison

NMDS ordination plot (Figure 4.5) illustrates how the FlowCam Macro classification clusters fall predominantly within the microscopy classification cluster, forming partially overlapping groups, with the microscopy 95 % confidence ellipse having a greater range. The 2-dimensional NMDS solution had a stress value of 0.11, below the cut-off of 0.2, indicating a good fit and representation of community dissimilarities. Similarities between the copepod numerical compositions obtained from the FlowCam Macro and microscopy are moreover illustrated in Figure 4.6.

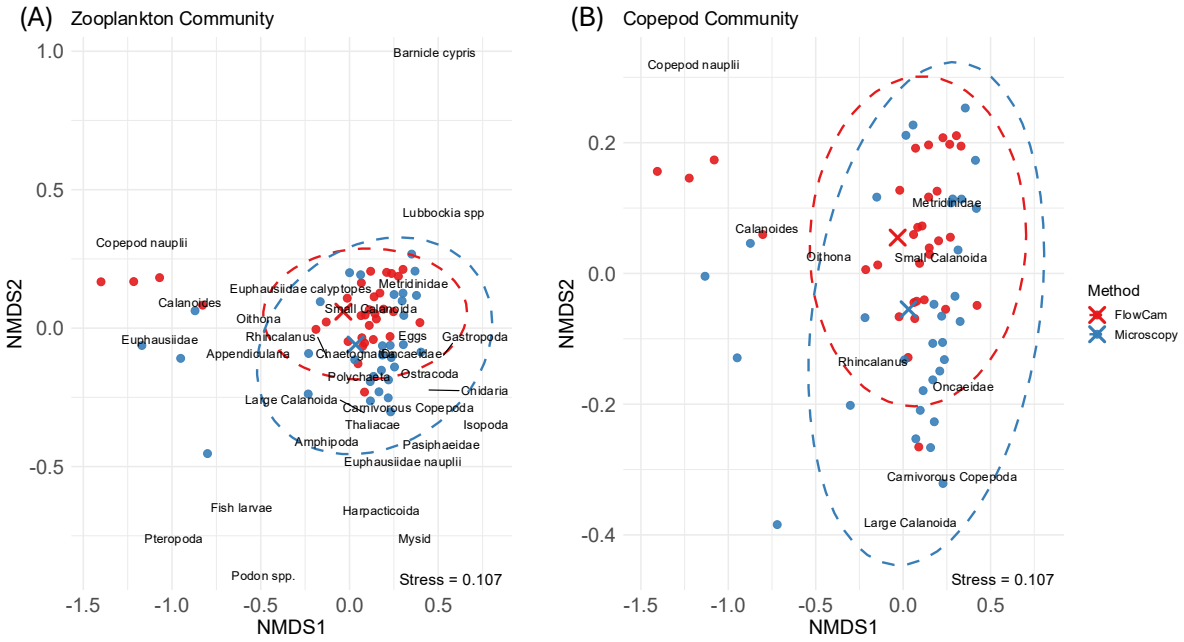

Figure 4.5. Non-metric multidimensional scaling (NMDS) ordination of (A) zooplankton and (B) copepod numerical proportional composition based on Bray-Curtis dissimilarities. Each point represents a sample, with colour indicating classification method (red = FlowCam, blue = microscopy). Ellipses represent 95% confidence intervals around group centroids (centroids marked by X). Taxa labels indicate the position of individual taxa grouping in the ordination space.

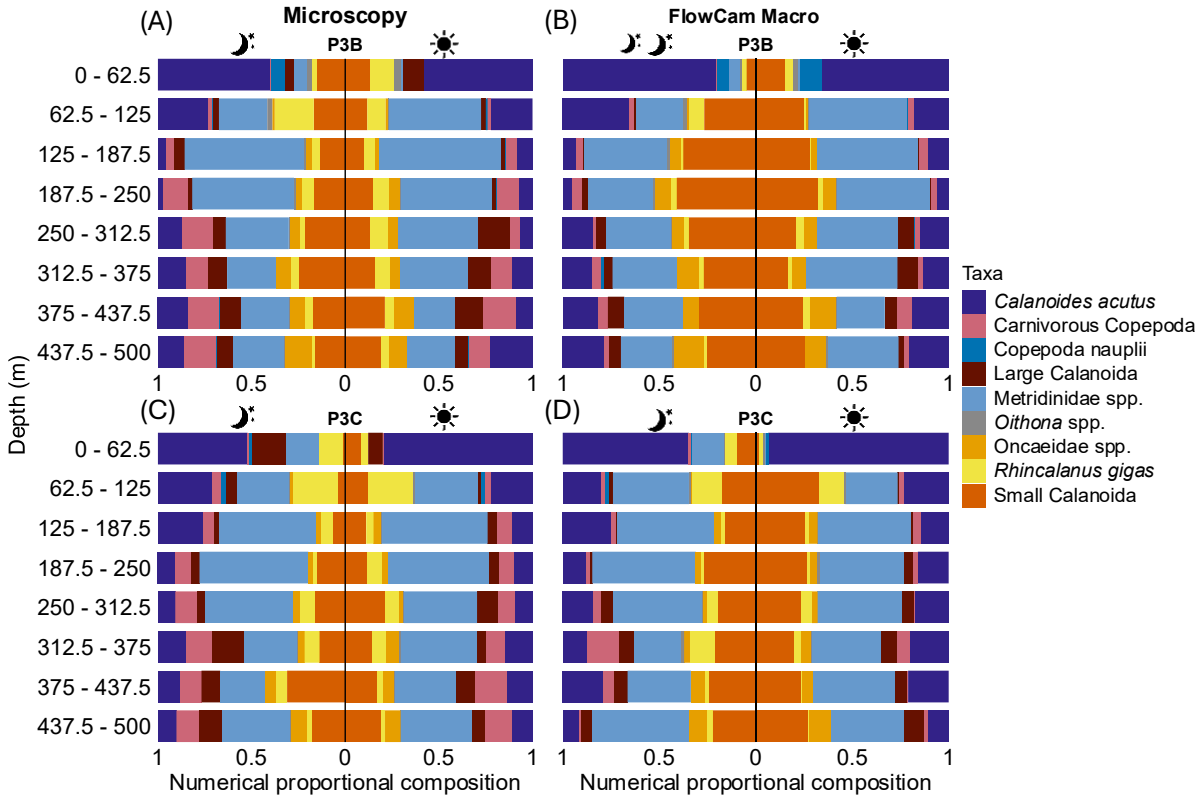

Figure 4.6. Vertical distribution of Copepoda taxonomic numerical proportional composition during night and day visits of station P3 (top P3B and bottom P3C) northwest of South Georgia in the Scotia Sea analysed using (A, C) microscopy and (B, D) the FlowCam Macro. *Calanoides acutus* grouping both <3000 and >3000 µm *Calanoides acutus*. Night nets: left of x-axis=0.

Both method and depth categories were observed to significantly influence the zooplankton community composition of the samples ($F=7.47_{1,63}$, $p=0.001$, $R^2=0.081$ and $F=23.92_{1,63}$, $p=0.001$, $R^2=0.26$, respectively), although depth explained a greater proportion of the variance (26 %) than method (8 %). SIMPER analysis indicated that differences in the two methods were mainly driven by small Calanoida (greater contribution in FlowCam), carnivorous Copepoda, *R. gigas*, large Calanoida (greater contributions in microscopy) classifications ($p< 0.01$), accounting for 75.8 % of the variability between the methods. Other taxa which significantly contributed to differences between the two methods, albeit in much smaller contributions, are summarised in Table 4.3.

Looking specifically at just the copepod composition, both method and depth categories were observed to significantly influence the copepod community composition of the samples ($F=6.76_{1,63}$, $p=0.001$, $R^2=0.074$ and $F=23.92_{1,63}$, $p=0.001$, $R^2=0.26$). Depth accounted for a greater proportion of the explained variance in copepod composition (26 %) compared to only 7.4 % of the variation explained by the method, suggesting stronger copepod composition changes by depth than by classification method. Similarly to the overall zooplankton composition, SIMPER

analysis indicated that differences in the two methods were mainly driven by small Calanoida (greater contribution in FlowCam), carnivorous Copepoda, *R. gigas*, large Calanoida (greater contributions in microscopy) classifications ($p < 0.01$).

Table 4.3. Summary of SIMPER (Similarity Percentages) analysis comparing zooplankton community composition between FlowCam Macro and Microscopy methods of analysis. The table shows each taxon's average contribution to the Bray–Curtis dissimilarity (mean contribution), the standard deviation of the contribution (SD), mean proportional compositions in each group (FlowCam Macro, Microscopy), cumulative contribution to total dissimilarity (Cumulative contribution), and the significance of each taxon's contribution (p). Significant taxa are marked with asterisks.

Taxon	Mean contribution	SD	Mean FlowCam	Mean Microscopy	Cumulative contribution	P-value
Calanoides acutus	0.0838	0.0998	0.2167	0.1669	0.216	0.213
Metridinidae	0.0815	0.0597	0.3148	0.3035	0.426	0.461
Small Calanoida	0.0517	0.0348	0.2096	0.1286	0.559	0.001*
Carnivorous Copepoda	0.0297	0.0201	0.0289	0.0751	0.636	0.001*
Rhincalanus gigas	0.0238	0.0237	0.0322	0.0616	0.698	0.001*
Large Calanoida	0.0234	0.0175	0.0345	0.0657	0.758	0.001*
Oncaeidae	0.0195	0.0153	0.0471	0.0372	0.808	0.434
Ostracoda	0.0132	0.0105	0.0277	0.0320	0.842	0.586
Cnidaria	0.0087	0.0094	0.0004	0.0169	0.865	0.001*
Pteropoda	0.0080	0.0188	-	0.0156	0.885	0.001*
Chaetognatha	0.0076	0.0068	0.0061	0.0195	0.905	0.001*
Euphausiidae calyptopes	0.0065	0.0089	0.0088	0.0073	0.922	0.904
Polychaeta	0.0062	0.0058	0.0121	0.0119	0.938	0.989
Copepoda nauplii	0.0054	0.0120	0.0072	0.0046	0.952	0.99
Euphausiidae	0.0048	0.0070	0.0043	0.0079	0.964	0.071
***Oithona* spp.**	0.0034	0.0035	0.0052	0.0055	0.973	0.61
Thaliacea	0.0029	0.0036	0.0030	0.0042	0.980	0.531
Isopoda	0.0028	0.0155	-	0.0054	0.987	0.022*

Taxon	Average contribution	SD	Average FlowCam	Average Microscopy	Cumulative contribution	P-value
Amphipoda	0.0017	0.0020	0.0013	0.0032	0.992	0.022*
Euphausiidae nauplii	0.0013	0.0026	0.0007	0.0019	0.995	0.043*
Appendicularia	0.0011	0.0026	-	0.0021	0.998	0.001*
Mysida	0.0003	0.0009	-	0.0006	0.999	0.002*
Eggs	0.0002	0.0007	0.0005	-	0.999	0.124
Gastropoda	0.0001	0.0003	-	0.0002	1.000	0.002*
Fish larvae	<0.0001	<0.0001	-	<0.0001	1.000	0.001*
Cirripedia cypris	<0.0001	0.0001	-	<0.0001	1.000	0.007*
***Podon* spp.**	<0.0001	0.0001	-	<0.0001	1.000	0.006*
***Lubbockia* spp.**	<0.0001	0.0001	-	<0.0001	1.000	0.011*
Harpacticoida	<0.0001	0.0001	-	<0.0001	1.000	0.003*
Pasiphaeidae	<0.0001	<0.0001	-	<0.0001	1.000	0.001*

4.4.3 Normalised biovolume size spectra (NBSS)

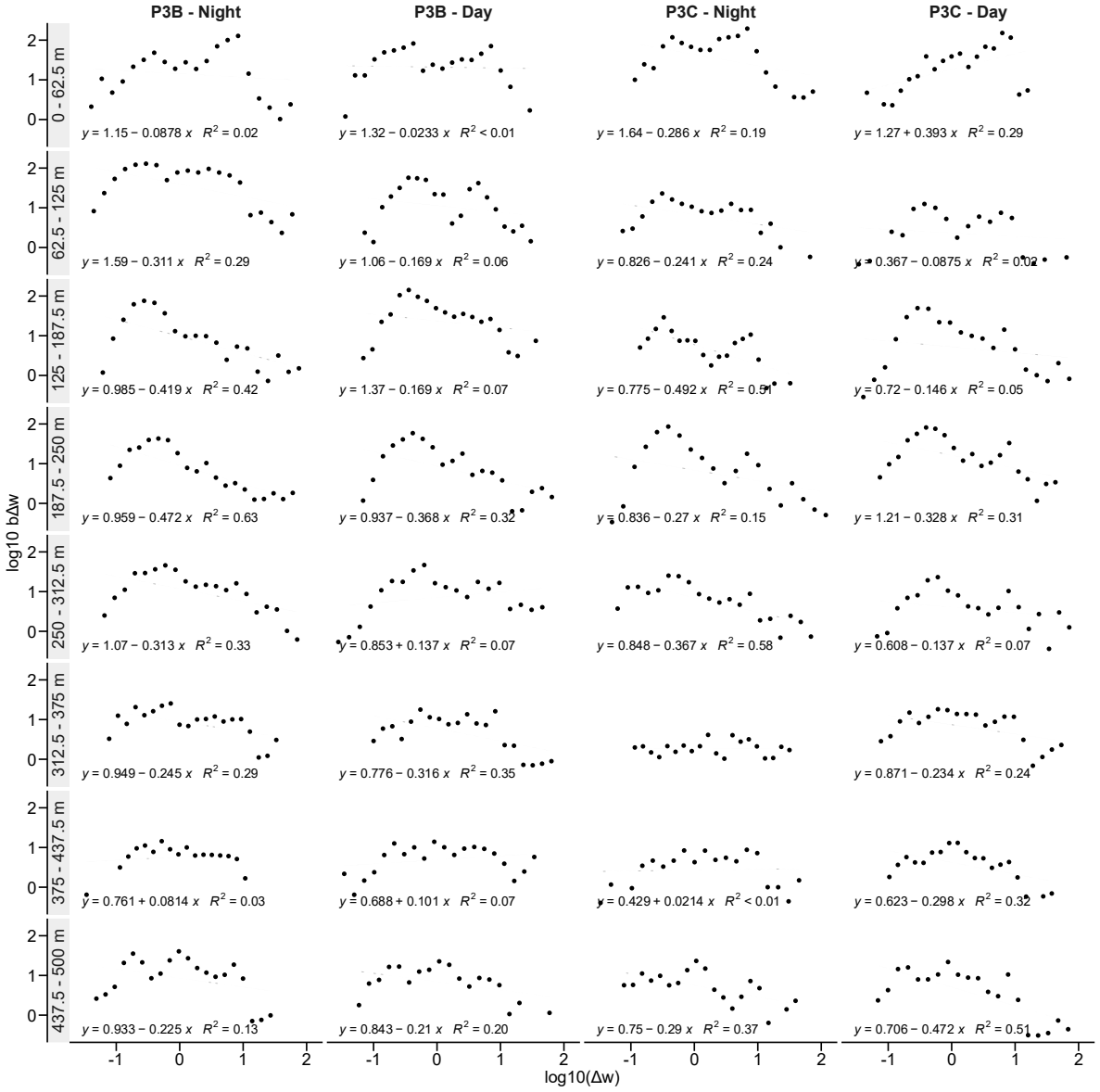

Figure 4.7. Vertically resolved normalised biovolume size spectra (NBSS) from 0 – 500 m at the P3 station in the Scotia Sea. Depth intervals are represented in the shaded boxes.

Results of the NBSS for each event and depth are shown in Figure 4.7. Surface waters (0 – 62 m) exhibited a bimodal size distribution (except for P3C Day), with peaks at $\log_{10}(0.396\ mm^3) \approx -0.40$ to $\log_{10}(0.450\ mm^3) \approx -0.35$, and $\log_{10}(6.27\ mm^3) \approx 0.80$ to $\log_{10}(8.30\ mm^3) \approx 0.92$. The first peak can be attributed to a mix of *C. acutus* < 3000 µm, *R. gigas* nauplii, small Calanoida and Metridinidae, whilst the second peak to *C. acutus* < 3000 µm (Figure 4.8). The size distribution then shifted towards smaller sizes (right-skewed distribution) in waters between 62 – 312 m. Notably, depths between 125 – 250 m showed a peak in organisms sized around $\log_{10}(0.27\ mm^3) \approx -0.57$ to $\log_{10}(0.46\ mm^3) \approx -0.34$, which can be attributed to Metridinidae and small Calanoida. Between 312 – 437 m, the size distribution flattened and became more normally distributed, peaking in the medium size classes, containing Metridinidae, and small Calanoida

on the left end and *C. acutus* > 3000 µm on the right end. In deeper waters (437 – 500 m), the distribution showed small peaks at $\log_{10}(0.15\ mm^3) \approx -0.82$ to $\log_{10}(0.25\ mm^3) \approx -0.60$, $\log_{10}(0.88\ mm^3) \approx -0.06$ to $\log_{10}(1.08\ mm^3) \approx 0.03$, and $\log_{10}(4.64\ mm^3) \approx 0.67$ to $\log_{10}(7.65\ mm^3) \approx 0.88$. The first peak (smallest size class) can be attributed to small Calanoida and Oncaeidae, the middle peak to Metridinidae, and the last peak (largest size class) can be attributed to *C. acutus* > 3000 um, large Calanoida and, to a lesser extent, Metridinidae, *R. gigas* and Polychaeta (Figure 4.8). Vertical changes in the NBSS slopes are expressed in the regression equations on Figure 4.7 and the boxplot in Figure 4.9. The slopes of the NBSS were very shallow in the surface layer (0 – 62 m), with one event (P3C - Day) being positive. NBSS slopes gradually steepened into mid-layer depths up to 250 m. The steepest (negative) NBSS slopes were observed in the depth horizon of 187 – 250 m. Past 250 m, the NBSS slopes then flattened down to 437 m. The last depth horizon sampled (437 – 500 m) had steeper slopes. Overall, there was a general negative trend in the intercept, with intercepts being higher in surface waters and lower at deeper depths.

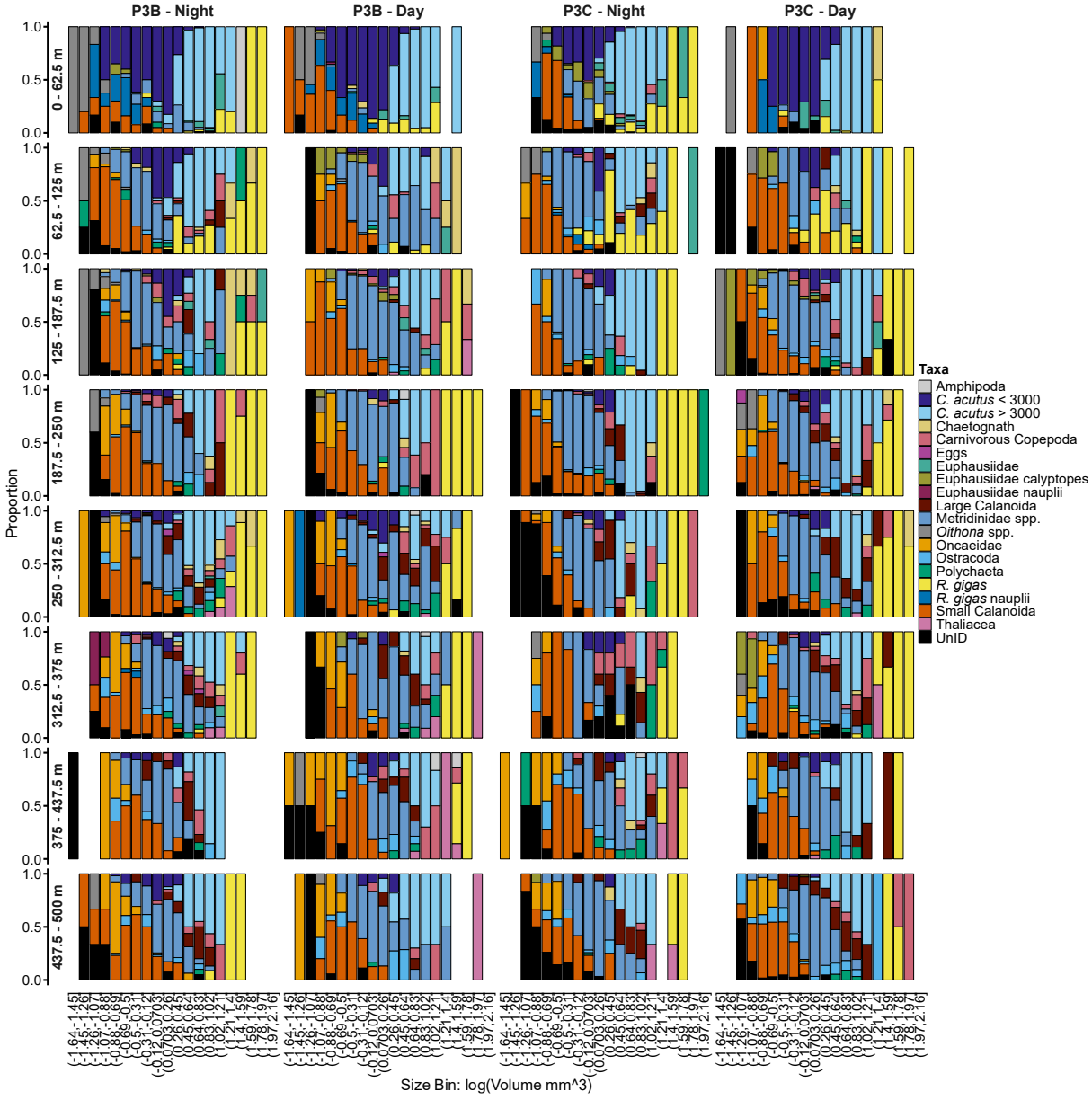

Figure 4.8. Vertical distribution of zooplankton composition within each NBSS size (volume) bin for each event and net at the P3 station in the Scotia Sea.

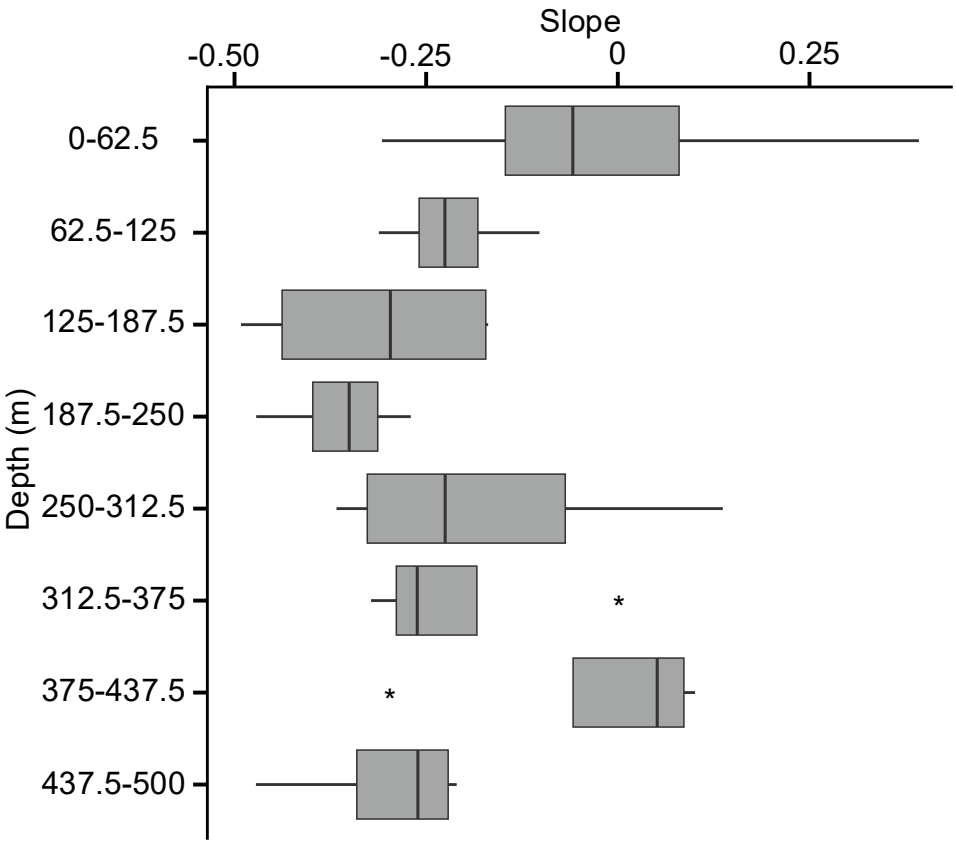

Figure 4.9. Boxplot of NBSS slope vs depth summarised across P3B and P3C station visits in the Scotia Sea. The boxplot represents the minimum, maximum, median, first quartile and third quartile values. Asterisks represent outliers.

4.5 Discussion

Knowledge of the vertical composition and size distribution of zooplankton within the upper mesopelagic is critical to understanding their trophic ecology and role in regulating the transfer of organic matter from the surface to the deeper layers of the ocean. Currently, data on depth-stratified mesopelagic zooplankton size spectra is sparse, with only a few studies having vertically resolved normalized biovolume size spectra (NBSS) into mesopelagic and bathypelagic layers (Dai *et al.*, 2017; Yamamae *et al.*, 2023; Kim *et al.*, 2025). The present study is the first to investigate epi- to upper mesopelagic zooplankton community NBSS changes across 8 discrete depths from the surface down to 500 m in the Scotia Sea. Our findings reveal clear depth-related patterns in zooplankton community composition and size structure across the Scotia Sea, shaped by the functional ecology and physiology of the zooplankton community. These vertical patterns are captured through both the NBSS and community composition, providing complementary insights into depth-stratified changes in body size.

4.5.1 Effect of sampling bias on NBSS

NBSS slopes observed in this study were significantly shallower than the theoretical value of -1 expected in stable marine ecosystems (Sheldon *et al.*, 1972). Shallower slopes can partly be attributed to a high abundance and biovolume of animals in larger size classes and partly to under sampling of smaller animals. It must firstly be acknowledged that the abundance of organisms, and hence biovolume at either end of the NBSS size bins are likely subject to sampling bias. At the larger end of the size range, active net avoidance by animals can occur, however this is suggested to only be important for the larger macrozooplankton, e.g., krill (> 4 mm) and not a significant problem for mesozooplankton (Skjoldal *et al.*, 2013; Christiansen *et al.*, 2024). Animals present in our net samples equal to or smaller than our net mesh size of 330 µm will not have been quantitively retained by our nets. This sampling bias may furthermore be extended beyond the size of the mesh due to issues with extrusion. For example, a 200 µm mesh net is estimated to most efficiently sample zooplankton with prosome lengths between 450 – 1400 µm (Hopcroft *et al.*, 2001), whilst the lower effective sampling capability of the MOCNESS 330 µm mesh net is suggested to stand at ~1000 µm (Barnes and Tranter, 1965; Böttger, 1987; Koppelmann and Weikert, 1992). Indeed, past studies in the Scotia Sea using smaller meshed nets (e.g. 53 µm, 100 µm and 200 µm) found that the small copepods *Oithona* spp., *Oncaea* spp., *Ctenocalanus citer* and *Microcalanus pygmaeus* dominated the abundance of mesozooplankton (Ward *et al.*, 2012b). Other studies have purposefully excluded particles smaller than the lower effective sampling capability from NBSS linear regressions (Lombard *et al.*, 2019; Cornils *et al.*, 2022). Our NBSS slope did indeed become steeper (Appendix C Figure C 1) when excluding anything captured by our nets with an areaABD < 0.785 mm^2 (area of a spherical diameter = 1 mm). This was mainly reflected in the 'cutting out' of the first NBSS dome of smaller size classes. Atkinson *et al.* (2021) has suggested that a range of at least 7 orders of magnitude is needed to reliably interpret NBSS slopes to effectively represent trophic transfer efficiency of marine ecosystems. The limitation of size range (~4 orders of magnitude) in this study therefore constrains accurate size spectrum analysis of the marine ecosystem. However, size spectrum analysis, in terms of using NBSS slopes to investigate the trophic transfer efficiency (TTE) of the ecosystem, was not the objective of this study. Rather NBSS were used to get an understanding of how size changes with depth and how this relates back to the composition and functional traits of the zooplankton communities at respective depths. Therefore, we only need consistent sampling efficiency of zooplankton (e.g., consistent sampling method) rather than 100 % sampling efficiency of the net.

4.5.2 Dome like features of NBSS

Rather than showing a linear distribution, the NBSS in this study showed bi- and tri-modal distributions (Figure 4.7). Dome and troughs have been widely observed in pelagic size spectra studies, with several explanations having been proposed including domes being representative of subsequent trophic levels in the food web (Boudreau *et al.*, 1991; Tarling *et al.*, 2012; Giering *et al.*, 2019b), predator-prey interactions (Sprules and Goyke, 1994; Tarling *et al.*, 2012), manifestations of top-down trophic cascades in eutrophic environments (Rossberg *et al.*, 2019), and bottom-up and/or top-down trophic cascades from fishing pressure (Andersen and Pedersen, 2009). NBSS studies covering large size ranges ~13 orders of magnitude, from microplankton up to macrozooplankton and fish, are able to capture several trophic levels within the food web (Tarling *et al.*, 2012). However considering the lower range in magnitude covered in the present study, we posit that the first NBSS peak/dome of smaller size classes is a result of sampling inefficiencies resulting in under sampling of smaller sized mesozooplankton. We then propose that subsequent domes reflect the prevalence of key functional groups within the mesozooplankton community.

NBSS in surface waters (0 – 62 m) had a bimodal distribution, with large herbivorous calanoid copepods *C. acutus* > 3000 µm dominating both numerically and in biovolume (Figure 4.4), resulting in the second dome. The dominance of *C. acutus* was reflected in NBSS slopes that were flat or even slightly positive – suggesting high biovolume and energy retention in larger size classes. Shallower slopes have previously been associated with cold-water systems where large, lipid-storing copepods dominate (Tarling *et al.*, 2012; Yamamae *et al.*, 2023). This aligns with our observations in the Scotia Sea, where lipid-storing *C. acutus* and *R. gigas* dominated biovolume. These species undergo ontogenetic vertical migration, overwintering at depth, during which they rely on internal lipid reserves, before ascending to surface waters during spring to exploit seasonal phytoplankton blooms (Atkinson, 1991; Huntley and Escritor, 1991). The overall high biomass retention in larger size classes, and hence second dome, in this study may partly be due to the large phytoplankton bloom and excellent feeding conditions during the sampling period (Ainsworth *et al.*, 2023; Giering *et al.*, 2023), a phenomenon attributed to eutrophic systems (Rossberg *et al.*, 2019; Atkinson *et al.*, 2024). However, we suggest that the dome may also be an artefact of the physiological ecology of *C. acutus* and *R. gigas*, with a proportion of the population being in or emerging from diapause, and therefore still relying on internal energy stores from the previous year. This is supported by lipid biomarker analyses (Savineau *et al.*, 2024) and observations of low carbon-specific ingestion rates for these species during this expedition (Cook *et al.*, 2023), suggesting limited grazing and reliance on external sources of energy from the diatom bloom due to the metabolism of internal lipid stores. Such conditions may contribute to the maintenance of a system with high zooplankton biomass

across large size classes, a phenomenon commonly observed in ecosystems subsidized by external energy sources (Trebilco *et al.*, 2013). This physiological state complicates the interpretation of shallow NBSS slopes, which are typically associated with high TTE but may instead reflect internal energy use rather than efficient energy transfer from primary production.

Between 125 – 250 m, the community structure shifted toward smaller detritivorous, omnivorous and particle-associated copepods, such as Metridinidae, small Calanoida and Oncaeidae (Figure 4.4). This shift coincided with steeper NBSS slopes and a less pronounced dome in the larger size class of *C. acutus*, indicating a reduced contribution of large-bodied zooplankton (Figure 4.7and Figure 4.8). Detritovores and particle associated copepods play a crucial role in the reworking and attenuation of sinking particulate organic matter (POM) in the upper mesopelagic zone (Mayor *et al.*, 2014; Koski *et al.*, 2020; Mayor *et al.*, 2020). Although our net mesh size will have under sampled these smaller species, lipid analyses also revealed an increased contribution of Oncaeidae and Oithonidae fatty alcohol biomarkers to the larger particle pool between 150 – 250 m (Savineau *et al.*, 2024), suggesting the presence of these small particle-associated copepod at these depths. Past studies have also reported an increased presence of Metridinidae*,* Oncaeidae and *Oithona* spp. at these depths (Longhurst *et al.*, 1984; Hattori, 1989; Atkinson and Sinclair, 2000; Gislason, 2008; Kosobokova and Hopcroft, 2010). Recent modelling using the MEDUSA ecosystem framework has hypothesized that particle-associated copepods (PACs) have a significant role in the attenuation of sinking POC fluxes in the upper ocean (Mayor *et al.*, 2020). Particle fragmentation by these copepods at the epipelagic-mesopelagic boundary may reduce the vertical transfer of organic material to deeper layers (Koski *et al.*, 2020), thereby influencing energy flow and ecosystem structure. The attenuation of POM may explain the flattening of NBSS slopes at greater depths, whereby the ecosystem becomes increasingly reliant on recycled energy and is characterized by a rise in detritivores, omnivores and carnivores.

Below 250 m, NBSS slopes became shallower again and displayed a trimodal distribution (Figure 4.7). These features may not represent full trophic levels, as in broader-spectrum NBSS studies e.g. Tarling *et al.* (2012), but more likely reflect the prevalence of key functional groups within the mesozooplankton community. The first dome represents the detritivore and particle feeding community, mainly consisting of small Calanoida and Oncaeidae, the middle dome detritivore/omnivore Metridinidae, and the final dome large Calanoida and *C. acutus* and to a lesser extent Metridinidae and *R. gigas* (Figure 4.8). Increases in large-sized zooplankton and shallowing of NBSS slopes with depth is a common phenomenon (Dai *et al.*, 2017; Yamamae *et al.*, 2023; Kim *et al.*, 2025). Several reasons can be responsible for this, including increased proportion of large-bodied carnivorous zooplankton (Steinberg *et al.*, 2008; Homma and Yamaguchi, 2010), lower temperature-induced metabolic rates allowing organisms to grow

larger (Atkinson, 1995), predation-mediated selection – i.e. reduced pressure of visual predation of larger zooplankton in deeper waters (De Robertis *et al.*, 2000), and the presence of large-bodied diapausing copepods (Yamaguchi *et al.*, 2002; Homma and Yamaguchi, 2010). In this study, the shallowing of the NBSS slope in deeper waters can at least be partly attributed to the presence of ontogenetic vertically migrating species, *Calanoides acutus* and *R. gigas*, which may have not yet emerged from diapause and migrated back up to surface waters (Cook *et al.*, 2023; Savineau *et al.*, 2024). Indeed, Kim *et al.* (2025) partly attributed more moderate NBSS slopes with increasing depth to the horizontal transportation and advection of subarctic diapausing copepods.

4.5.3 Importance of integrating zooplankton taxonomy and functional ecology into size spectrum interpretations

This study highlights the complexity of interpreting NBSS and the importance of accounting for taxonomic composition and functional ecology when interpreting zooplankton size spectra, as size-based assessments alone may result in a blind interpretation and misleading conclusions about ecosystem dynamics. High biovolumes of organisms in larger size classes are often indicative of ecosystems with high transfer efficiencies of energy up the food web (Zhou, 2006). However, in high-latitude environments, such as the Scotia Sea, this pattern may instead reflect seasonal physiological dynamics, specifically the dominance of lipid-storing herbivorous copepods (Tarling *et al.*, 2012). These organisms rely on internal energy reserves acquired weeks or months earlier, decoupling current observed NBSS patterns from active phytoplankton consumption and ecosystem dynamics. This time-disconnect may have far reaching consequences on if and how NBSS can be used to reliably assess and model ecosystem functioning. While shallow NBSS slopes and biovolume accumulation in larger size classes might suggest active energy transfer up the food web, potentially meaning reduced carbon export to depth, this is not necessarily the case when diapausing copepods are in a dormant state and not grazing, as noted by Cook *et al.* (2023) and Savineau *et al.* (2024). Without accounting for zooplankton physiology and life history dynamics, for which taxonomical knowledge is required, NBSS interpretations may overestimate ecosystem-level energy retention and underestimate vertical carbon flux.

Moreover, different zooplankton community compositions can produce similar NBSS patterns but reflect contrasting ecosystem dynamics. For example, in the Celtic Sea and subtropical Pacific, shallower NBSS slopes and accumulation of biomass in larger size classes were shaped by a dominance of gelatinous species, carnivorous feeding modes and an increased internal recycling of energy within the zooplankton community (Dai *et al.*, 2016; Dai *et al.*, 2017; Giering *et al.*, 2019b). Although these aforementioned NBSS studies may produce similar NBSS

patterns to those observed in the present study, the mechanisms shaping them differ greatly, all of which has implications for size-based ecosystem modelling. This highlights the importance of integrating taxonomic community composition, functional traits, and physiology when using size spectra to assess ecosystem processes.

4.5.4 Moving towards imaging technologies

Given the importance of taxonomic composition when interpreting size spectra, imaging technologies are revolutionising our ability to generate and reliably interpret NBSS data. High-throughput and semi-autonomous techniques, such as the FlowCam Macro used in this study, allow us to couple size-based assessments with taxonomic knowledge of zooplankton communities. The comparison of the taxonomic composition obtained from the FlowCam Macro vs that from microscopy (Figure 4.6) suggests that FlowCam Macro bench-top imaging may provide a cost-effective alternative to time- and labour-intensive microscopy, especially when the research question at hand is related to understanding patterns in overall community composition and size structure. Although some minor differences in numerical composition were observed between the two methods, with microscopy able to capture less abundant taxa (e.g. *Podon* spp. or Cirripedia cyprids), the two methods overlapped in overall composition of the dominant zooplankton and copepod species. The main difference between the two methods arose from the FlowCam Macro having a greater contribution of small Calanoida and the microscopy analysis having a greater contribution of large Calanoida. We suggest these differences resulted from juvenile stages of species categorised as 'Large Calanoida' in the microscopy analysis being classified within the 'Small Calanoida" category of the FlowCam Macro based on size. For example, all stages (but nauplii) of *Calanus propinquus* were classified as 'Large Calanoida' in the microscopy work, however, in the FlowCam Macro classification, unidentifiable calanoid copepods were classified as either small (< 3000 µm) or large (> 3000 µm) Calanoida, therefore juvenile stages of large Calanoida could be classified as small Calanoida depending on their size. Although current imaging technologies cannot yet fully replace physical sampling and traditional technologies, with scientists suggesting a period of overlap between the two methods (Giering *et al.*, 2022), our work highlights the utility of imaging technologies in providing broad-level taxonomy for supporting robust size-based data.

4.6 Conclusion

This work provides a new perspective on how size spectra alone may not provide the most robust understanding of zooplankton ecosystem dynamics and energy transfer in marine food webs and instead emphasizes the importance of knowledge of taxonomic composition to infer

the influence of zooplankton functional ecology in governing NBSS patterns and energy flows. Indeed, this study demonstrates the importance of accounting for functional and physiological dynamics when examining zooplankton size spectra, especially in high-latitude environments where ontogenetic vertical migration and diapausing behaviour of calanoid copepods will have significant effects on the structure of NBSS. Knowledge of the extent of active feeding, or not, by diapausing species on the spring phytoplankton bloom will significantly influence the interpretation of energy transfer within this environment. This highlights the need to reconsider if and how NBSS can be used as a tool to explore trophic transfer efficiencies in marine ecosystems and the potential implications of NBSS interpretations if we are to 'blindly' use size-spectra modelling alone without taxonomic compositional information. Lastly, our study demonstrates the importance of imaging technologies in integrating both size-based measurements and taxonomical information for the reliable interpretation of size spectral studies.

Chapter 5 Discussion

The aim of this thesis was to elucidate how zooplankton ecology and physiology changes from epi- to upper mesopelagic waters and how this impacts the cycling of carbon in the twilight zone. Zooplankton trophic ecology and physiology was studied in detail using observations made in the Scotia Sea (Southern Ocean) and the northern Benguela Upwelling System and a range of complementary methods (lipid biomarkers, stable isotopes, size-spectra, grazing experiments, respiration measurements).

5.1 Key findings

This work produced three key findings:

- Lipid-storing copepods were still in, or emerging from, metabolic inactivity during the spring diatom bloom in the Scotia Sea. The physiological ecology of diapausing calanoid copepods results in a decoupling between feeding dynamics and the spring diatom bloom in the upper 500 m of the water column. Understanding the timing of diapause is key to uncovering the impact of lipid-storing copepods on the turnover and flux of particulate organic matter (POM) in the upper mesopelagic (Chapter 2).
- High biomass of mesozooplankton in the lower boundary of the oxygen minimum zone (OMZ) of the northern Benguela Upwelling System (nBUS) suggests the OMZ may act as an important refuge for mesozooplankton from larger micronekton which were distributed above and below the OMZ. Elevated C:N ratios and animal-derived lipid biomarkers in POM indicate mesozooplankton and micronekton play a central role in the processing and fate of carbon in the mesopelagic and OMZ (Chapter 3).
- The presence of lipid-storing copepods causes high biovolume retention in large size classes and can mislead interpretations of ecosystem dynamics and carbon cycling unless taxonomic and physiological factors are considered when interpreting size spectra. Integrating these aspects into size-based approaches is crucial when assessing zooplankton-mediated carbon cycling (Chapter 4).

The following discussion synthesises how the results from the three data chapter of my thesis integrate to provide increased understanding of temporally and spatially resolved zooplankton-mediated carbon cycling in the mesopelagic. I furthermore discuss how my results fit into the wider context of other regions and in future warming climate.

5.2 Zooplankton as important actors in the decoupling of ocean carbon cycling in time and space

5.2.1 Lipid-storing copepod induced temporal decoupling between carbon fixation and remineralisation

Understanding the duration and timing of diapause by overwintering calanoid copepods is key to uncovering the effects of ontogenetic vertical migration and the lipid pump on the seasonal active transport of carbon into the mesopelagic. In this thesis I have highlighted how the presence of lipid-storing copepods in an ecosystem result in a temporal decoupling between primary production and biogeochemical cycling, specifically between carbon fixation and carbon remineralisation. Chapter 2, supported by findings from Cook et al. (2023), suggests that a portion of the *C. acutus* and *R. gigas* populations in the Scotia Sea (Southern Ocean) were still in, or emerging from, diapause. During this period, they relied on stored lipids for energy and were therefore not actively grazing on the intense phytoplankton bloom observed during the study. Chapter 4 moreover posits that high energy retention in larger size classes of NBSS is due to the presence of *C. acutus* and *R. gigas*, who's life cycle patterns result in much of the seasonal primary productivity being integrated into their lipid reserves for the entire year. Together, these chapters highlight how the influence of herbivorous calanoid copepods on fixed carbon loss via grazing may be felt in the summer of year one, when C5 copepodites build up their lipid reserves prior to ontogenetic migration to depth for diapause. However, the remineralisation of this carbon may only occur months later, in the following spring, when these C5 copepodite use their lipid stores to fuel growth into adults and reproduction/egg production (Hagen and Schnack-Schiel, 1996). Moreover, the timing of when lipid-storing copepods emerge from diapause in summer, and become metabolically active and begin grazing again, may results in short temporal offsets with the peak of the diatom bloom. Indeed, during the this study (COMICS DY086 Expedition), Giering *et al*. (2023) and Henson *et al*. (2023) reported a temporal offset between the significant accumulation of organic matter in the upper mesopelagic and when this carbon was lost 2 – 3 weeks later, with the offset being proposed to be linked to the inactivity of the mesopelagic ecosystem during the height of primary production. Temporal uncoupling has also been proposed to explain high procaryotic carbon demands relative to POC flux in deep waters, with the inclusion of temporal offsets found to balance the carbon budget over a year long time scale, suggesting prokaryotes are only weakly coupled to POC flux on a seasonal timescale (Uchimiya *et al.*, 2018). Considering *C. acutus* and *R. gigas* dominate mesozooplankton biomass in the upper 500 m of the water column in the Scotia Sea (Chapter 4, Kerkar *et al*. (2022), Cook *et al*. (2023)), assuming that these animals are actively grazing on the phytoplankton population during the peak of bloom events could lead to

a miscalculation of carbon flux, and suggests temporal offsets caused by lipid-storing copepod physiology should be taken into account when compiling carbon budgets.

5.2.2 Zooplankton-induced spatial decoupling between carbon fixation and remineralisation

The vertical distribution and migratory behaviour of zooplankton can lead to a spatial decoupling between primary production in surface waters and the processes of carbon cycling and remineralisation at depth. Both diel vertical migration (DVM) and ontogenetic vertical migration (OVM) can contribute to this decoupling, albeit on different timescales, with the former acting on a diel scale and the latter on a seasonal/yearly scale. Zooplankton that perform DVM feed in the surface layer at night and descend to deeper waters during the day, where respiration at depth results in the remineralisation of surface-derived carbon. This pattern leads to a daily, dynamic cycling of carbon. For example, members of the taxa Metridinidae were observed to undertake significant DVM, feeding in the surface waters at night and residing within the oxygen minimum zone (OMZ) during the day (Chapter 3). Although mesozooplankton DVM was reported to be asynchronous in this thesis, active carbon flux beyond 125 m via respiration (CO_2 - carbon remineralisation), excretion of dissolved organic carbon (DOC) and mortality at depth amounted to up to 0.761 µmol C m^{-3} d^{-1}. Giering *et al.* (2023) suggests that gut flux at depth by vertical migrating zooplankton and micronekton could be a possible mechanism to transport sufficient carbon to the lower mesopelagic zone to balance the lower mesopelagic carbon budget. OVM also represents a longer-term mechanism of spatial decoupling. Diapausing copepods feeding on surface-derived carbon will accumulate large-lipid stores before migrating to depth in late summer/autumn to diapause. Whilst in diapause, lipid-storing copepods will slowly metabolise stored carbon, effectively remineralising surface-fixed carbon at depth over extended periods. Yang *et al.* (2025) reported mesozooplankton in the Southern Ocean to contribute 26.5 million tons of carbon per year via OVM respiration at depths > 500 m. In addition, mortality at depth of diapausing copepods provides a further means by which zooplankton decouple carbon cycling over space. Yang *et al.* (2025) reported mesozooplankton in the Southern Ocean to contribute 25.5 million tons of carbon per year via OVM mortality at depths > 500 m. The spatial effect of zooplankton-mediated carbon cycling can also be observed when looking at how the lipidic and elemental signatures of POM change with depth. Both Chapter 2 and Chapter 3 observed an increase in zooplankton-derived lipid biomarker signatures and a decrease in phytoplankton-derived lipid biomarker signatures with depth, indicating zooplankton-sourced materials become increasingly more important in the mesopelagic particle pool in the Scotia Sea and nBUS. This indicates that zooplankton are important actors in the processing and fate of carbon in the mesopelagic. Spatial decoupling

has also been observed in terms of POC export transfer efficiency, with transfer efficiencies within the upper 100 m increasing but transfer efficiencies in the lower mesopelagic decreasing during a post-bloom phase in the Scotia Sea (Henson *et al.*, 2023). This underscores a spatial decoupling between the flux attenuation processes happening in the upper and lower mesopelagic. Understanding what drives spatial decoupling in mesopelagic carbon cycling is therefore an important avenue for future research.

Oxygen minimum zones (OMZs) have been widely identified as regions of high particle transfer efficiency to depth, largely related to reduced particle flux attenuation associated with lower rates of aerobic bacterial degradation and altered zooplankton activity (Weber and Bianchi, 2020). Results from Chapter 3 suggests particle transformation and repacking within the Benguela OMZ, with particles becoming increasingly refractory with depth and showing enhanced zooplankton and animal lipid signatures, particularly in the larger (>53 µm) particle size fraction. This pattern suggests active particle repackaging processes by zooplankton via production of faecal pellet material. Oxygen concentrations in the Benguela OMZ during this study were less extreme than in more intense OMZs such as the Arabian Sea, where oxygen concentrations are well below 20 µmol/kg (Liu *et al.*, 2024), potentially allowing for greater heterotrophic processing of particles in our study region. Kurian *et al.* (2026) reported sharp degradation of labile organic matter in the upper ~60 m due to zooplankton reworking above the OMZ in the easter Arabian Sea, however, our observation of peak zooplankton biomass both above and within the OMZ complicates the attribution of particle transformation and faecal material production to a single depth horizon. Indeed, Roullier *et al.* (2014) attributed an accumulation of large particles and enhanced particulate repackaging in zooplankton-enriched layers of the lower oxycline of the Arabian Sea OMZ. When comparing the accumulation of the animal biomarker 18:1(n-9) in POM of the nBUS OMZ (chapter 3) to that of the P3 site of the Scotia Sea (chapter 2), we can observe greater accumulation in 18:1(n-9) with depth in the Scotia Sea than in the nBUS, suggesting that the reduced zooplankton activity in the OMZ is potentially resulting in less particle repacking than in a well-oxygenated area such as the Scotia Sea, Southern Ocean. This further emphasizes the role of OMZ as areas of enhance carbon preservation and flux to depth (Weber and Bianchi, 2020).

5.3 Zooplankton in a warming climate and implications for the BCP

Our findings highlight the importance of copepod vertical migration in driving both a spatial and temporal decoupling between carbon fixation in surface waters and subsequent remineralisation at depth on both diel and seasonal time frames. Global oceans are experiencing pronounced warming and environmental change as a result of anthropogenic

climate warming (Pörtner *et al.*, 2019). The Southern Ocean is observed to show strong regional sensitivities in relation to climate change, with overall trends in phytoplankton blooms increasing in amplitude, decreasing in seasonality, initiating later and terminating earlier (Thomalla *et al.*, 2023). However, in areas of sea ice, blooms have been observed to initiate earlier and last longer (Thomalla *et al.*, 2023; Schlosser and Strutton, 2025). In the Scotia Sea, sea surface temperature (SST) has increased by approximately 0.98 °C between the *Discovery Investigations* period (1926–1938) and contemporary observations (1996–2013) (Tarling et al., 2017).

Changes in primary production phenology and duration may have important implications for herbivorous zooplankton, especially those undergoing seasonal migration and diapause, such as *C. acutus* and *R. gigas* discussed in chapters 2 and 4. An extended productive season could delay descent into diapause, and earlier bloom result in earlier exit from diapause, potentially reducing the magnitude or duration of seasonal vertical migration and thus carbon export to depth. Indeed, distinct regional variations in life cycle of *R. gigas* have been observed in the Southern Ocean, with northern populations in the Scotia sea exiting diapause and coming back to surface waters up to 2-3 months earlier than populations further south in the Eastern Weddell Sea (Ward *et al.*, 1997), potentially resulting in less carbon export via seasonal migration in the former sub-population. Such poleward lags in the timing of exist from diapause in relation to the progressively later appearance of the phytoplankton maxima further south have also been established in *C. acutus* and *C. propinquus* in the Southern Ocean (Voronina, 1970). Long-term increases in ocean temperatures and concurrent changes in bloom phenology may therefore lead to changes the prevalence/dominance of one regionally distinct sub-population over another, all of which would have consequences for their impacts/role in the BCP.

Ocean warming is also associated with a reduction in zooplankton body size, known as Bergmann's rule, whereby ectothermic animals such as zooplankton tend to grow faster, reach sexual maturity earlier and have smaller adult sizes under higher temperatures (Gillooly, 2000; Campbell *et al.*, 2021). Such phenomenon has also been termed the temperature-size rule, whereby ectothermic species mean sizes decrease with warming (Atkinson, 1994) and has been observed across aquatic systems (Garzke *et al.*, 2015; Doan *et al.*, 2019; Albini *et al.*, 2025). Smaller body size of calanoid copepods implies smaller lipid store capacity, potentially reducing the amount of carbon being transported to depth via the lipid shunt and released during diapause at depth. Warming-induced reductions in body size of zooplankton could therefore directly weaken the contribution of zooplankton migratory carbon to the BCP.

The cues that trigger the emergence from diapause remain to be fully understood, with observations of copepods exiting diapause in the absence of clear environmental cues

(Østvedt, 1955; Conover, 1965) suggesting that internal physiological cues, potentially linked to the internal biological clock, gene regulation or lipid content/composition are at play (Bandara *et al.*, 2021). Energetic limitations are suggested to play a role in the duration of diapause, with modelling by Saumweber and Durbin (2006) suggesting *Calanus finmarchicus* lipid reserves would sustain diapause for 280 days at 0 °C, but only 90 days at 11 °C, highlighting the strong influence of temperature on metabolic demand. Increased sea temperatures and metabolic rates could therefore accelerate lipid store depletion and potentially force calanoid copepods into earlier exit from diapause. Less time in deeper waters could furthermore potentially reduce the amount of carbon stored at depth via mortality and predation of calanoid copepods in deep waters.

Whilst surface waters in the Scotia Sea, have warmed by almost 1 °C since the 1920-30s, deeper waters have remained comparatively stable and are warming more slowly (Tarling et al., 2017). This suggests that ocean warming impacts on diapause duration may be more strongly determined by body size and lipid reserves at the time of descent than by temperature-dependent metabolic rates at depth. Zooplankton could descend to greater depths to reach colder waters, potentially enhancing carbon transfer to the deep ocean. Wilson *et al.* (2016) suggested *Calanus finmarchicus* in the Labrador Sea would have to diapause at depths >2000 m to counteract end-of-century temperature-induced shortening in diapause duration. However, the feasibility of this response depends on the ability of individuals to maintain neutral buoyancy at greater depths. Visser and Jónasdóttir (1999) highlighted that calanus copepods would become negatively buoyant at such depths, preventing successful diapause at >2000 m modelled by (Wilson *et al.*, 2016). Moreover, temperature-induced reduction in body size and lipid content would further exacerbate this negative buoyancy.

Increasing SST could moreover lead to poleward migrations of smaller, more temperate species towards the poles, as by *Calanus* species in the North Atlantic (Beaugrand *et al.*, 2002; Chust *et al.*, 2013). Such replacement of large species with smaller ones can have drastic implications with the amount of carbon biomass these animals would migrate to depth as well their life history strategies in terms of diapause. Although SST has warmed by ~1 °C in the Scotia sea, zooplankton biomass has increased over time (Ward *et al.*, 2018) and the geographical location of abundances have remained relatively stable despite the 1920s–1930s SST isotherms having shifted poleward by more than 500 km (Tarling et al., 2017). *Calanoides acutus*, *Rhincalanus gigas* and *Calanus simillimus*, have been observed to increase in abundance by 20–55 % compared to 70 years ago (Ward *et al.*, 2018), potentially meaning an increased carbon export at depth via ontogenetic vertical migration. This apparent resilience suggests that Southern Ocean zooplankton may be buffered against surface warming by spending much of the year at depth in cooler, more stable environments during diapause (Tarling *et al.*, 2018). Nevertheless, the

complex interplay between ocean warming, phytoplankton and zooplankton phenology, body size, and migration behaviour makes predicting future climate-driven changes in zooplankton-mediated carbon sequestration highly uncertain. Diapause furthermore remains a complicated process to study in the ocean and within laboratory settings, resulting in a lack of clear markers of the physiological mechanisms governing it (Baumgartner and Tarrant, 2017).

Global warming is moreover predicted to lead to a an expansion of mid-depth oxygen minimum zones, due to reduced dissolved oxygen solubility in water, enhanced respiration-induced oxygen consumption by organisms and increased vertical stratification (Oschlies *et al.*, 2018). Such expansions have already been observed in the Benguela Upwelling System (Stramma *et al.*, 2008) and the California current in the Eastern Pacific (Bograd *et al.*, 2008). The expansion of OMZs may influence the BCP by limiting the vertical migration of zooplankton if oxygen concentration in deeper waters are too low for survival, compressing communities in shallow surface layers of oxygenated water, as observed in the Eastern Pacific (Köhn *et al.*, 2022). This could both reduce the depth at which vertical migrators can descend to as well as how long they may be able to stay down before having to return to oxygenated waters to pay off higher oxygen debts (Bianchi *et al.*, 2013), all of which would negatively impact zooplankton active carbon export flux to deep waters. Moreover, lower oxygen concentrations may results in migrating zooplankton to further suppress their metabolism at depth, reducing the amount of carbon dioxide being released via respiration, hence decreasing the efficiency of the BCP (Seibel, 2011). Lower oxygen concentrations have moreover been observed to reduce survival of copepods under controlled laboratory conditions and also resulted in smaller-sized copepods due to oxygen-limited growth rates (reviewed by Roman and Pierson (2022)). Similarly to temperature mentioned above, reduced oxygen concentrations, are likely to have size-dependent impacts on zooplankton carbon export. In contrast however, expansion of OMZs may potentially result in increased passive carbon flux to depth due to reduced particle attenuation and degradation by microbes and heterotrophs within OMZs (Weber and Bianchi, 2020).

5.4 Future directions

This thesis addressed key uncertainties in the role of zooplankton in the biological carbon pump, highlighting the importance of integrating functional ecology and physiology into our understanding of zooplankton-mediated carbon cycling. However, this work also highlights themes for future research in zooplankton trophic ecology and physiology, and the tools required to study them.

5.4.1 Improving empirical understanding of zooplankton processes

Chapter 3 found large discrepancies between carbon ingested (via grazing) and carbon respired when quantifying mesozooplankton metabolic budgets for the nBUS. These were suggested to arise from poor food quality requiring high ingestion to meet metabolic requirements, but also potentially from uncertainties in estimating ingestion rates of mesozooplankton, especially in the mesopelagic where changes in environmental conditions were significant. This thesis therefore highlights the need to improve understanding of how grazing rates change throughout epi- and mesopelagic waters depending on environmental factors such as temperature, pressure, oxygen concentration and food concentration. Although some of these can be investigated through incubation experiments (e.g. the effects of temperature/oxygen/food concentration), discrepancies between measurements made at atmospheric pressure vs *in situ* pressure and environmental conditions must be considered. Studies have used pressurized chambers to reproduce conditions found in the mesopelagic when studying microbial respiration (Amano *et al.*, 2023). Past studies have also used hydrostatic chambers to look at egg hatch survival of the calanoid copepod, *Calanus sinicus* (Yoshiki *et al.*, 2006). Expanding the use of such pressurised chambers to conduct incubation experiments exploring metabolic rates (e.g., grazing and respiration) of zooplankton could significantly increase our understanding of how their physiology changes with depth throughout the mesopelagic.

This thesis has highlighted that diel vertical migration is not a conventional, synchronous behaviour undertaken by all zooplankton and micronekton, and is instead a complex phenomenon influenced by many factors including environmental conditions (e.g. food availability, oxygen concentration), body size and taxa-specific functional ecologies and physiologies. In the Scotia Sea, stable isotope signatures of mesozooplankton suggests these animals were feeding on fresh POM throughout the upper 500 m (Chapter 2), despite showing no evidence of synchronised DVM (Cook *et al.*, 2023), highlighting the influence of food availability on DVM behaviour. Indeed, increased food availability throughout the mixed layer has been suggested as a possible reason for lack of DVM by zooplankton (Cisewski and Strass, 2016). In the nBUS, the vertical expansion of the OMZ towards the end of the study period became a barrier to DVM of decapods which were able to perform DVM when the OMZ was shallower (Chapter 3). The presence of lipid-storing copepods at depth in both study sites may moreover explain the lack of synchronised DVM in mesozooplankton (Chapter 2, Chapter 3, Cook *et al.* (2023)). The lipid-storing copepods *Calanoides acutus/Rhincalanus gigas* in the Scotia Sea (Chapter 2, 4) and *C. natalis/R. nasutus* in the nBUS (Chapter 3) are dominant taxa, therefore it is possible that their ontogenetic diapausing state, at the time of the study could have significantly reduced the magnitude of mesozooplankton DVM compared to a time of year when they would be metabolically active. Moreover, body size may be an important determinant of

DVM activity, with DVM often attributed to larger zooplankton and micronekton which have increased risk of visual predation (Hays *et al.*, 1994; De Robertis *et al.*, 2000). Chapter 3 did observe a general trend in larger animals (macrozooplankton and micronekton) performing consistent DVM, whereas this was lacking in smaller animals (mesozooplankton). Improving our understanding of potential links between body size and DVM of zooplankton and micronekton should also be a key priority for future research.

More observational work is required to understand the drivers of DVM behaviour. Specifically quantifying what proportion of zooplankton communities undergo DVM, and how this changes seasonally (e.g., in response to environmental forcings or taxa-specific ontogenetic behaviours) and in different biogeographical regions. Aumont *et al.* (2018) attempted to explicitly integrate DVM into the ocean biogeochemical model NEMO-PISCES and found that evaluating the model behaviour was challenging due to scarcity of observational data. The model assumed all organisms swam synchronously in the same direction and to the same depth, however we know this is not the case, as is seen in Chapter 3, where different depths of DVM and reverse DVM are observed – all of which are influenced by environmental parameters such as oxygen concentrations and taxa-specific physiologies.

5.4.2 Sampling the entire zooplankton size spectrum

A key limitation discussed in Chapter 4 was the effects of zooplankton net sampling bias on the normalised biovolume size spectra (NBSS) produced, specifically the under sampling of smaller zooplankton, as the MOCNESS-330 µm lower effective sampling capability is estimated to stand ~1000 µm. This resulted in a misrepresentation of abundances of smaller sized zooplankton and thus an under-quantification and contribution of the biovolume of small size classes to the NBSS. Altogether, this influences the shape of the NBSS and how we may interpret it (Chapter 4). To get a broad understanding of ecosystem functioning, we need to ensure the complete spectrum of zooplankton is collected, including all sizes, functions, places, depths and time. However, historically and to this day, conventional nets to monitor zooplankton are of mesh sizes > 200 µm. For example, the western channel observatory L4 coastal time series run by Plymouth Marine Laboratory uses a 200 µm meshed WP2 net (McEvoy *et al.*, 2022), the Bermuda Atlantic Time-series Study (BATS) in the Sargasso Sea uses a 202 µm mesh (Steinberg and Cope, 2025), the continuous plankton recorder (CPR) uses a 270 µm silk mesh (Holland *et al.*, 2025), Line P transect time series in the North Pacific uses a 236 µm meshed net (Kwong *et al.*, 2022) and the Hawaii Ocean Time-Series (HOT) in the Pacific uses a 202 µm meshed net (Fujieki *et al.*, 2023). It is estimated that conventional 200 µm meshed nets significantly under-capture mesozooplankton between 200 – 800 µm, therefore under sampling small but important zooplankton such as *Oithona* spp. and Oncaeidae (Gallienne and Robins, 2001; Ward

et al., 2012b). Despite their small size, recent research suggests these taxa, referred to as 'particle-associated copepods' are key actors in the fragmentation of particles in the ocean (Mayor *et al.*, 2020). Improved sampling and thus representation of these animals when assessing zooplankton community size spectra will therefore improve our interpretations of zooplankton ecosystem dynamics and zooplankton-mediated carbon cycling. It is crucial that zooplankton research and monitoring move towards including smaller meshed nets (e.g. 64 µm) as the norm, so that small but critically important species are not quantitatively and qualitatively misrepresented.

5.4.3 Move towards imaging technologies. Are images the future?

Chapter 4 highlighted how functional ecology and physiology are key drivers of the size structure and shape of NBSS, and how we therefore need taxonomic information of the community being studied to be able to make the right conclusions as to what drives overall size-spectra patterns. Without such taxonomic information, we may be "blindly" interpreting and applying size-spectra approaches to study ecosystem functioning.

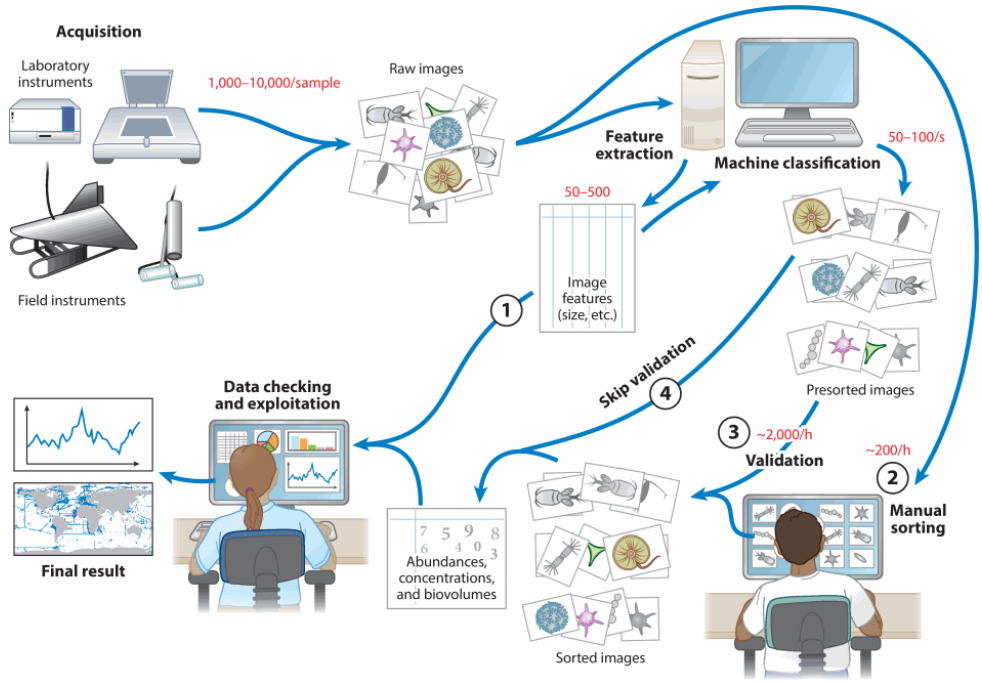

Figure 5.1 The plankton quantitative imaging process, illustrated by Irisson *et al.* (2022)

Imaging technologies are enhancing our ability to efficiently and quickly collect and process zooplankton taxonomic and abundance data compared to microscopy analysis and also collect associated morphological measurements from images such as size, which can be used to quantify biovolume or biomass (Figure 5.1). Growing infrastructure to process quantitative imaging datasets, such as EcoTaxa, are becoming increasingly useful to efficiently classify images within a universal taxonomic reference (World Register of Marine Species, WoRMS) and

associated metadata (Picheral *et al.*, 2025). Using a combination of machine learning, convolutional neural networks and human-based taxonomic knowledge and validation, all in a user-friendly, open-access web platform, it allows scientists to efficiently classify extremely large imaging datasets of hundreds of thousands to millions of images (Irisson *et al.*, 2022).

Although there are concerns that imaging-technologies cannot provide the taxonomic resolution that microscopy analysis can (Giering *et al.*, 2022), results from Chapter 4 do show that, at a broader taxonomic level, FlowCam Macro image-based taxonomy is comparable to microscopic taxonomy, therefore when looking at patterns of overall community composition and size structure, imaging technologies may be more advantageous. There is indeed growing interest in moving towards quantitative imaging, especially when it comes to observational data such as resolving plankton temporal and spatial patterns, monitoring biodiversity - especially of fragile, gelatinous species which break apart in nets (Christiansen *et al.*, 2018), and exploring size spectra and estimating carbon fluxes (Irisson *et al.*, 2022). Indeed, *in-situ* imaging technologies such as the Underwater Vision Profiler (UVP) can target and image particles > 100 µm and more efficiently capture gelatinous organisms, which together could increase resolution of zooplankton community size structure and help reduce net sampling size-biases (Chapter 4; section 5.4.2). *In-situ* imaging can also increase the spatial resolution of zooplankton vertical distributions, as zooplankton are imaged right at the depth at which they are found. This is particularly useful when it comes to limitations of coarser spatial resolutions in nets, as observed in Chapter 3, where broad sampling depth intervals make precise determination of peak mesozooplankton biomass distributions in relation to the OMZ difficult. However, it also must be acknowledged that quantitative imaging cannot fully replace physical sampling, due to the breadth of ecological and biogeochemical information that can be extracted from physical samples, e.g. metabolic rates, elemental information, molecular analyses. Therefore, the sampling tool used must be chosen in accordance with the research question at hand.

5.5 Conclusion

The research in this thesis furthers our understanding of the role of zooplankton trophic ecology and physiology in the cycling and fate of carbon in the mesopelagic zone, and have highlighted how:

- the physiological ecology of diapausing copepods causes a temporal decoupling between carbon fixation and remineralisation (Chapter 2).

- diel vertical migration (DVM), ontogenetic vertical migration (OVM) and oxygen minimum zones (OMZ) cause spatial decoupling between carbon fixation and remineralisation (Chapter 3 and Chapter 2).
- taxonomy, functional ecology and physiology drive changes in the size structure of zooplankton communities and subsequent size-based assessments of zooplankton-mediated carbon cycling (Chapter 4).

Future research into zooplankton-mediated carbon cycling should focus on:

- understanding what controls the timing of exit from diapause in lipid-storing copepods.
- understanding how zooplankton metabolic rates change under *in-situ* conditions within the mesopelagic.
- understanding what drives DVM behaviour of zooplankton and potential links between body size and the magnitude of DVM.
- improving the sampling of smaller-sized mesozooplankton to ensure complete representation of the entire size spectrum of zooplankton communities.

Appendix A Chapter 2

A.1 Supplementary tables for Chapter 2

Table A 1 Summary of the net deployments and zooplankton collected for the lipid biomarker analysis at the P3 (B+C) stations in the Scotia Sea.

Station	Date / Time of Day	Sampler	Event	Net	Depth (m)	Individuals collected
P3B	29/11/2017 Day	RMT 25	153	1	248 – 501.5	*Euphausia triacantha* *Thysanoessa* spp.
				2	18.3 – 256	Chaetognatha
	30/11/2017 Night	RMT 25	162	1	250.4 – 501.3	Chaetognatha *Euphausia triacantha*
				2	19.4 – 262.2	*Euphausia triacantha* *Salpa thompsoni* *Thysanoessa* spp.
	03/12/2017 Night	MOCNESS	217	2	436.9 – 501.3	*Calanoides acutus*
				5	250.9 – 312.9	*Rhincalanus gigas*
				6	187.8 – 251.5	*Rhincalanus gigas*
				9	12.6 – 61.8	*Calanoides acutus*
	04/12/2017 Day	MOCNESS	234	3	374.9 – 438.2	*Rhincalanus gigas*
				5	249.9 – 312.4	Chaetognatha
				6	187 – 249.8	*Calanoides acutus*
				9	13.7 – 64.5	*Rhincalanus gigas* *Themisto gaudichaudii*
P3C	10/12/2017 Night	RMT 25	286	2	14.8 – 259.8	*Salpa thompsoni* *Thysanoessa* spp.
	10/12/2017	RMT 25	295	1	248.8 – 501.5	*Thysanoessa* spp.

P3C	Day			2	12.9 – 259.8	Chaetognatha *Euphausia triacantha* (×2) *Themisto gaudichaudii* *Thysanoessa* spp.
	11/12/2017 Day	MOCNESS	315	3	374.9 – 438.5	*Calanoides acutus* Chaetognatha *Paraeuchaeta* spp. *Rhincalanus gigas*
				5	250.7 – 313.7	Chaetognatha *Euphausia triacantha* *Rhincalanus gigas*
				7	125 – 187.6	*Calanoides acutus* Chaetognatha *Rhincalanus gigas*
				9	9.7 – 58.3	*Calanoides acutus* *Themisto gaudichaudii*

Table A 2 Summary of the net deployments and zooplankton collected for the stable isotope analysis at the P3 (B+C) stations in the Scotia Sea.

Station	Date / Time of Day	Sampler	Event	Net	Depth (m)	Individuals collected
P3B	29/11/2017 Day	RMT 25	153	1	248 – 501.5	*Salpa thompsoni* (×3)
				2	18.3 – 256	*Thysanoessa* spp. (×5) *Salpa thompsoni* (×5)
	30/11/2017 Night	RMT 25	162	2	19.4 – 149.5	*Salpa thompsoni* (×2)
	30/11/2017 Day	Mammoth	175	2	375 – 438	*Calanoides acutus*
				6	125 – 188	*Calanoides acutus*
				9	5 33	*Calanoides acutus*
	30/11/2017 Twilight	MSC	180	6		*Rhincalanus gigas*
	03/12/2017 Night	MOCNESS	217	3	375.5 – 436.9	Chaetognatha *Paraeuchaeta* spp. *Thysanoessa* spp. (×2)
				5	250.9 – 312.9	*Euphausia triacantha* (×2) *Rhincalanus gigas* *Thysanoessa* spp. (×4)
				7	124.7 – 188.6	*Euphausia triacantha* (×5)
	04/12/2017 Day	MOCNESS	234	5	249.9 – 312.4	Chaetognatha (×4) *Euphausia triacantha* (×5)
				7	125.2 – 188.1	Chaetognatha (×3)
	04/12/2017	MOCNESS	234	9	13.7 – 64.5	Chaetognatha *Rhincalanus gigas*

	Day					*Themisto gaudichaudii* (×4) *Thysanoessa* spp. (×5)
P3C	10/12/2017 Night	RMT 25	286	2	14.8 – 259.8	*Euphausia triacantha* (×5) *Thysanoessa* spp. (×3) *Salpa thompsoni* (×2)
	10/12/2017 Day	RMT 25	295	1	248.8 – 501.5	*Thysanoessa* spp. (×4)
				2	12.9 – 259.8	Chaetognatha (×2) *Themisto gaudichaudii* (×5) *Thysanoessa* spp. (×2) *Salpa thompsoni* (×5)
	11/12/2017 Night	MOCNESS	305	3	375.2 – 437.7	*Calanoides acutus*
				5	249.8 – 299	*Rhincalanus gigas* (×2)
				7	125.2 – 187.6	*Calanoides acutus* Chaetognatha (×2) *Rhincalanus gigas* (×3)
				9	8.6 – 61.8	*Rhincalanus gigas* (×3) *Themisto gaudichaudii* (×2) *Thysanoessa* spp.
	11/12/2017 Day	MOCNESS	315	3	374.9 – 438.5	*Calanoides acutus* (×2) Chaetognatha *Paraeuchaeta* spp. (×2) *Rhincalanus gigas* (×3) *Thysanoessa* spp.
	11/12/2017 Day	MOCNESS	315	5	250.7 – 313.7	Chaetognatha *Euphausia triacantha* (×5) *Rhincalanus gigas*
				9	9.7 – 58.3	*Rhincalanus gigas*

						Themisto gaudichaudii (×2) *Thysanoessa* spp. (×3)

Table A 3 Linear regression output between depth and the relative abundances of fatty acids (mol%) in the <53 µm and >53 µm size-fractions of particulate organic matter (POM). Asterisks highlight fatty acids with significant linear regressions and slopes, and equations are given for these. Standard errors for the regression equation coefficients are given in bracket. Subscript numbers in brackets associated with the F value represent the degrees of freedom. The fatty acid 22:1 was tentatively assigned as 22:1(n-11) based on the knowledge of 22:1(n-11) being a fatty acid only biosynthesised by herbivorous calanoid copepods such as *C. acutus* (Hagen *et al.*, 1993; Dalsgaard *et al.*, 2003).

Fatty acid	**POM <53 µm**		**POM >53 µm**	
14:0	$F=2.98_{(1,20)}$, p=0.099, R^2=0.130		$F=7.54_{(1,20)}$, p=0.012, R^2=0.274 y= -30.60x(±11.2) + 297.09(±46.4)	*
16:0	$F=1.92_{(1,20)}$, p=0.182, R^2=0.087		$F=0.07_{(1,20)}$, p=0.794, R^2=0.003	
18:0	$F=42.6_{(1,20)}$, p<0.001, R^2=0.681 y= 90.12x(±13.8) + 79.25(±21.6)	*	$F=2.06_{(1,20)}$, p=0.166, R^2=0.094	
16:1(n-7)	$F=0.92_{(1,20)}$, p=0.349, R^2=0.044		$F=0.29_{(1,20)}$, p=0.593, R^2=0.015	
18:2(n-6)	$F=1.71_{(1,20)}$, p=0.205, R^2=0.079		$F=2.66_{(1,20)}$, p=0.119, R^2=0.117	
18:1(n-9)	$F=8.20_{(1,20)}$, p=0.009, R^2=0.291 y = 16.06x(±5.61) + 59.44(±43.9)	*	$F=23.6_{(1,20)}$, p<0.001, R^2=0.541 y = 11.08x(±2.28) + 24.41(±43.2)	*
18:2(tr-9)	$F=7.77_{(1,20)}$, p=0.011, R^2=0.280 y= 55.02x(±19.7) - 23.62(±71.0)	*	$F=6.16_{(1,20)}$, p=0.022, R^2=0.236 y = 27.40x(±11.0) + 39.05(±71.6)	*
20:5(n-3)	$F=2.56_{(1,20)}$, p=0.125, R^2=0.114		$F=0.35_{(1,20)}$, p=0.559, R^2= 0.017	
20:1(n-9)	$F=0.08_{(1,20)}$, p=0.775, R^2=0.004		$F=0.06_{(1,20)}$, p=0.811, R^2=0.003	
22:6(n-3)	$F<0.001_{(1,20)}$, p=0.988, R^2<0.001		$F=0.12_{(1,20)}$, p=0.735, R^2=0.006	
22:1	$F=0.677_{(1,20)}$, p=0.420, R^2=0.033		$F=1.01_{(1,20)}$, p=0.326, R^2=0.048	

A.2 Supplementary figures for Chapter 2

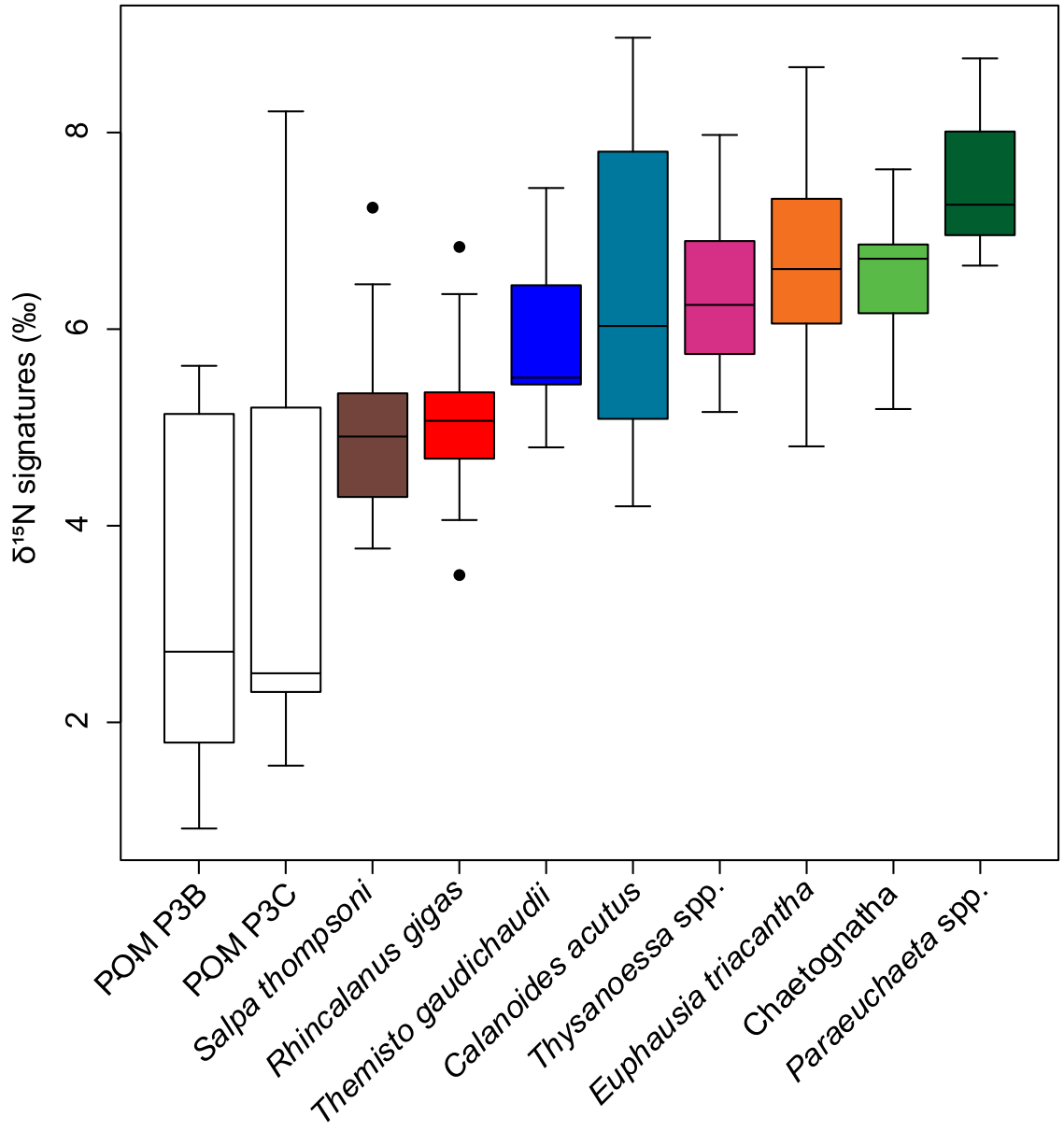

Figure A 1 $\delta^{15}N$ stable isotope signatures (‰) of POM at P3B and P3C (white boxes) and the eight zooplankton taxa at station P3 in the Scotia Sea (coloured boxes). The boxplot represents the minimum, maximum, median, first quartile and third quartile values. Circles represent outliers.

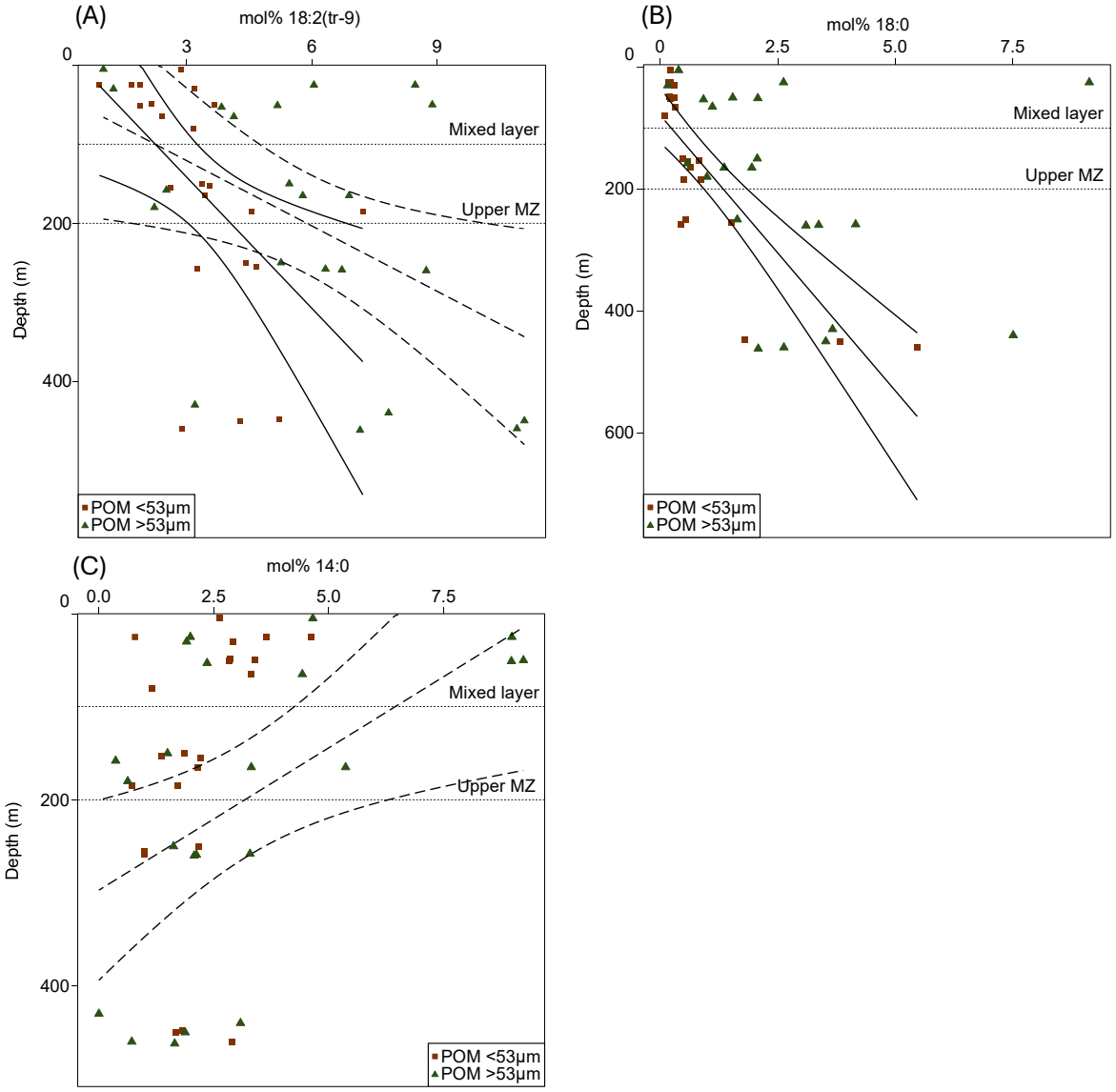

Figure A 2 Fatty acid composition of POM in relation to sampling depth at the P3 station in the Scotia Sea. The regression lines indicate a statistically significant ($p<0.05$) linear relationship between the fatty acids and depth. (A) 18:2(tr-9) in POM <53 µm = solid line: y= 55.02x(±19.7) – 23.62(±71.0); R^2 = 0.28; 18:2(tr-9) in >53 µm POM = dashed line: y = 27.40x(±11.0) + 39.05(±71.6); R^2 = 0.25. (B) 18:0 in POM <53 µm = solid line: y= 90.12x(±13.8) + 79.25(±21.6); R^2 = 0.68. (C) 14:0 in POM >53 µm = dashed line: y= -0.60x (±11.2) + 297.09(±46.4); R^2 = 0.27. Horizontal dotted lines indicate the boundaries of the mixed layer depth (0 – 95 m) and the upper (96 – 200 m) and lower mesopelagic zones (MZ) (201 – 1000 m) (Giering *et al.*, 2023).

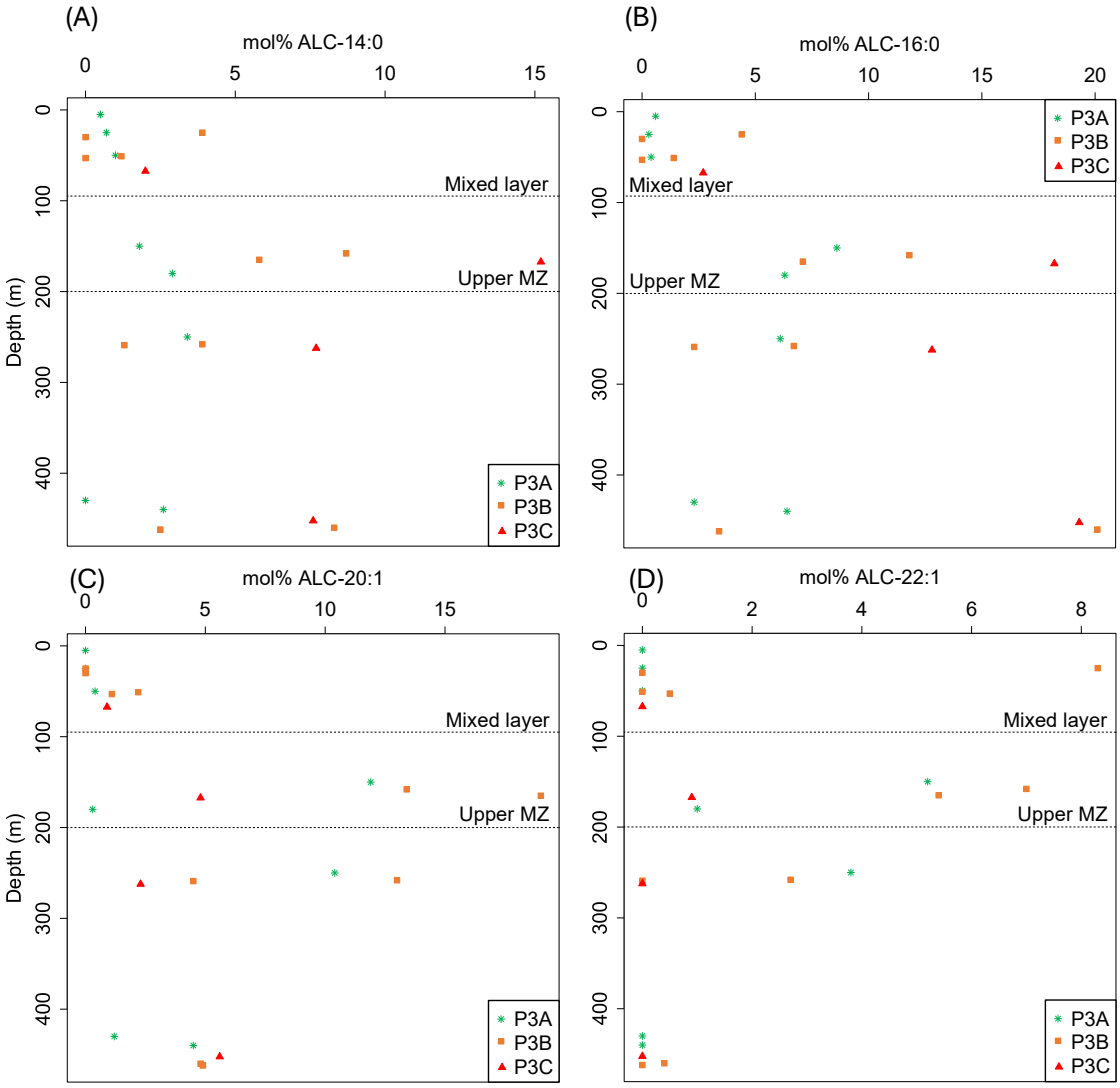

Figure A 3 Relative abundances (mol%) of fatty alcohols (A) ALC-14:0, (B) ALC-16:0, (C) ALC-20:1 and (D) ALC-22:,1 in the >53 µm size-fractions of particulate organic matter (POM) with depth at station P3 in the Scotia Sea. Horizontal dotted lines indicate the boundaries of the mixed layer depth (0 – 95 m) and the upper mesopelagic zone (96 – 200 m) (201 – 1000 m) (Giering *et al.*, 2023).

Appendix B Chapter 3

B.1 Supplementary tables for Chapter 3

Table B 1 Overview of different taxa sampled at station BN in the northern Benguela Upwelling System from the Mammoth-100, Mammoth-300 and RMT25. For taxa groups classified based on length, this refers to total length of the zooplankton calculated from the FlowCam .

Name of taxonomic group	**Sample gear**	**Group**	**Examples of taxa found in this category**
Eggs	Mammoth-100 Mammoth-300	Mesozooplankton	Eggs
Copepod nauplii	Mammoth-100 Mammoth-300	Mesozooplankton	Copepoda nauplii
Copepod 100 – 499 µm	Mammoth-100	Mesozooplankton	unID Copepoda
Copepod 500 – 999	Mammoth-100	Mesozooplankton	unID Copepoda
Copepod 1000 - 2999 µm	Mammoth-100	Mesozooplankton	*Paracalanus parvus parvus, Centropages* spp., *Microcalanus* spp., *Heterohabdus* spp.
Calanoida < 3000 µm	Mammoth-300	Mesozooplankton	*Paracalanus parvus parvus, Centropages* spp., *Microcalanus* spp., *Heterohabdus* spp.
Oithona spp.	Mammoth-100 Mammoth-300	Mesozooplankton	*Oithona* spp., *Oithona atlantica, Oithona similis*

Oncaeidae	Mammoth-100 Mammoth-300	Mesozooplankton	Oncaeidae spp., *Triconia spp*.
Harpacticoida	Mammoth-100 Mammoth-300	Mesozooplankton	Harpacticoida spp.
Mormonilloida	Mammoth-100 Mammoth-300	Mesozooplankton	Mormonilloida spp.
Lubbockiidae	Mammoth-300	Mesozooplankton	Lubbockiidae spp.
Metridinidae	Mammoth-100 Mammoth-300	Mesozooplankton	Metridinidae spp., *Metridia* spp., *Metridia lucens, Pleuromamma* spp.
Calanidae < 3000 µm	Mammoth-100 Mammoth-300	Mesozooplankton	*Calanoides natalis* (previously *Calanoides carinatus*), *Nannocalanus* spp.
Calanidae > 3000 µm	Mammoth-100 Mammoth-300	Mesozooplankton	*Calanoides natalis*
Copepod > 3000 µm	Mammoth-100 Mammoth-300	Mesozooplankton	Unidentifiable Copepoda
Eucalanidae	Mammoth-100 Mammoth-300	Mesozooplankton	*Rhincalanus nasutus, Eucalanus* spp.
Carnivorous Calanoida	Mammoth-100	Mesozooplankton	*Euchaeta* spp.

	Mammoth-300		
Ostracoda	Mammoth-100 Mammoth-300 RMT25	Mesozooplankton Micronekton	*Gigantocypris* spp., Ostracoda spp.
Pteropoda	Mammoth-100 RMT25	Mesozooplankton Micronekton	Pteropoda spp., *Clio* spp., *Cymbulia peronii*
Nemertea	RMT25	Micronekton	Nemertea spp.
Polychaeta	Mammoth-100 Mammoth-300 RMT25	Mesozooplankton Micronekton	Polychaeta spp.
Amphipoda	Mammoth-300 RMT25	Mesozooplankton Micronekton	Amphipoda spp., *Phrosina semilunata*, *Platyscelus* spp., Hyperiidae spp., *Oxycephalus clausi*, *Oxycephalus* spp., *Phronima* spp.
Appendicularia	Mammoth-100 Mammoth-300	Mesozooplankton	Appendicularia spp., *Oikopleura* spp., *Fritillaria* spp
Chaetognatha	Mammoth-100 Mammoth-300 RMT25	Mesozooplankton Micronekton	Chaetogntha spp., Sagittidae spp..
Salpa	Mammoth-100	Mesozooplankton	Salpidae spp., *Salpa* spp., *Cyclosalpa pinnata*, *Pyrosoma* spp., Pyrosomatida spp.

	Mammoth-300 RMT25	Micronekton	
Euphausiidae nauplii	Mammoth-100 Mammoth-300	Mesozooplankton	Euphausiidae nauplii
Euphausiidae calyptopes	Mammoth-100 Mammoth-300	Mesozooplankton	Euphausiidae calyptopes
Euphausiidae	Mammoth-100 Mammoth-300 RMT25	Mesozooplankton Micronekton	*Euphausia hanseni*, Euphausiacae spp., *Hansarsia megalops* (previously *Nematoscelis megalops*), *Stylocheiron* spp., *Thysanopoda* spp., *Euphausia gibboides*, *Euphausia recurva*, *Nematobrachion* spp., *Thysanoessa gregaria*
Fish larvae	Mammoth-100	Mesozooplankton	Fish larvae
Jellies	Mammoth-100 Mammoth-300	Mesozooplankton	Unidentifiable gelatinous organisms
UnID	Mammoth-100 Mammoth-300	Mesozooplankton	Unidentifiable zooplankton
Mysid	RMT25	Micronekton	Mysida spp.
Gastropoda	RMT25	Micronekton	Pterotracheoidea spp.

Decapoda	RMT25	Micronekton	*Oplophorus novaezeelandiae, Gennadas* spp., *Cristaspis cristata* (previously *Systellaspis cristata*), *Acanthephyra* spp., *Acanthephyra pelagica* (previously *Acanthephyra acanthitelsonis*), Decapoda spp., Brachyura spp.
Siphonophora	RMT25	Micronekton	*Diphyes* spp., Siphonophora spp., Calycophorae spp., Physonectae spp., Abylidae spp., Chelophyes spp., *Diphyes dispar*
Cnidaria	RMT25	Micronekton	*Atolla* spp., *Chrysaora* spp., *Colobonema sericeum*, Cnidaria spp., *Halicreas minimum*, *Halicreas* spp., Honey comb jelly, Moerisiidae spp., *Nausithoe punctata*, *Orchistoma pileus, Orchistoma* spp., *Pegantha triloba,* *Periphylla periphylla, Periphylla* spp.
Ctenophora	RMT25	Micronekton	*Boroe* spp., Ctenophora spp.,
Cephalopoda	RMT25	Micronekton	Teuthida spp., Decapodiformes spp., *Histioteuthis* spp., Octapoda spp.
Fish	RMT25	Micronekton	**Acropomatiformes** (e.g., lanternbellies) *Paradiplospinus gracilis*, Melamphaidae spp., **Anguilliformes** (e.g., eels) *Leptocephalus* spp., Nemichthyidae spp. **Argentiniformes** (e.g., smelts) *Bathylagus gracilis*, Bathylagidae spp. **Lophiiformes** (e.g., anglerfish) *Borostomias* spp., Angler fish, Melanostomiinae spp., Stomiidae spp., *Stomias* spp.

			Myctophiformes (e.g., lanternfishes) *Diaphus hudsoni, Diaphus* spp., *Electrona risso, Gymnoscopelus* spp., *Lampadena pontifex, Lampadena* sp., *Lampanyctus* spp., *Metelectrona* spp., Myctophidae spp., *Symbolophorus boops, Symbolophorus* spp. **Stomiiformes** (e.g., Sternoptychinae spp.) *Argyropelecus hemigymnus, Cyclothone* spp., *Howella sherboni*, Sternoptychidae spp. **UnID mesopelagic fish**

Table B 2 Area based diameter to dry weight (DW) and carbon (C) to DW conversion. Sources: (1) Lehette and Hernández-León (2009), (2) Giering *et al.* (2019b), (3) Hernández-León and Montero (2006), (4) Donnelly *et al.* (1994), (5) Huntley *et al.* (1989), (6) Ikeda and Mitchell (1982), (7) Koppelmann *et al.* (2013), (8) Clarke *et al.* (1992).

Mesozooplankton	**a**	**b**	**Source**	**C:DW**	**Source**
Calanidae	45.25	1.59	1	0.45	2
Chaetognath	23.45	1.19	1	0.29	4
Copepod carnivorous	45.25	1.59	1	0.45	2
Eucalanidae	45.25	1.59	1	0.45	2
Harpacticoida	45.25	1.59	1	0.45	2
Metridinidae	45.25	1.59	1	0.45	2
Mormonilloida	45.25	1.59	1	0.45	2
Oithona spp.	45.25	1.59	1	0.45	2
Oncaeidae	45.25	1.59	1	0.45	2
Ostracoda	44.78	1.56	1	0.45	2
Large Calanoida	45.25	1.59	1	0.45	2
Small Calanoida	45.25	1.59	1	0.45	2
UnID (general mesozooplankton)	43.38	1.54	1,3	0.45	2
Jellies	4.03	1.24	1	0.06	4,5,6
Amphipoda	44.78	1.56	1	0.45	2
Lubbockiidae	45.25	1.59	1	0.45	2
Polychaeta	4.03	1.24	1	0.37	8
Salpa	4.03	1.24	1	0.06	4,5,6
Copepod nauplii	45.25	1.59	1	0.45	2
Appendicularia	4.03	1.24	1	0.06	4,5,6
Euphausiidae	43.81	1.47	1	0.45	2
Euphausiidae calyptopes	43.81	1.47	1	0.45	2
Eggs (general mesozooplankton)	43.38	1.54	1,3	0.45	2
Euphausiidae nauplii	43.81	1.47	1	0.45	2
Copepod 1000-3000	45.25	1.59	1	0.45	2

Pteropoda (general mesozooplankton)	43.38	1.54	1	0.489	7
Copepod 500-1000	45.25	1.59	1	0.45	2
Copepod 100-500	45.25	1.59	1	0.45	2
Fish Larvae (general mesozooplankton)	43.38	1.54	1	0.45	2

Table B 3 Wet weight (WW) to dry weight (DW) conversions for micronekton based on the regression: log(DW) = a + b * log (WW). Coefficients were obtained from samples during this study and supplemented with published data where necessary. Carbon (C) to DW conversions. Sources: (1) This study, (2) Kiørboe (2013), (3) Giering *et al.* (2019b), (4) Donnelly *et al.* (1994), (5) Clarke *et al.* (1992), (6) Huntley *et al.* (1989), (7) Ikeda and Mitchell (1982), (8) Koppelmann *et al.* (2013), (9) (Reeve, 1980).

Taxa	**a**	**b**	**Source**	**C:DW**	**Source**
Amphipoda	-0.57	0.92	2	0.45	3
Chaetognatha	-0.8336	0.8747	1	0.29	4
Siphonophora	-1.33	0.99	2	0.0916	5
Cnidaria	-1.33	0.99	2	0.16	5
Salpa	-1.77	1.08	2	0.06	4, 6, 7
Pteropoda	-0.55	0.8	2	0.489	8
Gastropoda	-0.55	0.8	2	0.489	8
Ctenophora	-1.4	0.98	2	0.037	9
Copepoda	-0.67	0.96	2	0.45	3
Euphausiacea	-0.69	1.03	2	0.45	3
Oplophorus novaezeelandiae	-1.0338	1.1693	1	0.45	3
Gennadas spp.	-0.6158	1.0107	1	0.45	3
Euphausia hanseni	-0.553	0.9711	1	0.45	3
Acanthephyra pelagica	-0.5847	1.0043	1	0.45	3
Platyscelus spp.	-0.4914	0.9805	1	0.45	3
Hansarsia megalops	-0.6012	0.9557	1	0.45	3
Phronima spp.	-0.8549	0.966	1	0.45	3
Phrosina semilunata	-0.7079	0.9067	1	0.45	3

Table B 4 Wet weight (WW) to dry weight (DW) conversions for micronekton where DW=WW*c. C:DW ratio conversion. Sources: (1) Podeswa (2012), (2) Kiørboe (2013), (3) Giering *et al.* (2019b), (4) Clarke *et al.* (1992), (5) Childress and Nygaard (1974), (6) Penczak *et al.* (1984), (7) Sinclair *et al.* (2016), (8) Omori (1969), (9) Ricciardi and Bourget (1998), (10) Gogina *et al.* (2022).

Taxa	**c**	**Source**	**C:DW**	**Source**
Decapoda	0.179	1	0.45	3
Polychaeta	0.134	2	0.37	4
Ostracoda	0.05	5	0.45	3
Fish	0.2	6,7	0.4	8
Cephalopoda	0.2	9	0.45	3
Mysidacea	0.2	10	0.45	3
Nemertea	0.174	10	0.37	4
Other crustacea	0.183	2	0.45	3

Table B 5 Taxa specific coefficients for the allometric regressions relating WW (mg) to ETS-derived respiration (µL O_2 Ind^{-1} h^{-1}).

ln(respiration)=a0 + a1 *ln(WW)	**a0**	**a1**
Fish	-0.86936	0.72833
Phrosina semilunata	0.29	0.6262
Oplophorus novaezeelandiae	1.0941	0.5827
Chaetognatha	-3.9455	1.0871
Hansarsia megalops	-3.6171	1.5737
Euphausia hanseni	-2.273	1.1466
Euphausia gibboides	-2.273	1.1466

Table B 6 Taxa specific coefficients for the allometric regressions relating WW (mg) to ETS-derived respiration (µL O_2 Ind^{-1} h^{-1}), where T is temperature in Kelvin and z depth sampled in m.

ln(respiration)=a0 + a1 *ln(DW) + a2 * 1000/T + a3 * ln(z)				
	a0	**a1**	**a2**	**a3**
Other Euphausiidae	14.136	0.7546	-3.7539	-0.1102
Cephalopoda	28.326	0.779	7.903	-0.365
Polychaeta	5.7501	0.7713	-1.325	-0.2533
Pteropoda (Gastropoda)	12.62735	0.895441	-3.65232	-0.00805
Gastropoda (Mollusca)	12.62735	0.895441	-3.65232	-0.00805
Decapoda	28.86871	0.8722	-8.08446	-0.12409
Amphipoda	11.461	0.74635	-3.02074	-0.16809
Cnidaria	25.22874	0.877153	-7.44524	-0.00609
Ctenophora	2.54824	0.68545	-0.88331	-0.02113
Salpa (Thaliacea)	16.394	0.7213	-4.8272	0.4181
Siphonophora (Cnidaria)	25.22874	0.877153	-7.44524	-0.00609
Ostracoda	5.11907	0.70981	-1.61853	-0.10225
Mysidacea	23.80412	0.76976	-6.5796	-0.11221
Fish	19.491	0.885	-5.77	-0.261

Table B 7 Taxa specific daily ingestion rates from grazing experiments during this study and published estimates from literature. Sources: (1) This study, (2) Ikeda and Shiga (1999), (3) Saito and Kiørboe (2001), (4) Purcell and Kremer (1983), (5) D'Ambra *et al.* (2013), (6) Ishii and Tanaka (2001), (7) Hereu *et al.* (2010), (8) Hunt *et al.* (2008), (9) Reeve and Walter (1979), (10) Gurney *et al.* (2002), (11) Maynou and Cartes (1998), (12) Bode-Dalby *et al.* (2022), (13) Pakhomov *et al.* (1996), (14) Bruno *et al.* (2021), (15) Kremer *et al.* (2025), (16) Wells *et al.* (1997), (17) (Schukat *et al.*, 2013b).

Net	**Taxa**	**Daily carbon specific ingestion rates (d^{-1})**	**Source**
RMT25	Amphipoda	0.065	2
	Chaetognatha	0.144	3
	Siphonophora	0.02	4
	Cnidaria	0.0623	5,6
	Salpa	0.7	7
	Pteropoda	0.223	8
	Gastropoda	0.223	8
	Ctenophora	0.67	9
	Copepoda	0.0912	1
	Euphausiidae	0.106	10
	Oplophorus novaezeelandiae	0.039	11
	Gennadas spp.	0.039	11
	Euphausia hanseni	0.106	10
	Acanthephyra pelagica	0.106	10
	Platyscelus spp.	0.065	2
	Hansarsia megalops	0.106	10
	Phronima spp.	0.065	2

RMT25	*Phrosina semilunata*	0.065	2
	Decapoda	0.039	11
	Polychaeta	0.393	Average from other mesozooplankton
	Ostracoda	0.393	Average from other mesozooplankton
	Fish	0.03	13
	Cephalopoda	0.0394	14, 15, 16
	Mysidacea	0.106	10
	Nemertea	0.393	Average from other mesozooplankton
	Other crustacea	0.098	1
Mammoth	Calanidae	0.429	1
	Chaetognatha	0.144	3
	Copepoda carnivorous	0.1045	12
	Eucalanidae	0.078	17
	Harpacticoida	0.698	1
	Metridinidae	0.469	1
	Mormonilloida	0.698	1
	Oithona spp.	0.698	1
	Oncaeidae	0.698	1
	Ostracoda	0.393	Average from other mesozooplankton
	Large Calanoida	0.127	1
	Small Calanoida	0.536	1
	UnID	0.393	Average from other mesozooplankton
	Jellies	0.393	Average from other mesozooplankton
	Amphipoda	0.065	2
	Lubbockiidae	0.698	1
	Polychaeta	0.393	Average from other mesozooplankton
	Salpa	0.7097	7
	Copepod nauplii	0.393	Average from other mesozooplankton

Mammoth	Appendicularia	0.393	Average from other mesozooplankton
	Copepod 1000-3000	0.536	1
	Pteropoda	0.393	Average from other mesozooplankton
	Copepod 500-1000	0.536	1
	Copepod 100-500	0.536	1
	Fish Larvae	0.393	Average from other mesozooplankton

Table B 8 Lipid composition (mol%, mean) of <53 µm and >53 µm POM throughout epi- and mesopelagic waters at station BN in the northern Benguela Upwelling System. Saturated fatty acids (SFAs), branched fatty acids (Br. FAs), monounsaturated fatty acids (MUFAs), polyunsaturated fatty acids (PUFAs), Sterols, Other, fatty alcohols (ALC).

Station	Particle size	Depth (m)		SFAs	Br. FAs	MUFAs	PUFAs	Sterols	Other	ALC
BN1	<53 µm	30	mean	58.5	1.3	12.7	22.5	2.1	0	2.8
			sd	-	-	-	-	-	-	-
BN1	<53 µm	80	mean	49.5	2.6	14.9	18	11.5	0	3.6
			sd	-	-	-	-	-	-	-
BN1	<53 µm	120	mean	44.4	0.5	30.9	6.7	15.1	0	2.3
			sd	-	-	-	-	-	-	-
BN1	<53 µm	250	mean	30.3	0.2	33.3	20.7	12.6	0	3
			sd	-	-	-	-	-	-	-
BN1	<53 µm	400	mean	85	0	15	0	0	0	0
			sd	-	-	-	-	-	-	-
BN1	>53 µm	30	mean	36.02	0.76	26.08	13.33	4.43	1.17	18.21
			sd	-	-	-	-	-	-	-
BN1	>53 µm	80	mean	33.64	0.14	33.66	5.51	13.7	0.41	12.94
			sd	-	-	-	-	-	-	-
BN1	>53 µm	120	mean	44.41	0.18	39.65	3.43	5.76	0	6.57
			sd	-	-	-	-	-	-	-
BN1	>53 µm	250	mean	39.67	0.55	36.59	2.65	4.77	0	15.77
			sd	-	-	-	-	-	-	-
BN1	>53 µm	400	mean	25.81	0.43	30.77	21.89	2.97	0	18.13
			sd	-	-	-	-	-	-	-
BN2	<53 µm	20	mean	32.49	0.46	16.78	47.08	1.62	0.79	0.77
			sd	-	-	-	-	-	-	-
BN2	<53 µm	35	mean	25.38	2.13	25.7	21.49	10.29	8.15	7.38

Station	Particle size	Depth (m)		SFAs	Br. FAs	MUFAs	PUFAs	Sterols	Other	ALC
BN2	<53 µm	35	sd	-	-	-	-	-	-	-
BN2	<53 µm	75	mean	53.68	5.38	10.59	4.73	12.42	2.55	10.66
			sd	-	-	-	-	-	-	-
BN2	<53 µm	100	mean	36.69	3.01	5.36	14.3	23.38	0.65	16.88
			sd	6.75	3.12	2.11	3.87	3.94	0.59	0.15
BN2	<53 µm	250	mean	45.22	2.52	10.67	3.7	5.04	0.3	32.78
			sd	20.71	3.34	2.64	2.04	1.95	0.43	10.66
BN2	<53 µm	500	mean	50.25	3.33	7.84	4.87	5.42	0	28.93
			sd	23.52	3.85	0.87	3.79	1.92	0.00	25.48
BN2	>53 µm	20	mean	15.04	0.46	16.48	61.56	4.74	0.72	1
			sd	-	-	-	-	-	-	-
BN2	>53 µm	35	mean	20.02	1.27	14.77	40.14	17.31	4.46	2.03
			sd	-	-	-	-	-	-	-
BN2	>53 µm	75	mean	20.99	0	9.81	12.79	43.19	0	13.22
			sd	-	-	-	-	-	-	-
BN2	>53 µm	100	mean	25	0.46	13.61	11.14	36.44	0	13.35
			sd	2.47	0.66	2.95	7.85	3.93	0.00	2.16
BN2	>53 µm	250	mean	23.84	0	16.15	18.21	24.42	0	17.37
			sd	2.79	0.00	1.85	4.98	0.81	0.00	10.43
BN2	>53 µm	500	mean	22.28	0.27	31.63	13.77	10.15	0	21.89
			sd	7.16	0.38	11.69	9.16	10.18	0.00	14.43
BN3	<53 µm	35	mean	38.85	0.69	10.33	42.7	4.59	1.78	1.06
			sd	7.44	0.61	1.98	8.49	0.60	0.51	1.32
BN3	<53 µm	75	mean	31.58	2.19	12.03	35.17	8.14	0.5	10.67
			sd	4.32	2.31	1.12	6.72	4.47	0.08	1.06
BN3	<53 µm	100	mean	48.67	3.38	11.16	15.38	8.74	0.58	12.47
			sd	7.36	0.89	1.72	13.71	3.06	0.27	2.22

Station	Particle size	Depth (m)		SFAs	Br. FAs	MUFAs	PUFAs	Sterols	Other	ALC
BN3	<53 µm	250	mean	58.31	3.17	6.86	6.2	10.75	0.52	14.47
			sd	11.34	0.33	4.24	5.98	2.25	0.04	3.32
BN3	<53 µm	500	mean	59.18	2.06	3.13	18.52	3.69	0	14.07
			sd	8.37	0.27	0.83	4.33	0.10	0.00	3.40
BN3	>53 µm	35	mean	29.24	1.45	10.38	42.16	9.09	6.08	1.6
			sd	14.67	0.08	4.15	23.19	4.55	7.96	0.88
BN3	>53 µm	75	mean	25.69	0.97	16.1	27.74	19.41	0.03	10.06
			sd	4.95	0.02	1.45	8.12	2.30	0.04	2.38
BN3	>53 µm	100	mean	30.64	0.63	18.19	22.49	15.65	0	12.4
			sd	0.06	0.40	4.90	9.16	4.18	0.00	9.42
BN3	>53 µm	250	mean	17.77	0.33	12.39	20.49	8.29	29.03	11.7
			sd	4.62	0.47	7.45	17.76	0.98	41.05	9.77
BN3	>53 µm	500	mean	23.07	0.27	28.96	42.57	2.19	0	2.94
			sd	6.14	0.38	17.71	27.22	1.87	0.00	1.88

Table B 9 Fatty alcohol (ALC) composition (mol%) (mean (x̄) and standard deviation (sd)) of <53 µm and >53 µm POM throughout epi- and mesopelagic waters at station BN in the northern Benguela Upwelling System.

Particle size	Depth (m)		ALC-12:0	ALC-13:0	ALC-14:0	ALC-15:0	ALC-16:0	ALC-17:0	ALC-18:0	ALC-19:0	ALC-20:0	ALC-22:0	ALC-24:0	ALC-18:1	ALC-20:1	ALC-22:1	ALC-24:1
<53 µm	20	x̄	15.4	0	0	14.8	24	0	45.9	0	0	0	0	0	0	0	0
		sd	-	-	-	-	-	-	-	-	-	-	-	-	-	-	-
<53 µm	30	x̄	0	0	0	0	0	0	100	0	0	0	0	0	0	0	0
		sd	-	-	-	-	-	-	-	-	-	-	-	-	-	-	-
<53 µm	35	x̄	1.2	0	28.8	10.1	10.2	0	45.4	4.2	0	0	0	0	0	0	0
		sd	2.1	0.0	25.9	9.7	17.6	0.0	47.3	7.4	0.0	0.0	0.0	0.0	0.0	0.0	0.0
<53 µm	75	x̄	0.4	0.7	6.5	2.3	20.6	0	61.2	0	3.2	4.6	0.5	0	0	0	0
		sd	0.6	0.6	7.0	2.0	4.0	0.0	15.1	0.0	3.2	4.5	0.5	0.0	0.0	0.0	0.0
<53 µm	80	x̄	0	0	16.2	0	45.4	0	36.1	0	0	0	0	2.3	0	0	0
		sd	-	-	-	-	-	-	-	-	-	-	-	-	-	-	-
<53 µm	100	x̄	3.5	0	7.6	2.1	22	11.5	48.4	1.4	2.1	1.5	0	0	0	0	0

Particle size	Depth (m)		ALC-12:0	ALC-13:0	ALC-14:0	ALC-15:0	ALC-16:0	ALC-17:0	ALC-18:0	ALC-19:0	ALC-20:0	ALC-22:0	ALC-24:0	ALC-18:1	ALC-20:1	ALC-22:1	ALC-24:1
<53 µm	100	sd	4.2	0.0	10.4	2.5	23.2	13.3	10.4	2.8	2.5	2.0	0.0	0.0	0.0	0.0	0.0
<53 µm	120	x̄	0	0	0	0	0	0	100	0	0	0	0	0	0	0	0
		sd	-	-	-	-	-	-	-	-	-	-	-	-	-	-	-
<53 µm	250	x̄	1.2	0	23.5	3.4	29.1	2.4	35.4	1.3	2.9	0.7	0	0	0	0	0
		sd	2.6	0.0	23.3	3.9	24.0	3.4	22.9	2.2	3.1	1.0	0.0	0.0	0.0	0.0	0.0
<53 µm	400	x̄	0	0	0	0	0	0	0	0	0	0	0	0	0	0	0
		sd	-	-	-	-	-	-	-	-	-	-	-	-	-	-	-
<53 µm	500	x̄	1.6	0	0	1.1	9.9	14.3	61.4	6	3.3	2.2	0.2	0	0	0	0
		sd	3.2	0.0	0.0	2.2	11.6	16.7	38.1	6.4	2.2	3.7	0.4	0.0	0.0	0.0	0.0
>53 µm	20	x̄	0	0	16.2	24.7	39.6	5.3	14.1	0	0	0	0	0	0	0	0
		sd	-	-	-	-	-	-	-	-	-	-	-	-	-	-	-
>53 µm	30	x̄	0	0	8.4	1.8	10.2	2.5	76	0	1.2	0	0	0	0	0	0

Particle size	Depth (m)		ALC-12:0	ALC-13:0	ALC-14:0	ALC-15:0	ALC-16:0	ALC-17:0	ALC-18:0	ALC-19:0	ALC-20:0	ALC-22:0	ALC-24:0	ALC-18:1	ALC-20:1	ALC-22:1	ALC-24:1
>53 µm	30	sd	-	-	-	-	-	-	-	-	-	-	-	-	-	-	-
>53 µm	35	x̄	0	0	41.4	0	38.7	4.8	12.3	0	2.3	0	0.5	0	0	0	0
		sd	0.0	0.0	19.2	0.0	8.2	8.4	11.3	0.0	3.9	0.0	0.9	0.0	0.0	0.0	0.0
>53 µm	75	x̄	0	0	20.1	1.3	36.2	0	41	0	0.3	0	0.8	0	0	0	0.3
		sd	0.0	0.0	9.7	1.2	21.5	0.0	25.8	0.0	0.5	0.0	1.3	0.0	0.0	0.0	0.6
>53 µm	80	x̄	0	0	20.9	1.7	41.6	3.6	17.9	0	0	1.2	0	12.4	0	0	0.7
		sd	-	-	-	-	-	-	-	-	-	-	-	-	-	-	-
>53 µm	100	x̄	0	0	12.7	2.6	35.6	16.5	29.5	0	2.2	0	0.9	0	0	0	0
		sd	0.0	0.0	4.3	2.0	19.6	25.6	15.3	0.0	2.0	0.0	1.8	0.0	0.0	0.0	0.0
>53 µm	120	x̄	0	0	32.7	3.1	46.2	4.5	13.5	0	0	0	0	0	0	0	0
		sd	-	-	-	-	-	-	-	-	-	-	-	-	-	-	-
>53 µm	250	x̄	0	0	16.6	2.3	49.3	16.2	11.9	1.5	0.6	0.1	0	1.2	0	0.2	0.1

Particle size	Depth (m)		ALC-12:0	ALC-13:0	ALC-14:0	ALC-15:0	ALC-16:0	ALC-17:0	ALC-18:0	ALC-19:0	ALC-20:0	ALC-22:0	ALC-24:0	ALC-18:1	ALC-20:1	ALC-22:1	ALC-24:1
>53 µm	250	sd	0.0	0.0	5.2	1.4	8.8	11.6	2.8	3.4	0.3	0.2	0.0	2.6	0.0	0.4	0.2
>53 µm	400	$\bar{x}$	0	0	60	1.4	15.9	5.1	3	0	0.6	0	0	0	3.5	10.4	0
		sd	-	-	-	-	-	-	-	-	-	-	-	-	-	-	-
>53 µm	500	$\bar{x}$	0	0	17	3	58.5	0.3	17.1	0	0.6	0.1	0	0	0	2.4	1
		sd	0.0	0.0	6.2	2.8	13.2	0.6	8.8	0.0	1.0	0.1	0.0	0.0	0.0	4.9	2.1

Table B 10 Fatty acid composition (mol%) (mean (x̄) and standard deviation (sd)) of <53 µm and >53 µm POM throughout epi- and mesopelagic waters at station BN in the northern Benguela Upwelling System.

Particle size	**Depth (m)**		**14:0**	**16:0**	**18:0**	**16:1(n-7)**	**18:1(n-9)**	**18:1(tr-9)**	**20:5(n-3)**	**16:1**	**18:4**	**18:3**	**22:1**	**22:6(n-3)**
<53 µm	20	x̄	13.3	17.9	1.8	0.8	6.0	1.6	6.4	8.9	14.1	8.5	0.0	16.4
		sd	-	-	-	-	-	-	-	-	-	-	-	-
<53 µm	35	x̄	7.6	12.3	8.5	10.9	3.8	2.0	7.9	1.2	11.2	7.0	0.0	10.5
		sd	5.1	2.0	10.0	7.3	3.0	1.9	0.8	0.7	2.2	1.7	0.0	9.9
<53 µm	75	x̄	5.5	30.3	13.1	3.7	5.5	3.3	7.4	0.6	4.4	4.0	0.1	12.6
		sd	3.7	9.5	9.1	1.9	1.9	1.9	3.8	0.5	4.5	1.6	0.1	11.4
<53 µm	100	x̄	5.6	36.6	17.5	2.3	4.8	1.8	3.3	1.5	0.9	4.1	0.7	8.0
		sd	1.6	4.5	4.5	2.6	3.8	0.5	2.8	1.3	1.1	5.1	0.8	7.9
<53 µm	250	x̄	4.5	37.9	30.6	2.5	3.9	0.8	2.0	2.1	0.0	0.5	0.5	2.1
		sd	3.1	10.2	18.5	1.0	5.1	9.8	3.2	2.0	0.4	0.4	0.8	5.6
<53 µm	500	x̄	3.0	40.4	24.6	0.9	3.9	0.9	1.3	1.9	4.1	4.5	0.4	2.9

Particle size	Depth (m)		14:0	16:0	18:0	16:1(n-7)	18:1(n-9)	18:1(tr-9)	20:5(n-3)	16:1	18:4	18:3	22:1	22:6(n-3)
<53 µm	500	sd	1.9	1.8	3.5	1.1	4.8	0.6	0.9	2.7	6.5	7.9	0.5	2.5
>53 µm	20	x̄	6.1	8.2	1.3	12.7	2.6	1.1	12.1	0.8	9.1	2.3	0.2	12.3
		sd	-	-	-	-	-	-	-	-	-	-	-	-
>53 µm	35	x̄	5.9	15.1	9.2	8.9	2.7	1.9	10.5	0.3	4.7	1.0	0.2	13.8
		sd	2.9	4.6	7.1	4.7	1.3	0.7	3.6	0.3	0.5	0.2	0.1	10.9
>53 µm	75	x̄	1.8	25.6	9.3	5.8	8.8	3.6	2.9	0.0	1.8	0.0	2.2	4.4
		sd	1.4	5.9	2.8	1.2	1.9	1.3	1.3	0.0	2.0	0.0	1.1	2.8
>53 µm	100	x̄	2.1	31.2	10.9	5.7	11.1	3.6	2.5	0.0	2.1	0.9	3.5	3.0
		sd	1.0	7.4	1.3	1.0	4.4	1.3	1.8	0.0	4.3	1.8	2.4	2.3
>53 µm	250	x̄	2.2	24.5	10.8	6.7	11.9	3.8	4.1	0.0	0.6	0.0	1.6	6.9
		sd	1.9	8.0	5.1	2.3	3.3	10.5	1.3	0.0	1.1	0.3	0.9	2.9
>53 µm	500	x̄	1.9	18.4	6.6	14.0	17.9	3.5	4.4	0.2	1.4	0.4	1.2	3.3
		sd	1.9	7.0	3.4	12.1	17.7	1.4	4.9	0.3	1.9	0.7	1.3	1.8

Table B 11 Mean and standard deviation (SD) lipid content to carbon weight (µg gC^{-1}), lipid to dry weight (DW, mg gDW^{-1}), percent carbon of DW and percent lipid of DW of mesozooplankton and micronekton at station BN in the northern Benguela Upwelling System (nBUS).

Species	**Lipid (µg gC^{-1})**	**SD**	**Lipid (mg gDW^{-1})**	**SD**	**%C of DW**	**SD**	**% Lipids of DW**	**SD**
Calanoides natalis	349.6	118.9	216	55.3	63.2	6.7	21.6	5.5
Rhincalanus nasutus	382.9	97.1	233.4	77.4	60.6	7.8	23.3	7.7
Nannocalanus spp.	35	28.3	19.6	14.3	58.6	6.7	2	1.4
Eucalanus spp.	52.9	42.8	23.8	20.2	45.6	12.1	2.4	2
Euchaeta spp.	153.4	205.1	76.2	101.4	51.9	3.3	7.6	10.1
Euphausia hanseni	54.1	13.8	19.7	5.7	36.3	3.1	2	0.6
Phrosina semilunata	101.5	58.2	25.2	13.7	25.1	1.2	2.5	1.4
Oplophorus novaezeelandiae	327.1	123	119.5	40.6	37.4	5.2	12	4.1
Atolla spp.	1953.3	2880.5	135.2	159.5	13.7	8	13.5	15.9
Hansarsia megalops	66.8	20.7	25.2	8.2	37.6	1.3	2.5	0.8
Gennadas spp.	621.8	526.6	242.4	198.8	39.7	1.5	24.2	19.9
Nemichthyidae spp.	430.3	463.9	210.2	222.9	50.7	5.2	21	22.3
Platyscelus spp.	163.3	29.3	41.6	6	25.7	3.1	4.2	0.6
Phronima spp.	69.9	16.9	20.7	5.7	29.5	3.5	2.1	0.6
Systellaspis cristata	445	NA	172.9	NA	38.9	NA	17.3	NA

Species	**Lipid (µg gC^{-1})**	**SD**	**Lipid (mg gDW^{-1})**	**SD**	**%C of DW**	**SD**	**% Lipids of DW**	**SD**
Acanthephyra pelagica	92.8	46.5	40.5	20.2	44	5.4	4.1	2
Gymnoscopelus spp.	357.6	189	174.4	96.7	48	2.5	17.4	9.7
Sternoptychinae spp.	488.6	565.2	170.1	189.2	35.4	4.8	17	18.9
Chaetognatha spp.	171.7	NA	15.5	NA	9	NA	1.5	NA
Bathylagidae spp.	205.9	186.4	87.2	82.1	40.5	3.1	8.7	8.2
Cyclothone spp.	602.5	270.4	237	123.3	39.4	9.8	23.7	12.3

Table B 12 Carbon specific daily respiration rates (% d^{-1}) of mesozooplankton derived from ETS-assays for whole-community samples from the Mammoth-300 and Mammoth-100 from station BN in the northern Benguela Upwelling System (nBUS).

Depth (m)	**Mammoth-300 (% d^{-1})**						**Mammoth-100 (% d^{-1})**					
	BN1		BN2		BN3		BN1		BN2		BN3	
	Day	Night	Day	Night	Day	Night	Day	Night	Day	Night	Day	Night
5-33	2.42	1.18	1.47	1.57	1.20	2.18	4.02	5.62	1.18	1.76	-	4.92
33-63	3.42	2.72	5.27	0.90	0.47	5.01						
63-125	6.47	3.85	0.98	1.22	1.75	4.24						
125-188	0.93	1.52	0.31	0.81	0.53	2.38	0.57	0.90	0.93	0.43	0.96	4.44
188-250	0.72	0.90	0.26	0.26	0.50	1.19						
250-375	1.13	1.53	1.27	1.03	0.42	0.22	1.22	1.17	0.68	0.57	1.91	1.43
375-500	0.92	1.37	1.07	0.71	0.88	1.55						
500-625	0.32	0.52	0.98	0.26	0.84	0.51	0.57	0.35	0.47	0.42	0.62	0.43
625-750	0.31	0.54	0.77	0.28	0.55	0.43						

B.2 Supplementary figures for Chapter 3

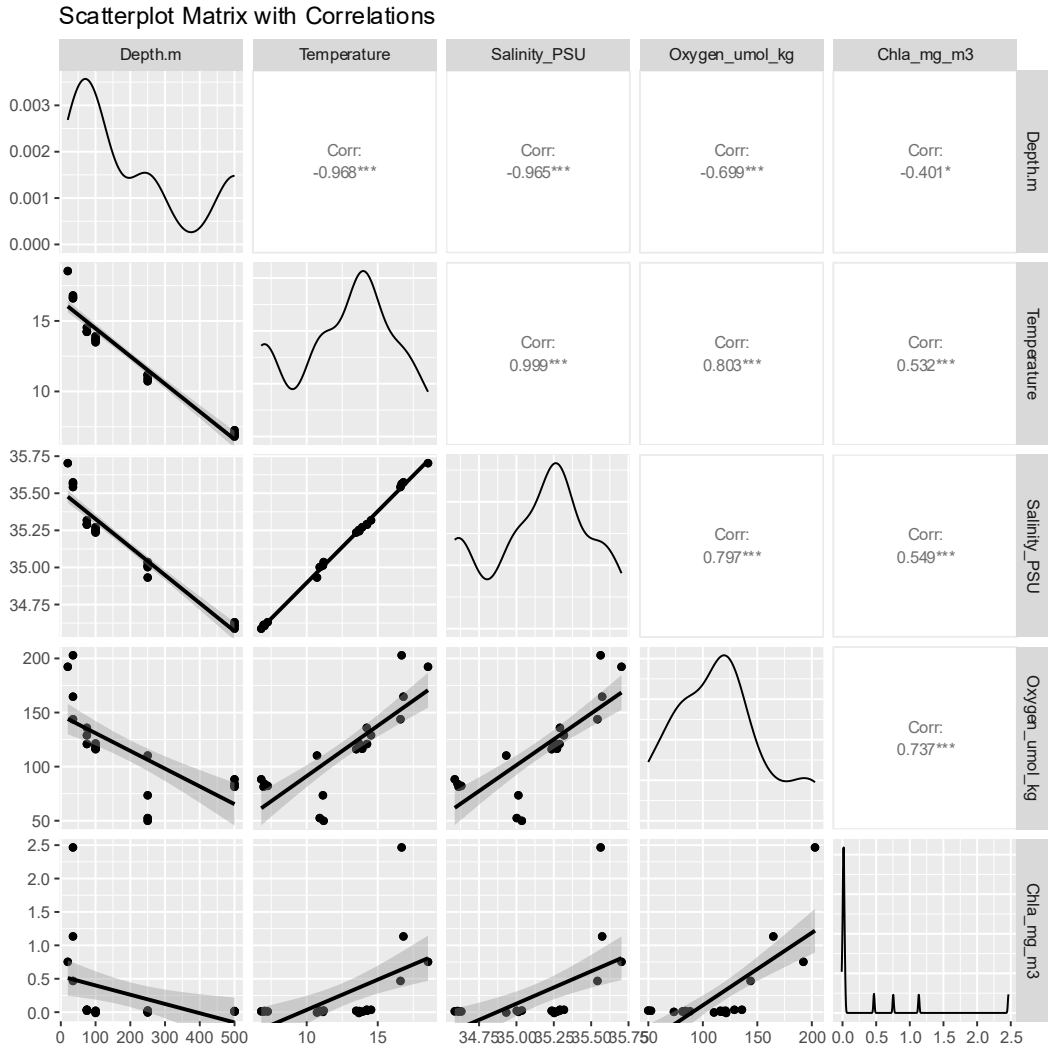

Figure B 1 Correlation matrix exploring collinearity between the different environmental variables sampled at the NB station in the northern Benguela Upwelling System.

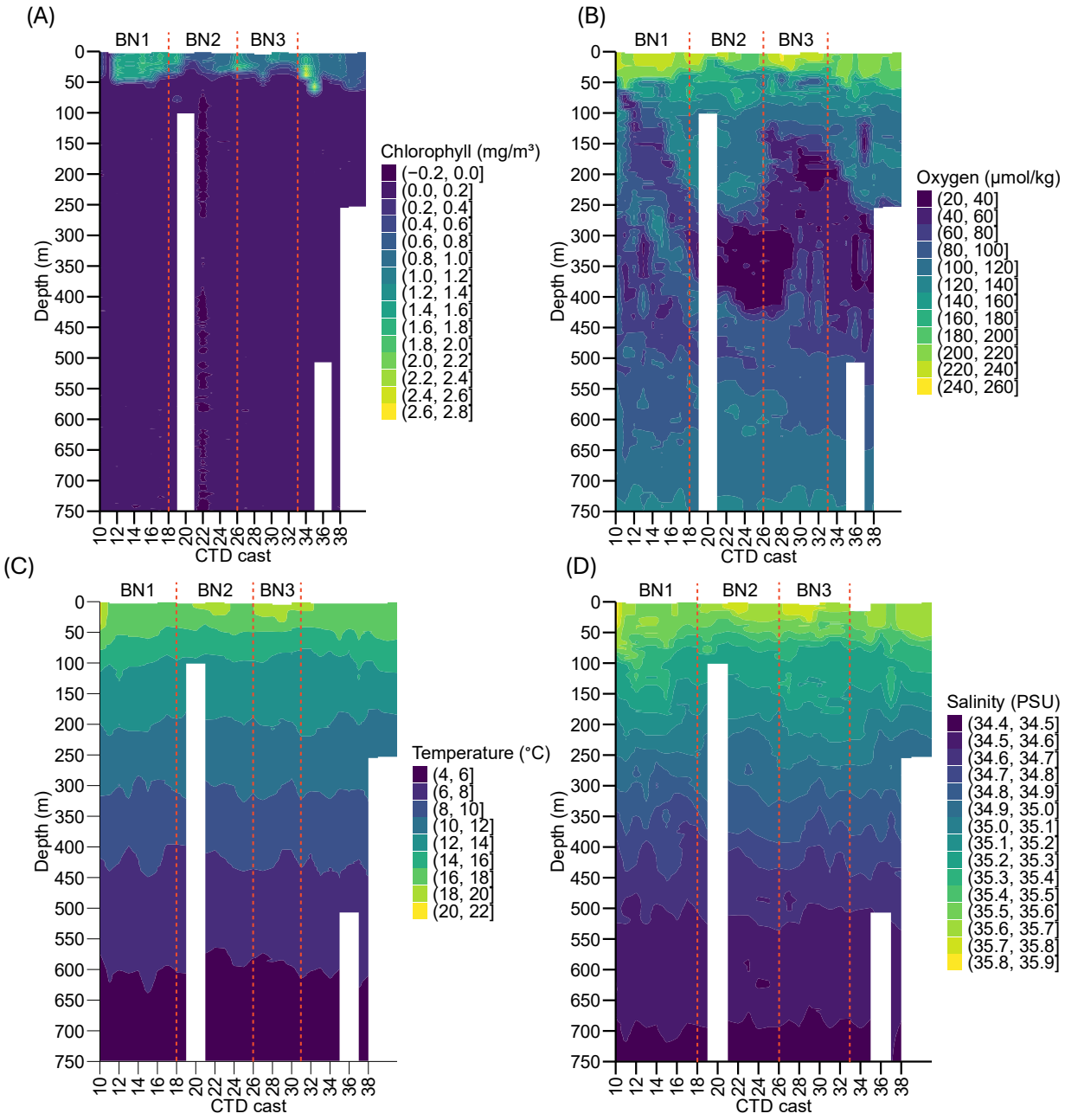

Figure B 2 (A) Chlorophyll (mg m^{-3}), (B) oxygen (µmol kg^{-1}), (C) temperature (°C) and (D) salinity (PSU), contour depth profile in the top 750 m of the water column at station BN in the northern Benguela Upwelling System. Red lines delimitate the station visits BN1, BN2 and BN3.

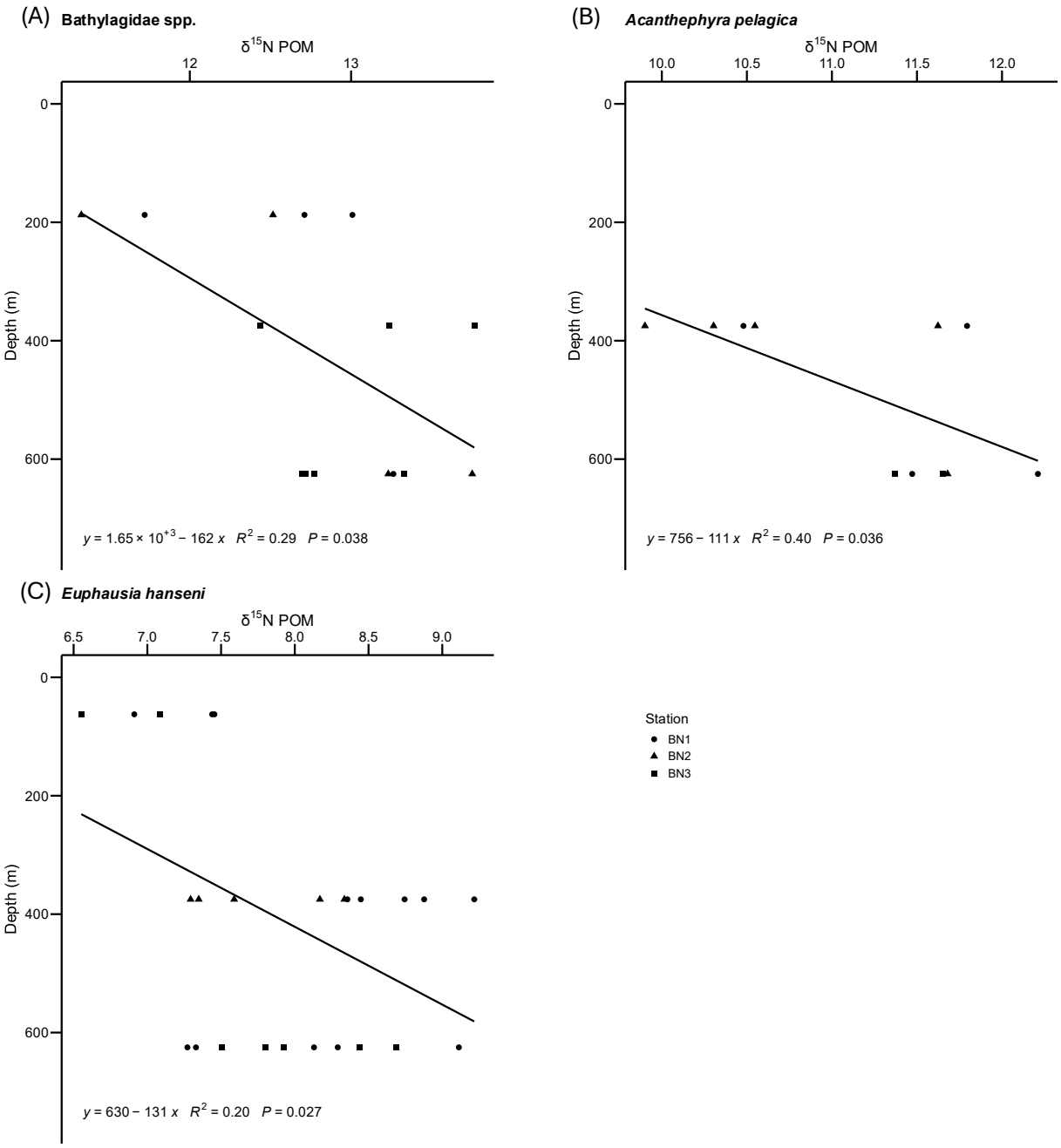

Figure B 3 Relationship between $\delta^{15}N$ of (A) Bathylagidae spp., (B) *Acanthephyra pelagica,* and (C) *Euphausia hanseni,* and depth at stations BN1-BN3 in the northern Benguela Upwelling system.

Appendix C Chapter 4

C.1 Supplementary figures for Chapter 4

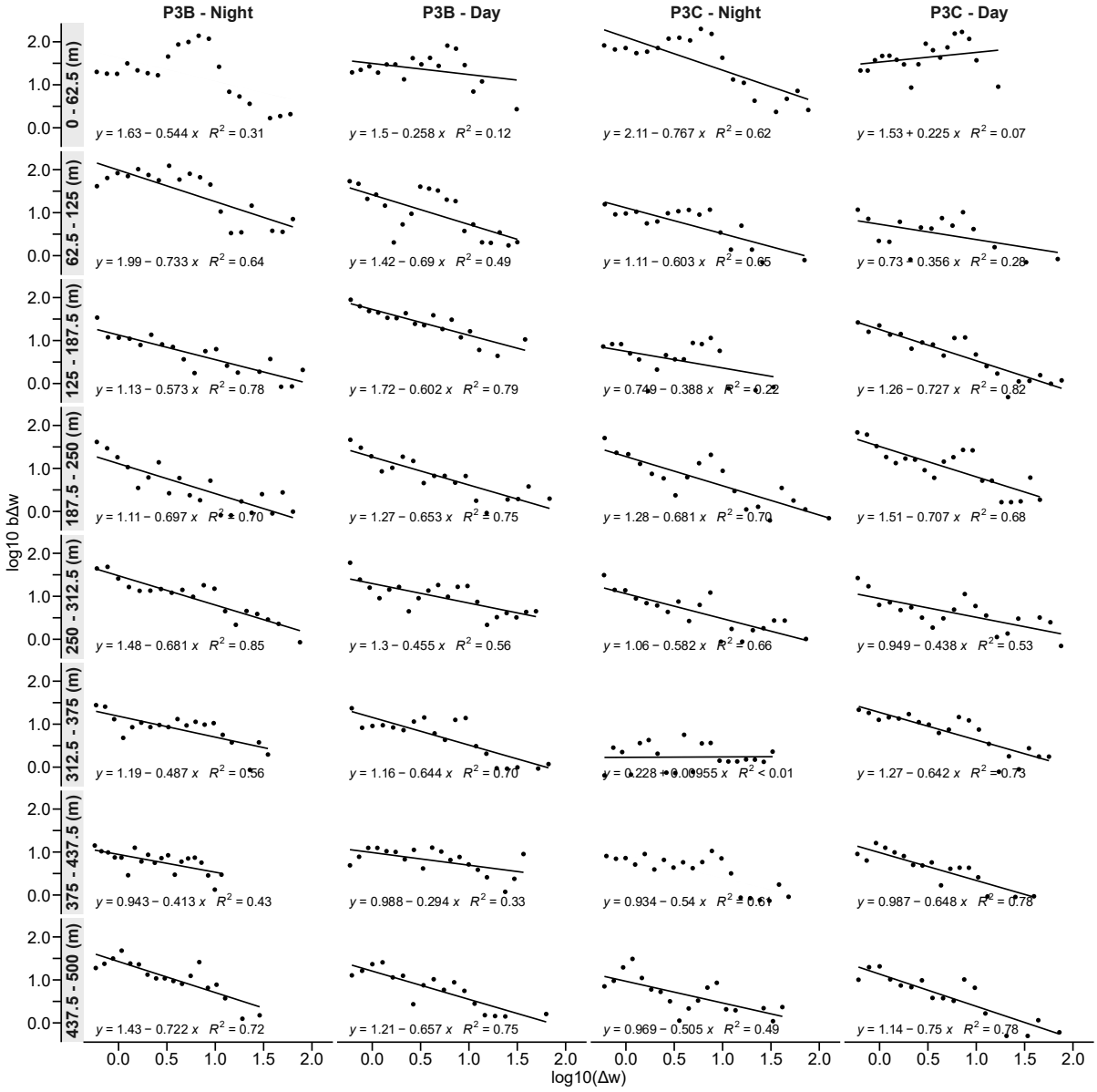

Figure C 1 Vertically resolved normalised biovolume size spectra (NBSS) plots for the zooplankton communities at station P3 in the Scotia Sea when only keeping particles with areaABD > 0.785 mm^2 = spherical circle with diameter = 1mm.

Bibliography

Ainsworth, J. *et al.* (2023) 'Iron cycling during the decline of a South Georgia diatom bloom', *Deep Sea Research Part II: Topical Studies in Oceanography*, 208, p. 105269. doi: https://doi.org/10.1016/j.dsr2.2023.105269.

Albers, C., Kattner, G. and Hagen, W. (1996) 'The compositions of wax esters, triacylglycerols and phospholipids in Arctic and Antarctic copepods: evidence of energetic adaptations', *Marine Chemistry*, 55(3-4), pp. 347-358. doi: https://doi.org/10.1016/S0304-4203(96)00059-X.

Albini, D. *et al.* (2025) 'Warming alters plankton body-size distributions in a large field experiment', *Communications Biology*, 8(1), p. 162. doi: 10.1038/s42003-024-07380-2.

Alldredge, A. (1998) 'The carbon, nitrogen and mass content of marine snow as a function of aggregate size', *Deep Sea Research Part I: Oceanographic Research Papers*, 45(4), pp. 529-541. doi: https://doi.org/10.1016/S0967-0637(97)00048-4.

Amano, C. *et al.* (2023) 'A device for assessing microbial activity under ambient hydrostatic pressure: The in situ microbial incubator (ISMI)', *Limnology and Oceanography: Methods*, 21(2), pp. 69-81. doi: https://doi.org/10.1002/lom3.10528.

Andersen, K.H. *et al.* (2016) 'Characteristic sizes of life in the oceans, from bacteria to whales', *Annual review of marine science*, 8(1), pp. 217-241. doi: https://doi.org/10.1146/annurev-marine-122414-034144.

Andersen, K.H. and Pedersen, M. (2009) 'Damped trophic cascades driven by fishing in model marine ecosystems', *Proceedings of the Royal Society B: Biological Sciences*, 277(1682), pp. 795-802. doi: https://doi.org/10.1098/rspb.2009.1512.

Anderson, T.R. (1994) 'Relating C:N ratios in Zooplankton food and faecal pellets using a biochemical model', *Journal of Experimental Marine Biology and Ecology*, 184(2), pp. 183-199. doi: https://doi.org/10.1016/0022-0981(94)90004-3.

Anderson, T.R. *et al.* (2022) 'Quantifying the roles of food intake and stored lipid for growth and development throughout the life cycle of a high-latitude copepod, and consequences for ocean carbon sequestration', *Frontiers in Marine Science*, 9, p. 928209. doi: https://doi.org/10.3389/fmars.2022.928209.

Anderson, T.R. *et al.* (2019) 'Quantifying carbon fluxes from primary production to mesopelagic fish using a simple food web model', *ICES Journal of Marine Science*, 76(3), pp. 690-701. doi: https://doi.org/10.1093/icesjms/fsx234.

Antezana, T. (2009) 'Species-specific patterns of diel migration into the Oxygen Minimum Zone by euphausiids in the Humboldt Current Ecosystem', *Progress in Oceanography*, 83(1), pp. 228-236. doi: https://doi.org/10.1016/j.pocean.2009.07.039.

Arashkevich, E.G., Drits, A.V. and Timonin, A.G. (1996) 'Diapause in the life cycle of *Calanoides carinatus* (Kroyer), (Copepoda, Calanoida)', *Hydrobiologia*, 320(1), pp. 197-208. doi: https://doi.org/10.1007/BF00016821.

Archibald, K.M., Siegel, D.A. and Doney, S.C. (2019) 'Modeling the impact of zooplankton diel vertical migration on the carbon export flux of the biological pump', *Global Biogeochemical Cycles*, 33(2), pp. 181-199. doi: https://doi.org/10.1029/2018GB005983.

Ariffian, N.N.A. *et al.* (2025) 'Feeding ecology of dominant copepods (Calanoida: Calanidae, Rhincalanidae) in the Southern Ocean inferred from mouthpart morphology and isotopic signatures', *Journal of Crustacean Biology*, 45(2). doi: https://doi.org/10.1093/jcbiol/ruaf028.

Ariza, A. *et al.* (2015) 'Migrant biomass and respiratory carbon flux by zooplankton and micronekton in the subtropical northeast Atlantic Ocean (Canary Islands)', *Progress in Oceanography*, 134, pp. 330-342. doi: https://doi.org/10.1016/j.pocean.2015.03.003.

Arts, M.T., Ackman, R.G. and Holub, B.J. (2001) '"Essential fatty acids" in aquatic ecosystems: a crucial link between diet and human health and evolution', *Canadian Journal of Fisheries and Aquatic Sciences*, 58(1), pp. 122-137. doi: https://doi.org/10.1139/f00-224.

Atkinson, A. (1991) 'Life cycles of *Calanoides acutus, Calanus simillimus* and *Rhincalanus gigas* (Copepoda: Calanoida) within the Scotia Sea', *Marine Biology*, 109(1), pp. 79-91. doi: https://doi.org/10.1007/BF01320234.

Atkinson, A. *et al.* (2021) 'Increasing nutrient stress reduces the efficiency of energy transfer through planktonic size spectra', *Limnology and Oceanography*, 66(2), pp. 422-437. doi: https://doi.org/10.1002/lno.11613.

Atkinson, A. *et al.* (2024) 'Steeper size spectra with decreasing phytoplankton biomass indicate strong trophic amplification and future fish declines', *Nature Communications*, 15(1), p. 381. doi: https://doi.org/10.1038/s41467-023-44406-5.

Atkinson, A. *et al.* (2004) 'Long-term decline in krill stock and increase in salps within the Southern Ocean', *Nature*, 432(7013), pp. 100-103. doi: https://doi.org/10.1038/nature02996.

Atkinson, A. and Sinclair, J.D. (2000) 'Zonal distribution and seasonal vertical migration of copepod assemblages in the Scotia Sea', *Polar Biology*, 23(1), pp. 46-58. doi: https://doi.org/10.1007/s003000050007.

Atkinson, A. *et al.* (1992a) 'Diel vertical migration and feeding of copepods at an oceanic site near South Georgia', *Marine Biology*, 113(4), pp. 583-593. doi: https://doi.org/10.1007/BF00349702.

Atkinson, A. *et al.* (1992b) 'Feeding rates and diel vertical migration of copepods near South Georgia: comparison of shelf and oceanic sites', *Marine Biology*, 114(1), pp. 49-56. doi: https://doi.org/10.1007/BF00350855.

Atkinson, D. (1994) 'Temperature and Organism Size—A Biological Law for Ectotherms?', in Begon, M. and Fitter, A.H. (eds.) *Advances in Ecological Research*. Academic Press, pp. 1-58. doi: https://doi.org/10.1016/S0065-2504(08)60212-3.

Atkinson, D. (1995) 'Effects of temperature on the size of aquatic ectotherms: Exceptions to the general rule', *Journal of Thermal Biology*, 20(1), pp. 61-74. doi: https://doi.org/10.1016/0306-4565(94)00028-H.

Auel, H. *et al.* (2005) 'Metabolic adaptations and reduced respiration of the copepod *Calanoides carinatus* during diapause at depth in the Angola-Benguela Front and northern Benguela upwelling regions', *African Journal of Marine Science*, 27(3), pp. 653-657. doi: https://doi.org/10.2989/18142320509504125.

Auel, H. *et al.* (2002) 'Lipid biomarkers indicate different ecological niches and trophic relationships of the Arctic hyperiid amphipods *Themisto abyssorum* and *T. libellula*', *Polar Biology*, 25(5), pp. 374-383. doi: https://doi.org/10.1007/s00300-001-0354-7.

Auel, H. and Verheye, H.M. (2007) 'Hypoxia tolerance in the copepod *Calanoides carinatus* and the effect of an intermediate oxygen minimum layer on copepod vertical distribution in the

northern Benguela Current upwelling system and the Angola–Benguela Front', *Journal of Experimental Marine Biology and Ecology*, 352(1), pp. 234-243. doi: https://doi.org/10.1016/j.jembe.2007.07.020.

Aumont, O. *et al.* (2018) 'Evaluating the Potential Impacts of the Diurnal Vertical Migration by Marine Organisms on Marine Biogeochemistry', *Global Biogeochemical Cycles*, 32(11), pp. 1622-1643. doi: https://doi.org/10.1029/2018GB005886.

Baker, K. *et al.* (2025) 'Carbon injection potential of the mesopelagic-migrant pump in the Southern Ocean during summer', *Frontiers in Marine Science*, 12, p. 1461723. doi: https://doi.org/10.3389/fmars.2025.1461723.

Båmstedt, U. *et al.* (2000) '8 - Feeding', in Harris, R. *et al.* (eds.) *ICES Zooplankton Methodology Manual*. London: Academic Press, pp. 297-399. doi: https://doi.org/10.1016/B978-012327645-2/50009-8.

Bandara, K. *et al.* (2021) 'Two hundred years of zooplankton vertical migration research', *Biological Reviews*, 96(4), pp. 1547-1589. doi: https://doi.org/10.1111/brv.12715.

Barange, M. (1990) 'Vertical migration and habitat partitioning of six euphausiid species in the northern Benguela upwelling system', *Journal of Plankton Research*, 12(6), pp. 1223-1237. doi: https://doi.org/10.1093/plankt/12.6.1223.

Barange, M., Gibbons, M.J. and Carola, M. (1991) 'Diet and feeding of *Euphausia hanseni* and *Nematoscelis megalops* (Euphausiacea) in the northern Benguela Current: ecological significance of vertical space partitioning', *Marine Ecology Progress Series*, 73, pp. 173-181.

Barnes, C. *et al.* (2010) 'Global patterns in predator–prey size relationships reveal size dependency of trophic transfer efficiency', *Ecology*, 91(1), pp. 222-232. doi: https://doi.org/10.1890/08-2061.1.

Barnes, C. *et al.* (2007) 'Effect of temperature and ration size on carbon and nitrogen stable isotope trophic fractionation', *Functional Ecology*, 21(2), pp. 356-362. doi: https://doi.org/10.1111/j.1365-2435.2006.01224.x.

Barnes, H. and Tranter, D. (1965) 'A statistical examination of the catches, numbers, and biomass taken by three commonly used plankton nets', *Marine and Freshwater Research*, 16(3), pp. 293-306. doi: https://doi.org/10.1071/MF9650293.

Barth, A., Johnson, R. and Stone, J. (2023) 'Size and transparency influence diel vertical migration patterns in copepods', *Limnology and Oceanography*, 68(12), pp. 2749-2758. doi: https://doi.org/10.1002/lno.12461.

BAS (2025) *Scotia Sea open-ocean biological laboratories - British Antarctic Survey*. Available at: https://www.bas.ac.uk/project/scoobies/.

Baumgartner, M.F. and Tarrant, A.M. (2017) 'The Physiology and Ecology of Diapause in Marine Copepods', *Annual Review of Marine Science*, 9(Volume 9, 2017), pp. 387-411. doi: https://doi.org/10.1146/annurev-marine-010816-060505.

Beaugrand, G. *et al.* (2002) 'Reorganization of North Atlantic Marine Copepod Biodiversity and Climate', *Science*, 296(5573), pp. 1692-1694. doi: 10.1126/science.1071329.

Belcher, A. *et al.* (2020) 'Respiration of mesopelagic fish: a comparison of respiratory electron transport system (ETS) measurements and allometrically calculated rates in the Southern Ocean and Benguela Current', *ICES Journal of Marine Science*, 77(5), pp. 1672-1684. doi: https://doi.org/10.1093/icesjms/fsaa031.

Bell, M.V. *et al.* (2007) 'Application of liposome and stable isotope tracer techniques to study polyunsaturated fatty acid biosynthesis in marine zooplankton', *Journal of Plankton Research*, 29(5), pp. 417-422. doi: https://doi.org/10.1093/plankt/fbm025.

Berkes, F. (1975) 'Some Aspects of Feeding Mechanisms of Euphausiid Crustaceans', *Crustaceana*, 29(3), pp. 266-270. doi: https://www.jstor.org/stable/20102261.

Bianchi, D. *et al.* (2013) 'Intensification of open-ocean oxygen depletion by vertically migrating animals', *Nature Geoscience*, 6(7), pp. 545-548. doi: https://doi.org/10.1038/ngeo1837.

Blanchard, J.L. *et al.* (2017) 'From Bacteria to Whales: Using Functional Size Spectra to Model Marine Ecosystems', *Trends in Ecology & Evolution*, 32(3), pp. 174-186. doi: https://doi.org/10.1016/j.tree.2016.12.003.

Bode-Dalby, M. *et al.* (2022) 'Small is beautiful: the important role of small copepods in carbon budgets of the southern Benguela upwelling system', *Journal of Plankton Research*, 45(1), pp. 110-128. doi: https://doi.org/10.1093/plankt/fbac061.

Bode, M. *et al.* (2014) 'Spatio-temporal variability of copepod abundance along the 20 S monitoring transect in the northern Benguela upwelling system from 2005 to 2011', *PLoS One*, 9(5), p. e97738. doi: https://doi.org/10.1371/journal.pone.0097738.

Bode, M. *et al.* (2013) 'Predicting metabolic rates of calanoid copepods', *Journal of Experimental Marine Biology and Ecology*, 444, pp. 1-7. doi: https://doi.org/10.1016/j.jembe.2013.03.003.

Bograd, S.J. *et al.* (2008) 'Oxygen declines and the shoaling of the hypoxic boundary in the California Current', *Geophysical Research Letters*, 35(12). doi: https://doi.org/10.1029/2008GL034185.

Böttger, R. (1987) 'The Vertical Distribution of Micro- and Small Mesozooplankton in the Central Red Sea', *Biological Oceanography*, 4(4), pp. 383-402. doi: https://doi.org/10.1080/01965581.1987.10749498.

Boudreau, P.R., Dickie, L.M. and Kerr, S.R. (1991) 'Body-size spectra of production and biomass as system-level indicators of ecological dynamics', *Journal of Theoretical Biology*, 152(3), pp. 329-339. doi: https://doi.org/10.1016/S0022-5193(05)80198-5.

Bowman, T.E., Cohen, A.C. and McGuiness, M. (1982) 'Vertical distribution of *Themisto gaudichaudii* (Amphipoda: Hyperiidea) in Deepwater Dumpsite 106 off the mouth of Delaware Bay', *Smithsonian Contributions to Zoology*, 351.

Boyd, P.W. *et al.* (2019) 'Multi-faceted particle pumps drive carbon sequestration in the ocean', *Nature*, 568(7752), pp. 327-335. doi: https://doi.org/10.1038/s41586-019-1098-2.

Brett, J.R. and Groves, T.D.D. (1979) '6 - Physiological Energetics', in Hoar, W.S., Randall, D.J. and Brett, J.R. (eds.) *Fish Physiology*. Academic Press, pp. 279-352. doi: https://doi.org/10.1016/S1546-5098(08)60029-1.

Brown, J.H. *et al.* (2004) 'Toward a metabolic theory of ecology', *Ecology*, 85(7), pp. 1771-1789. doi: https://doi.org/10.1890/03-9000.

Bruland, K. and Silver, M. (1981) 'Sinking rates of fecal pellets from gelatinous zooplankton (salps, pteropods, doliolids)', *Marine Biology*, 63, pp. 295-300. doi: https://doi.org/10.1007/BF00395999.

Bruno, C. *et al.* (2021) 'What is on the menu? Feeding, consumption and cannibalism in exploited stocks of the jumbo squid *Dosidicus gigas* in south-central Chile', *Fisheries Research*, 233, p. 105722. doi: https://doi.org/10.1016/j.fishres.2020.105722.

Bucklin, A. *et al.* (2024) 'Metabarcoding and morphological analysis of diets of mesopelagic fishes in the NW Atlantic Slope Water', *Frontiers in Marine Science*, Volume 11 - 2024. doi: https://doi.org/10.3389/fmars.2024.1411996.

Buesseler, K.O. *et al.* (2007a) 'An assessment of the use of sediment traps for estimating upper ocean particle fluxes', *Journal of Marine Research*, 65, pp. 345-416. doi: https://doi.org/10.1357/002224007781567621.

Buesseler, K.O. and Boyd, P.W. (2009) 'Shedding light on processes that control particle export and flux attenuation in the twilight zone of the open ocean', *Limnology and oceanography*, 54(4), pp. 1210-1232. doi: https://doi.org/10.4319/lo.2009.54.4.1210.

Buesseler, K.O. *et al.* (2020) 'Metrics that matter for assessing the ocean biological carbon pump', *Proceedings of the National Academy of Sciences*, 117(18), pp. 9679-9687. doi: https://doi.org/10.1073/pnas.1918114117.

Buesseler, K.O. *et al.* (2007b) 'Revisiting Carbon Flux Through the Ocean's Twilight Zone', *Science*, 316(5824), pp. 567-570. doi: 10.1126/science.1137959.

Buitenhuis, E.T. *et al.* (2013) 'MAREDAT: towards a world atlas of MARine Ecosystem DATa', *Earth Syst. Sci. Data*, 5(2), pp. 227-239. doi: https://doi.org/10.5194/essd-5-227-2013.

Cabana, G. and Rasmussen, J.B. (1996) 'Comparison of aquatic food chains using nitrogen isotopes', *Proceedings of the National Academy of sciences*, 93(20), pp. 10844-10847. doi: https://doi.org/10.1073/pnas.93.20.10844.

Campbell, M.D. *et al.* (2021) 'Testing Bergmann's rule in marine copepods', *Ecography*, 44(9), pp. 1283-1295. doi: https://doi.org/10.1111/ecog.05545.

Capen, R. (1967) *Swimbladder Morphology of Some Mesopelagic Fishes in Relation to Sound Scattering: Juvenile Pacific Lantern Fishes Contain Gas in Their Swimbladders And, Hence, are Probably Major Sound Scatterers*. US Navy Electronics Laboratory.

Cavan, E.L. *et al.* (2017) 'Role of zooplankton in determining the efficiency of the biological carbon pump', *Biogeosciences*, 14(1), pp. 177-186. doi: https://doi.org/10.5194/bg-14-177-2017.

Cavan, E.L., Kawaguchi, S. and Boyd, P.W. (2021) 'Implications for the mesopelagic microbial gardening hypothesis as determined by experimental fragmentation of Antarctic krill fecal pellets', *Ecology and evolution*, 11(2), pp. 1023-1036. doi: https://doi.org/10.1002/ece3.7119.

Ceballos, S., Viesca, L. and Álvarez-Marqués, F. (2006) 'Copepod egg production during highly productive late spring conditions: importance of freshly ingested food and lipid storage', *Marine Ecology Progress Series*, 317, pp. 171-186. doi: https://doi.org/10.3354/meps.

Chavez, F.P. and Messié, M. (2009) 'A comparison of eastern boundary upwelling ecosystems', *Progress in Oceanography*, 83(1-4), pp. 80-96. doi: https://doi.org/10.1016/j.pocean.2009.07.032.

Cherel, Y. *et al.* (2010) 'Isotopic niches and trophic levels of myctophid fishes and their predators in the Southern Ocean', *Limnology and Oceanography*, 55(1), pp. 324-332. doi: https://doi.org/10.4319/lo.2010.55.1.0324.

Childress, J.J. and Nygaard, M. (1974) 'Chemical composition and buoyancy of midwater crustaceans as function of depth of occurrence off Southern California', *Marine Biology*, 27(3), pp. 225-238. doi: https://doi.org/10.1007/BF00391948.

Christiansen, S. *et al.* (2024) 'Extensive avoidance behaviour of krill from predators and nets', *ICES Journal of Marine Science*, 81(9), pp. 1764-1773. doi: https://doi.org/10.1093/icesjms/fsae123.

Christiansen, S. *et al.* (2018) 'Particulate matter flux interception in oceanic mesoscale eddies by the polychaete *Poeobius* sp', *Limnology and Oceanography*, 63(5), pp. 2093-2109. doi: https://doi.org/10.1002/lno.10926.

Chust, G. *et al.* (2014) 'Biomass changes and trophic amplification of plankton in a warmer ocean', *Global Change Biology*, 20(7), pp. 2124-2139. doi: https://doi.org/10.1111/gcb.12562.

Chust, G. *et al.* (2013) 'Are *Calanus* spp. shifting poleward in the North Atlantic? A habitat modelling approach', *ICES Journal of Marine Science*, 71(2), pp. 241-253. doi: 10.1093/icesjms/fst147.

Cisewski, B. and Strass, V.H. (2016) 'Acoustic insights into the zooplankton dynamics of the eastern Weddell Sea', *Progress in Oceanography*, 144, pp. 62-92. doi: https://doi.org/10.1016/j.pocean.2016.03.005.

Cisewski, B. *et al.* (2010) 'Seasonal variation of diel vertical migration of zooplankton from ADCP backscatter time series data in the Lazarev Sea, Antarctica', *Deep Sea Research Part I: Oceanographic Research Papers*, 57(1), pp. 78-94. doi: https://doi.org/10.1016/j.dsr.2009.10.005.

Clarke, A., Holmes, L.J. and Gore, D.J. (1992) 'Proximate and elemental composition of gelatinous zooplankton from the Southern Ocean', *Journal of Experimental Marine Biology and Ecology*, 155(1), pp. 55-68. doi: https://doi.org/10.1016/0022-0981(92)90027-8.

Close, H.G., Wakeham, S.G. and Pearson, A. (2014) 'Lipid and 13C signatures of submicron and suspended particulate organic matter in the Eastern Tropical North Pacific: Implications for the contribution of Bacteria', *Deep Sea Research Part I: Oceanographic Research Papers*, 85, pp. 15-34. doi: https://doi.org/10.1016/j.dsr.2013.11.005.

Cohen, J.E. *et al.* (1993) 'Body sizes of animal predators and animal prey in food webs', *Journal of animal ecology*, pp. 67-78. doi: https://doi.org/10.2307/5483.

Conover, R.J. (1965) 'Notes on the Molting Cycle, Development of Sexual Characters and Sex Ratio in *Calanus hyperboreus*', *Crustaceana*, 8(3), pp. 308-320.

Conroy, J.A. *et al.* (2020) 'Zooplankton diel vertical migration during Antarctic summer', *Deep Sea Research Part I: Oceanographic Research Papers*, 162, p. 103324. doi: https://doi.org/10.1016/j.dsr.2020.103324.

Cook, K.B. *et al.* (2023) 'Carbon budgets of Scotia Sea mesopelagic zooplankton and micronekton communities during austral spring', *Deep Sea Research Part II: Topical Studies in Oceanography*, 210, p. 105296. doi: https://doi.org/10.1016/j.dsr2.2023.105296.

Cornils, A. *et al.* (2022) 'Testing the usefulness of optical data for zooplankton long-term monitoring: Taxonomic composition, abundance, biomass, and size spectra from ZooScan image analysis', *Limnology and Oceanography: Methods*, 20(7), pp. 428-450. doi: https://doi.org/10.1002/lom3.10495.

Cotté, C. *et al.* (2022) 'Macrozooplankton and micronekton diversity and associated carbon vertical patterns and fluxes under distinct productive conditions around the Kerguelen Islands', *Journal of Marine Systems*, 226, p. 103650. doi: https://doi.org/10.1016/j.jmarsys.2021.103650.

D'Ambra, I. *et al.* (2013) 'Predation patterns and prey quality of medusae in a semi-enclosed marine lake: implications for food web energy transfer in coastal marine ecosystems', *Journal of Plankton Research*, 35(6), pp. 1305-1312. doi: https://doi.org/10.1093/plankt/fbt065.

Dai, L. *et al.* (2017) 'Zooplankton abundance, biovolume and size spectra down to 3000 m depth in the western tropical North Pacific during autumn 2014', *Deep Sea Research Part I: Oceanographic Research Papers*, 121, pp. 1-13. doi: https://doi.org/10.1016/j.dsr.2016.12.015.

Dai, L. *et al.* (2016) 'Zooplankton abundance, biovolume and size spectra at western boundary currents in the subtropical North Pacific during winter 2012', *Journal of Marine Systems*, 155, pp. 73-83. doi: https://doi.org/10.1016/j.jmarsys.2015.11.004.

Dalsgaard, J. *et al.* (2003) 'Fatty acid trophic markers in the pelagic marine environment'. doi: https://doi.org/10.1016/S0065-2881(03)46005-7.

Daly, K.L., Cass, C.J. and Wakeham, S.G. (2011) 'Lipid composition of tropical and subtropical copepod species of the genus *Rhincalanus* (Copepoda: Eucalanidae): a novel fatty acid and alcohol signature', *Marine Ecology Progress Series*, 439, pp. 127-138. doi: https://doi.org/10.3354/meps09324.

Dam, H.G., Roman, M.R. and Youngbluth, M.J. (1995) 'Downward export of respiratory carbon and dissolved inorganic nitrogen by diel-migrant mesozooplankton at the JGOFS Bermuda time-series station', *Deep Sea Research Part I: Oceanographic Research Papers*, 42(7), pp. 1187-1197. doi: https://doi.org/10.1016/0967-0637(95)00048-B.

Davison, P. *et al.* (2013) 'Carbon export mediated by mesopelagic fishes in the northeast Pacific Ocean', *Progress in Oceanography*, 116, pp. 14-30. doi: https://doi.org/10.1016/j.pocean.2013.05.013.

De Figueiredo, G.G.A.A. *et al.* (2025) 'Zooplankton abundance and biovolume size-spectra in the western tropical Atlantic-From the shelf towards complex oceanic current systems', *Marine Environmental Research*, 204, p. 106906. doi: https://doi.org/10.1016/j.marenvres.2024.106906.

De Figueiredo, G.G.A.A. *et al.* (2020) 'Body size and stable isotope composition of zooplankton in the western tropical Atlantic', *Journal of Marine Systems*, 212, p. 103449. doi: https://doi.org/10.1016/j.jmarsys.2020.103449.

De Robertis, A., Jaffe, J.S. and Ohman, M.D. (2000) 'Size-dependent visual predation risk and the timing of vertical migration in zooplankton', *Limnology and Oceanography*, 45(8), pp. 1838-1844. doi: https://doi.org/10.4319/lo.2000.45.8.1838.

DeNiro, M.J. and Epstein, S. (1978) 'Influence of diet on the distribution of carbon isotopes in animals', *Geochimica et Cosmochimica Acta*, 42(5), pp. 495-506. doi: https://doi.org/10.1016/0016-7037(78)90199-0.

Detmer, T.M. *et al.* (2019) 'Comparison of microscopy to a semi-automated method (FlowCAM®) for characterization of individual-, population-, and community-level measurements of zooplankton', *Hydrobiologia*, 838(1), pp. 99-110. doi: https://doi.org/10.1007/s10750-019-03980-w.

Doan, N.X. *et al.* (2019) 'Extreme temperature impairs growth and productivity in a common tropical marine copepod', *Scientific Reports*, 9(1), p. 4550. doi: 10.1038/s41598-019-40996-7.

Doherty, S.C. *et al.* (2021) 'Distinguishing zooplankton fecal pellets as a component of the biological pump using compound-specific isotope analysis of amino acids', *Limnology and oceanography*, 66(7), pp. 2827-2841. doi: https://doi.org/10.1002/lno.11793.

Donnelly, J. *et al.* (1994) 'Chemical composition of antarctic zooplankton during austral fall and winter', *Polar Biology*, 14(3), pp. 171-183. doi: https://doi.org/10.1007/BF00240522.

Duncan, S.E. *et al.* (2023) 'Trophic ecology of mesopelagic fishes in the northern and southern Benguela Upwelling Systems revealed through stable isotope patterns', *Marine Ecology Progress Series*, 725, pp. 75-93. doi: https://doi.org/10.3354/meps14455.

Eduardo, L.N. *et al.* (2021) 'Distribution, vertical migration, and trophic ecology of lanternfishes (Myctophidae) in the Southwestern Tropical Atlantic', *Progress in Oceanography*, 199, p. 102695. doi: https://doi.org/10.1016/j.pocean.2021.102695.

Eduardo, L.N. *et al.* (2020a) 'Hatchetfishes (Stomiiformes: Sternoptychidae) biodiversity, trophic ecology, vertical niche partitioning and functional roles in the western Tropical Atlantic', *Progress in Oceanography*, 187, p. 102389. doi: https://doi.org/10.1016/j.pocean.2020.102389.

Eduardo, L.N. *et al.* (2020b) 'Trophic ecology, habitat, and migratory behaviour of the viperfish *Chauliodus sloani* reveal a key mesopelagic player', *Scientific Reports*, 10(1), p. 20996. doi: https://doi.org/10.1038/s41598-020-77222-8.

Egorova, Y. *et al.* (2025) 'Mesopelagic Mesozooplankton and Micronekton Database', *Scientific Data*, 12(1), p. 1294. doi: https://doi.org/10.1038/s41597-025-05638-w.

Ekau, W. *et al.* (2010) 'Impacts of hypoxia on the structure and processes in pelagic communities (zooplankton, macro-invertebrates and fish)', *Biogeosciences*, 7(5), pp. 1669-1699. doi: https://doi.org/10.5194/bg-7-1669-2010.

Falk-Petersen, S., Hopkins, C. and Sargent, J. (1990) *European Marine Biology Symposia*.

Falk-Petersen, S. *et al.* (1999) 'Functional biodiversity of lipids in Antarctic zooplankton: *Calanoides acutus, Calanus propinquus, Thysanoessa macrura* and *Euphausia crystallorophias*', *Polar Biology*, 21(1), pp. 37-47. doi: https://doi.org/10.1007/s003000050330.

Falk-Petersen, S., Sargent, J.R. and Tande, K.S. (1987) 'Lipid composition of zooplankton in relation to the sub-arctic food web', *Polar Biology*, 8(2), pp. 115-120. doi: 10.1007/BF00297065.

Falkowski, P.G., Barber, R.T. and Smetacek, V. (1998) 'Biogeochemical controls and feedbacks on ocean primary production', *science*, 281(5374), pp. 200-206. doi: https://doi.org/10.1126/science.281.5374.200.

Färber Lorda, J. and Färber Data, B. (2023) 'Autumn vertical distribution of zooplankton in the oxygen minimum zone of the Eastern Tropical North Pacific', *Marine Environmental Research*, 190, p. 106116. doi: https://doi.org/10.1016/j.marenvres.2023.106116.

Feagans-Bartow, J.N. and Sutton, T.T. (2014) 'Ecology of the oceanic rim: pelagic eels as key ecosystem components', *Marine Ecology Progress Series*, 502, pp. 257-266. doi: https://doi.org/10.3354/meps10707.

Flock, M.E. and Hopkins, T.L. (1992) 'Species Composition, Vertical Distribution, and Food Habits of the Sergestid Shrimp Assemblage in the Eastern Gulf of Mexico', *Journal of Crustacean Biology*, 12(2), pp. 210-223. doi: https://doi.org/10.2307/1549076.

Flynn, K.J. *et al.* (2025) 'More realistic plankton simulation models will improve projections of ocean ecosystem responses to global change', *Nature Ecology & Evolution*. doi: https://doi.org/10.1038/s41559-025-02788-3.

Freese, D. *et al.* (2016) 'A year-round study on metabolic enzymes and body composition of the Arctic copepod *Calanus glacialis*: implications for the timing and intensity of diapause', *Marine Biology*, 164(1), p. 3. doi: https://doi.org/10.1007/s00227-016-3036-2.

Fricke, H. and Oehlenschläger, J. (1988) 'Fatty acid and sterol composition of the Antarctic amphipod *Themisto gaudichaudii* Guerin 1828', *Comparative Biochemistry and Physiology, B (Comparative Biochemistry)*, 89(1), pp. 39–42.

Froneman, P.W. and Pakhomov, E.A. (1998) 'Trophic importance of the chaetognaths *Eukrohnia hamata* and *Sagitta gazellae* in the pelagic system of the Prince Edward Islands (Southern Ocean)', *Polar Biology*, 19(4), pp. 242-249. doi: https://doi.org/10.1007/s003000050241.

Froneman, P.W. *et al.* (1998) 'Feeding and predation impact of two chaetognath species, *Eukrohnia hamata* and *Sagitta gazellae*, in the vicinity of Marion Island (southern ocean)', *Marine Biology*, 131(1), pp. 95-101. doi: https://doi.org/10.1007/s002270050300.

Froneman, P.W., Pakhomov, E.A. and Treasure, A. (2000) 'Trophic importance of the hyperiid amphipod, *Themisto gaudichaudi*, in the Prince Edward Archipelago (Southern Ocean) ecosystem', *Polar Biology*, 23(6), pp. 429-436. doi: https://doi.org/10.1007/s003000050464.

Frost, B. (1972) 'Effects of size and concentration of food particles on the feeding behavior of the marine planktonic copepod *Calanus pacificus*', *Limnology and oceanography*, 17(6), pp. 805-815. doi: https://doi.org/10.4319/lo.1972.17.6.0805.

Fry, B. (2006) *Stable isotope ecology*. Springer.

Fry, B. and Sherr, E.B. (1984) '$\delta^{13}C$ measurements as indicators of carbon flow in marine and freshwater ecosystems', *Contributions in Marine Science*, 27, pp. 13-47.

Fry, B. and Wainright, S.C. (1991) 'Diatom sources of 13 C-rich carbon in marine food webs', *Marine Ecology Progress Series*, pp. 149-157.

Fujieki, L.A. *et al.* (2023) *Hawaii Ocean Time-series Data Report 33: 2021* (SOEST Publication #11724) (33). University of Hawaii, Honolulu. Available at: https://hahana.soest.hawaii.edu/hot/reports/rep_y33.pdf.

Gallienne, C. and Robins, D. (2001) 'Is *Oithona* the most important copepod in the world's oceans?', *Journal of Plankton Research*, 23(12), pp. 1421-1432. doi: https://doi.org/10.1093/plankt/23.12.1421.

Gannes, L.Z., Del Rio, C.M. and Koch, P. (1998) 'Natural abundance variations in stable isotopes and their potential uses in animal physiological ecology', *Comparative biochemistry and physiology Part A: Molecular & integrative physiology*, 119(3), pp. 725-737. doi: https://doi.org/10.1016/S1095-6433(98)01016-2.

Garzke, J., Ismar, S.M.H. and Sommer, U. (2015) 'Climate change affects low trophic level marine consumers: warming decreases copepod size and abundance', *Oecologia*, 177(3), pp. 849-860. doi: 10.1007/s00442-014-3130-4.

Getzlaff, J. and Kriest, I. (2024) 'Impacts of Vertical Migrants on Biogeochemistry in an Earth System Model', *Global Biogeochemical Cycles*, 38(7), p. e2023GB007842. doi: https://doi.org/10.1029/2023GB007842.

Gibbons, M.J., Stuart, V. and Verheye, H.M. (1992) 'Trophic ecology of carnivorous zooplankton in the Benguela', *South African Journal of Marine Science*, 12(1), pp. 421-437. doi: https://doi.org/10.2989/02577619209504716.

Giering, S. *et al.* (2019a) 'RRS Discovery Cruise DY086, 12 November–19 December 2017', *Controls Over Mesopelagic Carbon Storage (COMICS). Southampton, UK: National Oceanography Centre, Southampton, 265pp.(National Oceanography Centre Cruise Report, No. 55)*.

Giering, S.L. *et al*. (2014) 'Reconciliation of the carbon budget in the ocean's twilight zone', *Nature*, 507(7493), pp. 480-483. doi: https://doi.org/10.1038/nature13123.

Giering, S.L. *et al*. (2019b) 'Seasonal variation of zooplankton community structure and trophic position in the Celtic Sea: A stable isotope and biovolume spectrum approach', *Progress in Oceanography*, 177, p. 101943. doi: https://doi.org/10.1016/j.pocean.2018.03.012.

Giering, S.L.C. *et al*. (2022) 'Are plankton nets a thing of the past? An assessment of in situ imaging of zooplankton for large-scale ecosystem assessment and policy decision-making', *Frontiers in Marine Science*, Volume 9 - 2022. doi: https://doi.org/10.3389/fmars.2022.986206.

Giering, S.L.C. *et al*. (2023) 'Vertical imbalance in organic carbon budgets is indicative of a missing vertical transfer during a phytoplankton bloom near South Georgia (COMICS)', *Deep Sea Research Part II: Topical Studies in Oceanography*, 209, p. 105277. doi: https://doi.org/10.1016/j.dsr2.2023.105277.

Gillooly, J.F. (2000) 'Effect of body size and temperature on generation time in zooplankton', *Journal of Plankton Research*, 22(2), pp. 241-251. doi: 10.1093/plankt/22.2.241.

Gislason, A. (2008) 'Vertical distribution and seasonal dynamics of mesozooplankton in the Iceland Basin', *Marine Biology Research*, 4(6), pp. 401-413. doi: https://doi.org/10.1080/17451000802232882.

Gogina, M., Zettler, A. and Zettler, M.L. (2022) 'Weight-to-weight conversion factors for benthic macrofauna: recent measurements from the Baltic and the North seas', *Earth Syst. Sci. Data*, 14(1), pp. 1-4. doi: https://doi.org/10.5194/essd-14-1-2022.

Gómez, M., Torres, S. and Hernández-León, S. (1996) 'Modification of the electron transport system (ETS) method for routine measurements of respiratory rates of zooplankton', *South African Journal of Marine Science*, 17(1), pp. 15-20. doi: https://doi.org/10.2989/025776196784158446.

González, H.E. and Smetacek, V. (1994) 'The possible role of the cyclopoid copepod *Oithona* in retarding vertical flux of zooplankton faecal material', *Marine Ecology Progress Series*, 113(3), pp. 233-246.

Gordon, D.C. (1971) 'Distribution of particulate organic carbon and nitrogen at an oceanic station in the central Pacific', *Deep Sea Research and Oceanographic Abstracts*, 18(11), pp. 1127-1134. doi: https://doi.org/10.1016/0011-7471(71)90098-2.

Graeve, M., Albers, C. and Kattner, G. (2005) 'Assimilation and biosynthesis of lipids in Arctic *Calanus* species based on feeding experiments with a 13C labelled diatom', *Journal of Experimental Marine Biology and Ecology*, 317(1), pp. 109-125. doi: https://doi.org/10.1016/j.jembe.2004.11.016.

Graeve, M., Hagen, W. and Kattner, G. (1994) 'Herbivorous or omnivorous? On the significance of lipid compositions as trophic markers in Antarctic copepods', *Deep Sea Research Part I: Oceanographic Research Papers*, 41(5), pp. 915-924. doi: https://doi.org/10.1016/0967-0637(94)90083-3.

Guiet, J., Poggiale, J.-C. and Maury, O. (2016) 'Modelling the community size-spectrum: recent developments and new directions', *Ecological Modelling*, 337, pp. 4-14. doi: https://doi.org/10.1016/j.ecolmodel.2016.05.015.

Gurney, L.J. *et al*. (2002) 'Diel feeding patterns and daily ration estimates of three subantarctic euphausiids in the vicinity of the Prince Edward Islands (Southern Ocean)', *Deep Sea Research Part II: Topical Studies in Oceanography*, 49(16), pp. 3207-3227. doi: https://doi.org/10.1016/S0967-0645(02)00079-6.

Gutiérrez-Bravo, J.G. *et al.* (2025) 'Midwater anoxia disrupts the trophic structure of zooplankton and fish in an oxygen deficient zone', *Limnology and Oceanography*, 70(4), pp. 886-898. doi: https://doi.org/10.1002/lno.12813.

Hagen, W., Kattner, G. and Graeve, M. (1993) '*Calanoides acutus* and *Calanus propinquus*, Antarctic copepods with different lipid storage modes via wax esters or triacylglycerols', *Marine Ecology Progress Series*, pp. 135-142.

Hagen, W., Kattner, G. and Graeve, M. (1995) 'On the lipid biochemistry of polar copepods: compositional differences in the Antarctic calanoids *Euchaeta antarctica* and *Euchirella rostromagna*', *Marine Biology*, 123(3), pp. 451-457. doi: https://doi.org/10.1007/BF00349224.

Hagen, W. and Schnack-Schiel, S.B. (1996) 'Seasonal lipid dynamics in dominant Antarctic copepods: Energy for overwintering or reproduction?', *Deep Sea Research Part I: Oceanographic Research Papers*, 43(2), pp. 139-158. doi: https://doi.org/10.1016/0967-0637(96)00001-5.

Hama, T. (1999) 'Fatty acid composition of particulate matter and photosynthetic products in subarctic and subtropical Pacific', *Journal of Plankton Research*, 21(7), pp. 1355-1372. doi: https://doi.org/10.1093/plankt/21.7.1355.

Hansen, B., Bjornsen, P.K. and Hansen, P.J. (1994) 'The size ratio between planktonic predators and their prey', *Limnology and Oceanography*, 39(2), pp. 395-403. doi: https://doi.org/10.4319/lo.1994.39.2.0395.

Harris, R.P. (1988) 'Interactions Between Diel Vertical Migratory Behavior of Marine Zooplankton and the Subsurface Chlorophyll Maximum', *Bulletin of Marine Science*, 43(3), pp. 663-674.

Harvey, H.R. *et al.* (1987) 'Biotransformation and assimilation of dietary lipids by Calanus feeding on a dinoflagellate', *Geochimica et Cosmochimica Acta*, 51(11), pp. 3031-3040. doi: https://doi.org/10.1016/0016-7037(87)90376-0.

Hatton, I.A. *et al.* (2021) 'The global ocean size spectrum from bacteria to whales', *Science advances*, 7(46), p. eabh3732. doi: https://doi.org/10.1126/sciadv.abh3732.

Hattori, H. (1989) 'Bimodal vertical distribution and diel migration of the copepods *Metridia pacifica*, *M. okhotensis* and *Pleuromamma scutullata* in the western North Pacific Ocean', *Marine Biology*, 103(1), pp. 39-50. doi: https://doi.org/10.1007/BF00391063.

Hays, G. *et al.* (1994) 'Interspecific differences in the diel vertical migration of marine copepods: the implications of size, color, and morphology', *Limnology and Oceanography*, 39(7), pp. 1621-1629. doi: https://doi.org/10.4319/lo.1994.39.7.1621.

Hays, G.C. (2003) *Migrations and Dispersal of Marine Organisms: Proceedings of the 37 th European Marine Biology Symposium held in Reykjavík, Iceland, 5–9 August 2002*. Springer.

Heffernan, J.J. and L. Hopkins, T. (1981) 'Vertical Distribution and Feeding of the Shrimp Genera *Gennadas* and *Bentheogennema* (Decapoda: Penaeidea) in the Eastern Gulf of Mexico', *Journal of Crustacean Biology*, 1(4), pp. 461-473. doi: https://doi.org/10.2307/1548124.

Heisey, D. and Porter, K.G. (1977) 'The effect of ambient oxygen concentration on filtering and respiration rates of *Daphnia galeata mendotae* and *Daphnia magna*', *Limnology and Oceanography*, 22(5), pp. 839-845. doi: https://doi.org/10.4319/lo.1977.22.5.0839.

Hemsley, V. *et al.* (2023) 'Suspended particles are hotspots of microbial remineralization in the ocean's twilight zone', *Deep Sea Research Part II: Topical Studies in Oceanography*, 212, p. 105339. doi: https://doi.org/10.1016/j.dsr2.2023.105339.

Henderson, L.C. *et al*. (2024) 'Variable carbon isotope fractionation of photosynthetic communities over depth in an open-ocean euphotic zone', *Proceedings of the National Academy of Sciences*, 121(10), p. e2304613121. doi: https://doi.org/10.1073/pnas.2304613121.

Heneghan, R.F. *et al*. (2020) 'A functional size-spectrum model of the global marine ecosystem that resolves zooplankton composition', *Ecological Modelling*, 435, p. 109265. doi: https://doi.org/10.1016/j.ecolmodel.2020.109265.

Heneghan, R.F., Hatton, I.A. and Galbraith, E.D. (2019) 'Climate change impacts on marine ecosystems through the lens of the size spectrum', *Emerging Topics in Life Sciences*, 3(2), pp. 233-243. doi: https://doi.org/10.1042/ETLS20190042.

Henson *et al* (2018) *RRS Discovery Cruise DY090, 23 May – 28 June 2018, Walvis Bay, Namibia – Cape Town, South Africa. NMF Sensors and Moorings CTD, LADCP & SAPs Cruise*.

Henson, S. *et al*. (2024) 'Knowledge Gaps in Quantifying the Climate Change Response of Biological Storage of Carbon in the Ocean', *Earth's Future*, 12(6), p. e2023EF004375. doi: https://doi.org/10.1029/2023EF004375.

Henson, S.A. *et al*. (2023) 'A seasonal transition in biological carbon pump efficiency in the northern Scotia Sea, Southern Ocean', *Deep Sea Research Part II: Topical Studies in Oceanography*, 208, p. 105274. doi: https://doi.org/10.1016/j.dsr2.2023.105274.

Henson, S.A. *et al*. (2022) 'Uncertain response of ocean biological carbon export in a changing world', *Nature Geoscience*, 15(4), pp. 248-254. doi: https://doi.org/10.1038/s41561-022-00927-0.

Henson, S.A., Sanders, R. and Madsen, E. (2012) 'Global patterns in efficiency of particulate organic carbon export and transfer to the deep ocean', *Global Biogeochemical Cycles*, 26(1). doi: https://doi.org/10.1029/2011GB004099.

Henson, S.A. *et al*. (2011) 'A reduced estimate of the strength of the ocean's biological carbon pump', *Geophysical Research Letters*, 38(4). doi: https://doi.org/10.1029/2011GL046735.

Hereu, C.M., Lavaniegos, B.E. and Goericke, R. (2010) 'Grazing impact of salp (Tunicata, Thaliacea) assemblages in the eastern tropical North Pacific', *Journal of Plankton Research*, 32(6), pp. 785-804. doi: https://doi.org/10.1093/plankt/fbq005.

Hernández-León, S. and Gómez, M. (1996) 'Factors affecting the respiration/ETS ratio in marine zooplankton', *Journal of Plankton Research*, 18(2), pp. 239-255. doi: https://doi.org/10.1093/plankt/18.2.239.

Hernández-León, S. and Montero, I. (2006) 'Zooplankton biomass estimated from digitalized images in Antarctic waters: A calibration exercise', *Journal of Geophysical Research: Oceans*, 111(C5). doi: https://doi.org/10.1029/2005JC002887.

Hernández-León, S. *et al*. (2019a) 'Zooplankton and Micronekton Active Flux Across the Tropical and Subtropical Atlantic Ocean', *Frontiers in Marine Science*, Volume 6 - 2019. doi: https://doi.org/10.3389/fmars.2019.00535.

Hernández-León, S. *et al*. (2019b) 'Carbon export through zooplankton active flux in the Canary Current', *Journal of Marine Systems*, 189, pp. 12-21. doi: https://doi.org/10.1016/j.jmarsys.2018.09.002.

Hernández-León, S. *et al*. (2024) 'Seasonality of zooplankton active flux in subtropical waters', *Limnology and Oceanography*, 69(11), pp. 2564-2579. doi: https://doi.org/10.1002/lno.12689.

Herrera, A. *et al.* (2014) 'Zooplankton biomass and electron transport system activity around the Balearic Islands (western Mediterranean)', *Journal of Marine Systems*, 131, pp. 54-62. doi: https://doi.org/10.1016/j.jmarsys.2013.11.004.

Herrera, I. *et al.* (2017) 'The effect of a strong warm winter on subtropical zooplankton biomass and metabolism', *Journal of Marine Research*, 75, pp. 557–577.

Herrera, I. *et al.* (2019) 'Vertical variability of *Euphausia distinguenda* metabolic rates during diel migration into the oxygen minimum zone of the Eastern Tropical Pacific off Mexico', *Journal of Plankton Research*, 41(2), pp. 165-176. doi: https://doi.org/10.1093/plankt/fbz004.

Hidalgo, M. and Browman, H.I. (2019) 'Developing the knowledge base needed to sustainably manage mesopelagic resources', *ICES Journal of Marine Science*, 76(3), pp. 609-615. doi: https://doi.org/10.1093/icesjms/fsz067.

Hidalgo, P., Escribano, R. and Morales, C.E. (2005) 'Ontogenetic vertical distribution and diel migration of the copepod *Eucalanus inermis* in the oxygen minimum zone off northern Chile (20–21° S)', *Journal of Plankton Research*, 27(6), pp. 519-529. doi: https://doi.org/10.1093/plankt/fbi025.

Hirche, H.-J. (1996) 'Diapause in the marine copepod, *Calanus finmarchicus* — A review', *Ophelia*, 44(1-3), pp. 129-143. doi: https://doi.org/10.1080/00785326.1995.10429843.

Hirche, H.J. (1997) 'Life cycle of the copepod *Calanus hyperboreus* in the Greenland Sea', *Marine Biology*, 128(4), pp. 607-618. doi: https://doi.org/10.1007/s002270050127.

Hobson, K.A. (1995) 'Reconstructing avian diets using stable-carbon and nitrogen isotope analysis of egg components: patterns of isotopic fractionation and turnover', *The Condor*, 97(3), pp. 752-762. doi: https://doi.org/10.2307/1369183.

Hobson, K.A., Piatt, J.F. and Pitocchelli, J. (1994) 'Using stable isotopes to determine seabird trophic relationships', *Journal of animal ecology*, pp. 786-798. doi: https://doi.org/10.2307/5256.

Holland, M.M. *et al.* (2025) 'Mind the gap - The need to integrate novel plankton methods alongside ongoing long-term monitoring', *Ocean & Coastal Management*, 262, p. 107542. doi: https://doi.org/10.1016/j.ocecoaman.2025.107542.

Holm, M.W. *et al.* (2019) 'Influence of behavioral plasticity and foraging strategy on starvation tolerance of planktonic copepods', *Journal of Experimental Marine Biology and Ecology*, 511, pp. 19-27. doi: https://doi.org/10.1016/j.jembe.2018.11.002.

Homma, T. and Yamaguchi, A. (2010) 'Vertical changes in abundance, biomass and community structure of copepods down to 3000m in the southern Bering Sea', *Deep Sea Research Part I: Oceanographic Research Papers*, 57(8), pp. 965-977. doi: https://doi.org/10.1016/j.dsr.2010.05.002.

Hopcroft, R.R., Roff, J.C. and Chavez, F.P. (2001) 'Size paradigms in copepod communities: a re-examination', *Hydrobiologia*, 453(1), pp. 133-141. doi: https://doi.org/10.1023/A:1013167917679.

Hopkins, T.L. *et al.* (1993) 'Community structure and trophic ecology of zooplankton in the scotia sea marginal ice zone in winter (1988)', *Deep Sea Research Part I: Oceanographic Research Papers*, 40(1), pp. 81-105. doi: https://doi.org/10.1016/0967-0637(93)90054-7.

Hudson, J.M. *et al.* (2014) 'Myctophid feeding ecology and carbon transport along the northern Mid-Atlantic Ridge', *Deep Sea Research Part I: Oceanographic Research Papers*, 93, pp. 104-116. doi: https://doi.org/10.1016/j.dsr.2014.07.002.

Hulbert, A. (2003) 'Life, death and membrane bilayers', *Journal of Experimental Biology*, 206(14), pp. 2303-2311. doi: https://doi.org/10.1242/jeb.00399.

Hunt, B.P.V. *et al.* (2015) 'A coupled stable isotope-size spectrum approach to understanding pelagic food-web dynamics: A case study from the southwest sub-tropical Pacific', *Deep Sea Research Part II: Topical Studies in Oceanography*, 113, pp. 208-224. doi: https://doi.org/10.1016/j.dsr2.2014.10.023.

Hunt, B.P.V. *et al.* (2008) 'Pteropods in Southern Ocean ecosystems', *Progress in Oceanography*, 78(3), pp. 193-221. doi: https://doi.org/10.1016/j.pocean.2008.06.001.

Huntley, M. and Escritor, F. (1991) 'Dynamics of *Calanoides acutus* (Copepoda: Calanoida) in Antarctic coastal waters', *Deep Sea Research Part A. Oceanographic Research Papers*, 38(8), pp. 1145-1167. doi: https://doi.org/10.1016/0198-0149(91)90100-T.

Huntley, M.E., Sykes, P.F. and Marin, V. (1989) 'Biometry and trophodynamics of *Salpa thompsoni foxton* (Tunicata: Thaliacea) near the Antarctic Peninsula in austral summer, 1983–1984', *Polar Biology*, 10(1), pp. 59-70. doi: https://doi.org/10.1007/BF00238291.

Hutchings, L. *et al.* (2009) 'The Benguela Current: An ecosystem of four components', *Progress in Oceanography*, 83(1-4), pp. 15-32. doi: https://doi.org/10.1016/j.pocean.2009.07.046.

Iglesias, I.S. *et al.* (2023) 'Mesopelagic fishes are important prey for a diversity of predators', *Frontiers in Marine Science*, 10, p. 1220088. doi: https://doi.org/10.3389/fmars.2023.1220088.

Ikeda, T. (1966) 'Relationship between respiration rate and body size in marine plankton animals as a function of the temperature of habitat', *Bull. Fac. Fish., Hokkaido Univ*, 21, p. 2.

Ikeda, T. (1985) 'Metabolic rates of epipelagic marine zooplankton as a function of body mass and temperature', *Marine Biology*, 85(1), pp. 1-11. doi: https://doi.org/10.1007/BF00396409.

Ikeda, T. (1988) 'Metabolism and chemical composition of crustaceans from the Antarctic mesopelagic zone', *Deep Sea Research Part A. Oceanographic Research Papers*, 35(12), pp. 1991-2002. doi: https://doi.org/10.1016/0198-0149(88)90121-5.

Ikeda, T. (1996) 'Metabolism, body composition, and energy budget of the mesopelagic fish *Maurolicus muelleri* in the Sea of Japan', *Fish. Bull. US*, 94, pp. 49-58.

Ikeda, T. (2014) 'Respiration and ammonia excretion by marine metazooplankton taxa: synthesis toward a global-bathymetric model', *Marine Biology*, 161(12), pp. 2753-2766. doi: https://doi.org/10.1007/s00227-014-2540-5.

Ikeda, T. (2016) 'Routine metabolic rates of pelagic marine fishes and cephalopods as a function of body mass, habitat temperature and habitat depth', *Journal of Experimental Marine Biology and Ecology*, 480, pp. 74-86. doi: https://doi.org/10.1016/j.jembe.2016.03.012.

Ikeda, T. and Mitchell, A.W. (1982) 'Oxygen uptake, ammonia excretion and phosphate excretion by krill and other Antarctic zooplankton in relation to their body size and chemical composition', *Marine Biology*, 71(3), pp. 283-298. doi: https://doi.org/10.1007/BF00397045.

Ikeda, T. and Motoda, S. (1978) 'Estimated zooplankton production and their ammonia excretion in the Kuroshio and adjacent seas', *Fishery Bulletin*, 76(2), p. 357.

Ikeda, T. and Shiga, N. (1999) 'Production, metabolism and production/biomass (P/B) ratio of *Themisto japonical* (Crustacea: Amphipoda) in Toyama Bay, southern Japan Sea', *Journal of Plankton Research*, 21(2), pp. 299-308. doi: https://doi.org/10.1093/plankt/21.2.299.

Irigoien, X., Conway, D.V.P. and Harris, R.P. (2004) 'Flexible diel vertical migration behaviour of zooplankton in the Irish Sea', *Marine Ecology Progress Series*, 267, pp. 85-97. doi: https://doi.org/10.3354/meps.

Irigoien, X. *et al.* (2014) 'Large mesopelagic fishes biomass and trophic efficiency in the open ocean', *Nature communications*, 5(1), p. 3271. doi: https://doi.org/10.1038/ncomms4271.

Irisson, J.-O. *et al.* (2022) 'Machine Learning for the Study of Plankton and Marine Snow from Images', *Annual Review of Marine Science*, 14(Volume 14, 2022), pp. 277-301. doi: https://doi.org/10.1146/annurev-marine-041921-013023.

Ishii, H. and Tanaka, F. (2001) 'Food and feeding of Aurelia aurita in Tokyo Bay with an analysis of stomach contents and a measurement of digestion times', *Hydrobiologia*, 451(1), pp. 311-320. doi: https://doi.org/10.1023/A:1011814525325.

Isla, A., Scharek, R. and Latasa, M. (2015) 'Zooplankton diel vertical migration and contribution to deep active carbon flux in the NW Mediterranean', *Journal of Marine Systems*, 143, pp. 86-97. doi: https://doi.org/10.1016/j.jmarsys.2014.10.017.

Jackson, G.A. (1993) 'Flux feeding as a mechanism for zooplankton grazing and its implications for vertical particulate flux', *Limnology and Oceanography*, 38(6), pp. 1328-1331. doi: https://doi.org/10.4319/lo.1993.38.6.1328.

Jackson, G.A. and Checkley, D.M. (2011) 'Particle size distributions in the upper 100m water column and their implications for animal feeding in the plankton', *Deep Sea Research Part I: Oceanographic Research Papers*, 58(3), pp. 283-297. doi: https://doi.org/10.1016/j.dsr.2010.12.008.

Jaspers, C. *et al.* (2023) 'Gelatinous larvacean zooplankton can enhance trophic transfer and carbon sequestration', *Trends in Ecology & Evolution*, 38(10), pp. 980-993. doi: 10.1016/j.tree.2023.05.005.

Jónasdóttir, S.H. *et al.* (2015) 'Seasonal copepod lipid pump promotes carbon sequestration in the deep North Atlantic', *Proceedings of the National Academy of Sciences*, 112(39), pp. 12122-12126. doi: https://doi.org/10.1073/pnas.1512110112.

Jonsson, P.R. and Tiselius, P. (1990) 'Feeding behaviour, prey detection and capture efficiency of the copepod *Acartia tonsa* feeding on planktonic ciliates', *Marine Ecology Progress Series*, pp. 35-44.

Kaartvedt, S., Aksnes, D.L. and Staby, A. (2012) 'Efficient trawl avoidance by mesopelagic fishes causes large underestimation of their biomass', *Marine Ecology Progress Series*, 456, pp. 1-6. doi: https://doi.org/10.3354/meps.

Kahru, M. *et al.* (2007) 'Eddies enhance biological production in the Weddell-Scotia Confluence of the Southern Ocean', *Geophysical Research Letters*, 34(14). doi: https://doi.org/10.1029/2007GL030430.

Kates, M. and Volcani, B.E. (1966) 'Lipid components of diatoms', *Biochimica et Biophysica Acta (BBA) - Lipids and Lipid Metabolism*, 116(2), pp. 264-278. doi: https://doi.org/10.1016/0005-2760(66)90009-9.

Kattner, G. *et al.* (2003) 'Fatty acid and alcohol composition of the small polar copepods, *Oithona* and *Oncaea*: indication on feeding modes', *Polar Biology*, 26(10), pp. 666-671. doi: https://doi.org/10.1007/s00300-003-0540-x.

Kattner, G., Graeve, M. and Hagen, W. (1994) 'Ontogenetic and seasonal changes in lipid and fatty acid/alcohol compositions of the dominant Antarctic copepods *Calanus propinquus,*

Calanoides acutus and *Rhincalanus gigas*', *Marine Biology*, 118(4), pp. 637-644. doi: https://doi.org/10.1007/BF00347511.

Kattner, G. and Hagen, W. (1995) 'Polar herbivorous copepods–different pathways in lipid biosynthesis', *ICES Journal of Marine Science*, 52(3-4), pp. 329-335. doi: https://doi.org/10.1016/1054-3139(95)80048-4.

Keil, R.G. *et al.* (2016) 'A multiproxy approach to understanding the "enhanced" flux of organic matter through the oxygen-deficient waters of the Arabian Sea', *Biogeosciences*, 13(7), pp. 2077-2092. doi: https://doi.org/10.5194/bg-13-2077-2016.

Kerkar, A.U., Venkataramana, V. and Tripathy, S.C. (2022) 'Assessing the trophic link between primary and secondary producers in the Southern Ocean: A carbon-biomass based approach', *Polar Science*, 31, p. 100734. doi: https://doi.org/10.1016/j.polar.2021.100734.

Kim, D. *et al.* (2023) 'Vertical, spatial, size, and taxonomic variations in stable isotopes (δ13C and δ15N) of zooplankton and other pelagic organisms in the western North Pacific', *Deep Sea Research Part I: Oceanographic Research Papers*, 197, p. 104045. doi: https://doi.org/10.1016/j.dsr.2023.104045.

Kim, D. *et al.* (2025) 'Vertical variations in zooplankton size spectra down to 3,000 m depth and significant effects of the sizes of Calanoida and Ergasilida across the subarctic, transitional, and subtropical regions of the western North Pacific', *Deep Sea Research Part I: Oceanographic Research Papers*, 217, p. 104445. doi: https://doi.org/10.1016/j.dsr.2025.104445.

Kiørboe, T. (2000) 'Colonization of marine snow aggregates by invertebrate zooplankton: Abundance, scaling, and possible role', *Limnology and Oceanography*, 45(2), pp. 479-484. doi: https://doi.org/10.4319/lo.2000.45.2.0479.

Kiørboe, T. (2013) 'Zooplankton body composition', *Limnology and Oceanography*, 58(5), pp. 1843-1850. doi: https://doi.org/10.4319/lo.2013.58.5.1843.

Kiørboe, T. and Hirst, A.G. (2014) 'Shifts in Mass Scaling of Respiration, Feeding, and Growth Rates across Life-Form Transitions in Marine Pelagic Organisms', *The American Naturalist*, 183(4), pp. E118-E130. doi: https://doi.org/10.1086/675241.

Kiriakoulakis, K. *et al.* (2004) 'Organic biogeochemistry of the Darwin Mounds, a deep-water coral ecosystem, of the NE Atlantic', *Deep Sea Research Part I: Oceanographic Research Papers*, 51(12), pp. 1937-1954. doi: https://doi.org/10.1016/j.dsr.2004.07.010.

Kleckner, R.C. and Gibbs Jr, R.H. (1972) 'Swimbladder structure of Mediterranean midwater fishes and a method of comparing swimbladder data with acoustic profiles', *Mediterranean Biological Studies Final Report I*, p. 230.

Kleiber, M. (1932) 'Body size and metabolism', *Hilgardia*, 6(11), pp. 315-353.

Klevjer, T.A. *et al.* (2016) 'Large scale patterns in vertical distribution and behaviour of mesopelagic scattering layers', *Scientific reports*, 6(1), p. 19873. doi: https://doi.org/10.1038/srep19873.

Köhn, E.E. *et al.* (2022) 'Strong Habitat Compression by Extreme Shoaling Events of Hypoxic Waters in the Eastern Pacific', *Journal of Geophysical Research: Oceans*, 127(6), p. e2022JC018429. doi: https://doi.org/10.1029/2022JC018429.

Koppelmann, R. *et al.* (2009) 'Trophic relationships of zooplankton in the eastern Mediterranean based on stable isotope measurements', *Journal of Plankton Research*, 31(6), pp. 669-686. doi: https://doi.org/10.1093/plankt/fbp013.

Koppelmann, R. *et al*. (2013) 'Onshore–offshore distribution of *Thecosomata* (Gastropoda) in the Benguela Current upwelling region off Namibia: species diversity and trophic position', *Journal of the Marine Biological Association of the United Kingdom*, 93(6), pp. 1625-1640. doi: https://doi.org/10.1017/S0025315413000052.

Koppelmann, R. and Weikert, H. (1992) 'Full-depth zooplankton profiles over the deep bathyal of the NE Atlantic', *Marine Ecology-Progress Series*, 86, pp. 263-263.

Korb, R.E. and Whitehouse, M. (2004) 'Contrasting primary production regimes around South Georgia, Southern Ocean: large blooms versus high nutrient, low chlorophyll waters', *Deep Sea Research Part I: Oceanographic Research Papers*, 51(5), pp. 721-738. doi: https://doi.org/10.1016/j.dsr.2004.02.006.

Korb, R.E. *et al*. (2010) 'Summer microplankton community structure across the Scotia Sea: implications for biological carbon export', *Biogeosciences*, 7(1), pp. 343-356. doi: https://doi.org/10.5194/bg-7-343-2010.

Korb, R.E., Whitehouse, M.J. and Ward, P. (2004) 'SeaWiFS in the southern ocean: spatial and temporal variability in phytoplankton biomass around South Georgia', *Deep Sea Research Part II: Topical Studies in Oceanography*, 51(1-3), pp. 99-116. doi: https://doi.org/10.1016/j.dsr2.2003.04.002.

Korb, R.E. *et al*. (2012) 'Regional and seasonal differences in microplankton biomass, productivity, and structure across the Scotia Sea: Implications for the export of biogenic carbon', *Deep Sea Research Part II: Topical Studies in Oceanography*, 59, pp. 67-77. doi: https://doi.org/10.1016/j.dsr2.2011.06.006.

Koski, M., Kiørboe, T. and Takahashi, K. (2005) 'Benthic life in the pelagic: Aggregate encounter and degradation rates by pelagic harpacticoid copepods', *Limnology and Oceanography*, 50(4), pp. 1254-1263. doi: https://doi.org/10.4319/lo.2005.50.4.1254.

Koski, M. *et al*. (2020) 'The missing piece of the upper mesopelagic carbon budget? Biomass, vertical distribution and feeding of aggregate-associated copepods at the PAP site', *Progress in Oceanography*, 181, p. 102243. doi: https://doi.org/10.1016/j.pocean.2019.102243.

Kosobokova, K.N. and Hopcroft, R.R. (2010) 'Diversity and vertical distribution of mesozooplankton in the Arctic's Canada Basin', *Deep Sea Research Part II: Topical Studies in Oceanography*, 57(1), pp. 96-110. doi: https://doi.org/10.1016/j.dsr2.2009.08.009.

Kremer, K.I. *et al*. (2025) 'Trophic ecology of squids in the Benguela Upwelling System elucidated by combining stomach content, stable isotope and fatty acid analyses', *Marine Biology*, 172(2), p. 32. doi: https://doi.org/10.1007/s00227-024-04592-2.

Kruse, S., Hagen, W. and Bathmann, U. (2010) 'Feeding ecology and energetics of the Antarctic chaetognaths *Eukrohnia hamata, E. bathypelagica* and *E. bathyantarctica*', *Marine Biology*, 157(10), pp. 2289-2302. doi: https://doi.org/10.1007/s00227-010-1496-3.

Kurian, S. *et al*. (2026) 'Transformation of particulate matter while sinking through the oxygen minimum zone of the Eastern Arabian Sea', *Marine Environmental Research*, 215, p. 107858. doi: https://doi.org/10.1016/j.marenvres.2026.107858.

Kürten, B. *et al*. (2013) 'Tracking seasonal changes in North Sea zooplankton trophic dynamics using stable isotopes', *Biogeochemistry*, 113, pp. 167-187. doi: https://doi.org/10.1007/s10533-011-9630-y.

Kwiatkowski, L., Aumont, O. and Bopp, L. (2019) 'Consistent trophic amplification of marine biomass declines under climate change', *Global change biology*, 25(1), pp. 218-229. doi: https://doi.org/10.1111/gcb.14468.

Kwon, E.Y., Primeau, F. and Sarmiento, J.L. (2009) 'The impact of remineralization depth on the air–sea carbon balance', *Nature Geoscience*, 2(9), pp. 630-635. doi: https://doi.org/10.1038/ngeo612.

Kwong, L.E. *et al.* (2020) 'Mesozooplankton and Micronekton Active Carbon Transport in Contrasting Eddies', *Frontiers in Marine Science*, Volume 6 - 2019. doi: https://doi.org/10.3389/fmars.2019.00825.

Kwong, L.E. *et al.* (2022) 'Spatial, seasonal, and climatic variability in mesozooplankton size spectra along a coastal-to-open ocean transect in the subarctic Northeast Pacific', *Progress in Oceanography*, 201, p. 102728. doi: https://doi.org/10.1016/j.pocean.2021.102728.

Laakmann, S., Stumpp, M. and Auel, H. (2009) 'Vertical distribution and dietary preferences of deep-sea copepods (Euchaetidae and Aetideidae; Calanoida) in the vicinity of the Antarctic Polar Front', *Polar Biology*, 32(5), pp. 679-689. doi: https://doi.org/10.1007/s00300-008-0573-2.

Lalande, C., Bauerfeind, E. and Nöthig, E.-M. (2011) 'Downward particulate organic carbon export at high temporal resolution in the eastern Fram Strait: influence of Atlantic Water on flux composition', *Marine Ecology Progress Series*, 440, pp. 127-136. doi: https://doi.org/10.3354/meps.

Lampitt, R.S., Noji, T. and von Bodungen, B. (1990) 'What happens to zooplankton faecal pellets? Implications for material flux', *Marine Biology*, 104(1), pp. 15-23. doi: https://doi.org/10.1007/BF01313152.

Larsson, P. and Lampert, W. (2011) 'Experimental evidence of a low-oxygen refuge for large zooplankton', *Limnology and Oceanography*, 56(5), pp. 1682-1688. doi: https://doi.org/10.4319/lo.2011.56.5.1682.

Lee, R.F., Kattner, G. and Hagen, W. (2006) 'Lipid storage in marine zooplankton', *Marine Ecology Progress Series*, 307, pp. 273-306. doi: https://doi.org/10.3354/meps.

Lee, R.F., Nevenzel, J.C. and Paffenhöfer, G.A. (1971) 'Importance of wax esters and other lipids in the marine food chain: Phytoplankton and copepods', *Marine Biology*, 9(2), pp. 99-108. doi: https://doi.org/10.1007/BF00348249.

Lehette, P. and Hernández-León, S. (2009) 'Zooplankton biomass estimation from digitized images: a comparison between subtropical and Antarctic organisms', *Limnology and Oceanography: Methods*, 7(4), pp. 304-308. doi: https://doi.org/10.4319/lom.2009.7.304.

Lilley, M. and Lombard, F. (2015) 'Respiration of fragile planktonic zooplankton: extending the possibilities with a single method', *Journal of Experimental Marine Biology and Ecology*, 471, pp. 226-231. doi: https://doi.org/10.1016/j.jembe.2015.06.013.

Liu, T. *et al.* (2024) 'Dissolved Oxygen Recovery in the Oxygen Minimum Zone of the Arabian Sea in Recent Decade as Observed by BGC-Argo Floats', *Geophysical Research Letters*, 51(12), p. e2024GL108841. doi: https://doi.org/10.1029/2024GL108841.

Liu, Y. *et al.* (2022) 'Seasonal variation in diel vertical migration of zooplankton and micronekton in the Andaman Sea observed by a moored ADCP', *Deep Sea Research Part I: Oceanographic Research Papers*, 179, p. 103663. doi: https://doi.org/10.1016/j.dsr.2021.103663.

Loick, N., W., E. and and Verheye, H.M. (2005) 'Water-body preferences of dominant calanoid copepod species in the Angola-Benguela frontal zone', *African Journal of Marine Science*, 27(3), pp. 597-608. doi: https://doi.org/10.2989/18142320509504120.

Lombard, F. *et al.* (2019) 'Globally Consistent Quantitative Observations of Planktonic Ecosystems', *Frontiers in Marine Science*, Volume 6 - 2019. doi: https://doi.org/10.3389/fmars.2019.00196.

Longhurst, A. *et al.* (1990) 'Vertical flux of respiratory carbon by oceanic diel migrant biota', *Deep Sea Research Part A. Oceanographic Research Papers*, 37(4), pp. 685-694. doi: Vertical flux of respiratory carbon by oceanic diel migrant biota.

Longhurst, A., Sameoto, D. and Herman, A. (1984) 'Vertical distribution of Arctic zooplankton in summer: eastern Canadian archipelago', *Journal of Plankton Research*, 6(1), pp. 137-168. doi: https://doi.org/10.1093/plankt/6.1.137.

Lourenço, S. *et al.* (2017) 'Life cycle, distribution and trophodynamics of the lanternfish *Krefftichthys anderssoni* (Lönnberg, 1905) in the Scotia Sea', *Polar Biology*, 40, pp. 1229-1245. doi: https://doi.org/10.1007/s00300-016-2046-3.

Lovecchio, E. *et al.* (2022) 'Oxygen Variability in the Offshore Northern Benguela Upwelling System From Glider Data', *Journal of Geophysical Research: Oceans*, 127(11), p. e2022JC019063. doi: https://doi.org/10.1029/2022JC019063.

Lovecchio, E. *et al.* (2025) 'Mesopelagic particle layers in the dynamic hypoxic northern Benguela are shaped by zooplankton activity', *Journal of Geophysical Research: Oceans*, 130(3), p. e2024JC021039. doi: https://doi.org/10.1029/2024JC021039.

Maar, K. *et al.* (2023) 'Lipids in meso- and bathypelagic fishes from the North Atlantic Ocean: dietary inputs suggested from fatty acid trophic markers', *Marine Ecology Progress Series*, 717, pp. 127-141. doi: https://doi.org/10.3354/meps.

Maas, A.E. *et al.* (2014) 'Fine-scale vertical distribution of macroplankton and micronekton in the Eastern Tropical North Pacific in association with an oxygen minimum zone', *Journal of Plankton Research*, 36(6), pp. 1557-1575. doi: https://doi.org/10.1093/plankt/fbu077.

Mackas, D.L. and Tsuda, A. (1999) 'Mesozooplankton in the eastern and western subarctic Pacific: community structure, seasonal life histories, and interannual variability', *Progress in Oceanography*, 43(2), pp. 335-363. doi: https://doi.org/10.1016/S0079-6611(99)00012-9.

Macko, S.A. *et al.* (1986) 'Kinetic fractionation of stable nitrogen isotopes during amino acid transamination', *Geochimica et Cosmochimica Acta*, 50(10), pp. 2143-2146. doi: https://doi.org/10.1016/0016-7037(86)90068-2.

Maldonado, F., Packard, T.T. and Gómez, M. (2012) 'Understanding tetrazolium reduction and the importance of substrates in measuring respiratory electron transport activity', *Journal of Experimental Marine Biology and Ecology*, 434-435, pp. 110-118. doi: https://doi.org/10.1016/j.jembe.2012.08.010.

Manno, C. *et al.* (2022) 'Deep carbon export peaks are driven by different biological pathways during the extended Scotia Sea (Southern Ocean) bloom', *Deep Sea Research Part II: Topical Studies in Oceanography*, 205, p. 105183. doi: https://doi.org/10.1016/j.dsr2.2022.105183.

Marin, V. (1988) 'Qualitative models of the life cycles of *Calanoides acutus, Calanus propinquus*, and *Rhincalanus gigas*', *Polar Biology*, 8(6), pp. 439-446. doi: https://doi.org/10.1007/BF00264720.

Marin, V.H. and Schnack-Schiel, S.B. (1993) 'The occurrence of *Rhincalanus gigas, Calanoides acutus, and Calanus propinquus* (Copepoda: Calanoida) in late May in the area of the Antarctic Peninsula', *Polar Biology*, 13(1), pp. 35-40. doi: https://doi.org/10.1007/BF00236581.

Marohn, L. *et al.* (2021) 'Distribution and diel vertical migration of mesopelagic fishes in the Southern Sargasso Sea — observations through hydroacoustics and stratified catches', *Marine Biodiversity*, 51(6), p. 87. doi: https://doi.org/10.1007/s12526-021-01216-6.

Martin, B. *et al.* (2015) 'Spatio-temporal variability of zooplankton biomass and environmental control in the Northern Benguela Upwelling System: field investigations and model simulation', *Marine Ecology*, 36(3), pp. 637-658. doi: https://doi.org/10.1111/maec.12173.

Martin, J.H. *et al.* (1987) 'VERTEX: carbon cycling in the northeast Pacific', *Deep Sea Research Part A. Oceanographic Research Papers*, 34(2), pp. 267-285. doi: https://doi.org/10.1016/0198-0149(87)90086-0.

Maynard, S.D. (1975) 'Mesopelagic micronekton in Hawaiian waters : faunal composition, standing stock, and diel vertical migration', *Fish. Bull.*, 73, pp. 726-736.

Maynou, F. and Cartes, J.E. (1998) 'Daily ration estimates and comparative study of food consumption in nine species of deep-water decapod crustaceans of the NW Mediterranean', *Marine Ecology Progress Series*, 171, pp. 221-231. doi: https://doi.org/10.3354/meps.

Mayor, D.J. *et al.* (2006) 'Feeding and reproduction of *Calanus finmarchicus* during non-bloom conditions in the Irminger Sea', *Journal of plankton research*, 28(12), pp. 1167-1179. doi: https://doi.org/10.1093/plankt/fbl047.

Mayor, D.J. *et al.* (2011) 'Absorption efficiencies and basal turnover of C, N and fatty acids in a marine Calanoid copepod', *Functional Ecology*, 25(3), pp. 509-518. doi: https://doi.org/10.1111/j.1365-2435.2010.01791.x.

Mayor, D.J., Gentleman, W.C. and Anderson, T.R. (2020) 'Ocean carbon sequestration: Particle fragmentation by copepods as a significant unrecognised factor? Explicitly representing the role of copepods in biogeochemical models may fundamentally improve understanding of future ocean carbon storage', *BioEssays*, 42(12), p. 2000149. doi: https://doi.org/10.1002/bies.202000149.

Mayor, D.J. *et al.* (2014) 'Microbial gardening in the ocean's twilight zone: Detritivorous metazoans benefit from fragmenting, rather than ingesting, sinking detritus', *Bioessays*, 36. doi: https://doi.org/10.1002/bies.201400100.

Mayor, D.J. *et al.* (2013) 'Tissue and size-related changes in the fatty acid and stable isotope signatures of the deep sea grenadier fish *Coryphaenoides armatus* from the Charlie-Gibbs Fracture Zone region of the Mid-Atlantic Ridge', *Deep Sea Research Part II: Topical Studies in Oceanography*, 98, pp. 421-430. doi: https://doi.org/10.1016/j.dsr2.2013.02.030.

Mayzaud, P. and Boutoute, M. (2015) 'Dynamics of lipid and fatty acid composition of the hyperiid amphipod *Themisto*: a bipolar comparison with special emphasis on seasonality', *Polar Biology*, 38(7), pp. 1049-1065. doi: https://doi.org/10.1007/s00300-015-1666-3.

Mayzaud, P. *et al.* (2005) 'Respiration in marine zooplankton—the other side of the coin: CO2 production', *Limnology and Oceanography*, 50(1), pp. 291-298. doi: https://doi.org/10.4319/lo.2005.50.1.0291.

Mayzaud, P., Claustre, H. and Augier, P. (1990) 'Effect of variable nutrient supply on fatty acid composition of phytoplankton grown in an enclosed experimental ecosystem', *Marine Ecology Progress Series*, 60, pp. 123-140.

McDonnell, A., Boyd, P. and Buesseler, K. (2015) 'Effects of sinking velocities and microbial respiration rates on the attenuation of particulate carbon fluxes through the mesopelagic zone', *Global Biogeochemical Cycles*, 29(2), pp. 175-193. doi: https://doi.org/10.1002/2014GB004935.

McEvoy, A., Atkinson, A. and Beesley, A. (2022) 'Zooplankton abundance time series from net hauls at site L4 off Plymouth, UK between 1988-2021'.

McMahon, K.W. *et al.* (2015) 'Carbon and nitrogen isotope fractionation of amino acids in an avian marine predator, the gentoo penguin (*Pygoscelis papua*)', *Ecology and evolution*, 5(6), pp. 1278-1290. doi: https://doi.org/10.1002/ece3.1437.

McMeans, B.C. *et al.* (2012) 'Seasonal patterns in fatty acids of *Calanus hyperboreus* (Copepoda, Calanoida) from Cumberland Sound, Baffin Island, Nunavut', *Marine Biology*, 159(5), pp. 1095-1105. doi: https://doi.org/10.1007/s00227-012-1889-6.

McMonagle, H. *et al.* (2023) 'High uncertainty in fish bioenergetics impedes precision of fish-mediated carbon transport estimates into the ocean's twilight zone', *Progress in Oceanography*, 217, p. 103078. doi: https://doi.org/10.1016/j.pocean.2023.103078.

Menden-Deuer, S. and Lessard, E.J. (2000) 'Carbon to volume relationships for dinoflagellates, diatoms, and other protist plankton', *Limnology and Oceanography*, 45(3), pp. 569-579. doi: https://doi.org/10.4319/lo.2000.45.3.0569.

Menden-Deuer, S., Slade, W.H. and Dierssen, H. (2021) 'Promoting Instrument Development for New Research Avenues in Ocean Science: Opening the Black Box of Grazing', *Frontiers in Marine Science*, Volume 8 - 2021. doi: https://doi.org/10.3389/fmars.2021.695938.

Metfies, K. *et al.* (2014) 'Molecular analyses of gut contents: elucidating the feeding of co-occurring salps in the Lazarev Sea from a different perspective', *Antarctic Science*, 26(5), pp. 545-553. doi: https://doi.org/10.1017/S0954102014000157.

Mill, A., Pinnegar, J. and Polunin, N. (2007) 'Explaining isotope trophic-step fractionation: why herbivorous fish are different', *Functional Ecology*, pp. 1137-1145.

Minagawa, M. and Wada, E. (1984) 'Stepwise enrichment of 15N along food chains: further evidence and the relation between δ15N and animal age', *Geochimica et cosmochimica acta*, 48(5), pp. 1135-1140. doi: https://doi.org/10.1016/0016-7037(84)90204-7.

Minutoli, R. *et al.* (2017) 'Zooplankton electron transport system activity and biomass in the western Ross Sea (Antarctica) during austral summer 2014', *Polar Biology*, 40(6), pp. 1197-1209. doi: https://doi.org/10.1007/s00300-016-2043-6.

Miyake, Y. and Wada, E. (1967) 'The abundance ratio of 15N/14N in marine environments', *Rec. Oceanogr. Works Jpn*, 9, pp. 37-53.

Monteiro, P. *et al.* (2006) 'Variability of natural hypoxia and methane in a coastal upwelling system: Oceanic physics or shelf biology?', *Geophysical Research Letters*, 33(16). doi: https://doi.org/10.1029/2006GL026234.

Moriarty, R. and O'Brien, T.D. (2013) 'Distribution of mesozooplankton biomass in the global ocean', *Earth Syst. Sci. Data*, 5(1), pp. 45-55. doi: https://doi.org/10.5194/essd-5-45-2013.

Moura, G.C.d. *et al.* (2016) 'Seasonal and spatial shifts in copepod diets within tropical estuaries measured by fatty acid profiles', *Ecological Indicators*, 69, pp. 284-294. doi: https://doi.org/10.1016/j.ecolind.2016.04.037.

Negrete-García, G. *et al.* (2022) 'Plankton energy flows using a global size-structured and trait-based model', *Progress in Oceanography*, 209, p. 102898. doi: https://doi.org/10.1016/j.pocean.2022.102898.

Nelson, M.M. *et al.* (2001) 'Lipids of Antarctic Ocean amphipods: food chain interactions and the occurrence of novel biomarkers', *Marine Chemistry*, 73(1), pp. 53-64. doi: https://doi.org/10.1016/S0304-4203(00)00072-4.

Nelson, M.M. *et al.* (2000) 'Lipids of gelatinous antarctic zooplankton: Cnidaria and Ctenophora', *Lipids*, 35(5), pp. 551-559. doi: https://doi.org/10.1007/s11745-000-555-5.

Nguyen, T.T. *et al.* (2022) 'Microbes contribute to setting the ocean carbon flux by altering the fate of sinking particulates', *Nature communications*, 13(1), p. 1657. doi: https://doi.org/10.1038/s41467-022-29297-2.

Nielsdóttir, M.C. *et al.* (2012) 'Seasonal and spatial dynamics of iron availability in the Scotia Sea', *Marine Chemistry*, 130, pp. 62-72. doi: https://doi.org/10.1016/j.marchem.2011.12.004.

Nielsen, J.M. *et al.* (2018) 'Diet tracing in ecology: Method comparison and selection', *Methods in Ecology and Evolution*, 9(2), pp. 278-291. doi: https://doi.org/10.1111/2041-210X.12869.

O'Leary, T. *et al.* (2001) 'Euphotic zone variations in bulk and compound-specific δ13C of suspended organic matter in the Subantarctic Ocean, south of Australia', *Journal of Geophysical Research: Oceans*, 106(C12), pp. 31669-31684. doi: https://doi.org/10.1029/2000JC000288.

O'Reilly, J. and Sherman, K. (2016) 'Chapter 5.1: Primary productivity patterns and trends', *Large marine ecosystems: Status and trends. United Nations Environment Programme, Nairobi*, pp. 91-99.

Ohman, M.D. (1990) 'The Demographic Benefits of Diel Vertical Migration by Zooplankton', *Ecological Monographs*, 60(3), pp. 257-281. doi: https://doi.org/10.2307/1943058.

Ohman, M.D. *et al.* (1998) 'Differential dormancy of co-occurring copepods', *Deep Sea Research Part II: Topical Studies in Oceanography*, 45(8), pp. 1709-1740. doi: https://doi.org/10.1016/S0967-0645(98)80014-3.

Ohman, M.D., Frost, B.W. and Cohen, E.B. (1983) 'Reverse diel vertical migration: an escape from invertebrate predators', *Science*, 220(4604), pp. 1404-1407. doi: https://doi.org/10.1126/science.220.4604.1404.

Oksanen, J. *et al.* (2020a) 'Vegan: Community Ecology Package', (Accessed November 2020).

Oksanen, J. *et al.* (2020b) *vegan: Community Ecology Package*[Computer program]. Available at: https://CRAN.R-project.org/package=vegan.

Oksanen, J. *et al.* (2022) *vegan: Community Ecology Package*[Computer program]. Available at: https://CRAN.R-project.org/package=vegan.

Olivar, M.P. *et al.* (2012) 'Vertical distribution, diversity and assemblages of mesopelagic fishes in the western Mediterranean', *Deep Sea Research Part I: Oceanographic Research Papers*, 62, pp. 53-69. doi: https://doi.org/10.1016/j.dsr.2011.12.014.

Olivar, M.P. *et al.* (2017) 'Mesopelagic fishes across the tropical and equatorial Atlantic: Biogeographical and vertical patterns', *Progress in Oceanography*, 151, pp. 116-137. doi: https://doi.org/10.1016/j.pocean.2016.12.001.

Olsen, E.M., Jørstad, T. and Kaartvedt, S. (2000) 'The feeding strategies of two large marine copepods', *Journal of Plankton Research*, 22(8), pp. 1513-1528. doi: https://doi.org/10.1093/plankt/22.8.1513.

Omori, M. (1969) 'Weight and chemical composition of some important oceanic zooplankton in the North Pacific Ocean', *Marine Biology*, 3(1), pp. 4-10. doi: https://doi.org/10.1007/BF00355587.

Omori, M. (1975) 'The Biology of Pelagic Shrimps in the Ocean', in Russell, F.S. and Yonge, M. (eds.) *Advances in Marine Biology*. Academic Press, pp. 233-324. doi: https://doi.org/10.1016/S0065-2881(08)60459-9.

Øresland, V. (1991) 'Feeding of the carnivorous copepod *Euchaeta antarctica* in Antarctic waters', *Mar Ecol Prog Ser*, 78, pp. 41-47.

Øresland, V. and Ward, P. (1993) 'Summer and winter diet of four carnivorous copepod species around South Georgia', *Marine Ecology Progress Series*, pp. 73-78.

Oschlies, A. *et al.* (2018) 'Drivers and mechanisms of ocean deoxygenation', *Nature Geoscience*, 11(7), pp. 467-473. doi: 10.1038/s41561-018-0152-2.

Østvedt, O.J. (1955) 'Zooplankton investigations from weather ship M in the Norwegian Sea, 1948-49', *Hvalrådets Skrifter*, 40, pp. 1-93.

Owens, T. and King, F. (1975) 'The measurement of respiratory electron-transport-system activity in marine zooplankton', *Marine Biology*, 30(1), pp. 27-36. doi: https://doi.org/10.1007/BF00393750.

Ozaki, K. and Ikeda, T. (1999) 'Vertical distribution, population structure and life cycle of the mesopelagic copepod *Paraeuchaeta elongata* off Cape Esan, southwestern Hokkaido, Japan', *Plankton Biology and Ecology*, 46(1), pp. 48-53.

Packard, T.T. and Christensen, J. (2004) 'Respiration and vertical carbon flux in the Gulf of Maine water column', *Journal of Marine Research*, 62(1).

Packard, T.T., Devol, A.H. and King, F.D. (1975) 'The effect of temperature on the respiratory electron transport system in marine plankton', *Deep Sea Research and Oceanographic Abstracts*, 22(4), pp. 237-249. doi: https://doi.org/10.1016/0011-7471(75)90029-7.

Pakhomov, E.A. *et al.* (2019) 'Utility of salps as a baseline proxy for food web studies', *Journal of plankton research*, 41(1), pp. 3-11. doi: https://doi.org/10.1093/plankt/fby051.

Pakhomov, E.A. and Perissinotto, R. (1996) 'Trophodynamics of the hyperiid amphipod *Themisto gaudichaudi* in the South Georgia region during late austral summer', *Marine Ecology Progress Series*, 134, pp. 91-100. doi: https://doi.org/10.3354/meps.

Pakhomov, E.A., Perissinotto, R. and Froneman, P.W. (1999) 'Predation impact of carnivorous macrozooplankton and micronekton in the Atlantic sector of the Southern Ocean', *Journal of Marine Systems*, 19(1), pp. 47-64. doi: https://doi.org/10.1016/S0924-7963(98)00023-2.

Pakhomov, E.A., Perissinotto, R. and McQuaid, C.D. (1996) 'Prey composition and daily rations of myctophid fishes in the Southern Ocean', *Marine Ecology Progress Series*, 134, pp. 1-14. doi: https://doi.org/10.3354/meps.

Papadimitraki, M., Maar, K. and Jónasdóttir, S.H. (2023) 'Meso- and bathypelagic fish feeding ecology: A meta-analysis on fatty acids and stable isotope trophic studies', *Deep Sea Research Part I: Oceanographic Research Papers*, 198, p. 104083. doi: https://doi.org/10.1016/j.dsr.2023.104083.

Parekh, P. *et al.* (2006) 'Atmospheric carbon dioxide in a less dusty world', *Geophysical research letters*, 33(3). doi: https://doi.org/10.1029/2005GL025098.

Park, J. *et al.* (2010) 'Variability of SeaWiFs chlorophyll-a in the southwest Atlantic sector of the Southern Ocean: Strong topographic effects and weak seasonality', *Deep Sea Research Part I: Oceanographic Research Papers*, 57(4), pp. 604-620. doi: https://doi.org/10.1016/j.dsr.2010.01.004.

Parrish, C.C. (2013) 'Lipids in marine ecosystems', *International Scholarly Research Notices*, 2013(1), p. 604045. doi: https://doi.org/10.5402/2013/604045.

Pasternak, A.F. and Schnack-Schiel, S.B. (2001) 'Feeding patterns of dominant Antarctic copepods: an interplay of diapause, selectivity, and availability of food', *Hydrobiologia*, 453(1), pp. 25-36. doi: https://doi.org/10.1023/A:1013147413136.

Penczak, T. *et al.* (1984) 'Food consumption and energy transformations by fish populations in two small lowland rivers in Poland', *Hydrobiologia*, 108, pp. 135-144. doi: https://doi.org/10.1007/BF00014873.

Perry, G.J. *et al.* (1979) 'Fatty acids of bacterial origin in contemporary marine sediments', *Geochimica et Cosmochimica Acta*, 43(11), pp. 1715-1725. doi: https://doi.org/10.1016/0016-7037(79)90020-6.

Picheral, M. *et al.* (2022) 'The Underwater Vision Profiler 6: an imaging sensor of particle size spectra and plankton, for autonomous and cabled platforms', *Limnology and Oceanography: Methods*, 20(2), pp. 115-129. doi: https://doi.org/10.1002/lom3.10475.

Picheral, M., Colin, S. and Irisson, J.-O. (2025) *EcoTaxa, a tool for the taxonomic classification of images*. Available at: http://ecotaxa.obs-vlfr.fr.

Pillar, S.C. *et al.* (1992) 'Community structure and trophic ecology of euphausiids in the Benguela ecosystem', *South African Journal of Marine Science*, 12(1), pp. 393-409. doi: https://doi.org/10.2989/02577619209504714.

Pinti, J. *et al.* (2023) 'Model estimates of metazoans' contributions to the biological carbon pump', *Biogeosciences*, 20(5), pp. 997-1009. doi: https://doi.org/10.5194/bg-20-997-2023.

Platt, T. and Denman, K. (1977) 'Organisation in the pelagic ecosystem', *Helgoländer Wissenschaftliche Meeresuntersuchungen*, 30, pp. 575-581. doi: https://doi.org/10.1007/BF02207862.

Ploug, H., Iversen, M.H. and Fischer, G. (2008) 'Ballast, sinking velocity, and apparent diffusivity within marine snow and zooplankton fecal pellets: Implications for substrate turnover by attached bacteria', *Limnology and Oceanography*, 53(5), pp. 1878-1886. doi: https://doi.org/10.4319/lo.2008.53.5.1878.

Podeswa, Y. (2012) *Active carbon transport and feeding ecology of pelagic decapods in the North Pacific Subtropical Gyre*. Available at: https://open.library.ubc.ca/collections/24/items/1.0053487.

Pond, D.W. (2012) 'The physical properties of lipids and their role in controlling the distribution of zooplankton in the oceans', *Journal of Plankton Research*, 34(6), pp. 443-453. doi: https://doi.org/10.1093/plankt/fbs027.

Pond, D.W. *et al.* (2002) 'Origins of long-chain polyunsaturated fatty acids in the hydrothermal vent worms *Ridgea piscesae* and *Protis hydrothermica*', *Marine Ecology Progress Series*, 225, pp. 219-226. doi: https://doi.org/10.3354/meps.

Pond, D.W. and Tarling, G.A. (2011) 'Phase transitions of wax esters adjust buoyancy in diapausing *Calanoides acutus*', *Limnology and Oceanography*, 56(4), pp. 1310-1318. doi: https://doi.org/10.4319/lo.2011.56.4.1310.

Pond, D.W., Tarling, G.A. and Mayor, D.J. (2014) 'Hydrostatic pressure and temperature effects on the membranes of a seasonally migrating marine copepod', *PLoS One*, 9(10), p. e111043. doi: https://doi.org/10.1371/journal.pone.0111043.

Pond, D.W. *et al.* (2012) 'Wax ester composition influences the diapause patterns in the copepod *Calanoides acutus*', *Deep Sea Research Part II: Topical Studies in Oceanography*, 59, pp. 93-104. doi: https://doi.org/10.1016/j.dsr2.2011.05.009.

Pond, D.W. and Ward, P. (2011) 'Importance of diatoms for *Oithona* in Antarctic waters', *Journal of plankton research*, 33(1), pp. 105-118. doi: https://doi.org/10.1093/plankt/fbq089.

Pörtner, H.-O. *et al.* (2019) 'Technical Summary', *IPCC Special Report on the Ocean and Cryosphere in a Changing Climate*.

Post, D.M. (2002) 'Using stable isotopes to estimate trophic position: models, methods, and assumptions', *Ecology*, 83(3), pp. 703-718. doi: https://doi.org/10.1890/0012-9658(2002)083[0703:USITET]2.0.CO;2.

Post, D.M. *et al.* (2007) 'Getting to the fat of the matter: models, methods and assumptions for dealing with lipids in stable isotope analyses', *Oecologia*, 152(1), pp. 179-189. doi: https://doi.org/10.1007/s00442-006-0630-x.

Potier, M. *et al.* (2007) 'Forage fauna in the diet of three large pelagic fishes (lancetfish, swordfish and yellowfin tuna) in the western equatorial Indian Ocean', *Fisheries Research*, 83(1), pp. 60-72. doi: https://doi.org/10.1016/j.fishres.2006.08.020.

Poulsen, L.K. and Kiørboe, T. (2006) 'Vertical flux and degradation rates of copepod fecal pellets in a zooplankton community dominated by small copepods', *Marine Ecology Progress Series*, 323, pp. 195-204. doi: https://doi.org/10.3354/meps.

Power, M., Guiguer, K.R.R.A. and Barton, D.R. (2003) 'Effects of temperature on isotopic enrichment in *Daphnia magna*: implications for aquatic food-web studies', *Rapid Communications in Mass Spectrometry*, 17(14), pp. 1619-1625. doi: https://doi.org/10.1002/rcm.1094.

Preece, C. *et al.* (in prep) 'Particulate organic matter and the influence of zooplankton on its composition and fate in the mesopelagic zone, Scotia Sea, (Southern Ocean)'.

Protopapa, M. *et al.* (2019a) 'Trophic positioning of prominent copepods in the epi- and mesopelagic zone of the ultra-oligotrophic eastern Mediterranean Sea', *Deep Sea Research Part II: Topical Studies in Oceanography*, 164, pp. 144-155. doi: https://doi.org/10.1016/j.dsr2.2019.04.011.

Protopapa, M. *et al.* (2019b) 'Zooplankton distribution, growth and respiration in the Cretan Passage, Eastern Mediterranean', *Deep Sea Research Part II: Topical Studies in Oceanography*, 164, pp. 156-169. doi: https://doi.org/10.1016/j.dsr2.2019.03.001.

Proud, R. *et al.* (2019) 'From siphonophores to deep scattering layers: uncertainty ranges for the estimation of global mesopelagic fish biomass', *ICES Journal of Marine Science*, 76(3), pp. 718-733. doi: https://doi.org/10.1093/icesjms/fsy037.

Purcell, J.E. and Kremer, P. (1983) 'Feeding and metabolism of the siphonophore Sphaeronectes gracilis1', *Journal of Plankton Research*, 5(1), pp. 95-106. doi: https://doi.org/10.1093/plankt/5.1.95.

Quillfeldt, P. *et al.* (2015) 'Variability of higher trophic level stable isotope data in space and time–a case study in a marine ecosystem', *Rapid Communications in Mass Spectrometry*, 29(7), pp. 667-674. doi: https://doi.org/10.1002/rcm.7145.

R Core Team (2022) 'R: A language and environment for statistical computing. R Foundation for Statistical Computing'.

R Core Team (2023) *R: A language and environment for statistical computing. R Foundation for Statistical Computing*[Computer program]. Available at: https://www.R-project.org/.

Rae, C.D. (2005) 'A demonstration of the hydrographic partition of the Benguela upwelling ecosystem at 26 40'S', *African Journal of Marine Science*, 27(3), pp. 617-628. doi: https://doi.org/10.2989/18142320509504122.

Ratnarajah, L. *et al.* (2023) 'Monitoring and modelling marine zooplankton in a changing climate', *Nature Communications*, 14(1), p. 564. doi: https://doi.org/10.1038/s41467-023-36241-5.

Reeve, M.R. (1980) 'Comparative experimental studies on the feeding of chaetognaths and ctenophores', *Journal of Plankton Research*, 2(4), pp. 381-393. doi: https://doi.org/10.1093/plankt/2.4.381.

Reeve, M.R. and Walter, M.A. (1979) 'Nutritional Ecology of Ctenophores—A Review of Recent Research', in Russell, F.S. and Yonge, M. (eds.) *Advances in Marine Biology*. Academic Press, pp. 249-287. doi: https://doi.org/10.1016/S0065-2881(08)60406-X.

Ricciardi, A. and Bourget, E. (1998) 'Weight-to-weight conversion factors for marine benthic macroinvertebrates', *Marine Ecology Progress Series*, 163, pp. 245-251. doi: https://doi.org/10.3354/meps.

Richoux, N.B. (2010) 'Trophic ecology of zooplankton at a frontal transition zone: fatty acid signatures at the subtropical convergence, Southern Ocean', *Journal of Plankton Research*, 33(3), pp. 491-505. doi: https://doi.org/10.1093/plankt/fbq132.

Riquelme-Bugueño, R. *et al.* (2020) 'Diel vertical migration into anoxic and high-pCO2 waters: acoustic and net-based krill observations in the Humboldt Current', *Scientific Reports*, 10(1), p. 17181. doi: https://doi.org/10.1038/s41598-020-73702-z.

Robinson, C. *et al.* (2010) 'Mesopelagic zone ecology and biogeochemistry–a synthesis', *Deep Sea Research Part II: Topical Studies in Oceanography*, 57(16), pp. 1504-1518. doi: https://doi.org/10.1016/j.dsr2.2010.02.018.

Rohr, T. *et al.* (2023) 'Zooplankton grazing is the largest source of uncertainty for marine carbon cycling in CMIP6 models', *Communications Earth & Environment*, 4(1), p. 212. doi: https://doi.org/10.1038/s43247-023-00871-w.

Roman, M.R. *et al.* (2019) 'Interactive effects of hypoxia and temperature on coastal pelagic zooplankton and fish', *Frontiers in Marine Science*, 6, p. 139. doi: https://doi.org/10.3389/fmars.2019.00139.

Roman, M.R. and Pierson, J.J. (2022) 'Interactive Effects of Increasing Temperature and Decreasing Oxygen on Coastal Copepods', *The Biological Bulletin*, 243(2), pp. 171-183. doi: 10.1086/722111.

Romero-Romero, S. *et al.* (2016) 'Body size-based trophic structure of a deep marine ecosystem', *Ecology*, 97(1), pp. 171-181. doi: https://doi.org/10.1890/15-0234.1.

Rossberg, A.G., Gaedke, U. and Kratina, P. (2019) 'Dome patterns in pelagic size spectra reveal strong trophic cascades', *Nature communications*, 10(1), p. 4396. doi: https://doi.org/10.1038/s41467-019-12289-0.

Roullier, F. *et al.* (2014) 'Particle size distribution and estimated carbon flux across the Arabian Sea oxygen minimum zone', *Biogeosciences*, 11(16), pp. 4541-4557. doi: https://doi.org/10.5194/bg-11-4541-2014.

Rounick, J. and Winterbourn, M. (1986) 'Stable carbon isotopes and carbon flow in ecosystems', *BioScience*, 36(3), pp. 171-177. doi: https://doi.org/10.2307/1310304.

Saito, H. and Kiørboe, T. (2001) 'Feeding rates in the chaetognath Sagitta elegans: effects of prey size, prey swimming behaviour and small-scale turbulence', *Journal of Plankton Research*, 23(12), pp. 1385-1398. doi: https://doi.org/10.1093/plankt/23.12.1385.

Saltzman, J. and Wishner, K.F. (1997) 'Zooplankton ecology in the eastern tropical Pacific oxygen minimum zone above a seamount: 2. Vertical distribution of copepods', *Deep Sea Research Part I: Oceanographic Research Papers*, 44(6), pp. 931-954. doi: https://doi.org/10.1016/S0967-0637(97)00006-X.

Sanders, R.J. *et al.* (2016) 'Controls over ocean mesopelagic interior carbon storage (COMICS): fieldwork, synthesis, and modeling efforts', *Frontiers in Marine Science*, 3, p. 136. doi: https://doi.org/10.3389/fmars.2016.00136.

Sargent, J.R. and Falk-Petersen, S. (1988) 'The lipid biochemistry of calanoid copepods', *Hydrobiologia*, 167(1), pp. 101-114. doi: 10.1007/BF00026297.

Saumweber, W.J. and Durbin, E.G. (2006) 'Estimating potential diapause duration in *Calanus finmarchicus*', *Deep Sea Research Part II: Topical Studies in Oceanography*, 53(23), pp. 2597-2617. doi: https://doi.org/10.1016/j.dsr2.2006.08.003.

Saunders, R.A. *et al.* (2018) 'Seasonal variation in the predatory impact of myctophids on zooplankton in the Scotia Sea (Southern Ocean)', *Progress in Oceanography*, 168, pp. 123-144. doi: https://doi.org/10.1016/j.pocean.2018.09.017.

Savineau, E.L.-R. *et al.* (2024) 'Investigating the physiological ecology of mesopelagic zooplankton in the Scotia sea (Southern ocean) using lipid and stable isotope signatures', *Deep Sea Research Part I: Oceanographic Research Papers*, 208, p. 104317. doi: https://doi.org/10.1016/j.dsr.2024.104317.

Schlosser, T.L. and Strutton, P.G. (2025) 'Phytoplankton blooms in the new Southern Ocean sea-ice regime', *Elementa: Science of the Anthropocene*, 13(1), p. 00055. doi: 10.1525/elementa.2024.00055.

Schnack-Schiel, S.B. *et al.* (2008) 'Population dynamics and life strategies of *Rhincalanus nasutus* (Copepoda) at the onset of the spring bloom in the Gulf of Aqaba (Red Sea)', *Journal of Plankton Research*, 30(6), pp. 655-672. doi: https://doi.org/10.1093/plankt/fbn029.

Schramski, J.R. *et al.* (2015) 'Metabolic theory predicts whole-ecosystem properties', *Proceedings of the National Academy of Sciences*, 112(8), pp. 2617-2622. doi: https://doi.org/10.1073/pnas.1423502112.

Schukat, A. *et al.* (2014) 'Complex trophic interactions of calanoid copepods in the Benguela upwelling system', *Journal of Sea Research*, 85, pp. 186-196. doi: https://doi.org/10.1016/j.seares.2013.04.018.

Schukat, A. *et al.* (2013a) 'Pelagic decapods in the northern Benguela upwelling system: Distribution, ecophysiology and contribution to active carbon flux', *Deep Sea Research Part I: Oceanographic Research Papers*, 75, pp. 146-156. doi: https://doi.org/10.1016/j.dsr.2013.02.003.

Schukat, A. *et al.* (2013b) 'Energetics and carbon budgets of dominant calanoid copepods in the northern Benguela upwelling system', *Journal of Experimental Marine Biology and Ecology*, 442, pp. 1-9. doi: https://doi.org/10.1016/j.jembe.2013.01.024.

Scott, C.L. *et al.* (2002) 'Species differences, origins and functions of fatty alcohols and fatty acids in the wax esters and phospholipids of *Calanus hyperboreus, C. glacialis* and *C. finmarchicus* from Arctic waters', *Marine Ecology Progress Series*, 235, pp. 127-134.

Seibel, B.A. (2011) 'Critical oxygen levels and metabolic suppression in oceanic oxygen minimum zones', *Journal of Experimental Biology*, 214(2), pp. 326-336. doi: https://doi.org/10.1242/jeb.049171.

Sheldon, R., Prakash, A. and Sutcliffe Jr, W. (1972) 'The size distribution of particles in the ocean', *Limnology and oceanography*, 17(3), pp. 327-340. doi: https://doi.org/10.4319/lo.1972.17.3.0327.

Sheridan, C.C. *et al.* (2002) 'Suspended particle organic composition and cycling in surface and midwaters of the equatorial Pacific Ocean', *Deep Sea Research Part I: Oceanographic Research Papers*, 49(11), pp. 1983-2008. doi: https://doi.org/10.1016/S0967-0637(02)00118-8.

Sinclair, E.H., Walker, W.A. and Thomason, J.R. (2016) 'Correction: Body Size Regression Formulae, Proximate Composition and Energy Density of Eastern Bering Sea Mesopelagic Fish and Squid', *PLOS ONE*, 11(7), p. e0159353. doi: https://doi.org/10.1371/journal.pone.0132289.

Skjoldal, H.R. *et al.* (2013) 'Intercomparison of zooplankton (net) sampling systems: Results from the ICES/GLOBEC sea-going workshop', *Progress in Oceanography*, 108, pp. 1-42. doi: https://doi.org/10.1016/j.pocean.2012.10.006.

Søreide, J.E. *et al.* (2008) 'Seasonal feeding strategies of *Calanus* in the high-Arctic Svalbard region', *Deep Sea Research Part II: Topical Studies in Oceanography*, 55(20), pp. 2225-2244. doi: https://doi.org/10.1016/j.dsr2.2008.05.024.

Sprules, W.G. and Barth, L.E. (2016) 'Surfing the biomass size spectrum: some remarks on history, theory, and application', *Canadian Journal of Fisheries and Aquatic Sciences*, 73(4), pp. 477-495. doi: https://doi.org/10.1139/cjfas-2015-0115.

Sprules, W.G. and Goyke, A.P. (1994) 'Size-Based Structure and Production in the Pelagia of Lakes Ontario and Michigan', *Canadian Journal of Fisheries and Aquatic Sciences*, 51(11), pp. 2603-2611. doi: https://doi.org/10.1139/f94-260.

Steinberg, D.K. *et al.* (2000) 'Zooplankton vertical migration and the active transport of dissolved organic and inorganic carbon in the Sargasso Sea', *Deep Sea Research Part I: Oceanographic Research Papers*, 47(1), pp. 137-158. doi: https://doi.org/10.1016/S0967-0637(99)00052-7.

Steinberg, D.K. and Cope, J.S. (2025) 'Zooplankton biomass measured from net tows conducted during ongoing monthly cruises, from April 1994 to June 2024, at the Bermuda Atlantic Time-series Study (BATS) site in the Sargasso Sea'.

Steinberg, D.K. *et al.* (2008) 'A comparison of mesopelagic mesozooplankton community structure in the subtropical and subarctic North Pacific Ocean', *Deep Sea Research Part II: Topical Studies in Oceanography*, 55(14), pp. 1615-1635. doi: https://doi.org/10.1016/j.dsr2.2008.04.025.

Steinberg, D.K. and Landry, M.R. (2017) 'Zooplankton and the ocean carbon cycle', *Annual review of marine science*, 9(1), pp. 413-444. doi: https://doi.org/10.1146/annurev-marine-010814-015924.

Steinberg, D.K., Pilskaln, C.H. and Silver, M.W. (1998) 'Contribution of zooplankton associated with detritus to sediment trap\'swimmer\'carbon in Monterey Bay, California, USA', *Marine Ecology Progress Series*, 164, pp. 157-166. doi: https://doi.org/10.3354/meps.

Steinberg, D.K. and Saba, G.K. (2008) 'Chapter 26 - Nitrogen Consumption and Metabolism in Marine Zooplankton', in Capone, D.G. *et al.* (eds.) *Nitrogen in the Marine Environment (Second Edition)*. San Diego: Academic Press, pp. 1135-1196. doi: https://doi.org/10.1016/B978-0-12-372522-6.00026-8.

Stevens, C. *et al.* (2022) 'Total lipid and fatty acid composition of mesozooplankton functional group members in the NE Pacific over a range of productivity regimes', *Marine Ecology Progress Series*, 687, pp. 43-64. doi: https://doi.org/10.3354/meps.

Stowasser, G. *et al.* (2012) 'Food web dynamics in the Scotia Sea in summer: a stable isotope study', *Deep Sea Research Part II: Topical Studies in Oceanography*, 59, pp. 208-221. doi: https://doi.org/10.1016/j.dsr2.2011.08.004.

Straile, D. (1997) 'Gross growth efficiencies of protozoan and metazoan zooplankton and their dependence on food concentration, predator-prey weight ratio, and taxonomic group', *Limnology and Oceanography*, 42(6), pp. 1375-1385. doi: https://doi.org/10.4319/lo.1997.42.6.1375.

Stramma, L. *et al.* (2008) 'Expanding Oxygen-Minimum Zones in the Tropical Oceans', *Science*, 320(5876), pp. 655-658. doi: https://doi.org/10.1126/science.1153847.

Stramma, L. *et al.* (2010) 'Ocean oxygen minima expansions and their biological impacts', *Deep Sea Research Part I: Oceanographic Research Papers*, 57(4), pp. 587-595. doi: https://doi.org/10.1016/j.dsr.2010.01.005.

Stukel, M.R. *et al.* (2023) 'Carbon sequestration by multiple biological pump pathways in a coastal upwelling biome', *Nature Communications*, 14(1), p. 2024. doi: https://doi.org/10.1038/s41467-023-37771-8.

Stukel, M.R. *et al.* (2013) 'Contributions of mesozooplankton to vertical carbon export in a coastal upwelling system', *Marine Ecology Progress Series*, 491, pp. 47-65. doi: https://doi.org/10.3354/meps.

Sutton, T. (2013) 'Vertical ecology of the pelagic ocean: classical patterns and new perspectives', *Journal of fish biology*, 83(6), pp. 1508-1527. doi: https://doi.org/10.1111/jfb.12263.

Svensen, C. *et al.* (2011) 'Zooplankton distribution across Fram Strait in autumn: Are small copepods and protozooplankton important?', *Progress in Oceanography*, 91(4), pp. 534-544. doi: https://doi.org/10.1016/j.pocean.2011.08.001.

Sweetman, C.J. *et al.* (2014) 'Diet composition of *Bathylagus euryops* (Osmeriformes: Bathylagidae) along the northern Mid-Atlantic Ridge', *Deep Sea Research Part I: Oceanographic Research Papers*, 92, pp. 107-114. doi: https://doi.org/10.1016/j.dsr.2014.06.010.

Takahashi, K. *et al.* (2009) 'Downward carbon transport by diel vertical migration of the copepods *Metridia pacifica* and *Metridia okhotensis* in the Oyashio region of the western subarctic Pacific Ocean', *Deep Sea Research Part I: Oceanographic Research Papers*, 56(10), pp. 1777-1791. doi: https://doi.org/10.1016/j.dsr.2009.05.006.

Tao, Z. *et al.* (2022) 'The diel vertical distribution and carbon biomass of the zooplankton community in the Caroline Seamount area of the western tropical Pacific Ocean', *Scientific Reports*, 12(1), p. 18908. doi: https://doi.org/10.1038/s41598-022-23522-0.

Tarling, G.A. *et al.* (2002) 'Midnight sinking behaviour in *Calanus finmarchicus*: a response to satiation or krill predation?', *Marine Ecology Progress Series*, 240, pp. 183-194. doi: https://doi.org/10.3354/meps.

Tarling, G.A., Shreeve, R.S. and Ward, P. (2007) 'Life-cycle and population dynamics of *Rhincalanus gigas* (Copepoda: Calanoida) in the Scotia Sea', *Marine Ecology Progress Series*, 338, pp. 145-158. doi: https://doi.org/10.3354/meps.

Tarling, G.A. *et al.* (2012) 'Seasonal trophic structure of the Scotia Sea pelagic ecosystem considered through biomass spectra and stable isotope analysis', *Deep Sea Research Part II: Topical Studies in Oceanography*, 59, pp. 222-236. doi: https://doi.org/10.1016/j.dsr2.2011.07.002.

Tarling, G.A., Ward, P. and Thorpe, S.E. (2018) 'Spatial distributions of Southern Ocean mesozooplankton communities have been resilient to long-term surface warming', *Global Change Biology*, 24(1), pp. 132-142. doi: https://doi.org/10.1111/gcb.13834.

Teuber, L. *et al.* (2013) 'Distribution and ecophysiology of calanoid copepods in relation to the oxygen minimum zone in the eastern tropical Atlantic', *PloS one*, 8(11), p. e77590. doi: https://doi.org/10.1371/journal.pone.0077590.

Thomalla, S.J. *et al.* (2023) 'Widespread changes in Southern Ocean phytoplankton blooms linked to climate drivers', *Nature Climate Change*, 13(9), pp. 975-984. doi: 10.1038/s41558-023-01768-4.

Timonin, A.G. *et al.* (1992) 'Zooplankton dynamics in the northern Benguela ecosystem, with special reference to the copepod *Calanoides carinatus*', *South African Journal of Marine Science*, 12(1), pp. 545-560. doi: https://doi.org/10.2989/02577619209504724.

Tjiputra, J.F., Couespel, D. and Sanders, R. (2025) 'Marine ecosystem role in setting up preindustrial and future climate', *Nature Communications*, 16(1), p. 2206. doi: https://doi.org/10.1038/s41467-025-57371-y.

Trebilco, R. *et al.* (2013) 'Ecosystem ecology: size-based constraints on the pyramids of life', *Trends in Ecology & Evolution*, 28(7), pp. 423-431. doi: https://doi.org/10.1016/j.tree.2013.03.008.

Turner, J.T. (2002) 'Zooplankton fecal pellets, marine snow and sinking phytoplankton blooms', *Aquatic microbial ecology*, 27(1), pp. 57-102. doi: https://doi.org/10.3354/ame.

Turner, J.T. (2004) 'The importance of small planktonic copepods and their roles in pelagic marine food webs', *Zool. stud*, 43(2), pp. 255-266.

Turner, J.T. (2015) 'Zooplankton fecal pellets, marine snow, phytodetritus and the ocean's biological pump', *Progress in Oceanography*, 130, pp. 205-248. doi: https://doi.org/10.1016/j.pocean.2014.08.005.

Tutasi, P. and Escribano, R. (2020) 'Zooplankton diel vertical migration and downward C flux into the oxygen minimum zone in the highly productive upwelling region off northern Chile', *Biogeosciences*, 17(2), pp. 455-473. doi: https://doi.org/10.5194/bg-17-455-2020.

Uchimiya, M. *et al.* (2018) 'Balancing organic carbon supply and consumption in the ocean's interior: Evidence from repeated biogeochemical observations conducted in the subarctic and subtropical western North Pacific', *Limnology and Oceanography*, 63(5), pp. 2015-2027. doi: https://doi.org/10.1002/lno.10821.

Ullah, H. *et al.* (2018) 'Climate change could drive marine food web collapse through altered trophic flows and cyanobacterial proliferation', *PLoS biology*, 16(1), p. e2003446. doi: https://doi.org/10.1371/journal.pbio.2003446.

Underwood, M.J. *et al.* (2020) 'An acoustic method to observe the distribution and behaviour of mesopelagic organisms in front of a trawl', *Deep Sea Research Part II: Topical Studies in Oceanography*, 180, p. 104873. doi: https://doi.org/10.1016/j.dsr2.2020.104873.

Valentine, R.C. and Valentine, D.L. (2004) 'Omega-3 fatty acids in cellular membranes: a unified concept', *Progress in lipid research*, 43(5), pp. 383-402. doi: https://doi.org/10.1016/j.plipres.2004.05.004.

Van Mooy, B.A.S., Keil, R.G. and Devol, A.H. (2002) 'Impact of suboxia on sinking particulate organic carbon: Enhanced carbon flux and preferential degradation of amino acids via denitrification', *Geochimica et Cosmochimica Acta*, 66(3), pp. 457-465. doi: https://doi.org/10.1016/S0016-7037(01)00787-6.

Vega, M.P. (1999) 'Life-stage differences in the diet of Parabroteas sarsi (Daday)(Copepoda, Calanoida): a field study', *Limnologica*, 29(2), pp. 186-190. doi: https://doi.org/10.1016/S0075-9511(99)80066-8.

Ventura, M. (2006) 'Linking biochemical and elemental composition in freshwater and marine crustacean zooplankton', *Marine Ecology Progress Series*, 327, pp. 233-246. doi: https://doi.org/10.3354/meps.

Verheye, H. *et al.* (2005) 'Life strategies, energetics and growth characteristics of *Calanoides carinatus* (Copepoda) in the Angola-Benguela frontal region', *African Journal of Marine Science*, 27(3), pp. 641-651. doi: https://doi.org/10.2989/18142320509504124.

Vestheim, H., Kaartvedt, S. and Edvardsen, B. (2005) 'State-dependent vertical distribution of the carnivore copepod *Pareuchaeta norvegica*', *Journal of Plankton Research*, 27(1), pp. 19-26. doi: https://doi.org/10.1093/plankt/fbh144.

Viso, A.-C. and Marty, J.-C. (1993) 'Fatty acids from 28 marine microalgae', *Phytochemistry*, 34(6), pp. 1521-1533. doi: https://doi.org/10.1016/S0031-9422(00)90839-2.

Visser, A.W., Grønning, J. and Jónasdóttir, S.H. (2017) '*Calanus hyperboreus* and the lipid pump', *Limnology and Oceanography*, 62(3), pp. 1155-1165. doi: https://doi.org/10.1002/lno.10492.

Visser, A.W. and Jónasdóttir, S.H. (1999) 'Lipids, buoyancy and the seasonal vertical migration of *Calanus finmarchicus*', *Fisheries Oceanography*, 8, pp. 100-106. doi: https://doi.org/10.1046/j.1365-2419.1999.00001.x.

Volkman, J.K. *et al.* (1980) 'Microbial lipids of an intertidal sediment—I. Fatty acids and hydrocarbons', *Geochimica et Cosmochimica Acta*, 44(8), pp. 1133-1143. doi: https://doi.org/10.1016/0016-7037(80)90067-8.

von Harbou, L. *et al.* (2011) 'Salps in the Lazarev Sea, Southern Ocean: I. Feeding dynamics', *Marine Biology*, 158(9), pp. 2009-2026. doi: https://doi.org/10.1007/s00227-011-1709-4.

Voronin, V.P. *et al.* (2022) 'Lipids and Fatty Acids in Some Mesopelagic Fish Species: General Characteristics and Peculiarities of Adaptive Response to Deep-Water Habitat', *Journal of Marine Science and Engineering*, 10(7). doi: https://doi.org/10.3390/jmse10070949.

Voronina, N.M. (1970) 'Seasonal cycles of some common Antarctic copepod species', *Antarctic ecology*, 1, pp. 162-172.

Wakeham, S.G. *et al.* (1984) 'Biogeochemistry of particulate organic matter in the oceans: results from sediment trap experiments', *Deep Sea Research Part A. Oceanographic Research Papers*, 31(5), pp. 509-528. doi: https://doi.org/10.1016/0198-0149(84)90099-2.

Wang, F. *et al.* (2019) 'δ13C and fatty acid composition of mesopelagic fishes in the South China Sea and their influence factors', *Chemistry and Ecology*, 35(9), pp. 788-804. doi: https://doi.org/10.1080/02757540.2019.1651844.

Ward, B.A. *et al*. (2012a) 'A size-structured food-web model for the global ocean', *Limnology and Oceanography*, 57(6), pp. 1877-1891. doi: https://doi.org/10.4319/lo.2012.57.6.1877.

Ward, P. *et al*. (1997) 'Regional variation in the life cycle of *Rhincalanus gigas* (Copepoda: Calanoida) in the Atlantic Sector of the Southern Ocean--re-examination of existing data (1928 to 1993)', *Marine Ecology Progress Series*, 157, pp. 261-275. doi: https://doi.org/10.3354/meps.

Ward, P., Atkinson, A. and Tarling, G. (2012b) 'Mesozooplankton community structure and variability in the Scotia Sea: a seasonal comparison', *Deep Sea Research Part II: Topical Studies in Oceanography*, 59, pp. 78-92. doi: https://doi.org/10.1016/j.dsr2.2011.07.004.

Ward, P. *et al*. (2004) 'Mesozooplankton community structure in the Scotia Sea during the CCAMLR 2000 survey: January–February 2000', *Deep Sea Research Part II: Topical Studies in Oceanography*, 51(12-13), pp. 1351-1367. doi: https://doi.org/10.1016/j.dsr2.2004.06.016.

Ward, P. *et al*. (2006) 'Plankton community structure and variability in the Scotia Sea: austral summer 2003', *Marine Ecology Progress Series*, 309, pp. 75-91. doi: https://doi.org/10.3354/meps.

Ward, P., Shreeve, R.S. and Cripps, G.C. (1996) '*Rhincalanus gigas* and *Calanus simillimus*: lipid storage patterns of two species of copepod in the seasonally ice-free zone of the Southern Ocean', *Journal of Plankton Research*, 18(8), pp. 1439-1454. doi: https://doi.org/10.1093/plankt/18.8.1439.

Ward, P., Tarling, G.A. and Thorpe, S.E. (2018) 'Temporal changes in abundances of large calanoid copepods in the Scotia Sea: comparing the 1930s with contemporary times', *Polar Biology*, 41(11), pp. 2297-2310. doi: https://doi.org/10.1007/s00300-018-2369-3.

Watts, J. and Tarling, G.A. (2012) 'Population dynamics and production of *Themisto gaudichaudii* (Amphipoda, Hyperiidae) at South Georgia, Antarctica', *Deep Sea Research Part II: Topical Studies in Oceanography*, 59-60, pp. 117-129. doi: https://doi.org/10.1016/j.dsr2.2011.05.001.

Webb, T.J., Vanden Berghe, E. and O'Dor, R. (2010) 'Biodiversity's Big Wet Secret: The Global Distribution of Marine Biological Records Reveals Chronic Under-Exploration of the Deep Pelagic Ocean', *PLOS ONE*, 5(8), p. e10223. doi: https://doi.org/10.1371/journal.pone.0010223.

Weber, T. and Bianchi, D. (2020) 'Efficient Particle Transfer to Depth in Oxygen Minimum Zones of the Pacific and Indian Oceans', *Frontiers in Earth Science*, Volume 8 - 2020. doi: 10.3389/feart.2020.00376.

Wells, M.J., Clarke, A. and Clarke, M.R. (1997) 'Energetics: the costs of living and reproducing for an individual cephalopod', *Philosophical Transactions of the Royal Society of London. Series B: Biological Sciences*, 351(1343), pp. 1083-1104. doi: https://doi.org/10.1098/rstb.1996.0095.

Wiebe, P.H., Lavery, A.C. and Lawson, G.L. (2023) 'Biogeographic variations in diel vertical migration determined from acoustic backscattering in the northwest Atlantic Ocean', *Deep Sea Research Part I: Oceanographic Research Papers*, 193, p. 103887. doi: https://doi.org/10.1016/j.dsr.2022.103887.

Wilson, R.J. *et al*. (2016) 'Projected impacts of 21st century climate change on diapause in *Calanus finmarchicus*', *Global Change Biology*, 22(10), pp. 3332-3340. doi: https://doi.org/10.1111/gcb.13282.

Wilson, S. *et al*. (2010) 'Feeding ecology of mesopelagic zooplankton of the subtropical and subarctic North Pacific Ocean determined with fatty acid biomarkers', *Deep Sea Research Part I: Oceanographic Research Papers*, 57(10), pp. 1278-1294. doi: https://doi.org/10.1016/j.dsr.2010.07.005.

Wishner, K.F. *et al.* (2013) 'Zooplankton in the eastern tropical north Pacific: Boundary effects of oxygen minimum zone expansion', *Deep Sea Research Part I: Oceanographic Research Papers*, 79, pp. 122-140. doi: https://doi.org/10.1016/j.dsr.2013.05.012.

Wishner, K.F., Seibel, B. and Outram, D. (2020) 'Ocean deoxygenation and copepods: coping with oxygen minimum zone variability', *Biogeosciences*, 17(8), pp. 2315-2339. doi: https://doi.org/10.5194/bg-17-2315-2020.

Yamaguchi, A. *et al.* (2002) 'Community and trophic structures of pelagic copepods down to greater depths in the western subarctic Pacific (WEST-COSMIC)', *Deep Sea Research Part I: Oceanographic Research Papers*, 49(6), pp. 1007-1025. doi: https://doi.org/10.1016/S0967-0637(02)00008-0.

Yamamae, K. *et al.* (2023) 'Vertical changes in zooplankton abundance, biomass, and community structure at seven stations down to 3000 m in neighboring waters of Japan during the summer: Insights from ZooScan imaging analysis', *Progress in Oceanography*, 219, p. 103155. doi: https://doi.org/10.1016/j.pocean.2023.103155.

Yang, G. *et al.* (2025) 'Seasonally migrating zooplankton strongly enhance Southern Ocean carbon sequestration', *Limnology and Oceanography*, n/a(n/a). doi: https://doi.org/10.1002/lno.70120.

Yang, G. *et al.* (2016) 'Feeding strategies of four dominant copepod species in Prydz Bay, Antarctica: insights from a combined fatty acid biomarker and stable isotopic approach', *Deep Sea Research Part I: Oceanographic Research Papers*, 114, pp. 55-63. doi: https://doi.org/10.1016/j.dsr.2016.04.016.

Yebra, L. *et al.* (2018) 'Zooplankton production and carbon export flux in the western Alboran Sea gyre (SW Mediterranean)', *Progress in oceanography*, 167, pp. 64-77. doi: https://doi.org/10.1016/j.pocean.2018.07.009.

Yebra, L. *et al.* (2017) 'Chapter Four - Advances in Biochemical Indices of Zooplankton Production', in Curry, B.E. (ed.) *Advances in Marine Biology*. Academic Press, pp. 157-240. doi: https://doi.org/10.1016/bs.amb.2016.09.001.

Yoshiki, T. *et al.* (2006) 'A new hydrostatic pressure apparatus for studies of marine zooplankton', *Journal of Plankton Research*, 28(6), pp. 563-570. doi: https://doi.org/10.1093/plankt/fbi141.

Yvon-Durocher, G. and Allen, A.P. (2012) 'Linking community size structure and ecosystem functioning using metabolic theory', *Philosophical Transactions of the Royal Society B: Biological Sciences*, 367(1605), pp. 2998-3007. doi: https://doi.org/10.1098/rstb.2012.0246.

Yvon-Durocher, G. *et al.* (2012) 'Reconciling the temperature dependence of respiration across timescales and ecosystem types', *Nature*, 487(7408), pp. 472-476. doi: https://doi.org/10.1038/nature11205.

Zahuranec, B.J. and Pugh, W.L. (1971) *Proceedings of an international symposium on biological sound scattering in the ocean*. Maury Center for Ocean Science.

Zanden, M.J.V. and Rasmussen, J.B. (2001) 'Variation in δ15N and δ13C trophic fractionation: implications for aquatic food web studies', *Limnology and oceanography*, 46(8), pp. 2061-2066. doi: https://doi.org/10.4319/lo.2001.46.8.2061.

Zaret, T.M. and Suffern, J.S. (1976) 'Vertical migration in zooplankton as a predator avoidance mechanism 1', *Limnology and oceanography*, 21(6), pp. 804-813. doi: https://doi.org/10.4319/lo.1976.21.6.0804.

Zhang, X. and Dam, H.G. (1997) 'Downward export of carbon by diel migrant mesozooplankton in the central equatorial Pacific', *Deep Sea Research Part II: Topical Studies in Oceanography*, 44(9-10), pp. 2191-2202. doi: https://doi.org/10.1016/S0967-0645(97)00060-X.

Zhou, M. (2006) 'What determines the slope of a plankton biomass spectrum?', *Journal of Plankton Research*, 28(5), pp. 437-448. doi: https://doi.org/10.1093/plankt/fbi119.

Zuur, A.F., Ieno, E.N. and Smith, G.M. (2007) 'Principal component analysis and redundancy analysis', in *Analysing Ecological Data*. New York, NY: Springer New York, pp. 193-224. doi: 10.1007/978-0-387-45972-1_12.